

Review

Selective C–C and C–O bond cleavage strategies for the thermochemical upgrading of (hemi)cellulosic biomass



Ruiyan Sun^a, Cui Yang^a, Zheng Fang^a, Ning Zhu^a, Mingyuan Zheng^{c,*}, Kai Guo^{a,b,**}, Tao Zhang^{c,*}

^a College of Biotechnology and Pharmaceutical Engineering, Nanjing Tech University, Nanjing 211816, China

^b State Key Laboratory of Materials-Oriented Chemical Engineering, Nanjing Tech University, Nanjing 211816, China

^c State Key Laboratory of Catalysis, Dalian Institute of Chemical Physics, Chinese Academy of Sciences, Dalian 116023, China

ARTICLE INFO

Keywords:
 (hemi)cellulose upgrading
 Platform molecules
 C–C/C–O bond cleavage
 Heterogeneous catalysis
 Catalyst design

ABSTRACT

Utilizing lignocellulose as an alternative green carbon resource is recognized as a vital approach to drive the ongoing transition towards a sustainable manufacture of chemicals, fuels, and materials with a low-carbon footprint. Unlike fossil resources, lignocellulose and its derivatives are featured by ubiquitous C–C and C–O bonds constituting carbon skeletons and various oxygenated moieties, respectively. Breaking these C–C/C–O bonds, in particular, the selective cleavage of specific C–C/C–O bonds present in biomass is of pivotal importance for the selective valorization of lignocellulose into targeted products. Hence, considerable attention has paid to searching for selective bond-breaking methods/strategies capable of tailoring different C–C/C–O bonds. Numerous conversion pathways based on selective C–C/C–O bond cleavage reactions have been developed to upgrade biomass into a broad spectrum of valuable products. In this review, we attempt to present a summary of existing selective C–C/C–O bond cleavage strategies frequently used for the upgrading of (hemi)cellulose, the dominant components of lignocellulose and also the major source of non-food carbohydrates. Each strategy is illustrated in terms of bond cleavage mechanism, utility in synthesizing various chemicals, representative catalyst systems, and coupling with other reactions to form cascade upgrading processes. Finally, pending challenges and potential opportunities related to selective bond cleavage strategies are discussed to propose future research directions. We hope that this review will help inspire further progress in designing new selective approaches for (hemi)cellulose valorization.

1. Introduction

Environmental issues, especially the pressing global warming situation, associated with the utilization of conventional fossil resources have largely accelerated the exploitation of renewable carbon resources aimed at carbon-neutral chemical industries. In this context, lignocellulosic biomass, a natural form of organic matter containing abundant carbon, oxygen, and hydrogen atoms, stands out as a very promising renewable carbon feedstock to reduce the heavy reliance on fossil sources of carbon. In comparison with the limited reserves of fossil resources, the production of lignocellulosic biomass on earth is estimated to amount to 181 billion tonnes per annum, which provides a huge pool of renewable carbon resources potentially available for establishing the targeted carbon-neutral bio-based chemical industry [1–3]. The vision

of bio-based chemical industry is to realize the sustainable valorization of lignocellulosic biomass into a wide spectrum of drop-in products (molecularly identical to the existing petro-based products with mature markets) including chemicals, fuels, and materials, as well as novel bio-based products (e.g., furandicarboxylic acid) bearing peculiar functionalities and properties [4–10]. However, lignocellulose typically exists as a complex polymer featuring heterogeneous compositions (cellulose, hemicellulose, lignin), robust structures, and complicated chemical linkages, which pose a great challenge for the selective valorization of lignocellulose to target products [11,12].

Central to lignocellulose upgrading lies in devising innovative conversion methods/techniques applicable to processing its diverse components. The past decade has witnessed intensive endeavors in developing various thermo-chemical conversion approaches to realize

* Corresponding authors.

** Corresponding author at: College of Biotechnology and Pharmaceutical Engineering, Nanjing Tech University, Nanjing 211816, China.

E-mail addresses: myzheng@dicp.ac.cn (M. Zheng), guok@njtech.edu.cn (K. Guo), taozhang@dicp.ac.cn (T. Zhang).

the efficient depolymerization and conversion of lignocellulose [5, 13–16]. For example, gasification and pyrolysis (also called liquefaction) represent two simplest thermochemical techniques capable of depolymerizing the whole components of lignocellulose in one step [17]. Nevertheless, the applied high reaction temperatures (above 400 °C) render the bond cleavage of lignocellulose occurring mostly in an uncontrolled manner, thus giving rise to many kinds of oxygenated compounds (bio-oils) as well as gaseous molecules (CO, CO₂, hydrocarbons, etc.). In contrast, the directional and selective upgrading of lignocellulose into targeted products can be realized by adopting a cascade conversion strategy which integrates upstream deconstruction/fractionation of lignocellulose into three major components (cellulose, hemicellulose, lignin) or their derivatives with downstream upgrading. Product selectivity control is primarily dependent on the choice of downstream upgrading protocols whereby lignocellulose-derived building blocks such as sugar monomers, sugar alcohols, aromatic monomers, hydroxymethylfurfural (HMF), and furfural can be transformed into various end products of high value. Such a multistep cascade strategy to bridge raw lignocellulose with end products has received increasing attention as a new paradigm for lignocellulose valorization [18]. Impressive advancements have been achieved with the emergence of various cascade conversion routes and relevant catalyst systems. For instance, ethylene glycol can be selectively obtained over tungsten-based catalysts via one-pot multistep conversion of cellulose involving hydrolysis, retro-aldol condensation (RAC), and hydrogenation [19,20]. Similarly, by the rational integration of hydrolysis, isomerization, RAC, and (de)hydration in one reactor, direct conversion of cellulose into lactic acid can be realized over a homogeneous Pb catalyst [21].

Lignocellulosic matrixes are comprised of aromatic and aliphatic carbon skeletons modified with abundant oxygen-containing moieties and linkages including hydroxyl, carbonyl, acetal, ether, carboxyl, and acetyl groups. C–C and C–O linkages are the two basic structural motifs present in lignocellulose. In terms of the reaction chemistry behind these reported cascade conversion protocols, most of them are based on the rational integration of diverse C–C/C–O bond cleavage or coupling reactions. In general, the upstream depolymerization of lignocellulose necessitates breaking the prevailing C–O (ether) linkages within (hemi)cellulose and lignin to release monosaccharide units and alkylphenolic monomers, respectively. As for the downstream upgrading of these monomers, C–O bond cleavage, C–C bond cleavage, and C–C coupling reactions are usually needed depending on the targeted products. For instance, when aiming for bio-fuels typically containing long-chain hydrocarbon molecules, the removal of oxygen atoms by C–O cleavage reactions along with an increase in carbon-chain length by C–C coupling reactions are frequently employed to endow bio-based chemicals with fuel-like properties [6,22,23]. Owing to the robust nature of C–C and C–O connections in biomass, high energy barriers need to be overcome in breaking these bonds, especially for C–C bonds. On the other hand, there are multiple configurations of C–C and C–O bonds within lignocellulose structures, most of which possess similar reactivities. Taking glucose (the basic unit of cellulose) as an example, its carbon skeleton comprises five C–C bonds featuring same binding environments, thus showing very similar bond energies. This renders the precise cleavage at desired connections quite challenging. To address aforementioned challenges, ongoing research efforts have been devoted to seeking for selective reactions and related catalyst systems applicable for the efficient cleavage of specific chemical bonds in lignocellulose. A number of reactions such as hydrolysis, RAC, oxidative fragmentation, demethoxylation, dealkylation, decarboxylation, and deoxydehydration (DODH) have been identified as efficient C–C or C–O bond cleavage methods in upgrading lignocellulose into valuable chemicals such as polyols, organic acids, aromatics, alkanes, etc. [5,24–32].

In recent years, the selective conversion of lignocellulose into targeted products by leveraging bond cleavage and C–C coupling reactions has become an active field of research. Several excellent reviews have

addressed the utilization of C–C coupling reactions/strategies to upgrade lignocellulose-derived molecules into long-carbon-chain chemicals as fuel components [6,33–36]. The application of bond cleavage reactions to break C–C/C–O linkages have been recently summarized primarily focusing on the lignin fraction [5,37–41]. An overview of bond cleavage reactions/strategies targeted for the C–C/C–O linkages in (hemi)cellulose and its derived building blocks is still scarce. As the major component of biomass, (hemi)cellulose has been demonstrated to be converted into a broad spectrum of chemicals and fuels by tailoring the C–C/C–O linkages. In particular, the selective cleavage of specific C–C/C–O bonds is of pivotal importance for steering the upgrading pathways of (hemi)cellulose into targeted products. Many different conversion pathways/routes have been reported for (hemi)cellulose valorization, and most of them are based on the rational combination of C–C/C–O bond cleavage reactions/strategies. Therefore, the current review is dedicated to a summary of relevant C–C and C–O bond cleavage reactions/strategies to upgrade (hemi)cellulose and its derivatives.

The main body of this review is organized into two major sections covering C–C and C–O bond cleavage strategies, respectively. Note that this review is not intended to present an exhaustive collection of a myriad of reports that involve the cleavage of C–C/C–O bonds in (hemi)cellulose and its derivatives, but rather to summarize the general bond cleavage reactions/strategies behind these reports. According to the reaction type of bond cleavage, we propose four frequently-used C–O bond cleavage strategies including glycosidic bond hydrolysis, dehydration of hydroxyl group, DODH of adjacent hydroxyl groups, and hydrogenolysis of internal C–O bond (Fig. 1). Similarly, available C–C bond cleavage strategies could be summarized into four main types consisting of RAC, oxidative cleavage, decarbonylation, and decarboxylation (Fig. 1). For each strategy, we select representative examples to illustrate the underlying bond-breaking mechanism, typical applications in synthesizing valuable products, and key factors (e.g., catalysts, reaction conditions) to affect the performance. Particular attention is paid to two prominent strategies, that is, DODH of adjacent hydroxyl groups and RAC, since both of them manifest high versatility for a broad scope of bio-based molecules. The combination of these bond cleavage reactions with other reactions to form novel cascade upgrading approaches will be discussed as well. We hope this review could provide informative knowledge to advance the development of precisely-controlled upgrading approaches for (hemi)cellulose based on selective C–O/C–C bond cleavage reactions.

2. C–O bond cleavage strategies

As a highly-oxygenated biopolymer, (hemi)cellulose bears a high fraction of oxygen-containing moieties mainly including hydroxyl groups and glycosidic linkages. Correspondingly, two types of C–O bonds in the forms of free hydroxyl group and glycosidic linkage are ubiquitous in (hemi)cellulose molecular structures. These oxygen-containing moieties can be tailored by several C–O bond cleavage strategies mainly including acid-promoted glycosidic bond hydrolysis, dehydration of hydroxyl groups, DODH of adjacent hydroxyl groups, and hydrogenolysis of internal C–O bond. The major function of the former strategy is to break glycosidic linkages within (hemi)cellulosic networks, while the latter three strategies aim at selectively removing hydroxyl groups. These strategies have found broad applications in both upstream depolymerization and downstream biorefining of (hemi)cellulose. Detailed descriptions of each strategy will be shown in following sections.

2.1. Glycosidic bond hydrolysis

Glucose and xylose, the basic units of cellulose and hemicellulose, are connected by glycosidic bonds to form polymeric networks. In spite of distinct structural units, cellulose and hemicellulose possess the same

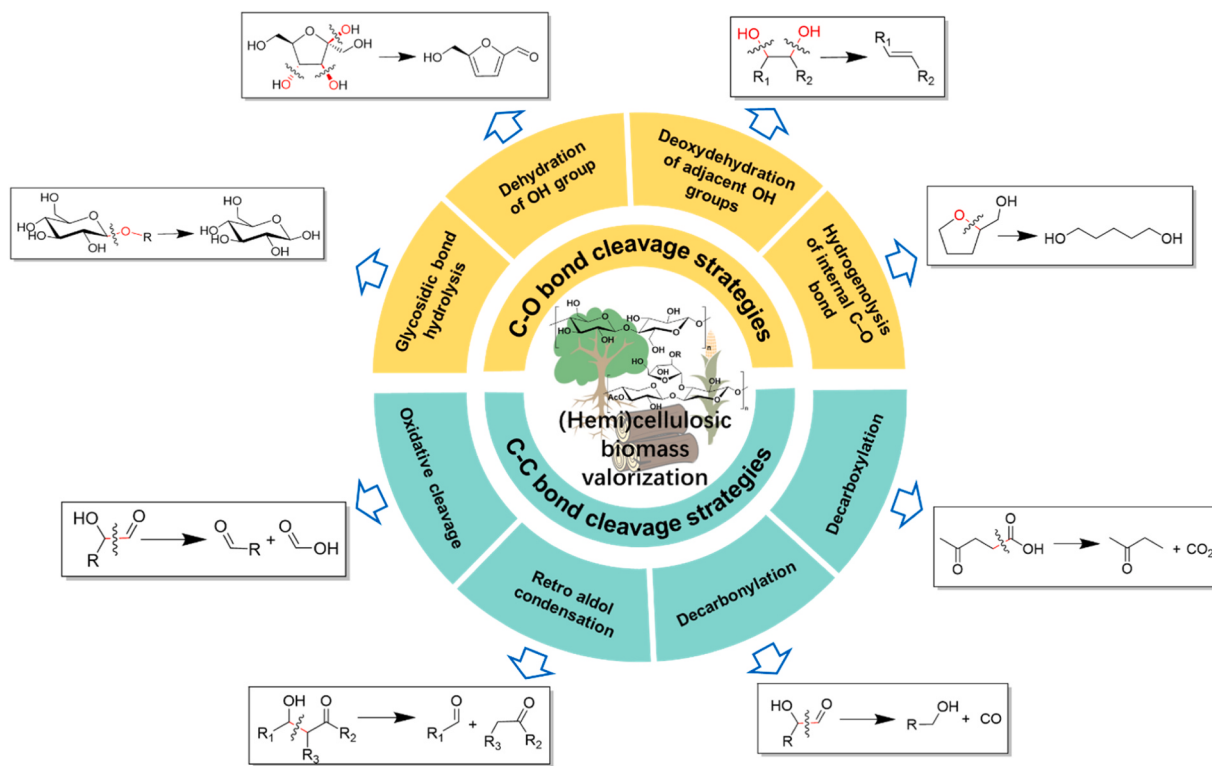


Fig. 1. Commonly-used C–O and C–C bond cleavage strategies for the selective valorization of (hemi)cellulose and its derivatives.

chemical linkages, that is, glycosidic bonds (Fig. 2). Existing glycosidic bond hydrolysis methods are basically applicable to both cellulose and hemicellulose. One major structural difference between cellulose and hemicellulose is their different degree of crystallinity and polymerization, which strongly affect the hydrolysis efficiency of glycosidic bonds. The glycosidic bonds of hemicellulose are more readily to be cleaved than cellulose, owing to the loose and amorphous structures of hemicellulose [42]. Irrespective of the substrates used, the overwhelming majority of glycosidic bond cleavage reactions are catalyzed by acid catalysts, typically following an acid hydrolysis mechanism. In principle, acid hydrolysis of glycosidic bond entails the participation of water molecules and protons, serving as nucleophilic reagents and catalytic active species, respectively. Protons are typically provided by Brønsted acid catalysts and normally exist in the form of hydronium ions upon dissolving in water. It should be noted that, in the absence of acid catalysts, the hydrolysis of glycosidic bonds can still proceed slowly, assisted by the protons from self-ionization of water at high temperatures. The depolymerization of cellulose is proposed to proceed in a

stepwise manner analogous to enzymatic hydrolysis, i.e., the first breakage of long cellulose strands to form short-chain oligomers which continue to yield glucose by cleaving glycosidic linkages [43,44]. Taking cellobiose as a model substrate (Scheme 1), the initial step of glycosidic bond hydrolysis is believed to involve the activation of acetal linkages (C–O–C), which entails the protonation of the oxygen atom in acetal linkage to generate an oxonium intermediate [43,45–47]. Upon the formation of oxonium species, the cleavage of acetal linkage readily happens, yielding one glucose unit and one carbocation intermediate. In the final step, one water molecule reacts with the carbocation intermediate via nucleophilic attack, giving rise to another glucose unit as well as one proton. As such, the regenerated proton can enter another catalysis cycle of glycosidic bond hydrolysis. In addition to protons, Lewis acid sites such as high-valence Sn and Ru species alone or combined with solid acids have been reported to catalyze the hydrolysis of glycosidic bonds [48,49]. However, it is still debatable whether or not these Lewis acids indeed serve as the catalytic active sites for glycosidic bonds hydrolysis. Considering that a Lewis acidic site could transform to its Brønsted acid counterpart by hydroxylation upon reaction with water, the observed catalytic performances might arise from the generated protons [50,51]. More work is required to clarify the role of Lewis acids.

In general, glycosidic bond cleavage in (hemi)cellulose is carried out in aqueous solutions or ionic liquids, at a wide temperature range from 100 to 250 °C, achieving glucose or xylose in moderate to high yields varying from 40 to 90%, depending on employed catalyst systems. With regard to catalyst development, research attention has been mostly devoted to exploring various homogeneous and heterogeneous acids for the depolymerization of cellulose and hemicellulose [42,43,52,53]. As an old hydrolysis process, homogeneous mineral acids such as sulfuric acid, hydrochloric acid, and phosphoric acid have long been applied for glycosidic linkage cleavage [54,55]. The application of other homogeneous Brønsted acids like heteropoly acids (phosphomolybdc acid, phosphotungstic acid, silicotungstic acid, etc.) and organic acids (oxalic acid, maleic acid, acetic acid, formic acid, p-toluenesulfonic acid, etc.) as

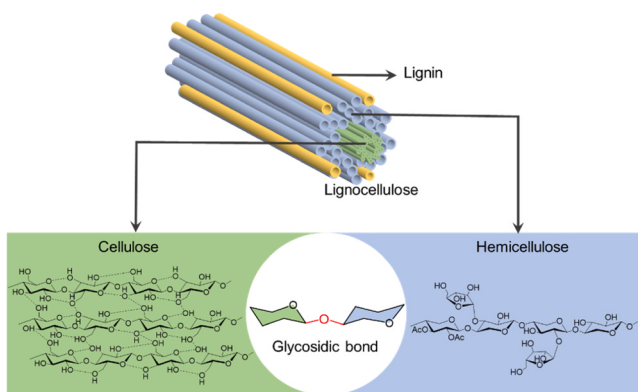
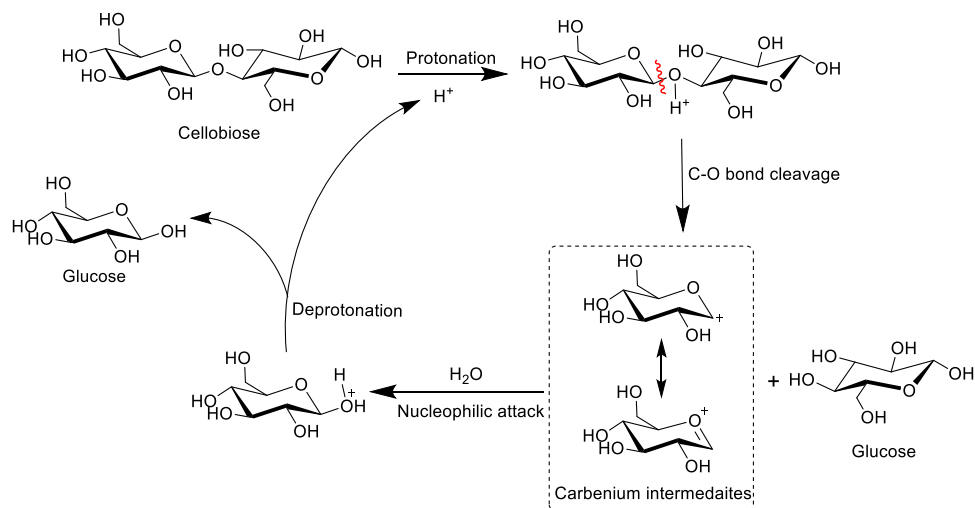


Fig. 2. Typical molecular structures of cellulose and hemicellulose present in lignocellulose.



Scheme 1. Proposed reaction mechanism for acid-catalyzed hydrolysis of glycosidic bonds (using cellobiose as a typical example). Adapted with permission from ref. [44].

glycosidic bond-cleavage catalysts have also been demonstrated [49, 56–58]. Of these acids, maleic acid was discovered to deliver superior glucose selectivity over conventional H_2SO_4 for (hemi)cellulose hydrolysis [56,58]. The unique configuration of dual carboxyl group in maleic acid, resembling the catalytic active centers in cellulolytic enzymes, as well as the weak acid strength of maleic acid are proposed to account for its high selectivity. Kinetic studies reveal that the conversion rate of (hemi)cellulose over homogeneous acids are primarily dependent on the concentration of proton (i.e., Brønsted acid sites) and reaction temperatures [42,56]. The former is closely related to the intrinsic acid strength of acid catalysts, as indicated by pK_a . For example, strong acids ($pK_a < 0$) like sulfuric acid and high temperatures (≥ 150 °C) are usually required for a satisfactory cellulose conversion owing to the structural recalcitrance of cellulose [45,59,60]. By contrast, moderate acids (pK_a around 2) like oxalic acid along with low temperatures (around 130 °C) are already sufficient to achieve almost full conversion of hemicellulose featuring an amorphous structure and a low polymerization degree [61]. Capitalizing on the higher reactivity of hemicellulose, the selective extraction of xylose from biomass without deconstructing cellulose fraction can be realized. For example, Stein et al. reported the high-yield formation of xylose (17.7 wt%) directly from beech wood at 125 °C by using oxalic acid in a biphasic reaction system containing water and 2-methyltetrahydrofuran [57]. The choice of solvent also strongly affects the hydrolysis efficiency of glycosidic bonds. For example, the hydrolysis of cellulose could be markedly enhanced by performing the reaction in salt-containing solvents capable of dissolving and swelling cellulose to increase its accessibility, such as ionic liquids, molten salts (e.g., LiBr), concentrated $ZnCl_2$ solution, etc [59,62–66]. Overall, homogeneous acids possess a prominent advantage related to their soluble nature in water, which ensures sufficient interactions between glycosidic bonds and catalytic active sites, i.e., proton-containing moieties. However, the utilization of homogeneous acids faces several long-standing drawbacks, that is, severe equipment corrosion, substantial waste streams, degradation of glucose/xylose, and costly catalyst recycling.

To address the issues associated with mineral acids, the application of heterogeneous acids, well-known for its facile separation and recycling, for glycosidic bond hydrolysis has become the subject of intensive studies in recent years. Numerous heterogeneous acid catalysts have proven effective in breaking glycosidic bonds such as sulfonated polystyrene resins, sulfonated tetrafluoroethylene resins, sulfonated materials (e.g., carbon and silica), proton-form zeolites, metal oxides, etc [52, 53]. In essence, acidic functions of these solid acid catalysts stem from the proton-containing moieties present in their frameworks, such as the

bridging hydroxyl groups in zeolites and the sulfonic groups in resins, carbons, and silicas. The synthesis, characterization, performance, and structure-activity relationships associated with solid acid-catalyzed (hemi)cellulose hydrolysis have been comprehensively reviewed [43, 67–70], and will not be detailed herein. The major issue of solid acid-catalyzed (hemi)cellulose hydrolysis is the poor interaction/contact between solid acids and insoluble cellulose, thus leading to unsatisfactory yields of glucose/xylose and higher mass ratio of catalyst/substrate. Feasible strategies reported to enhance the interaction/contact between solid acids and cellulose include the structural engineering of solid acids for mesoporous channels and high surface areas, as well as introducing cellulose-binding sites onto catalyst surface such as boronic acid groups [71], phenolic hydroxyl groups (PhOH) [72], carboxyl groups [73], and chlorides [74], mimicking the microenvironments of cellulase (Fig. 3). Employing carbon-based materials as supports can also enhance the adsorption of cellulose onto catalyst surface. The existing $CH-\pi$ interaction (van der Waals forces) between aromatic structure of graphene sheet and CH moieties of cellulose is proposed to account for the improved performance over carbon-based acid catalysts [75–77]. Poor stability presents another common issue encountered in the hydrolysis of (hemi)cellulose over solid acids. Under hydrothermal conditions, the acidic centers of solid acids such as zeolites and sulfonated carbon tend to undergo gradual degrading or leaching, which will become pronounced with increasing reaction temperatures [78,79]. One promising solution is to lower reaction temperature, but this in turn would require the design of more active solid catalysts through the aforementioned strategies to improve interaction between solid acid and cellulose.

The pretreatment of (hemi)cellulose, prior to acid hydrolysis, has been identified as an essential approach to improve reactivity. This process is especially necessary when it comes to hydrolyzing cellulose featuring crystalline structures, high polymerization degree, compact molecular arrangement, and extensive hydrogen bonds. These natural properties have imposed great hurdles for the efficient contact/interaction between acid catalysts and glycosidic linkages. Therefore, it is imperative to pretreat cellulose in order to disrupt complex hydrogen bond networks, open up the crystalline structure, and increase the accessibility of glycosidic bonds towards acid catalysts. A series of chemical, physical, and physico-chemical pretreatment methods have been developed, such as acid prehydrolysis, ionic liquid treatment, alkaline treatment, organosolvolysis, steam explosion, microwave irradiation, mechanical milling, etc. For detailed introduction of these methods, which is beyond the scope of this review, the reader is referred to several excellent review articles [80–82].

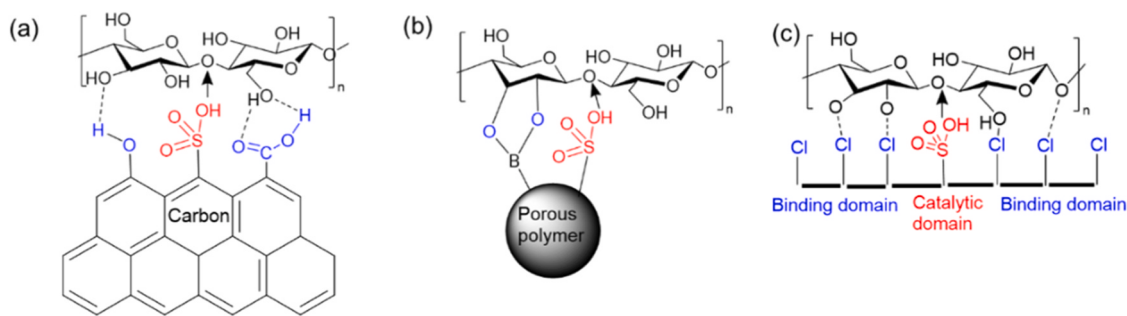


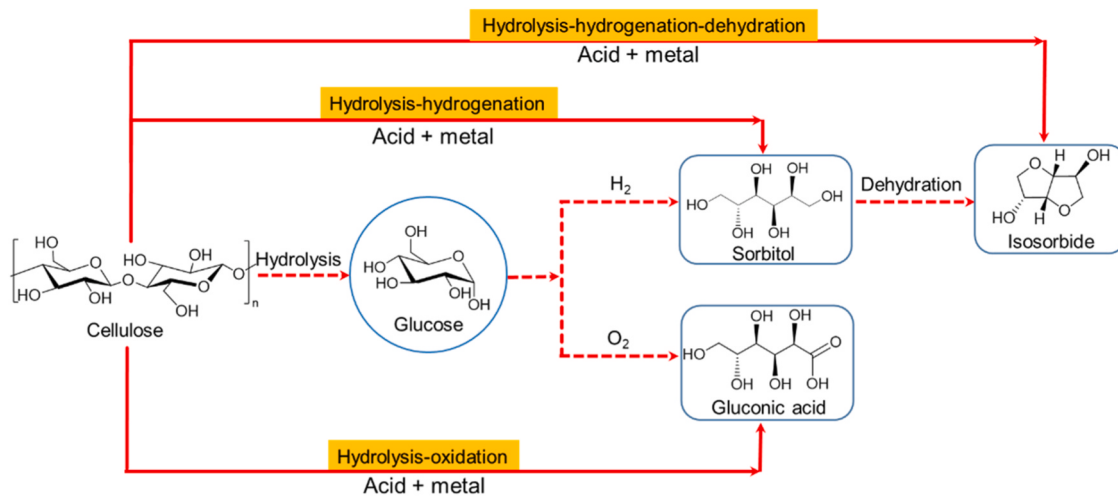
Fig. 3. Typical cellulase-like solid acid catalysts containing both acidic sites (e.g., sulfonic groups) and various binding sites for cellulose hydrolysis: (a) phenolic hydroxyl groups and carboxyl groups as binding sites; (b) boronic acid groups as binding sites; (c) chlorides as binding sites. Adapted with permission from ref. [71–74].

Glycosidic bond hydrolysis not only enables the depolymerization of cellulose into glucose, but also opens the access to more value-added chemicals when combined with other reaction strategies such as hydrogenation and oxidation (Scheme 2 and Table 1). For example, by integrating glycosidic bond hydrolysis and glucose hydrogenation (hydrolysis-hydrogenation), one-pot hydrolytic hydrogenation of cellulose to sorbitol with moderate to high yields was achieved over a series of bifunctional catalysts comprising acidic moieties and metal species, e.g., Pt/Al₂O₃, Ru/C + H₄SiW₁₂O₄₀, Ni₂P/AC, Ni/oxidized CNF[83–86]. In these examples, cellulose first undergoes glycosidic bond cleavage over acid sites to yield glucose as an intermediate, followed by an immediate hydrogenation over metal sites to give sorbitol. Key to this hydrolysis-hydrogenation process is the balance between acidic properties and hydrogenation ability of metals. Acid sites are believed to arise from acidic supports (e.g., Al₂O₃, oxidized CNF) and the doped metals such as phosphors. Besides, the heterolysis of H₂ on metal sites as well as the high-pressure hot water could also provide protons for cellulose hydrolysis. Sorbitol yield is also dependent on the crystallinity of cellulose. In the case of applying Ru/C + H₄SiW₁₂O₄₀, ball-milled cellulose with higher reactivity could deliver a very high hexitol yield of 85% at 190 °C and 95 bar H₂ in 1 h, whereas only 36% yield of hexitol was obtained for untreated microcrystalline cellulose [84]. Note that this hydrolysis-hydrogenation strategy is also applicable to upgrading hemicellulose with the formation of xylitol as the main product via xylose intermediate [87–89].

A synthetic route for gluconic acid, a valuable chemical in food, pharmaceutical, and materials industries, can be conceived by combining glycosidic bond hydrolysis with glucose oxidation (hydrolysis-oxidation). However, the realization of this hydrolysis-oxidation

route in one pot faces a big challenge in terms of reaction compatibility. The catalytic oxidation of glucose to gluconic acid typically proceeds under basic conditions, which is incompatible with the acid-catalyzed hydrolysis of cellulose. So far, only a few bifunctional Au catalysts including Au/Cs_{1.2}H_{1.8}PW₁₂O₄₀, Au/Cs₃PW₁₂O₄₀ + H₃PW₁₂O₄₀, and Au/HY have been reported to catalyze this hydrolysis-oxidation route giving appreciable gluconic acid yields (23–85%) [90,91]. In these Au-based catalysts, the acidic supports facilitate cellulose hydrolysis, while Au nanoparticles catalyze the selective oxidation of aldehyde groups in glucose. Among these catalysts, the combination of Au/Cs₃PW₁₂O₄₀ with H₃PW₁₂O₄₀ exhibited an excellent yield of up to 85% [90]. The superior performance was ascribed to the synergistic catalysis of H₃PW₁₂O₄₀ (cellulose hydrolysis) and Au/Cs₃PW₁₂O₄₀ (glucose oxidation). In contrast to the easy degradation of Cs_{1.2}H_{1.8}PW₁₂O₄₀ and HY under hydrothermal conditions, Au/Cs₃PW₁₂O₄₀ is relatively stable during recycling tests with only slight decrease in gluconic acid yield. Interestingly, Pan et al. reported the direct conversion of cellulose into gluconic acid in concentrated FeCl₃ aqueous solution without catalysts [92]. Under mild reaction conditions (120 °C, 1 bar of air, 2 h), 50% yield of gluconic acid with 100% conversion of cellulose was achieved by using 60% FeCl₃ for the first cellulose hydrolysis step followed by 40% FeCl₃ for the subsequent glucose oxidation step. The sequential utilization of 60% and 40% FeCl₃ solution enables the well-dissolution and hydrolysis of cellulose and meanwhile offers moderate oxidation ability to suppress the over-oxidation of gluconic acid as well as other side reactions.

In addition, the integration of glycosidic bond hydrolysis, glucose hydrogenation, and sorbitol dehydration offers another interesting approach to valorize cellulose. Such a three-step reaction strategy could



Scheme 2. The combination of glycosidic bond hydrolysis with different reactions to constitute a series of one-pot cascade routes for cellulose valorization.

Table 1

Representative catalyst systems for the hydrolysis-oxidation, hydrolysis-hydrogenation, and hydrolysis-hydrogenation-dehydration of cellulose into gluconic acid, sorbitol, and isosorbide, respectively.

Reaction	Catalyst	Product	Solvent	Temp. (°C)	Time (h)	Atm./pressure	Conv. (%)	Yield (%)	Ref.
Hydrolysis-oxidation	Au/Cs _{1.2} H _{1.8} PW ₁₂ O ₄₀	Gluconic acid	H ₂ O	145	11	O ₂ / 10 bar	72	60 ^a	90
	H ₃ PW ₁₂ O ₄₀ and Au/Cs ₃ PW ₁₂ O ₄₀	Gluconic acid	H ₂ O	145	11	O ₂ / 10 bar	97	85 ^a	90
	Au/HY	Gluconic acid	H ₂ O	110	3	O ₂ / 5 bar	41	23 ^b	91
	–	Gluconic acid	FeCl ₃	120	2	Air/ 1 bar	100	50	92
Hydrolysis-hydrogenation	Pt/Al ₂ O ₃	Sorbitol	H ₂ O	190	24	H ₂ / 50 bar	–	25	83
	Ru/C + H ₄ SiW ₁₂ O ₄₀	Sorbitol	H ₂ O	190	1	H ₂ / 95 bar	100	85 ^c	84
	Ni ₂ P/AC	Sorbitol	H ₂ O	225	1.5	H ₂ / 60 bar	100	48.4	85
Hydrolysis-hydrogenation-dehydration	Ni/oxidized CNF	Sorbitol	H ₂ O	190	24	H ₂ / 60 bar	92.6	64 ^a	86
	Ru/mNbPO	Isosorbide	H ₂ O	220	1	H ₂ / 60 bar	100	50	93
	Ru/C + HCl	Isosorbide	H ₂ O	215	6	H ₂ / 60 bar	100	49.5	94
	Ru/C + H ₄ SiW ₁₂ O ₄₀	Isosorbide	H ₂ O	210	1	H ₂ / 50 bar	–	63 ^d	95

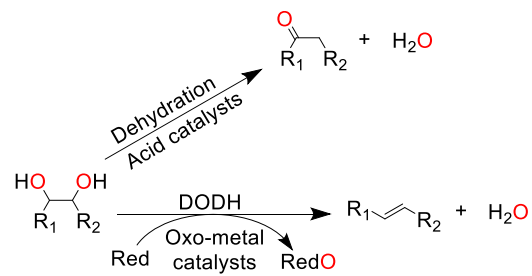
^a ball-milled cellulose as substrate; ^b proline-treated cellulose as substrate; ^c ball-milled cellulose as substrate, overall yield of sorbitol and mannitol; ^d delignified wheat straw as substrate.

ultimately give rise to isosorbide, a novel diol of great interest for polymer and drug synthesis, further extending the cellulose-to-chemical value chain towards fine chemicals of higher value (Scheme 1). The smooth running of these three reactions in sequence necessitates a bifunctional catalyst with tailored acidic and hydrogenation functions as well as appropriate reaction conditions. For instance, Li et al. designed a bifunctional heterogeneous catalyst by depositing Ru nanoparticles onto mesoporous niobium phosphate (Ru/mNbPO), achieving an isosorbide yield of ca. 50% in one pot at 220 °C and 60 bar H₂ in 1 h [93]. This high activity is attributed to the synergistic catalysis between the strong acidity of mNbPO and the hydrogenation ability of metallic Ru sites, responsible for glycosidic bond cleavage/sorbitol dehydration and glucose hydrogenation, respectively. Physically mixing hydrogenation catalysts with acids represent a straightforward method to realize the hydrolysis-hydrogenation-dehydration of cellulose into isosorbide. Zhao et al. examined the activity of noble metal catalysts (Ru, Pt, Pd) with mineral acids (HCl, H₂SO₄). The combination of Ru/C with HCl was found to exhibit the highest isosorbide yield of 49.5% at 215 °C and 60 bar H₂ in 6 h [94]. By replacing HCl with H₄SiW₁₂O₄₀, the yield of isosorbide could be improved to 63% using crude cellulose obtained from the delignification of wheat straw [95]. A considerable amount of H₄SiW₁₂O₄₀ (547 mmol/L) is required to provide sufficient H⁺ for the dehydration of reaction intermediates including sorbitol, 1,4-sorbitan, and 3,6-sorbitan.

2.2. DODH of adjacent hydroxyl groups

2.2.1. General chemistry

DODH reaction, also termed as didehydroxylation, refers to the simultaneous elimination of two adjacent hydroxyl groups (in *cis* position) to produce alkenes in the presence of oxo-metal catalysts and reductants. DODH is a selective reaction strategy dedicated to hydroxyl group removal without triggering C–C bond cleavage. The two hydroxyl groups are removed in the form of one water molecule and one oxygen atom (Scheme 3). The reductant is concurrently oxidized by the abstracted oxygen atom via an oxygen atom transfer (OAT) process. Mechanistically, DODH reaction can be perceived as the integration of deoxygenation and dehydration reactions, enabling the cleavage of two vicinal C–O bonds in one reaction. This unique feature renders DODH reaction highly useful in converting polyhydroxy compounds like sugars and sugar alcohols into olefin products. This is in sharp contrast with the well-known acid-catalyzed dehydration approach that normally eliminates one hydroxyl group and affords mixed products containing enols, ketos, and condensation products (Scheme 3).



Scheme 3. DODH of diols to alkenes.

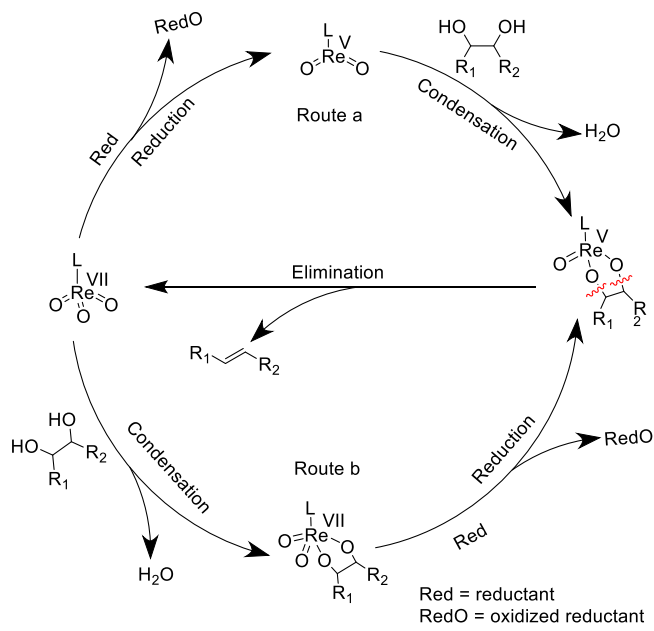
DODH of biomass derivatives can proceed in a non-catalytic or a catalytic manner. The non-catalytic DODH reaction usually occurs at temperatures above 200 °C in the presence of a stoichiometric reaction mediator mainly including formic acid or orthoformate [96,97]. The catalytic DODH can proceed at lower temperatures ranging from 100 to 200 °C by using a transition metal catalyst (mostly Re-based catalysts) bearing redox properties along with a reductant [98,99]. A number of electron-donating chemicals have been explored as reductants such as secondary alcohols, triphenylphosphine (PPh₃), sulfite, H₂, and zero-valence metals (e.g., Zn, Fe, Mn) [100,101]. Transition metal catalysts can provide the oxophilic binding sites to activate and abstract hydroxyl groups from substrates, while the reductant serves as an oxygen acceptor capable of reducing the oxidized metal catalysts to restore their redox activity. The reported DODH catalysts are dominated by diverse oxo-rhenium compounds, e.g., CH₃ReO₃ (MTO), cyclopentadienyl-based trioxorhenium (Cp*ReO₃), perrhenic acid (HReO₄), dirhenium decacarbonyl (Re₂(CO)₁₀), etc [98]. These oxo-rhenium compounds can be directly utilized as homogeneous catalysts. Alternatively, the immobilization or dispersion of these oxo-rhenium compounds onto solid supports (e.g., carbon, ZrO₂, TiO₂, SiO₂, CeO₂, zeolites, polystyrene) has been proved to be a feasible approach to synthesize heterogeneous Re catalysts giving moderate to high activities [102,103]. In addition to oxo-rhenium catalysts, a few oxo-molybdenum, oxo-vandium compounds, and ruthenium complexes were reported to act as DODH catalysts, but most of them show lower alkene yields [103–105]. The superior activity/selectivity of oxo-rhenium catalysts is attributed to their rich oxidation states (+1 to +7), excellent oxophilic nature of Re to abstract oxygen atoms from substrates, and the medium bond strength between Re and hydroxyl groups to enable the facile cleavage of Re=O bonds.

With respect to reaction mechanism, it is believed that oxo-metal-

catalyzed DODH reaction could proceed via two possible catalytic cycles: (a) reduction-condensation-elimination or (b) condensation-reduction-elimination [106–108]. As depicted in **Scheme 4**, taking ReO_3 as an example, the reduction-condensation-elimination route (a) starts with the reduction of one $\text{Re}=\text{O}$ bond in $\text{LRe(VII)}\text{O}_3$ complex by the reductant, giving rise to the catalytically active species of $\text{LRe(V)}\text{O}_2$. The subsequent condensation of $\text{LRe(V)}\text{O}_2$ complex with the diol substrate generates the key intermediate of Re(V) -diolate and one water molecule, followed by the eventual elimination of alkene product from Re(V) -diolate with the concurrent regeneration of $\text{LRe(VII)}\text{O}_3$ complex to complete the catalytic cycle. Alternatively, Wang et al. proposed a distinct catalytically active species of methyl oxodihydroxyrhenium(V) (MODH) resulting from the initial reduction of $\text{LRe(VII)}\text{O}_3$ according to density functional theory (DFT) calculations [109]. The formation of MODH involves the reduction of two $\text{Re}=\text{O}$ bonds to yield two OH groups attached to rhenium, in contrast to the abstraction of one oxygen atom in $\text{LRe(VII)}\text{O}_3$ complex to form $\text{LRe(V)}\text{O}_2$. For the other condensation-reduction-elimination route (b), the $\text{LRe(VII)}\text{O}_3$ complex first condenses with the diol substrate to generate the Re(VII) -diolate complex, which undergoes reduction to give a Re(V) -diolate intermediate by the reductant, finally leading to the elimination of alkene product and the re-oxidation to form $\text{LRe(VII)}\text{O}_3$ complex. Mechanistic studies indicate that the rate-determining step for both catalytic cycles concerns either the alkene elimination or the reduction of Re(VII) to Re(V) , depending on the choice of reductant and catalyst [102,109].

2.2.2. Applications in (hemi)cellulose valorization

In fact, DODH reaction has long been known as a useful tool for the synthesis of olefinic compounds in the field of synthetic chemistry. In 1996, Andrews and coworkers are the first to apply this reaction for catalytic biomass valorization aiming at the removal of hydroxyl groups from glycerol and tetritol [99]. Later, the enormous potential of DODH reaction was further disclosed by Toste et al., who demonstrated its broad applications in valorizing a series of biomass-derived molecules including sugar monomers, hexitols, inositol, and sugar acids [107, 110]. With continuous efforts devoted to DODH reaction in terms of catalyst design, reductant optimization, and substrate exploration, DODH reaction has evolved as a powerful protocol to selectively cleave the C–O bonds in vicinal diols derived from biomass. A broad spectrum of value-added chemicals containing double bonds can be obtained from



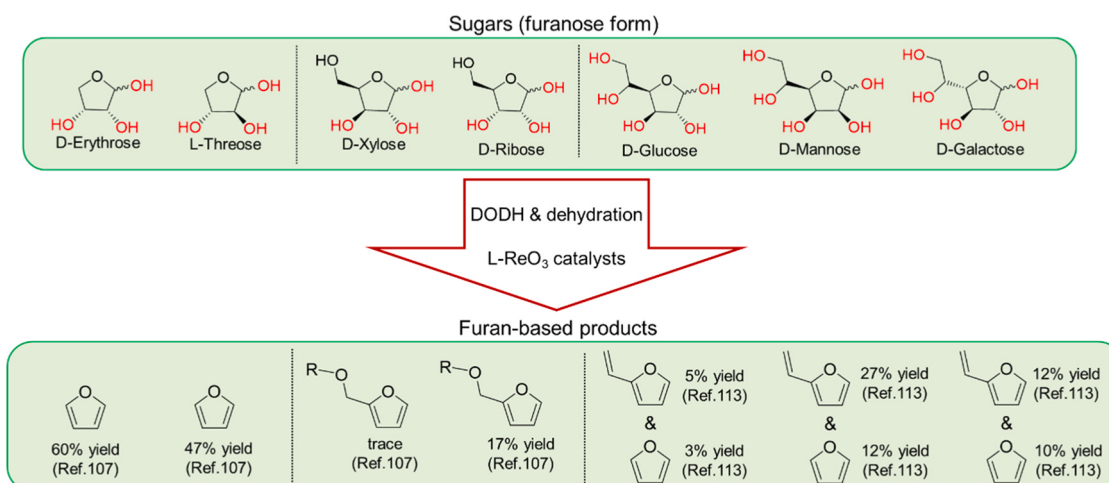
Scheme 4. Two general catalytic cycles proposed for oxo-rhenium-catalyzed DODH reaction. Adapted with permission from ref. [106].

the DODH of (hemi)cellulose including butadiene, pentadiene, hexatriene, benzene, muconic acid, dideoxy sugars, etc. [104,105]. These bio-based unsaturated compounds hold the potential to act as either “drop-in” molecules to in part replace existing fossil-derived unsaturated chemicals or emerging molecules featuring novel moieties with new usage. Importantly, the formed C=C bonds in these products are highly reactive towards further transformations such as hydrogenation, hydroformylation, and Diels-Alder (D-A) reaction. Combining these reactions with DODH could constitute new cascade valorization routes, further broadening the product scope accessible from DODH reaction. For instance, a tandem synthetic protocol of bio-based adipic acid has been demonstrated by combining mucic acid DODH and subsequent muconic acid hydrogenation in one pot [111,112]. In this section, we will concentrate on diverse applications of DODH reaction in breaking the C–O bonds in (hemi)cellulose derivatives, mainly involving the DODH of sugars, sugar alcohols, and sugar acids.

2.2.2.1. DODH reaction of sugars. DODH reaction of lignocellulose-derived sugars have received increasing attention in recent years, due to the straightforward and mature production of sugars by acid or enzymatic hydrolysis, as mentioned above. Research efforts have focused largely on the DODH of monosaccharides with 4–6 carbon atoms such as erythrose, ribose, xylose, mannose, glucose, and galactose. One challenge related to these sugar monomers is their instabilities, that is, being apt to undergo intramolecular dehydration and cyclization to form more stable furan or pyran derivatives as well as condensed products upon heating.

It was found that the DODH products of sugars are dominated by furan-based compounds (e.g., furan, 2-vinylfuran) in low to moderate yields (**Scheme 5**). The formation of furan moieties from sugars actually requires a DODH reaction and also a dehydration step to remove three OH groups on furan ring. For instance, Toste and coworkers demonstrated that D-erythrose could be converted to furan (60% yield) via a tandem DODH reaction followed by dehydration at 155 °C by utilizing MTO as the catalyst and 3-octanol as the reductant [107]. Notably, the DODH of L-threose, a diastereomer of D-erythrose, also provided 47% yield of furan, despite bearing a pair of *trans* hydroxyl groups. The authors proposed that the *trans* geometry can be shifted to *cis* geometry by the epimerization of C1 and C2 hydroxyl groups in D-erythrose, thus meeting the *cis*-diol requirement of DODH reaction. When applying DODH to convert pentoses (i.e., D-xylose, D-ribose) and hexoses (i.e., D-mannose, D-glucose, D-galactose), 2-(alkoxymethyl)furan (the ether form of furfuryl alcohol) and a mixture of 2-vinylfuran and furan were produced as primary products, respectively (**Scheme 5**) [107]. However, these furan products were produced in comparatively low yields (below 40%), probably due to the successive conversion of 2-(alkoxymethyl) furan and 2-vinylfuran to unknown products. Gebbink et al. reported the utilization of a trioxo-rhenium complex with a bulky Cp^{tt} ligand ($\text{Cp}^{\text{tt}}\text{ReO}_3$, $\text{Cp}^{\text{tt}} = 1,3\text{-di-tertbutylcyclopentadienyl}$) as the catalyst for the DODH of D-glucose, D-mannose, and D-galactose in the presence of 3-pentanol or 3-octanol as the reductant [113]. All these sugars gave low yields (below 39%) towards 2-vinylfuran and furan. The highest yield of 2-vinylfuran/furan up to 39% was observed for D-mannose, whereas only 8% yield of 2-vinylfuran/furan was obtained for the DODH of D-glucose. Likewise, D-ribose afforded much higher yield of 2-(alkoxymethyl)furan than D-xylose (17% vs. trace) in the presence of MTO and 3-octanol [107]. These results indicate that catalytic performance is dependent on the stereo conformations of hydroxyl groups in sugar molecules. Further studies are required to clarify the effect imposed by the different stereochemistries of sugars.

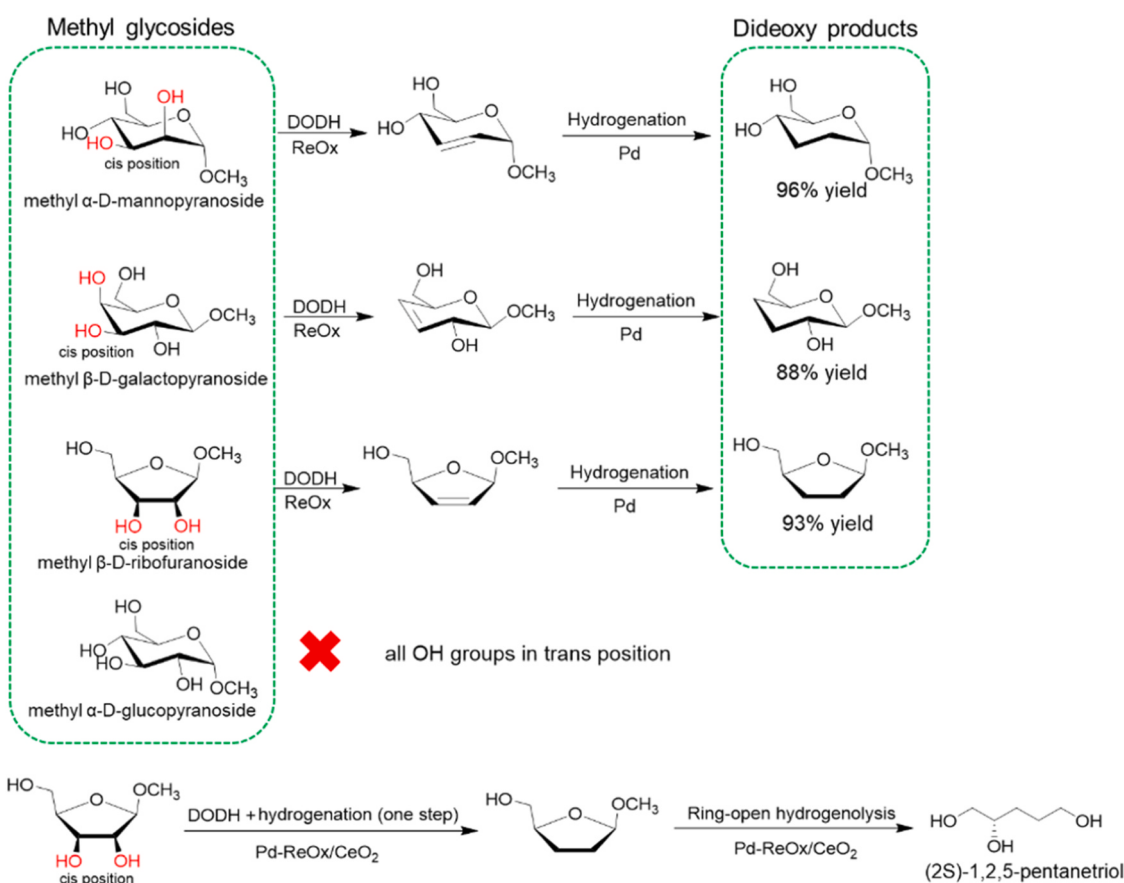
The instability of sugar monomers arising from the reactive aldehyde moiety is considered as the main cause of low product yields for the DODH of sugars. In order to improve the yield of targeted products, researchers turn to study the DODH of methyl glycosides, a cyclic acetal form of monosaccharide with improved stability. In contrast to the



Scheme 5. A summary of the DODH of various sugars into furan-based compounds.

dominated formation of furans from monosaccharides, unsaturated dideoxy glycosides are generated as major products for the DODH of methyl glycosides. The integration of glycoside DODH with hydrogenation in one step (i.e., DODH-hydrogenation) over a bifunctional catalyst led to saturated dideoxy glycosides, precursors to dideoxy sugars. For example, Tomishige et al. reported the DODH-hydrogenation of various methyl glycosides (e.g., methyl α -D-mannopyranoside, methyl β -D-ribofuranoside, methyl β -D-galactopyranoside, etc.) into the corresponding dideoxy glycosides in excellent yields (above 82%) by using a bifunctional catalyst $\text{ReO}_x\text{-Pd/CeO}_2$ and H_2 as a reductant at 140 °C [114]. Highly-dispersed ReO_x species in monomeric form on

CeO_2 was proposed as the active sites for the DODH of methyl glycosides to unsaturated methyl glycosides, which subsequently undergoes hydrogenation over metallic Pd species to yield dideoxy glycosides (Scheme 6). Analogous to MTO, the redox cycle between high-valence (i.e., VII or VI) and reduced (i.e., V or IV) ReO_x species was believed to play a key role in promoting DODH catalysis cycle. When substituting Pd with a weak-hydrogenation-activity metal such as Au, the obtained catalyst $\text{ReO}_x\text{-Au/CeO}_2$ could shift the major product from saturated dideoxy glycosides to unsaturated ones [115]. It should be noted that no dideoxy products were observed when applying methyl α -D-glucopyranoside as substrate, which possesses only *trans* vicinal hydroxyl groups



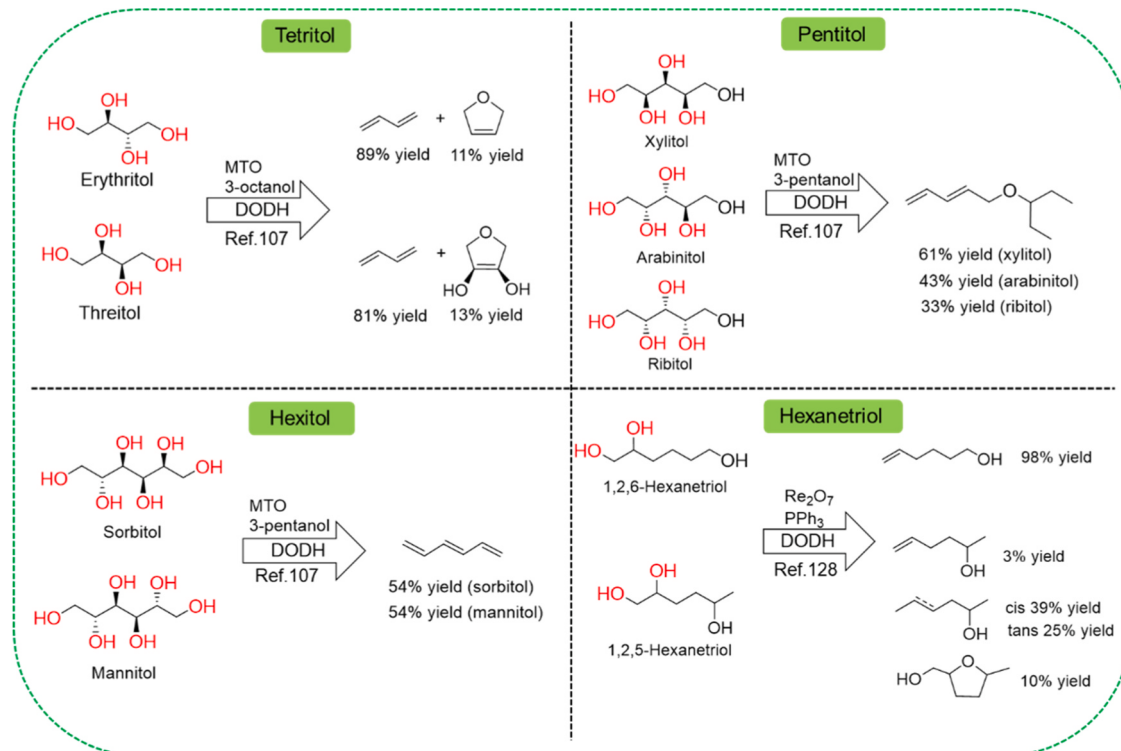
Scheme 6. A summary of the DODH-hydrogenation of various methyl glycosides into dideoxy sugars.

on its pyran ring. Moreover, owing to the stable cyclic acetal structure of methyl glycosides, the potential transformation from *trans* conformation into its corresponding *cis* epimer via epimerization, as reported for L-threose [107], is probably blocked in the case of methyl glycosides. The authors therefore concluded that the presence of *cis* adjacent hydroxyl groups is essential for DODH-hydrogenation of methyl glycosides, in line with the aforementioned requirement of DODH reaction. A prominent feature for the DODH of methyl glycosides presents the maintained stereostructures of chiral atoms and moieties after the reaction. Therefore, the produced unsaturated methyl glycosides and saturated dideoxy glycosides can serve as chiral building blocks. For example, 2,3-dideoxy ribofuranoside generated from methyl β -D-ribofuranoside can be converted into (2 S)-1,2,5-pentanetriol with high enantioselectivity up to 96% ee via a cascade reaction of hydration and hydrogenation over the same catalyst $\text{ReO}_x\text{-Pd/CeO}_2$ (Scheme 6) [114]. Following this strategy, the synthesis other complex chiral polyols (e.g., (2 R,5 S)-1,2,5,6-hexanetetrol, (4 R,5 S)-1,4,5-hexanetriol, etc.) in high ee values were also demonstrated by selecting corresponding methyl glycosides as substrates [116]. Overall, the DODH of methyl glycosides not only realizes the selective cleavage of C–O bond but also opens a new pathway to synthesize valuable sugar-derived chiral molecules of great interest for pharmaceuticals, food additives, and biologically-active compounds.

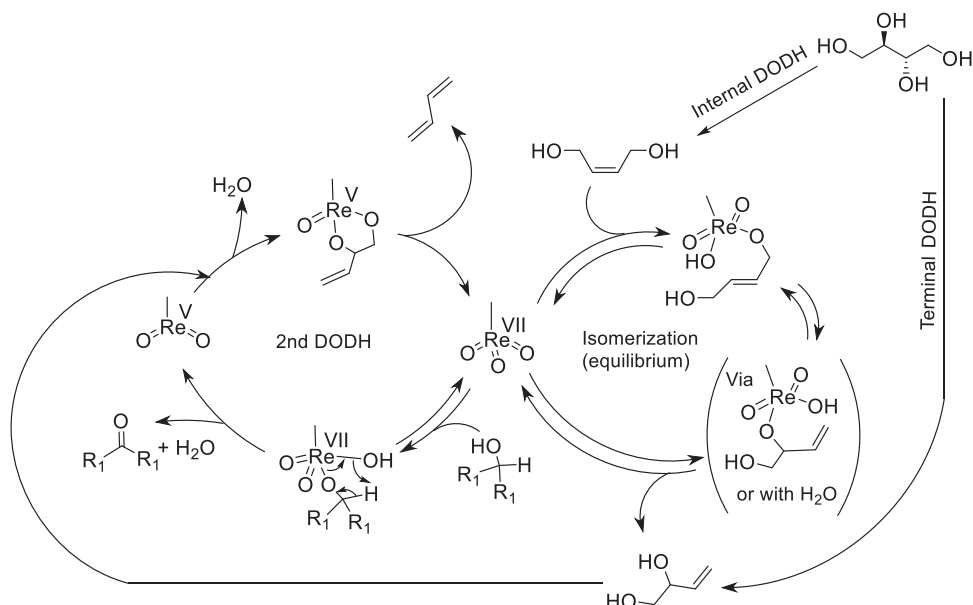
2.2.2.2. DODH reaction of sugar alcohols. Sugar alcohols, featured by fully hydroxylated carbon skeletons, appear as a promising substrate category for DODH reaction. The most widely studied sugar alcohols are tetritols, pentitols, and hexitols, represented by erythritol, xylitol, and sorbitol, respectively. These sugar alcohols are easily obtained from the reduction of corresponding sugar monomers. The absence of aldehyde moiety endows these sugar alcohols higher stability and more hydroxyl groups available for DODH reaction. For sugar alcohols containing an even number of vicinal OH groups like erythritol and sorbitol, DODH reaction can theoretically remove all hydroxyl groups and affords high-value conjugated olefin products including butadiene and hexatriene (Scheme 7). Among various sugar alcohols, erythritol is often selected as

a model substrate in many studies of DODH reaction. For example, Andrews et al. first described the DODH reaction of erythritol to 1,3-butadiene, an important monomer for the manufacture of synthetic rubber, in a high yield of 80% at 135 °C in 28 h, in the presence of Cp^*ReO_3 as catalyst and PPh_3 as reductant [99]. Following this study, various combinations of catalyst and reductant have been developed for the DODH of erythritol and threitol into 1,3-butadiene in medium to high yields, such as MTO + 3-octanol [107], MTO + indoline [117], $\text{Cp}^{\text{tr}}\text{ReO}_3$ + 3-octanol [113], $\text{Cp}^{\text{tt}}\text{ReO}_3$ + 3-octanol [118], Bu_4NReO_4 + Na_2SO_3 [119], $\text{ReO}_x\text{-Au/CeO}_2$ + H_2 [120], $\text{ReO}_x\text{-Ag/CeO}_2$ + H_2 [121], ReO_x nanoparticles + 3-octanol [122]. It was found that the addition of a Brønsted acid catalyst (e.g., TsOH , H_2SO_4) beneficial to the extrusion of alkene products would lead to the formation of 2,5-dihydrofuran as the main product (62% yield) instead of 1,3-butadiene from erythritol over $\text{Re}_2\text{CO}_{10}$ + 3-octanol [123]. The production of 2,5-dihydrofuran is speculated to occur via a cascade pathway including the first cyclodehydration of erythritol to 1,4-anhydroerythritol over acid catalyst followed by the DODH of 1,4-anhydroerythritol to 2,5-dihydrofuran.

Interestingly, although erythritol (*trans* internal diols) and threitol (*cis* internal diols) feature different diol conformations, both of them gave similar 1,3-butadiene yields (81% vs. 89%), implying a special DODH reaction pathway for C4 sugar alcohols. [107,110] To understand this point, control experiments using different diols in *trans* or *cis* conformations have been conducted. As shown in Scheme 8, a plausible reaction pathway of MTO-catalyzed erythritol and threitol DODH to 1,3-butadiene was proposed based on control experiments. The DODH reaction can start by removing either internal or terminal diols in erythritol, affording 2-butene-1,4-diol or 3-butene-1,2-diol as intermediates, respectively. The remaining hydroxyl groups in 3-butene-1,2-diol are readily eliminated by a second DODH reaction accompanied by the formation of 1,3-butadiene. Alternatively, the DODH reaction of 2-butene-1,4-diol can take place via MTO-catalyzed OH group shift (i.e., isomerization) to form a vicinal diol (i.e., 3-butene-1,2-diol) followed by DODH to ultimately yield 1,3-butadiene as well. As such, olefinic compounds containing non-vicinal hydroxyl groups could act as reactive



Scheme 7. A summary of the DODH of sugar alcohols containing an even or odd number of OH groups.

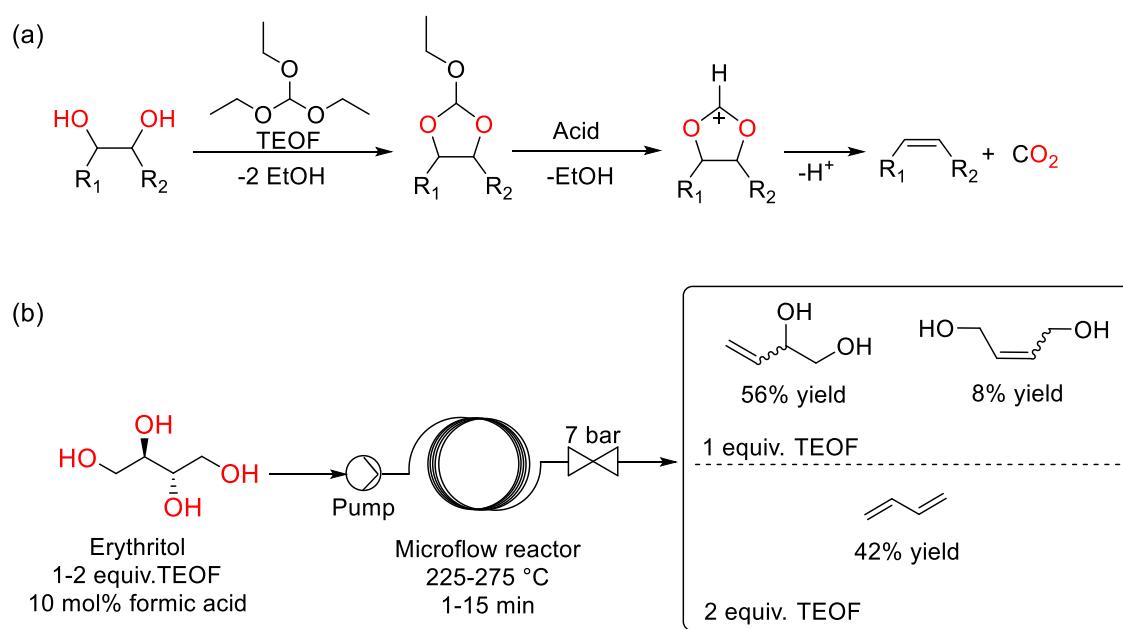


Scheme 8. Proposed catalysis cycle for the MTO-catalyzed DODH of erythritol to 1,3-butadiene. Reproduced with permission from ref. [110].

substrates towards DODH reaction which normally needs vicinal diols as substrates. Besides, control experiments indicate that the transformation of *trans* diols into its *cis* counterparts likely occurred during the isomerization of OH groups [110]. Evidently, the key step within the proposed catalytic cycle is the generation of allylic alcohol-like intermediates, which can undergo *in situ* shift of OH groups towards vicinal and *cis* configuration. This key step along with second DODH reaction accounts for the selective conversion of different intermediates into 1,3-butadiene, regardless of the first DODH reaction occurring at internal or terminal OH groups.

A metal-free DODH protocol to transform erythritol into 1,3-butadiene and 3-butene-1,2-diol has been proposed by Monbaliu and co-workers [124]. In contrast to the commonly-used oxo-metal catalysts along with reductants, the metal-free DODH protocol relies on the utilization of triethyl orthoformate (TEOF) as a deoxygenation reagent in

combination with a catalytic amount of formic acid in a continuous-flow reactor. This reaction is believed to proceed following a Eastwood olefination pathway (Scheme 9a), which comprises the reaction between diols and TEOF catalyzed by formic acid to yield an intermediate of dioxolane-based orthoester [97,125]. This intermediate can be transformed into a reactive dioxolane-based carbocation intermediate, which readily undergoes decomposition (C–O bond cleavage) by extruding one CO_2 molecule and thus generating an alkene product. These mechanistic insights indicate that the removal of one vicinal diol (i.e., one DODH reaction) necessitates the participation of one TEOF molecule. Thus, by varying the molar ratio of erythritol/TEOF, the major product produced from erythritol DODH can be switched between 1,3-butadiene (by removing four OH groups) and 3-butene-1,2-diol (by removing two OH groups). The latter can be formed in a high yield of 56% at 1 equiv. of TEOF and 275 °C within 6 min of residence time (Scheme 9b). Notably,



Scheme 9. (a) Reaction mechanism proposed for TEOF-mediated DODH of vicinal diols. (b) The DODH of erythritol in a continuous microflow reactor with switchable product selectivities. Adapted with permission from ref. [124].

owing to the employed microfluidic continuous-flow reaction system capable of allowing feed solutions fast exposure to high temperatures, the reaction time to complete erythritol DODH can be shortened to 1–15 min with maintained high yields. This is significantly shorter than traditional batch-mode DODH reaction of erythritol, usually taking a couple of hours to reach completion.

With respect to the DODH of hexitols such as D-sorbitol and D-mannitol, the removal of six hydroxyl groups necessitates three DODH reactions occurring successively in one pot, finally generating hexatriene as the main product (Scheme 7). Compared to the DODH of erythritol, a high reaction temperature of 200 °C is required to eliminate six hydroxyl groups in sorbitol (triple DODH). A moderate yield of 54% towards (E)-1,3,5-hexatriene was reported by using MTO as catalyst and 3-pentanol as reductant [107]. The DODH of D-mannitol, a stereoisomer of D-sorbitol, gave a same yield of 54% towards (E)-1,3,5-hexatriene [107]. Considering the presence of *trans* OH groups in both D-sorbitol and D-mannitol, the smooth elimination of all OH groups to yield (E)-1,3,5-hexatriene presumably involves the shift of OH groups to form *cis* conformation, as proposed for erythritol in Scheme 8.

When applying DODH reaction to upgrade sugar alcohols containing an odd number of vicinal OH groups like pentitols (e.g., xylitol, arabinitol, ribitol) and hexanetriol, unsaturated alcohols are usually produced as main product owing to the presence of one spare hydroxyl group which cannot be removed by DODH (Scheme 7). This free OH group is liable to be etherified or esterified during the reaction. For instance, xylitol, a readily available chemical from hemicellulose, can be transformed into (E)-5-penta-1,3-diene ether (the ether form of 2,4-pentadiene-1-ol) in 61% yield at 170 °C in the presence of MTO and 3-pentanol by two DODH reactions [107]. Under the same conditions, D-arabinitol and ribitol, two isomers of xylitol, were also converted to (E)-5-penta-1,3-diene ether but in lower yields of 43% and 33%, respectively. The utilization of indoline as the reductant to replace alcohols enabled the clean formation of (E)-2,4-pentadiene-1-ol as the major product (56%) instead of its ether from [117]. This is due to the blocked etherification between (E)-2,4-pentadiene-1-ol with alcoholic solvents. The combined utilization of CP^{tr}ReO₃ and 3-octanol has been proven to catalyze the DODH of pentitols (e.g., xylitol, arabinitol, ribitol) to (E)-5-penta-1,3-diene ethers in moderate yields (42–48%) at 135 °C [113]. In addition, Sun et al. described a meal-free DODH of xylitol into (E)-2,4-pentadiene-1-ol and (E)-2,4-pentadien-1-ol formate in a total yield of 70.5% by using formic acid as the deoxygenation reagent and tetraglyme as the solvent at 235 °C [126]. An excessive amount of formic acid (8–12 eq.) is preferred considering the thermal decomposition of formic acid at 235 °C. This formic acid-mediated DODH reaction is proposed to proceed via a dioxolane orthoester intermediate (Scheme 9a) [96,127], analogous to aforementioned TEOF-mediated DODH reaction of erythritol. The elimination of two vicinal OH groups (one DODH reaction) requires the participation of one formic acid molecule, which offers two hydrogen species to abstract two OH groups with concomitant formation of two H₂O molecules and one CO₂ molecule.

HMF-derived 1,2,5- and 1,2,6-hexanetriol appear as another group of polyols bearing odd numbers of OH groups for DODH reaction. Among these hexanetriols, only two vicinal OH groups can be eliminated by DODH giving rise to diverse hexenols as products. Oxo-rhenium catalysts including MTO and Re₂O₇ have been reported to catalyze the DODH of 1,2,6-hexanetriol exclusively to 5-hexen-1-ol in excellent yields ($\geq 96\%$) in the presence of PPh₃ (1.1 eq.) as reductant at 165 °C within 1 h (Scheme 7) [128]. By contrast, a complex product mixture containing 5-hexen-2-ol (3% yield), *cis*-2-hexen-5-ol (39% yield), *trans*-2-hexen-5-ol (25% yield), and 5-methyltetrahydrofurfuryl alcohol (10% yield) was produced from the DODH of 1,2,5-hexanetriol over Re₂O₇ under similar reaction conditions (Scheme 7). The formation of 2-hexen-5-ol is considered as the result of Re-catalyzed double-bond isomerization of 5-hexen-2-ol, indicating the higher reactivity of 1,2,5-hexanetriol towards double-bond isomerization than 1,2,

6-hexanetriol. Interestingly, in the absence of PPh₃, Re₂O₇-catalyzed conversion of 1,2,5-hexanetriol followed a cyclodehydration procedure rather than DODH, leading to 5-methyltetrahydrofurfuryl alcohol as the major product (90% yield). The Lewis acidity of Re₂O₇ is proposed to account for the acid-catalyzed cyclodehydration of 1,2,5-hexanetriol.

Gebbink and coworkers studied the catalytic performances of CP^{tr}ReO₃ for the DODH of various C3–C6 linear polyols under identical reaction conditions (135 °C, 15 h, N₂, 3-octanol as reductant) [113]. The highest product yield (99% towards allyl alcohol) was obtained for glycerol, the simplest polyol among the examined substrates, whereas sorbitol featuring the longest carbon chain gave the lowest product yield (17% towards 1,3,5-hexatriene). The DODH of xylitol gave (E)-5-penta-1,3-diene ether in a moderate yield of 46%. It could be seen that there exists an interesting relationship between olefin product yields and the carbon chain lengths of polyol substrates, that is, the gradual decrease of alkene yields with the increase of carbon chain lengths from C3 to C6 (Fig. 4). This structure-activity correlation presumably arises from the increased steric hindrance associated with the bulky polyols, hampering the complexation of polyols with oxo-rhenium active centers.

2.2.2.3. DODH reaction of sugar acids. Sugar acids represent an attractive class of substrates for DODH reaction due to the presence of both vicinal OH groups and carboxyl groups. In particular, sugar-derived dicarboxylic acids with two terminal carboxyl groups are considered as promising feedstocks to produce bio-based diacid monomers for polyamides (nylons) and polyesters. The most widely investigated sugar diacids are mucic acid and glucaric acid, which are readily accessible from (hemi)cellulose-derived galactose and glucose, respectively, by selectively oxidizing their end groups. Considering the presence of four internal OH groups and two terminal carboxyl groups in both acids, two DODH reactions are needed to achieve complete dehydroxylation, affording muconic acid as the main product (Scheme 10). The subsequent catalytic reduction of muconic acid would produce adipic acid, a key monomer to synthesize nylon 66. Therefore, the DODH of mucic acid and glucaric acid provides the opportunity to develop a bio-based synthesis process for adipic acid. In terms of reactivity towards DODH, mucic acid featuring two pairs of *cis*-OH groups is superior to glucaric acid which has one pair of *trans*-OH groups (unfavorable for DODH) and one pair of *cis*-OH groups.

Mucic acid.

The DODH of mucic acid to muconic acid was first explored by Shiramizu and Toste, who employed HReO₄ as catalyst and 1-butanol as reductant [110]. At 170 °C under N₂ atmosphere, *trans,trans*-dibutyl muconate, a diester of muconic acid, was obtained as the major product in a yield of 71% (Scheme 11). During the reaction, HReO₄ plays dual roles: a redox catalyst for DODH and a Brønsted acid catalyst for esterification. When utilizing the mucic acid dibutyl ester as the substrate for DODH, the yield of dibutyl muconate was further increased to 94% under same reaction conditions. The improved yield is ascribed to the enhanced solubility of esterified mucic acid in alcoholic solvents, leading to better contact/interaction between catalyst (HReO₄) and mucic acid ester. As a proof of concept, the authors demonstrated the synthesis of adipate directly from mucic acid by a one-pot two step reaction strategy (i.e., DODH-hydrogenation) involving the DODH of mucic acid to dibutyl muconate at 170 °C followed by room-temperature hydrogenation catalyzed by Pd/C to afford 62% yield of dibutyl adipate under 6.9 bar H₂ (Scheme 11). Later, the same group developed a one-pot procedure to realize the catalytic transformation of mucic acid to adipate by merging DODH and hydrogenation in one reactor under identical reaction conditions [129]. The integration of these two reactions relies on the utilization of H₂ as the reductant for KReO₄-catalyzed mucic acid DODH reaction and also for Pd/C-catalyzed hydrogenation of muconate (Scheme 11). This one-pot strategy could enable the direct production of dimethyl adipate directly from mucic acid in a high yield

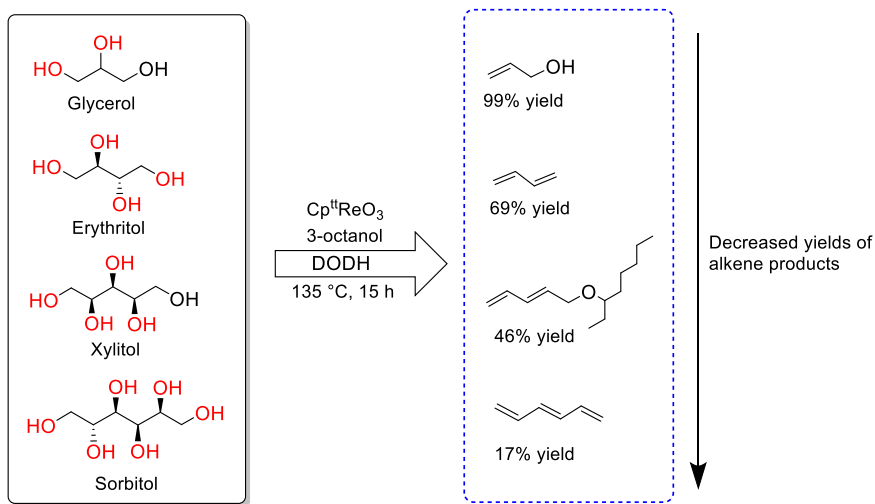
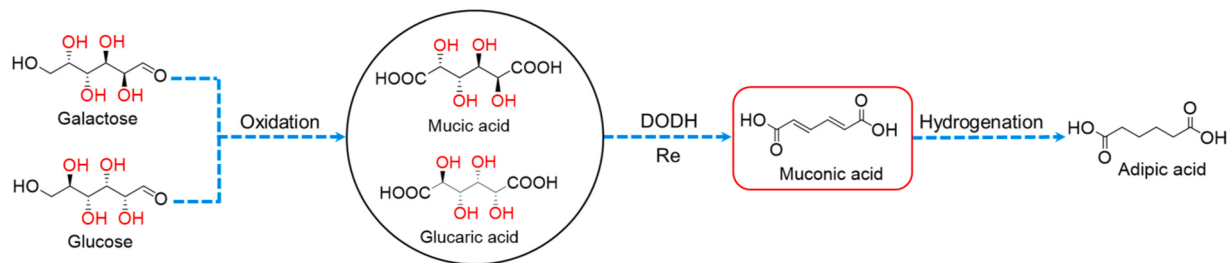


Fig. 4. Cp^*ReO_3 -catalyzed DODH of polyol substrates from glycerol to sorbitol under identical reaction conditions.



Scheme 10. Selective removal of internal OH groups in (hemi)cellulose-derived mucic and glucaric acids by Re-catalyzed DODH towards muconic acid and adipic acid.

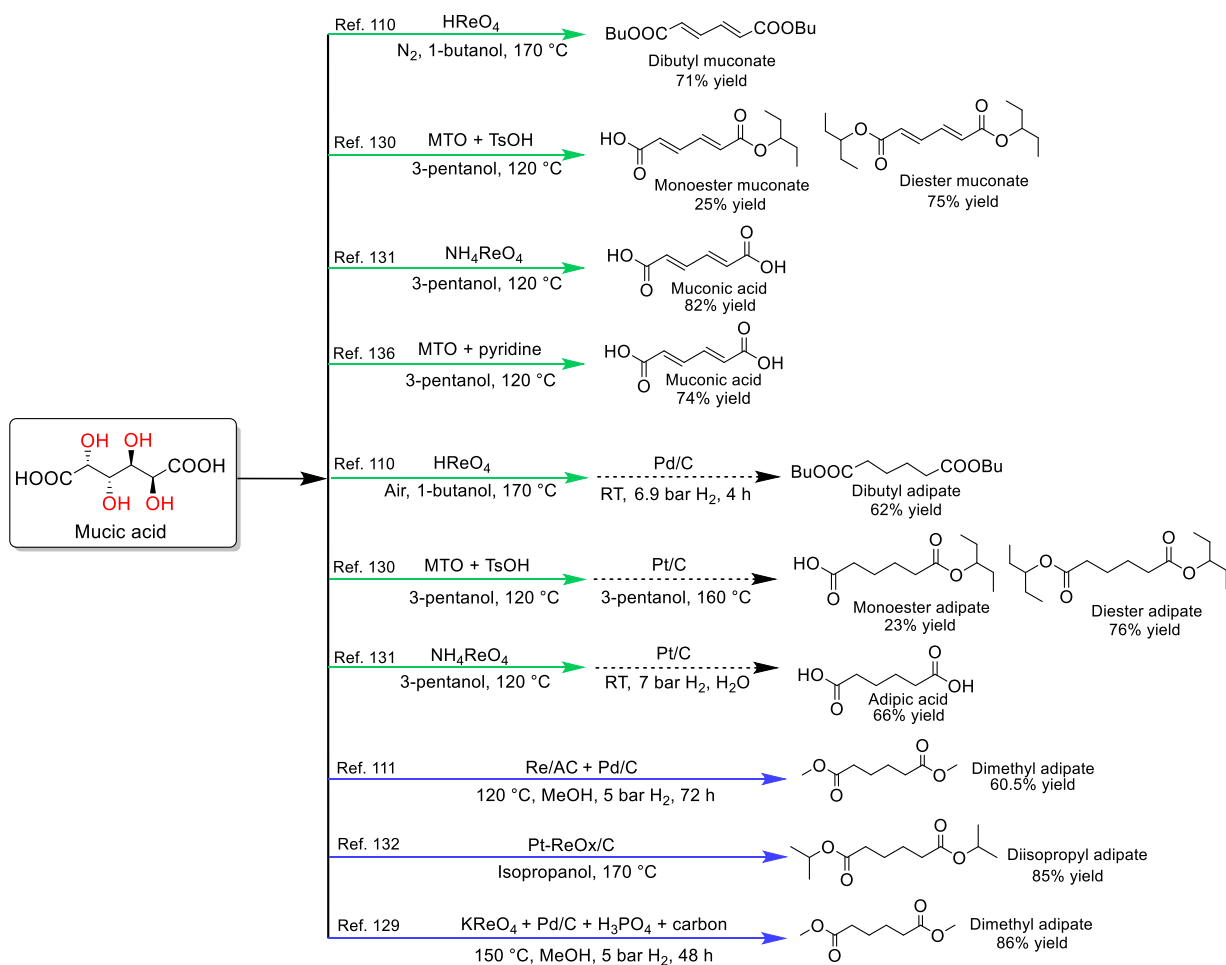
of 86% in the presence of H_3PO_4 as the co-catalyst under 5 bar H_2 at 150 °C in 48 h.

Zhang and coworkers further optimized the DODH of mucic acid by utilizing MTO as the DODH catalyst, *para*-toluene sulfonic acid (TsOH) as the co-catalyst, and 3-pentanol as the reductant (Scheme 11) [130]. An excellent yield of 99% towards muconic acid esters (a mixture of monoester and diester) was obtained at a mild temperature of 120 °C within 24 h. The addition of TsOH not only accelerated the esterification of mucic acid thus improving its solubility in 3-pentanol, but also promoted the extrusion of alkene during MTO-catalyzed DODH reaction. Therefore, the excellent performance is a result of the synergic effect of MTO, TsOH, and 3-pentanol. By using 3-pentanol as the hydrogen donor, the obtained crude muconic acid esters could be quantitatively reduced into adipate without forming side products via Pt/C-catalyzed transfer hydrogenation at 160 °C. Based on these results, a one-pot two step synthetic protocol for adipic acid ester was designed by combining MTO-catalyzed DODH of mucic acid (120 °C, 12 h) with Pt/C-catalyzed transfer hydrogenation (160 °C, 12 h), which ultimately afforded adipate in a total yield of up to 99% (Scheme 11).

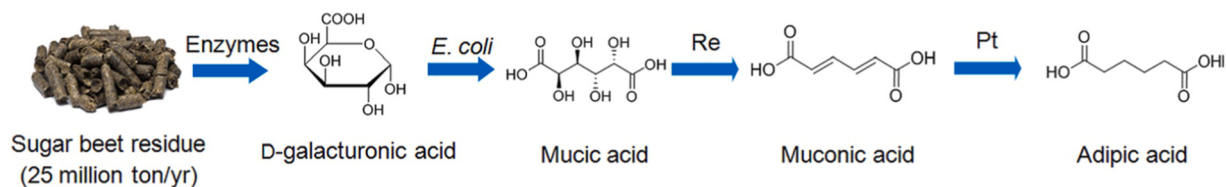
Despite these promising yields reported for adipate, it is more attractive to produce muconic acid and adipic acid in their free acid forms rather than ester forms, since bio-based adipic acid can be directly used to synthesize nylon without pre-hydrolysis. Zhang and coworkers found that the concomitant esterification of carboxyl groups can be inhibited by blocking the Brønsted or Lewis acidity of oxo-rhenium catalysts, therefore leading to the generation of DODH products primarily in free acid form instead of esterified form (Scheme 11) [131]. For instance, a high yield of 72% towards free muconic acid was obtained over NH_4ReO_4 (with negligible acidity) at 120 °C in 8 h in 3-pentanol as the solvent, whereas the exclusive formation of muconic acid ester was observed for HReO_4 . A further Pt/C-catalyzed hydrogenation

of the obtained muconic acid in water at room temperature under 7 bar H_2 afforded adipic acid as the desired product in a high yield of 92%. Based on these results, the authors demonstrated a cascade process to synthesize free adipic acid (8.4% yield) from sugar beet residue by integrating bio-catalysis and chemo-catalysis (Scheme 12). Sugar beet residue first undergoes enzymatic hydrolysis to yield D-galacturonic acid, which is further oxidized to mucic acid by the engineered *E. coli* strain followed by the aforementioned DODH-hydrogenation over NH_4ReO_4 and Pt/C to finally yield adipic acid.

In addition to homogeneous Re catalysts, developing solid Re catalysts to enable heterogeneous DODH of mucic acid has received great interest recently. Likozar and coworkers claimed that the DODH of mucic acid followed by hydrogenation to give adipic acid ester could proceed smoothly over pre-reduced Re/activated carbon catalysts (Re/AC) [111]. In the presence of methanol as solvent, mucic acid was fully converted to various dehydroxylated products, including adipic acid ester (30.9% yield), muconic acid ester (0.5% yield), and partially-reduced muconic acid ester containing one double bond (66.5%), in an overall yield of up to 98% under N_2 at 175 °C within 72 h. The formation of saturated adipic acid ester in methanol without H_2 indicates the moderate hydrogenation ability of reduced Re species to hydrogenate double bonds using methanol as the hydrogen donor. The yield of adipic acid ester can be further improved to 60.5% by adding Pd/C to promote the hydrogenation of muconic acid ester at 120 °C under 5 bar H_2 (Scheme 11). Catalyst characterization results disclosed that the pre-reduction (400 °C) of oxidized Re species to generate metallic Re and Re(III) species is the key to achieve high DODH and hydrogenation activities. This is opposite to the general understanding that high-valence Re(IV, V, VI, VII) oxides serve as the active site for DODH. In terms of recyclability, reduced Re/AC catalysts showed unchanged activities during the first two runs, whereas the activity of



Scheme 11. A summary of mucic acid DODH into muconate/muconic acid followed by hydrogenation to from adipate/adipic acid over different Re catalysts.

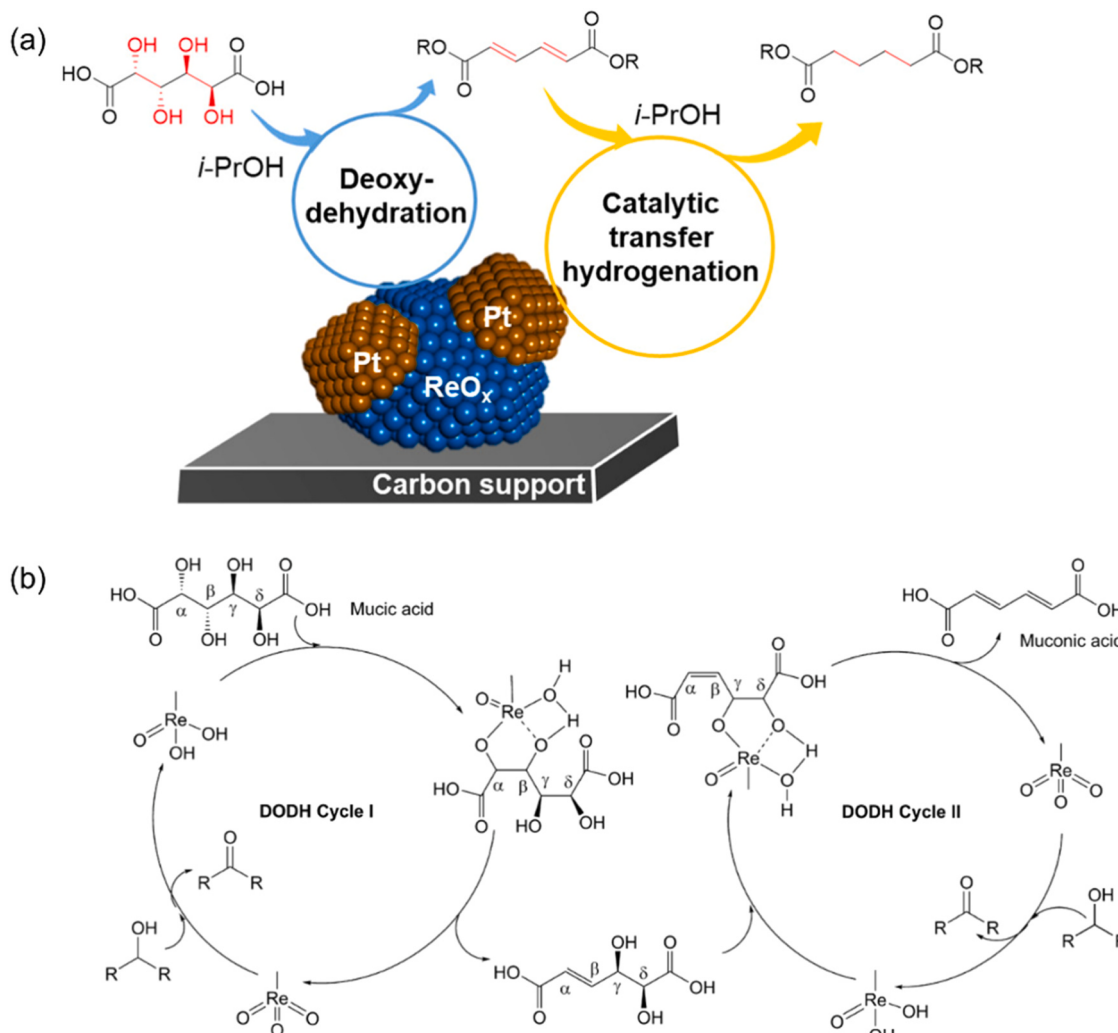


Scheme 12. A sustainable route for the synthesis of adipic acid from sugar beet residue by coupling biological and chemical catalysis. Reproduced with permission from ref. [131].

oxidized Re catalysts dropped by 60% in the second run. These results indicated that reduced Re(0, III) species presented improved stability in alcohol solvents with less dissolution than high-valence Re(IV, V, VI, VII) species. Abu-Omar et al. designed a heterogeneous bifunctional Pt-ReO_x/C catalyst capable of integrating mucic acid DODH and subsequent transfer hydrogenation of muconic acid ester in one pot (Scheme 13a) [132]. By using isopropanol as a reductant for DODH and also a hydrogen donor for transfer hydrogenation, the Pt-ReO_x/C catalyst gave an 85% yield of diisopropyl adipate at 170 °C under N₂ atmosphere in 24 h (Scheme 11). Catalyst characterization results revealed the co-existence of high-valence Re species (VII and VI) and metallic Pt species on AC, which were identified as the catalytically active sites for mucic acid DODH and muconic acid ester hydrogenation, respectively.

Mechanistic insights into Re-catalyzed DODH of mucic acid into muconic acid was gained primarily from computational studies [130]. The reaction is generally believed to proceed on high-valence Re(VI/VII)

species, analogous to aforementioned catalysis cycle in Scheme 4. Taking MTO-catalyzed DODH as an example, four internal OH groups of mucic acid are stepwise eliminated via two DODH reactions (Scheme 13b). Firstly, MTO is reduced by alcohol to form MODH as the catalytically active species, which condenses with the α - and β -OH groups of mucic acid to form the activated mucic acid bound to Re atom (i.e., Re-diolate). This Re-diolate species subsequently undergoes two C–O bond cleavage reactions to extrude an olefin intermediate (i.e., alkene elimination step) with concurrent regeneration of MTO complex. Similar to the first DODH cycle, the second DODH reaction involves the activation and elimination of the remaining γ - and δ -OH groups by MODH, giving muconic acid as the final product. It was found that the energy barrier of alkene elimination step in DODH cycle I is higher than that in DODH cycle II (21.1 vs. 17.6 kcal/mol), indicating that the second DODH reaction proceeds faster than the first DODH reaction. The reduction of MTO(VII) to MODH(V) was calculated as the rate-determining step with the highest energy barrier of 39.6 kcal/mol

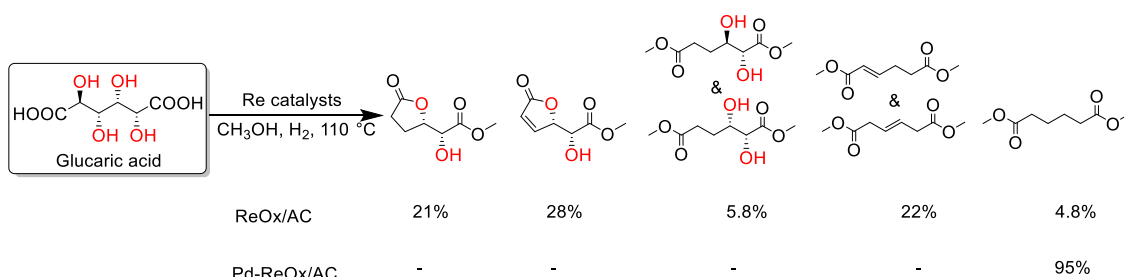


Scheme 13. (a) DODH of mucic acid followed by hydrogenation into adipate in one pot over a heterogeneous Pt-ReO_x/C catalyst; (b) Proposed catalysis cycle for double DODH of mucic acid into muconic acid in the presence of MTO and alcohol as reductant. Reproduced with permission from ref. [130,132].

in both DODH cycle I and II. The authors also considered an alternative DODH route including the first elimination of β - and γ -OH groups of mucic acid followed by the elimination of α - and δ -OH groups. However, the elimination of β - and γ -OH groups followed by α - and δ -OH groups were calculated to have energy barriers of 29.5 and 25.4 kcal/mol, respectively, which are much higher than the route starting with α - and β -OH groups and subsequent γ - and δ -OH groups. Therefore, the DODH of mucic acid is believed to proceed via firstly removing α - and β -OH groups rather than β - and γ -OH groups. This conclusion can be explained by the favorable coordination of *cis*-conformation α - and β -OH groups with Re in contrast to the *trans*-conformation β - and γ -OH groups.

Glucaric acid.

Glucaric acid, a stereoisomer of mucic acid, can be obtained from a low-cost and easily-available C6 sugar, namely glucose. Hence, glucaric acid is considered as a more attractive substrate for DODH targeting adipate/adipic acid compared to mucic acid typically derived from galactose with limited availability. However, it is challenging to eliminate the four internal OH groups in glucaric acid via DODH, since the presence of one pair of *trans* OH groups in glucaric acid would hinder the coordination of OH groups with Re. The addition of Pd as a co-catalyst has been demonstrated as an effective strategy to completely remove four OH groups in glucaric acid by two DODH reactions [112]. The sole utilization of ReO_x/AC catalyst delivered a very low yield of 26.8% towards fully dehydroxylated products (the last two columns in Scheme



Scheme 14. Synergistic catalysis of Pd and ReO_x in the DODH of glucaric acid towards fully dehydroxylated products.

14) from the double DODH of potassium glucarate at 110 °C under 20 bar H₂, whereas Pd-doped ReO_x/AC catalyst (Pd-ReO_x/AC) gave an excellent yield of up to 95% towards adipic acid ester (**Scheme 14**). Clearly, the addition of Pd not only catalyzed the anticipated hydrogenation of C=C bonds in dehydroxylated products, but also dramatically accelerated the elimination of four internal OH groups. Characterizations of Pd-ReO_x/AC catalyst indicated the co-existence of high-valence Re(VI)O_x species and Pd nanoparticles in close proximity. Along with control experiment results, the authors concluded that the synergy effect between ReO_x and Pd species is responsible for the superb DODH efficiency of Pd-ReO_x/AC catalyst. Specifically, ReO_x with a high valence (Re(VI)) probably serves as the active site for glucaric acid DODH, while the neighbouring Pd nanoparticles are speculated to assist the DODH by providing the active H species arising from H₂ dissociation on Pd nanoparticles. The formed active H species was speculated to facilitate the elimination of OH group and also contribute to the redox cycle between Re(VI) and Re(IV).

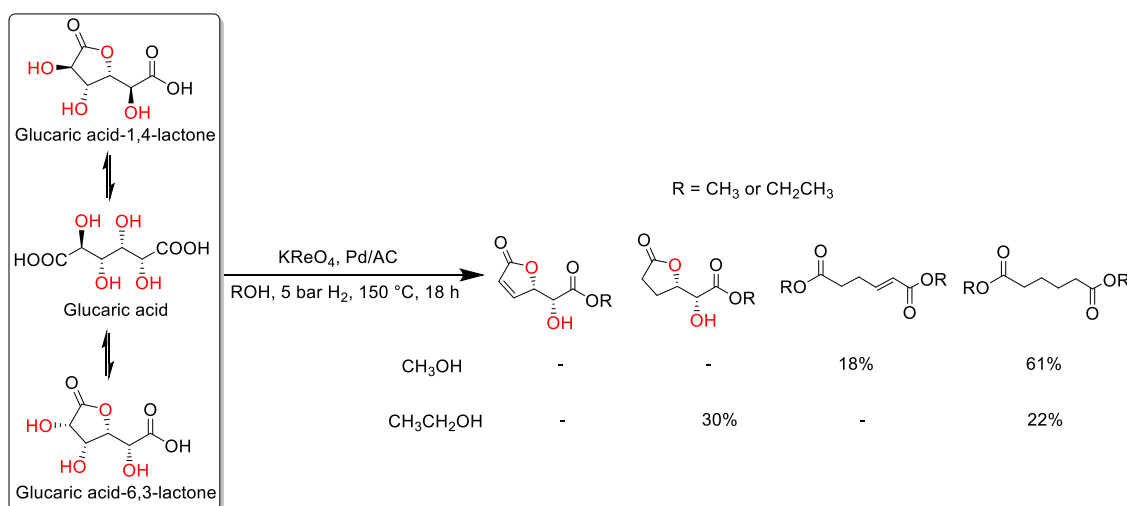
In addition, the choice of solvent could significantly affect the removal of four OH groups in glucaric acid through Re-catalyzed DODH. For example, F. Dean Toste's group reported the employment of methanol as solvent afforded a high yield of 61% towards dimethyl adipate via the DODH-hydrogenation of over KReO₄ catalyst together with Pd/C at 150 °C under 5 bar H₂ in 18 h (**Scheme 15**) [129]. As discussed above, the DODH of glucaric acid is promoted by the synergistic catalysis of KReO₄ and Pd, while the following hydrogenation of C=C bonds mainly occurs on Pd sites. The yield of dimethyl adipate could be further improved to 88% when adding H₃PO₄ as a co-catalyst to accelerate the ring-opening of lactone and AC as a support for the deposition of soluble rhenium species. In contrast, a very low yield of 22% towards diethyl adipate was achieved in the presence of ethanol as solvent under identical reaction conditions (**Scheme 15**). The authors suggested that the facilitated removal of four OH groups in glucaric acid by using methanol as solvent is probably related to the altered equilibria among 1, 4-lactone, 6,3-lactone, and linear forms of glucaric acid. Yet, further studies are needed to clarify the underlying cause of the beneficial effect of methanol.

Recently, a heterogeneous ZrO₂-supported oxo-rhenium catalyst (ReO_x/ZrO₂) was developed for the DODH of glucaric acid-1,4-lactone into partially dehydroxylated products and muconate, giving a total yield of 93% in butanol at 120 °C under N₂ atmosphere [133]. In contrast, the classical homogeneous catalyst MTO afforded a much lower yield of 50% under identical reaction conditions. Such superior DODH activity of ReO_x/ZrO₂ is attributed to the high reducibility of ReO_x on ZrO₂ surface, as evidenced by H₂ temperature-programmed reduction (H₂-TPR) and X-ray photoelectron spectroscopy (XPS). The

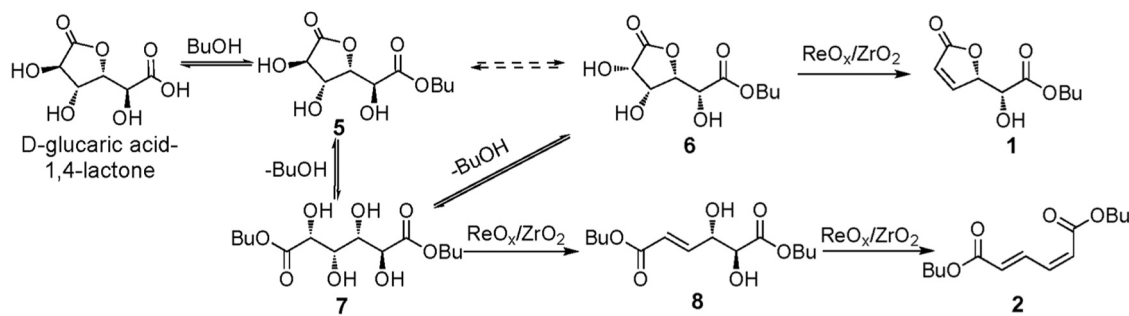
obtained muconate can undergo a separate hydrogenation step to yield adipate over Pd/C at 120 °C under H₂ atmosphere. Through this two-step DODH-hydrogenation strategy, glucaric acid-1,4-lactone can be finally transformed into adipate in a high yield of 82%. As shown in **Scheme 16**, a plausible reaction network for the DODH of glucaric acid-1,4-lactone was proposed by monitoring the evolution of various reaction intermediates and products during the reaction. It is known that three interconvertible intermediates including two cyclic lactones (i.e., glucaric acid-1,4-lactone and glucaric acid-3,6-lactone) and one linear glucaric acid ester are usually derived from glucaric acid upon dissolving in alcoholic solvents (**Scheme 15**). At the beginning of the reaction, ReO_x/ZrO₂ catalyst shifts the equilibrium established among these three products towards the formation of glucaric acid-3,6-lactone and linear glucaric acid ester, since both of them possess a pair of *cis* OH groups available for DODH reaction. The DODH of glucaric acid-1,4-lactone is hard to proceed owing to the presence of only *trans* OH groups on its five-membered ring. The first DODH reaction of glucaric acid-3, 6-lactone and linear glucaric acid ester give rise to partially dehydroxylated 1,4-lactone (1) and linear glucaric acid ester (6). Muconic acid ester is finally generated by the second DODH reaction of 6, which very likely involves a prior isomerization step to transform the remaining *trans* OH groups in 6 into *cis* conformation. Additionally, it is worthy to note that the dehydroxylated intermediate 1 possesses a pair of *cis* OH groups available for DODH reaction, thus offering another possible route to synthesize muconic acid ester and adipic acid ester. Following a two-step reaction sequence comprising ring-open of lactone and DODH, the dehydroxylated intermediate 1 can be converted into muconic acid ester as well.

Other bio-based carboxylic acids.

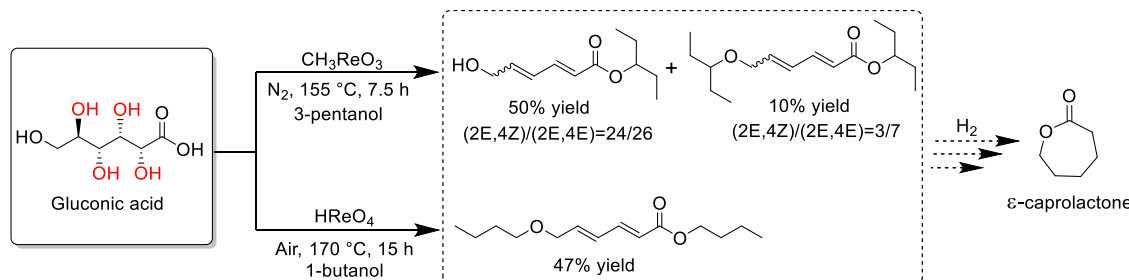
Apart from aforementioned sugar-derived dicarboxylic acids, gluconic acid bearing one carboxyl group as well as five adjacent OH groups appears as an interesting substrate for DODH reaction. In contrast to glucose-derived glucaric acid, it is easier to obtain gluconic acid through the facile oxidation of aldehyde group of glucose by established microbial fermentation or chemical oxidation technologies [134,135]. During the DODH of gluconic acid, four internal OH groups are eliminated by two DODH reactions accompanied by the formation of various derivatives of 6-hydroxy-2,4-hexadienoic acid as the main products. Toste et al. have explored the catalytic performance of different oxo-rhenium catalysts in the DODH of gluconic acid [110]. Under the catalysis of MTO, 6-hydroxy-2,4-hexadienoic acid ester was preferentially formed in a yield of 50% at 155 °C in 3-pentanol under N₂ atmosphere (**Scheme 17**). By contrast, utilizing HReO₄ as the catalyst afforded etherified 6-hydroxy-2,4-hexadienoic acid ester in a yield of 47% at 170 °C in 1-butanol. This is attributed to the accelerated etherification of terminal



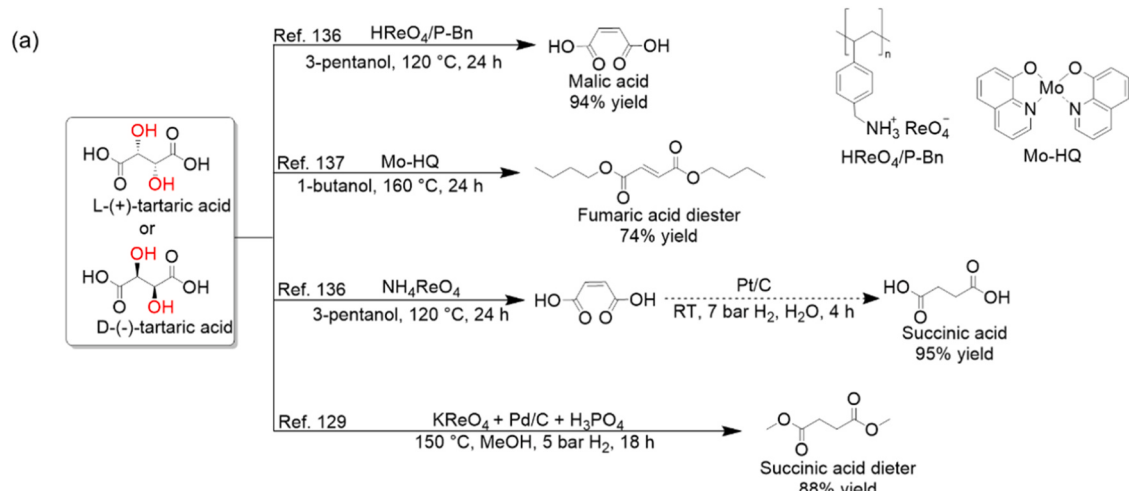
Scheme 15. DODH of glucaric acid and its lactones over KReO₄ + Pd/AC catalysts using ethanol or methanol as solvent.



Scheme 16. Proposed reaction pathway for the DODH of glucaric acid-1,4-lactone into dibutyl muconate over $\text{ReO}_x/\text{ZrO}_2$. Reproduced with permission from ref. [133].



Scheme 17. Re-catalyzed DODH of gluconic acid into various derivatives of 6-hydroxy-2,4-hexadienoic acid.



Scheme 18. (a) A summary of the DODH of tartaric acid into maleic acid/fumaric acid followed by hydrogenation to form succinic acid over Re- and Mo-based catalysts; (b) Proposed reaction mechanism for Mo-HQ-catalyzed DODH of tartaric acid into fumaric acid. Reproduced with permission from ref. [137].

OH group with solvent by the Brønsted acidity of HReO_4 . These dehydroxylated products can act as potential precursors to ϵ -caprolactone, a high-value monomer for specialized polymers, upon a facile reduction of the diene moieties present in 6-hydroxy-2,4-hexadienoic acid derivatives (Scheme 17).

Tartaric acid, a natural C4 α -hydroxy acids present in plants and fruits, can be biologically accessed from glucose fermentation. Tartaric acid is considered as a potential substrate to produce useful C4 oxygenated chemicals owing to the existence of two internal adjacent OH groups along with two terminal carboxyl groups. The removal of internal OH groups in tartaric acid by one DODH reaction will lead to maleic acid/fumaric acid containing one $\text{C}=\text{C}$ bond, which can be readily reduced to succinic acid, a key C4 building block, by catalytic hydrogenation. Zhang et al. reported a heterogeneous Re catalyst by immobilizing HReO_4 onto poly-benzylamine ($\text{HReO}_4/\text{P-Bn}$) for the DODH of L-(+)-tartaric acid into malic acid (Scheme 18a) [136]. A high maleic acid of up to 94% was achieved at 120 °C in 3-pentanol after 24 h. This high selectivity of free maleic acid was ascribed to the reduced acidity of HReO_4 by amine groups. However, a pronounced leaching of Re species (21% leaching) was observed during recycling experiments due to the weak electrostatic interaction between HReO_4 and benzylamine. By coupling DODH and hydrogenation in one pot over physically mixed catalysts of KReO_4 , H_3PO_4 , and Pd/C , D-(+)-tartaric acid could be directly transformed into succinic acid ester in 88% yield at 150 °C under 5 bar H_2 in 18 h (Scheme 18a) [129]. Notably, Zhang and Li developed a two-step process to realize the synthesis of succinic acid instead of its esters from L-(+)-tartaric acid [136]. This two-step process relies on the combined utilization of NH_4ReO_4 and Pt/C catalysts without introducing any acidic sites to suppress esterification reaction (Scheme 18a). The first DODH reaction of L-(+)-tartaric acid to maleic acid was catalyzed by NH_4ReO_4 in 3-pentanol at 120 °C, affording a high isolated yield of 91% in 24 h. The isolated maleic acid was further subjected to a Pt-catalyzed hydrogenation at room temperature under 7 bar H_2 , giving rise to 95% yield of succinic acid.

In addition to oxo-rhenium catalysts, a mononuclear molybdenum complex (Mo-HQ) containing two 8-hydroxyquinoline ligands was demonstrated to catalyze the DODH of L-(+)-tartaric acid into fumaric acid ester in a yield of 74% in the presence of butanol as reductant at 160 °C in air [137]. The excellent performance of molybdenum complex is ascribed to the electron-rich Mo centers induced by the electron-donating effect of 8-hydroxyquinoline ligands. The DODH of tartaric acid over Mo-HQ was proposed to follow a similar mechanism as that of Re catalysts, involving the reduction of Mo(VI) to Mo(IV), condensation to form a Mo(IV)-diolate intermediate, and the extrusion of fumaric acid accompanied with the regeneration of Mo(VI) centers (Scheme 18 b).

2.2.2.4. DODH coupled with various reactions. DODH-hydrogenation.

The obtained products from DODH reaction contain abundant alkene moieties which are synthetically useful to be converted into valuable saturated chemicals by metal-catalyzed hydrogenation. So far, the integration of DODH and hydrogenation (DODH-hydrogenation) has found many applications in the cascade upgrading of bio-based molecules into a range of valuable products such as monoalcohols [128,138], diols [138–140], dicarboxylic acids [110,111,129], and deoxy sugars [114]. In principle, DODH and hydrogenation reaction can proceed sequentially in a two-step manner under different reaction conditions, thus requiring two catalysts active for DODH and hydrogenation, respectively. Such a two-step strategy has been practiced for the step-wise synthesis of adipic acid from mucic acid and succinic acid from tartaric acid, as discussed above. Alternatively, DODH-hydrogenation reaction can proceed in a cascade manner in one pot without isolating reaction intermediates. In this case, physically mixed catalysts or bifunctional catalysts comprising oxo-metals for DODH and metallic sites for hydrogenation are usually needed. As stated above, physically

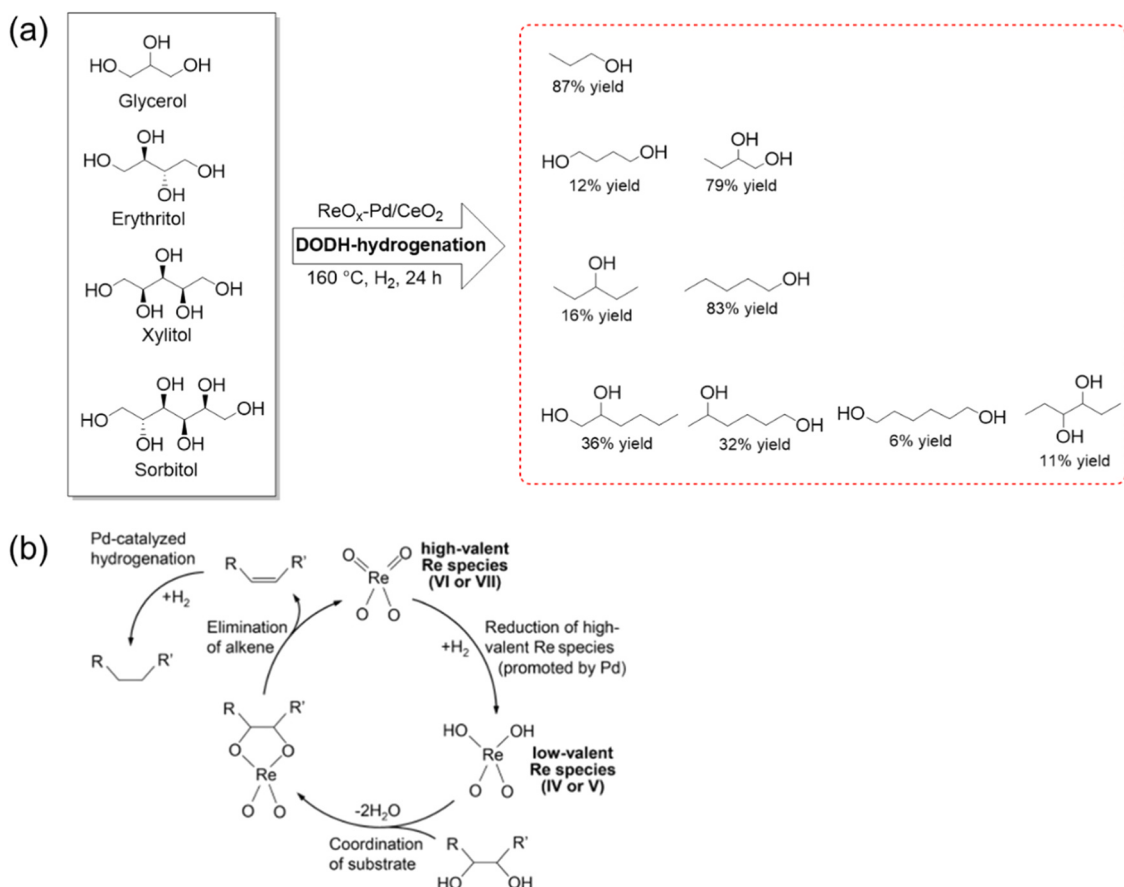
mixed catalysts such as $\text{Re/C} + \text{Pd/C}$, $\text{Re}_2\text{O}_7 + \text{Ru/C}$, and $\text{KReO}_4 + \text{Pd/C}$ [111,128,129], as well as bifunctional catalysts such as $\text{Pd-ReO}_x/\text{C}$ and $\text{Pt-ReO}_x/\text{C}$ have been demonstrated to realize the one-pot DODH-hydrogenation of mucic, glucaric, and tartaric acids into adipate and succinate [112,132].

In addition, Tomishige et al. developed a solid bifunctional catalyst by depositing rhenium oxides and metallic Pd components onto ceria ($\text{ReO}_x\text{-Pd/CeO}_2$) for DODH-hydrogenation [138]. $\text{ReO}_x\text{-Pd/CeO}_2$ exhibited excellent activities and selectivities for the DODH-hydrogenation of various sugar alcohols into corresponding mono-alcohols and diols using H_2 as reductant (Scheme 19a). In the case of glycerol, its DODH product allyl alcohol was hydrogenated into 1-propanol in a yield of 87% at 160 °C under 80 bar H_2 . Xylitol was converted to 1-pentanol in a yield of 83% via an intermediate of 2,4-pentadiene-1-ol. The formation of 3-pentanol (16%) indicated the parallel DODH of xylitol at C1/C2 and C4/C5 position. Unlike glycerol and xylitol, when utilizing erythritol and sorbitol containing even numbers of OH groups as substrates, their OH groups in theory could be completely eliminated via multiple DODH reactions leading to fully-dehydroxylated low-value alkanes (n-butane and n-hexane) upon hydrogenation. However, $\text{ReO}_x\text{-Pd/CeO}_2$ catalyst could direct the DODH-hydrogenation of erythritol and sorbitol towards valuable diols (partially dehydroxylated products) such as 1,2-butanediol (79% yield) and hexanediols (85% overall yield) instead of alkanes as main products (Scheme 19a). The excellent performance of $\text{ReO}_x\text{-Pd/CeO}_2$ was attributed to matched DODH abilities and hydrogenation abilities of $\text{ReO}_x\text{-Pd/CeO}_2$ catalysts. As depicted in Scheme 19b, DODH reaction was proposed to proceed via the condensation of vicinal OH groups with high-valence Re(IV)/Re(VI) or Re(V)/Re(VII) redox couples. These high-valence Re oxides were stabilized by CeO_2 to inhibit over-reduction to form low-valence Re species (such as metallic Re) featuring poor activity. Metallic Pd sites are able to activate H_2 for the hydrogenation of carbon–carbon double bonds. In addition, the same authors applied the DODH-hydrogenation strategy to transform methyl glycosides into corresponding deoxy sugars using $\text{ReO}_x\text{-Pd/CeO}_2$ catalysts in one pot [114]. As discussed above, various cyclic methyl glycosides with *cis* OH groups first underwent ReO_x -catalyzed DODH to selectively yield unsaturated deoxy methyl glycosides as intermediates, which were further reduced into deoxy sugars on metallic Pd sites. For more details, the reader is directed to the previous Section 2.2.2.1.

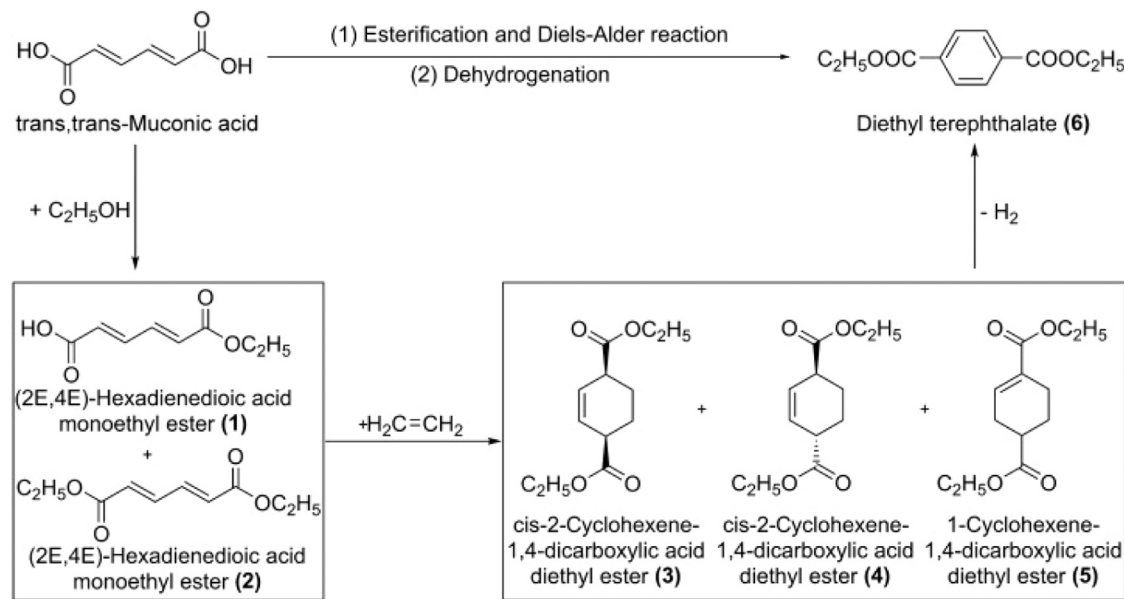
DODH-Diels-Alder.

As mentioned above, conjugated products containing diene moiety such as butadiene and muconic acid were usually obtained when performing the DODH of erythritol and mucic acid. The presence of reactive conjugated diene structures in butadiene and muconic acid allows for further reaction with dienophiles via Diels-Alder cycloaddition to generate six-membered ring chemicals including aromatics or cyclohexene derivatives. Therefore, coupling DODH with Diels-Alder reaction offers sustainable pathways to synthesize value-added aromatics or cyclohexene derivatives from bio-based compounds [141,142].

Of great interest is to synthesize terephthalic acid or its ester, an important bulk chemical for polyester industry (polyethylene terephthalate), through the Diels-Alder cycloaddition of muconic acid with ethylene. Lu and coworkers reported a two-step protocol to transform *trans,trans*-muconic acid into diethyl terephthalate in a yield of 80.6% by a tandem reaction sequence including esterification, Diels-Alder cycloaddition, and dehydrogenation (Scheme 20) [143]. The initial occurrence of esterification and Diels-Alder cycloaddition of *trans,trans*-muconic acid using a silicotungstic acid catalyst in the presence of ethanol and ethylene at 200 °C afforded a mixture of cyclohexene-based cycloadducts (99% selectivity) as reaction intermediates. The exclusive formation of cycloadducts is related to the utilization of esterified *trans,trans*-muconic acid, which possesses high solubility in ethanol as well as enhanced Diels-Alder reactivity owing to the electron donating effects of ethoxy groups. Without an isolation step, crude cycloadducts can be directly subjected to a Pd/C -catalyzed dehydrogenation reaction at



Scheme 19. (a) DODH-hydrogenation of various sugar alcohols into alkanols and alkanediols over $\text{ReO}_x\text{-Pd/CeO}_2$; (b) Proposed reaction mechanism for the DODH-hydrogenation of diols into alkanes over $\text{ReO}_x\text{-Pd/CeO}_2$. Reproduced with permission from ref. [138].



Scheme 20. A two-step protocol for the conversion of trans,trans-muconic acid into diethyl terephthalate by a tandem process including esterification, Diels-Alder cycloaddition, and dehydrogenation. Reproduced with permission from ref. [143].

200 °C under neutral or slightly basic conditions, eventually affording 80.6% yield of diethyl terephthalate. As such, diethyl terephthalate was successfully synthesized from muconic acid by two steps in one reactor. Moreover, novel variants of terephthalic acid (e.g., ethyl-terephthalic

acid, cyano-terephthalic acid, dihydroisobenzofuran-dicarboxylic acid) can be generated when utilizing complex dienophiles such as maleic anhydride, butene, and acrylonitrile to react with muconic acid. [141, 144] Despite these promising results, the possibility of combining DODH

reaction with Diels-Alder and dehydrogenation in a cascade manner has not been demonstrated yet. Further efforts are needed to explore the utilization of crude DODH product as the feedstock instead of commercial muconic acid.

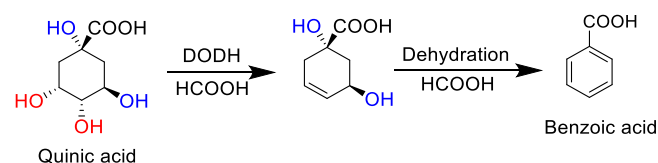
Toste et al. reported one successful example of applying DODH-Diels-Alder reaction strategy to convert erythritol and L-(+)-tartaric acid into 4-cyclohexene-1,2-dicarboxylic acid ester, a potential precursor of plasticizers, in one reactor by two steps (Scheme 21) [110]. The first step involved the HReO₄-catalyzed DODH of mixed erythritol and L-(+)-tartaric acid to form butadiene and fumaric acid ester, respectively, using 2-methyl-1-butanol as solvent and reductant. Then the generated crude mixture of butadiene and fumaric acid ester (a dienophile) underwent spontaneous Diels-Alder cycloaddition at 120 °C to give rise to 4-cyclohexene-1,2-dicarboxylic acid ester as the final product in a yield of 70%. This example clearly demonstrated the potential of DODH-Diels-Alder strategy in constructing complex molecules with desired functional groups by the rational selection of substrates and design of reaction sequence.

DODH-dehydration.

DODH reaction is specifically efficient to remove *cis* diols, while acid-catalyzed dehydration reaction is able to remove single OH group. These two methods are complementary in realizing the cleavage of C–O bonds. Therefore, the combination of DODH with dehydration (DODH-dehydration) could cooperatively eliminate all OH groups in polyhydroxy compounds to yield fully-dehydroxylated products like aromatics and furans. As discussed in Section 2.2.2.1, the DODH-dehydration of various sugar monomers led to the formation of furan and 2-vinylfuran as major products. Besides, DODH-dehydration strategy has been demonstrated to be useful in upgrading glucose-derived quinic acid into benzoic acid by removing all OH groups of quinic acid [145]. In the presence of formic acid, quinic acid was converted into benzoic acid in a high yield of 92% at 220 °C in 1.5 h using sulfolane as solvent. The reaction was proposed to proceed in a two-step mechanism (Scheme 22). Firstly, two vicinal OH groups in *cis* conformation on the ring of quinic acid were removed by formic acid-mediated DODH reaction affording an intermediate possessing cyclohexene structure. This formic acid-mediated DODH reaction likely proceeds via a same orthoester intermediate as that of TEOF-mediated DODH, as described in Scheme 9a. Subsequently, acid-catalyzed dehydration of two nonadjacent OH groups on the ring gives rise to benzoic acid. Note that formic acid plays two important roles: a deoxygenation reagent for DODH and a Brønsted acid catalyst for dehydration. Likewise, DODH-dehydration strategy was applied to the complete dehydration of shikimic acid into benzoic acid, affording a high yield of 89% in the presence of formic acid at 190 °C via a similar pathway [145].

2.3. Dehydration of OH groups

In addition to DODH, the cleavage of C–O bonds can be fulfilled by a classical acid-catalyzed dehydration of OH groups, which involves the elimination of single OH group in the form of water with the concomitant formation of one carbon–carbon double bond. Acid-catalyzed

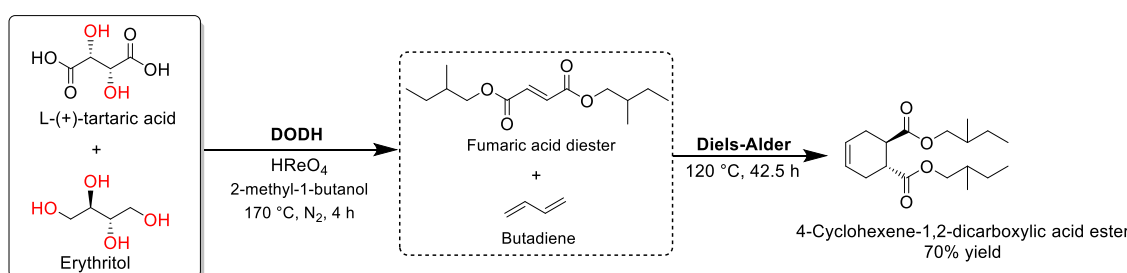


Scheme 22. One-pot conversion of quinic acid into benzoic acid via formic acid-mediated DODH-dehydration reaction. Adapted with permission from ref. [145].

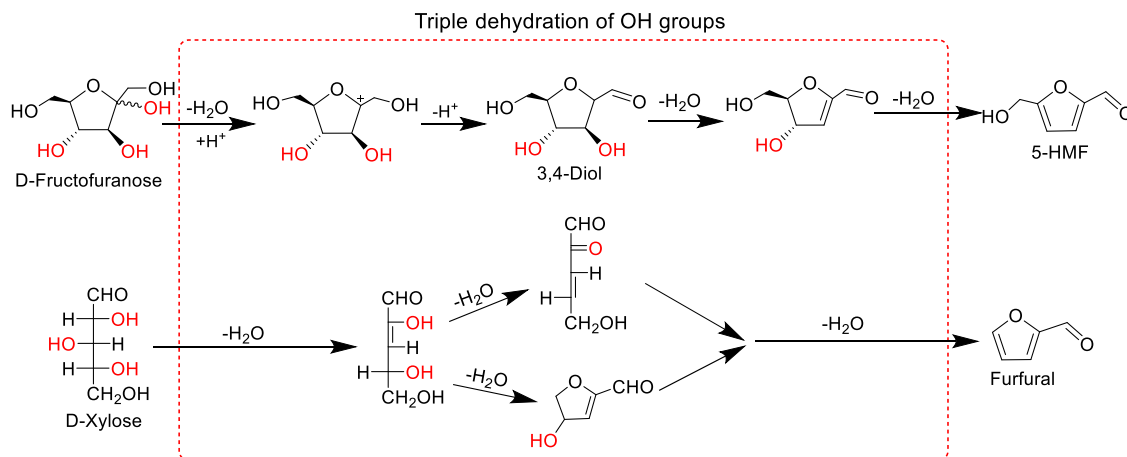
dehydration of OH groups has been used as an efficient deoxygenation method in numerous biomass upgrading processes. The most representative examples are the dehydration of sugar monomers (e.g., glucose, fructose, xylose) into furanic compounds such as HMF and furfural, two versatile building blocks to synthesize a wide variety of chemicals and fuels [16,146–153]. As the key conversion routes to valorize (hemi) cellulose, the dehydration of OH groups in hexoses and pentoses into HMF and furfural has been summarized in many reviews in the aspect of catalysts, solvents, mechanistic insights, process engineering [2,16, 153–162]. Therefore, the dehydration of sugars into HMF and furfural will be only briefly discussed herein.

HMF and furfural, featured by a furan ring, are produced by the acid-catalyzed cyclodehydration of glucose/fructose and xylose, respectively. In view of multiple isomers of glucose/fructose/xylose present in water and various reaction conditions applied, a number of reaction pathways involving cyclic or acyclic intermediates have been proposed for the synthesis of HMF and furfural [163–170]. The common steps to synthesize HMF and furfural involve three successive acid-catalyzed dehydration steps to cleave three C–O bonds in sugars with the coproduction of three H₂O molecules (Scheme 23). In the case of HMF formation, D-fructose in a cyclic form (D-fructofuranose) was proposed as the most likely species that actually undergoes three successive dehydration reactions through a series of cyclic intermediates (Scheme 23) [155,164, 167,170]. The reaction is initiated by the protonation of OH group at C2 position and the concurrent dehydration to form a carbocation intermediate followed by deprotonation to form 3,4-diol. Eliminating two OH groups on the ring of 3,4-diol through consecutive dehydration steps ultimately gives rise to HMF. When utilizing D-glucose as the substrate for HMF production, an isomerization step to transform D-glucose into D-fructose is believed to proceed prior to dehydration. The isomerization process can be facilitated by a Lewis acid or a Brønsted base catalyst to reach the equilibrium conversion of glucose [171,172]. The dehydration of xylose into furfural is usually believed to start with the linear form of xylose through either enol intermediates or cyclic unsaturated aldehyde intermediates (Scheme 23) [168,169,173]. Both routes involved three consecutive dehydration/cyclization steps to eliminate three OH groups.

In contrast to the combined utilization of oxo-rhenium catalysts and reductants for DODH, acid catalysts alone are sufficient for the dehydration of OH groups under moderate reaction temperatures (mostly 80–200 °C). Typically, the dehydration reaction is triggered by the protonation of either OH groups or pyranose oxygen atoms in hexoses/



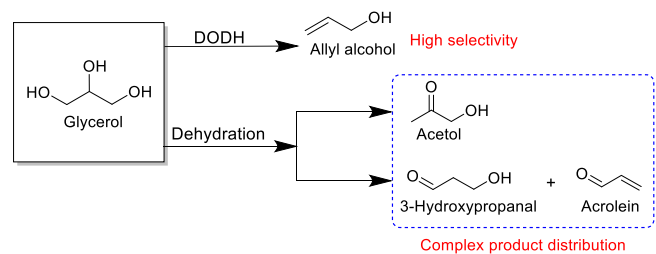
Scheme 21. Catalytic conversion of erythritol and tartaric acid into 4-cyclohexene-1,2-dicarboxylic acid ester via a DODH-Diels-Alder cascade reaction. Adapted with persimmon from ref. 110.



Scheme 23. Proposed reaction pathway for the triple dehydration of D-fructofuranose and D-xylose into 5-HMF and furfural. Adapted with persimmon from ref. [164 and 168].

pentoses in the presence of a homogeneous or heterogeneous acid catalyst containing protons. The protonated OH groups can be facilely eliminated in the form of H_2O molecules to form corresponding enol or carbocation intermediates (Scheme 23). A wide range of homogenous and heterogeneous catalysts, such as mineral acids, organic acids, zeolites, sulfonated resins, heteropolyacids, metal chlorides, and acidic oxides have been demonstrated to afford moderate to high HMF and furfural yields [153,154,157,159,174]. Ionic liquids (mostly imidazolium types) and organic solvents (e.g., DMSO, MIBK, DMF, THF, lactone) are the preferred choice of reaction media for the dehydration of sugars to HMF and furfural, since these solvents are able to extract and stabilize the formed HMF/furfural, thus suppressing competitive side reactions such as HMF rehydration [175–179].

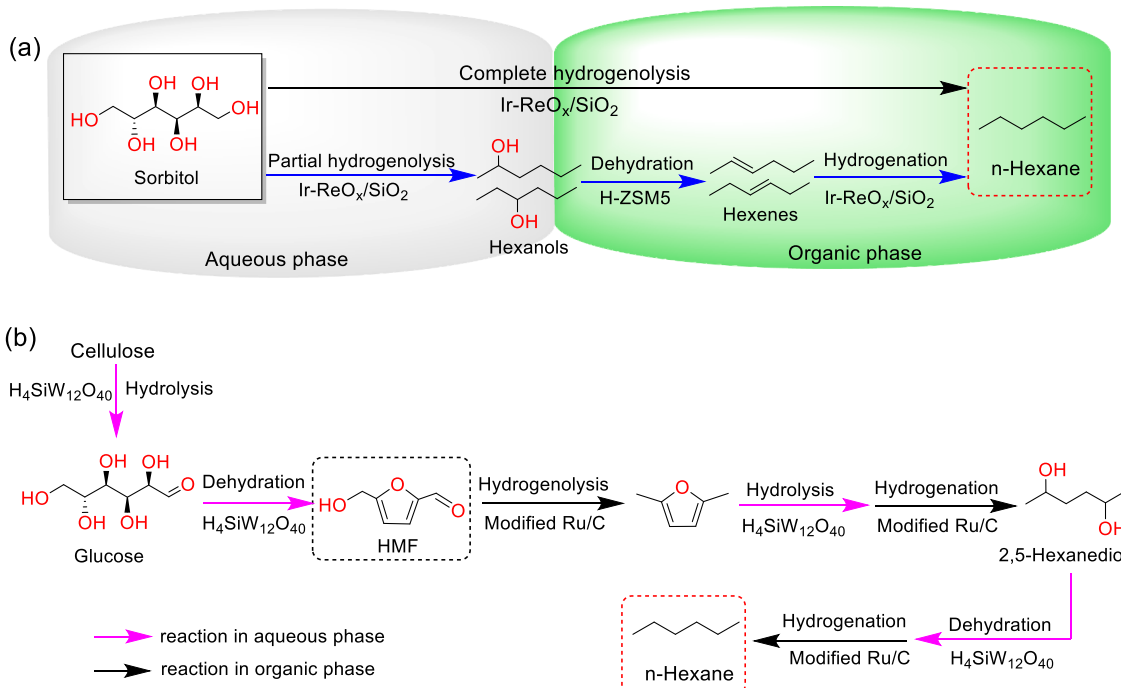
Noteworthy, unlike aforementioned DODH reaction capable of selectively cleaving *cis* vicinal OH groups, acid-catalyzed dehydration reaction is in principle applicable to single OH group without the requirement of stereochemistry. However, such a broad applicability of acid-catalyzed dehydration reaction results in poor selectivity control in eliminating specific OH groups. Especially for the dehydration of carbohydrates with multiple hydroxyl groups featuring similar reactivity, diverse products from competitive reaction pathways are often obtained. This is ascribed to the fact that acid-catalyzed dehydration can initiate at different hydroxyl groups, depending on reaction conditions as well as the structure and stereochemistry of sugar molecules. For example, glucose dehydration into HMF is always accompanied by the generation of side products, which are proposed to be correlated to the initial protonation of OH groups at which carbon atoms of glucose. As revealed by ab initio molecular dynamics calculations, the initial protonation of OH group at the C2 atom in D-glucose favors the formation HMF, whereas the formation of humins is dominated when the protonation of OH group initiates at the C4 atom in D-glucose [180,181]. Note that these computational studies were mostly implemented without considering the influence of reaction conditions (solvent, pH, salts) which could alter the initial protonation sites and also subsequent reaction pathways. Horváth et al. reported that the product distribution of D-fructose dehydration is also affected by the isomer structure D-fructose present in water [164]. As indicated by in situ nuclear magnetic resonance (NMR), the formation of humins and HMF probably arose from the protonation of OH groups in D-fructopyranose and D-fructofuranose, respectively. A prominent example to illustrate the different features between DODH and acid-catalyzed dehydration is the C–O bond breakage of glycerol (Scheme 24). Acid-catalyzed dehydration of glycerol generally leads to various products including acrolein/3-hydroxypropanal and acetol via the dehydration of glycerol at its secondary and primary OH groups, respectively [182]. In contrast, the exclusive production of allyl alcohol can be realized by removing



Scheme 24. Comparison of product selectivities for the C–O bond cleavage of glycerol via DODH and acid-catalyzed dehydration.

two adjacent OH groups of glycerol through a DODH reaction [183]. Obviously, DODH reaction is superior to the dehydration of OH groups in terms of steering product selectivity with less chances of generating multiple products during the C–O bond cleavage of biomass derivatives.

It is worth mentioning that the dehydration of OH groups is regarded as one elementary reaction of the hydrodeoxygenation (HDO) of bio-based oxygenates such as sugars and sugar alcohols. HDO does not refer to a specified type of reaction, but rather covers a series of reactions that enable the removal of oxygen (deoxygenation) along with the hydrogenation of unsaturated intermediates. One common approach in HDO chemistry is the dehydration of oxygenates into reactive intermediates followed by hydrogenation to generate less-oxygenated or fully-deoxygenated products such as alkanols and alkanes for drop-in transportation fuels. This kind of HDO process usually necessitates bifunctional catalysts containing acidic components for dehydration and metallic components for hydrogenation. For example, the OH groups of sorbitol can be completely removed via HDO over $\text{Ir}-\text{ReO}_x/\text{SiO}_2$ and H-ZSM-5, affording a high hexane yield of ca. 95% at 140 °C under 8 MPa H_2 in a biphasic system of water and dodecane [184]. In the absence of H-ZSM-5, hexane yield was decreased to 50% with the formation of 2-hexanol and 3-hexanol as major side products, suggesting that the removal of these secondary OH groups likely proceeds via H-ZSM-5-catalyzed dehydration. As indicated by control experiments with 1-pentanol, 2-pentanol, and 3-pentanol (model compounds to study the reaction behaviors of mono-alcohols), 2-pentanol and 3-pentanol prefer to undergo dehydration to form pentene, whereas 1-pentanol tends to undergo hydrogenolysis over $\text{Ir}-\text{ReO}_x/\text{SiO}_2$ to form pentane. Based on these observations, the HDO of sorbitol was proposed to proceed via two parallel pathways (Scheme 25a): a) the deep hydrogenolysis of all OH groups of sorbitol over $\text{Ir}-\text{ReO}_x/\text{SiO}_2$, and b) the partial hydrogenolysis of sorbitol to 2-hexanol and 3-hexanol followed by dehydration-hydrogenation via hexenes.



Scheme 25. (a) Proposed reaction pathway for the biphasic HDO of sorbitol into hexane over bifunctional Ir-ReO_x/SiO₂ and H-ZSM-5 catalysts; (b) Proposed reaction pathway for the biphasic HDO of cellulose into hexane over bifunctional H₄SiW₁₂O₄₀ and H₄SiW₁₂O₄₀-modified Ru/C catalysts. Adapted with permission from ref. [184 and 185].

Sels et al. reported a one-pot biphasic protocol for the HDO of cellulose into hexane over a bifunctional catalyst consisting of H₄SiW₁₂O₄₀-modified Ru/C and H₄SiW₁₂O₄₀, affording hexane in a yield of 52% at 220 °C in a biphasic system of decane and water [185]. The modified Ru/C was found to exist in the organic phase, while H₄SiW₁₂O₄₀ primarily existed in the aqueous phase. As a result, the released glucose from cellulose hydrolysis preferentially underwent H₄SiW₁₂O₄₀-catalyzed dehydration to generate HMF rather than Ru-catalyzed reduction into sorbitol. Hence, the direct conversion of cellulose into hexane was proposed to follow a distinct pathway involving HMF as an intermediate followed by sequential hydrogenolysis/hydrolysis/hydrogenation/dehydration/hydrogenation reactions (Scheme 25b). The modified Ru/C is responsible for the hydrogenation/hydrogenolysis of unsaturated intermediates (e.g., HMF and hexanedione), while H₄SiW₁₂O₄₀ catalyzes the hydrolysis and dehydration steps.

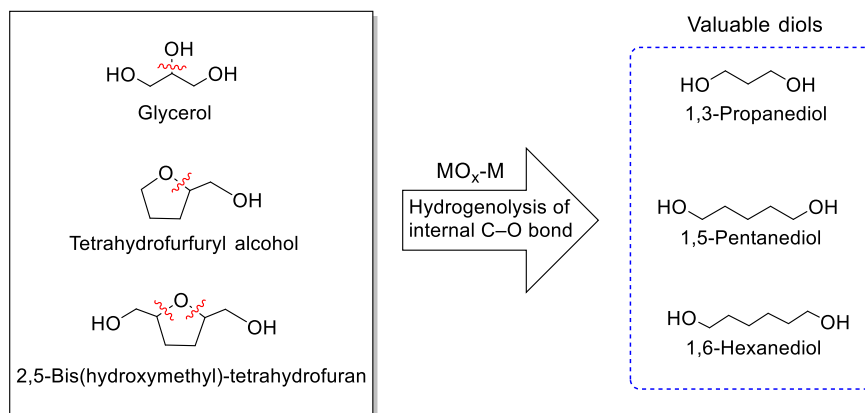
Ma and coworkers reported the direct aqueous-phase HDO of cellulose into hexanes (72% yield) under the synergistic catalysis of H₃PO₄, Ru/C, and layered LiNbMoO₆ [186]. H₃PO₄ is responsible for cellulose hydrolysis and sorbitol dehydration, while Ru/C is responsible for the hydrogenation of unsaturated reaction intermediates. The addition of layered LiNbMoO₆ is essential in controlling the reaction selectivity towards hexanes. The layered structure of LiNbMoO₆ can effectively inhibit the competitive cyclodehydration of sorbitol to form isosorbide through steric confinement effect, thus leading to the selective HDO of sorbitol into hexanes. Notably, such a multicomponent catalyst system, H₃PO₄ + Ru/C + layered LiNbMoO₆, was also demonstrated to be highly efficient for the direct aqueous-phase HDO of raw biomass into complex products mainly including C5 and C6 alkanes and monophenols [187]. Among the examined raw biomass, 82.4% yield (based on (hemi)cellulose fraction) of gasoline-range alkanes was achieved using corn stalk as feedstock at 230 °C under 6 MPa H₂, and 51.4% yield of volatile products could be obtained from the lignin fraction of corncob. The formation of C6 alkanes was proposed to arise from the cellulose HDO via three types of intermediates including HMF, sorbitol, and lactones. The HDO of hemicellulose into C5 alkanes was proposed to proceed via a series of C5 intermediates such as pentanol, tetrahydrofurfuryl alcohol

(THFA), pentanoic acid, and gamma-valerolactone (GVL). As for the HDO of lignin, the released lignin monomers (phenols and guaiacols) could further undergo HDO to yield a mixture of C6-C19 alcohols and hydrocarbons.

2.4. Hydrogenolysis of internal C–O bond

Hydrogenolysis is known as a powerful reaction strategy in the realm of hydrocarbon cracking capable of breaking C–X bonds (X = O, N, S) to remove heteroatoms in the presence of H₂. With the rise of biorefinery, hydrogenolysis has found important applications in removing excessive oxygen atoms present in biomass, for example, aforementioned hydrogenolysis of (hemi)cellulose-derived sugars and sugar alcohols into alkanes over metal-acid bifunctional catalysts. The formation of alkanes involves the removal of all OH groups without requiring selectivity control in breaking C–O bonds. As such, hydrogenolysis of C–O bonds with poor selectivity control is beyond the scope of this review and the interested reader is redirected to recent reviews involving this topic [29, 188–195].

In the case of targeting more valuable diol products (e.g., α,ω -diols) instead of alkanes, it is necessary to ensure hydrogenolysis proceeding in a controlled manner, that is, the selective scission of desired C–O bonds among several similar C–O bonds present in (hemi)cellulose derivatives. Herein, we mainly focus on the cleavage of internal C–O bond by hydrogenolysis, since it offers a highly useful strategy to eliminate the internal OH groups (secondary OH groups) of (hemi)cellulose derivatives as well as glycerol (Scheme 26). The selective cleavage of internal C–O bonds is usually realized over a composite catalyst (M–MO_x) containing noble metals (Ir, Rh, Pt, Pd) modified with oxophilic metal oxides (ReO_x, WO_x, MoO_x). Therein, noble metal sites are responsible for the heterolytic dissociation of H₂ into active hydride and proton species to promote C–O bond cleavage, while oxophilic metal oxides serve as the binding sites to interact with the OH groups in substrate. As a result of the synergy between noble metals and oxophilic metal oxide species, the internal C–O bonds (secondary OH groups) adjacent to primary OH group is more readily to be cleaved over other C–O bonds. This



Scheme 26. Selective hydrogenolysis of internal C–O bond in (hemi)cellulose-derived furanics and glycerol into α,ω -diols.

prominent feature has been utilized for the synthesis of α,ω -diols, important monomers for polymer industry, by the selective scission of internal C–O bonds of (hemi)cellulose-derived furanics as well as glycerol, for example, the hydrogenolysis of THFA into 1,5-pentanediol, 2,5-bis(hydroxymethyl)-tetrahydrofuran (BHMTHF) into 1,6-hexanediol, and glycerol into 1,3-propanediol (Scheme 26).

The combination of Rh with ReO_x ($\text{Rh}-\text{ReO}_x$) has been reported to catalyze the formation of 1,5-pentanediol by selectively breaking the internal C–O bond adjacent to hydroxymethyl (CH_2OH) group within THFA, a saturated product from furfural hydrogenation [196,197]. As shown in Table 2, a high 1,5-pentanediol yield of 77% was obtained over $\text{Rh}-\text{ReO}_x/\text{SiO}_2$ with a Re/Rh ratio of 0.5 at 120 °C in water under 8 MPa H_2 after 24 h. [196] The yield of 1,5-pentanediol could be further improved to 94% when using carbon-supported $\text{Rh}-\text{ReO}_x$ catalysts, probably due to the inhibited decomposition of 1,5-pentanediol on carbon support [198]. In addition to $\text{Rh}-\text{ReO}_x$, the combination of Ir or Rh with other oxophilic metal oxides (WO_x , MoO_x) also gave high selectivities (>90%) towards 1,5-pentanediol (Table 2) [199,200]. In contrast, in the absence of ReO_x , Rh/SiO_2 catalyst alone afforded 1,2-pentanediol as the major product (61.7% selectivity) but in a very low yield of 3.5% [196]. Evidently, the addition of ReO_x not only altered the hydrogenolysis pathway (reaction selectivity) but also improved the activity of Rh catalyst.

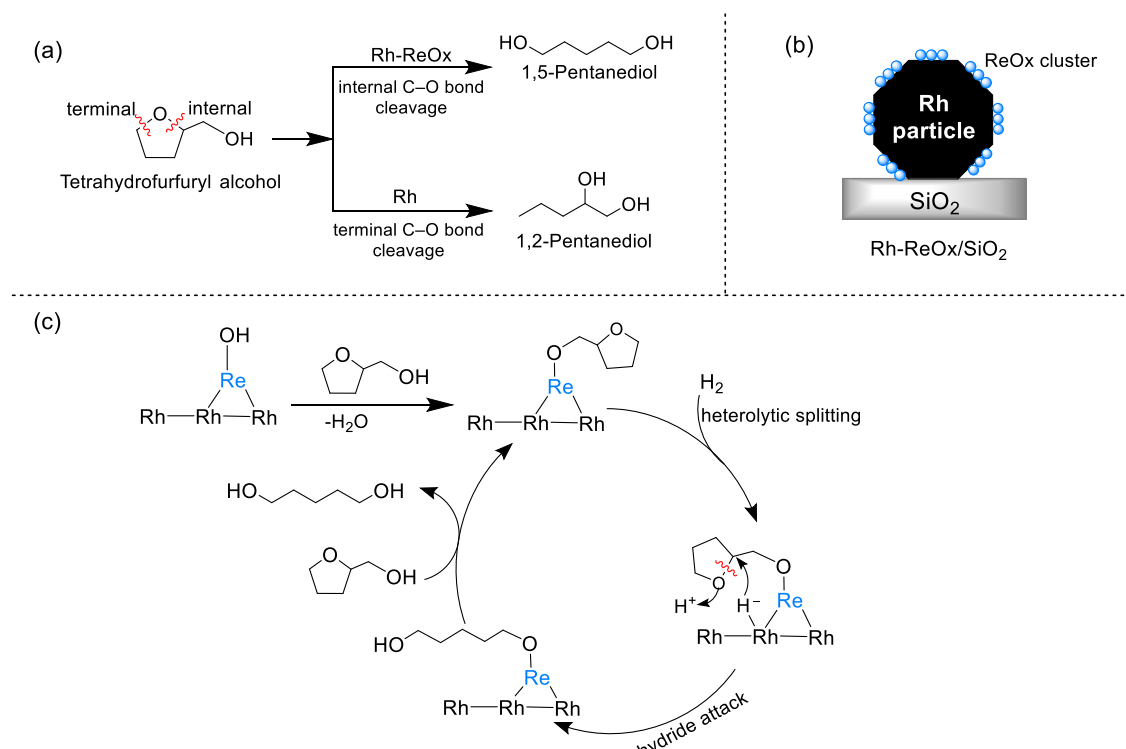
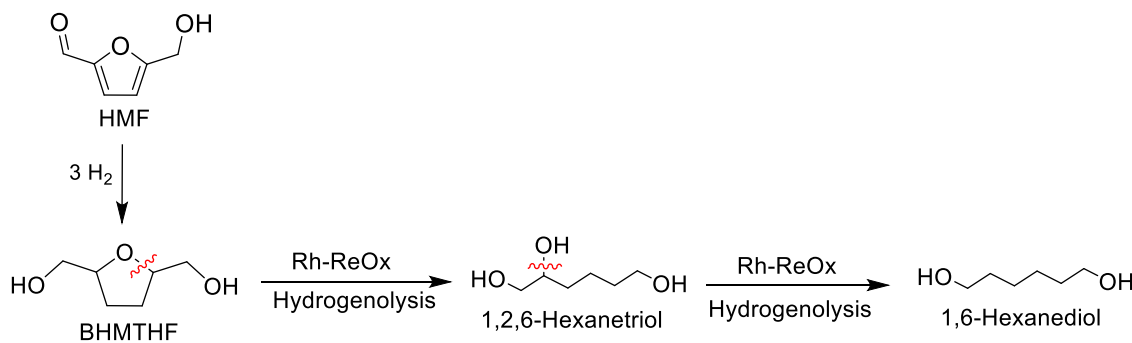
Analogous to THFA, BHMTHF, the hydrogenation product of HMF, has been demonstrated to undergo selective hydrogenolysis of its internal OH groups to yield 1,6-hexanediol via 1,2,6-hexanetriol [206–208]. As depicted in Scheme 27, the reaction involves the first hydrogenolysis of BHMTHF by breaking its internal C–O bond adjacent to the primary OH group (ring-opening reaction) to afford 1,2,6-hexanetriol, followed by a second hydrogenolysis reaction to break the internal C–O bond of 1,2,6-hexanetriol. Both hydrogenolysis steps can be catalyzed by same noble metals combined with oxophilic metal oxides (Table 2). For example, using $\text{Rh}-\text{ReO}_x/\text{SiO}_2$ (6.5 wt% Rh, 6 wt% Re) as the hydrogenolysis catalyst, a high 1,2,6-hexanetriol selectivity of up to 97% was obtained at 21% conversion of BHMTHF at 80 °C under

8 MPa H_2 after 20 h [206]. The subsequent hydrogenolysis of 1,2,6-hexanetriol into 1,6-hexanediol can also occur on $\text{Rh}-\text{ReO}_x/\text{SiO}_2$ but necessitates higher reaction temperatures. Increasing the reaction temperature to 180 °C led to a high 1,6-hexanediol selectivity of 73% at 17% conversion of 1,2,6-hexanetriol after 3 h, accompanied by the minor formation of 1,5-hexanediol (23% selectivity) [207]. The combination of $\text{Rh}-\text{ReO}_x/\text{SiO}_2$ with a solid acid catalyst (e.g., Nafion SAC-13) could enable the hydrogenolysis of BHMTHF to 1,6-hexanediol in one pot, affording a high yield of 86% [206]. Huber and coworkers developed a $\text{Pt}-\text{WO}_x/\text{TiO}_2$ catalyst for the direct hydrogenolysis of BHMTHF to 1,6-hexanediol with a yield of up to 70% without adding acids [209]. The authors proposed that the released H atoms from H_2 dissociation on Pt could react with WO_x to form Brønsted acid sites (W-OH). The synergistic catalysis of Pt and W-OH sites account for the high yields of 1,6-hexanediol. Furthermore, one-pot conversion of HMF into 1,6-hexanediol was demonstrated by integrating BHMTHF hydrogenolysis with upstream HMF hydrogenation in a fixed-bed reactor over a double-layer catalyst system containing upper Pd/SiO_2 and lower $\text{Ir}-\text{ReO}_x/\text{SiO}_2$ [210]. HMF was first hydrogenated into BHMTHF over Pd/SiO_2 , while $\text{Ir}-\text{ReO}_x/\text{SiO}_2$ promoted the subsequent cascade hydrogenolysis of BHMTHF into 1,6-hexanediol in a yield of 57.8% at 100 °C under 7 MPa H_2 .

As shown in Fig. 5a, the formation of 1,5-pentanediol and 1,2-pentanediol necessitates the cleavage of the internal and terminal C–O bonds of the furan ring, respectively. Considering the steric hindrance of hydroxymethyl (CH_2OH) group, the terminal C–O bond is more easily to undergo hydrogenolysis, which can account for the dominant formation of 1,2-pentanediol over Rh/SiO_2 . The preferential cleavage of internal C–O bond is attributed to the special structure of $\text{Rh}-\text{ReO}_x$ active sites, wherein small ReO_x clusters are located on the surface of Rh nanoparticles with the formation of Rh-Re bonds (Fig. 5b), as revealed by catalyst characterizations [197,198,201]. The interfaces between Rh nanoparticles and ReO_x clusters were proposed as the active sites for the cleavage of internal C–O bond. Based on kinetic analysis and control experiments of various ethers, Tomishige et al. proposed a

Table 2
Representative catalysts for the selective hydrogenolysis of internal C–O bond in THFA, BHMTHF, 1,2,6-hexanetriol, and HMF.

Substrate	Catalyst	Major Product	Conv. (%)	Temp. (°C)	Time (h)	Pressure of H_2 (bar)	Yield (%)	Ref.
THFA	$\text{Rh}-\text{ReO}_x/\text{SiO}_2$	1,5-Pentanediol	96.2	120	24	80	77	196
	$\text{Rh}-\text{ReO}_x/\text{AC}$	1,5-Pentanediol	100	100	36	80	94	198
	$\text{Rh}-\text{MoO}_x/\text{SiO}_2$	1,5-Pentanediol	94.2	100	24	80	85.1	199
	$\text{Ir}-\text{ReO}_x/\text{SiO}_2$	1,5-Pentanediol	58.2	100	2	80	55.8	200
	Ni-La	1,5-Pentanediol	97.6	150	24	30	87.9	228
BHMTHF	$\text{Rh}-\text{ReO}_x/\text{SiO}_2$ + Nafion SAC-13	1,6-Hexanediol	100	120	20	80	86	206
BHMTHF	$\text{Pt}-\text{WO}_x/\text{TiO}_2$	1,6-Hexanediol	100	160	5	55	70	209
1,2,6-Hexanetriol	$\text{Rh}-\text{ReO}_x/\text{SiO}_2$	1,6-Hexanediol	17	180	4	80	12.4	207
HMF	Pd/SiO_2 + $\text{Ir}-\text{ReO}_x/\text{SiO}_2$	1,6-Hexanediol	100	100	–	70	57.8	210



hydride-attack mechanism for the hydrogenolysis of THFA into 1,5-pentanediol over Rh-ReO_x (Fig. 5c) [202,203]. THFA is first converted into an adsorbed alkoxide intermediate by reacting with Re–OH species. A heterolytic splitting of H₂ at the interface of Rh and ReO_x affords hydride and proton species. Subsequently, the kinetically relevant cleavage of the internal C–O bond in the adsorbed alkoxide intermediate is triggered by the nucleophilic attack of hydride at the carbon atom of the internal C–O bond. The concurrent proton transfer leads to an adsorbed form of 1,5-pentanediol (alkoxide), which is finally released by a replacement reaction with another THFA molecule. A similar catalytic cycle was also proposed for Ir-ReO_x-catalyzed hydrogenolysis of THFA into 1,5-pentanediol [200]. Note that this hydride attack mechanism (also called “direct hydrogenolysis” by the authors) is different from another prevailing C–O bond cleavage mechanism via the dehydration of OH groups into alkene intermediates followed by hydrogenation [204]. Alternatively, in view of the Brønsted acidity of Re–OH species, the internal C–O bond scission is believed to be initiated by protonating the cyclic O atom in THFA following a proton-catalyzed ring-opening mechanism via a secondary carbonium intermediate [205]. Subsequent hydrogenation of

this carbonium intermediate on Rh nanoparticles gives 1,5-pentanediol.

Although this review concentrates on (hemi)cellulose-derived feedstocks, glycerol represents another important bio-based feedstock that can undergo internal C–O bond cleavage to yield 1,3-propanediol over M–MO_x catalysts [211]. The hydrogenolysis of glycerol usually leads to 1,2-propanediol as the major product owing to the facile cleavage of terminal C–O bonds. Tomishige and coworkers first described the catalytic function of ReO_x species in breaking the internal C–O bond of glycerol to afford 1,3-propanediol as the major product (Scheme 26) [212–215]. In the presence of Ir-ReO_x/SiO₂ (Re/Ir = 0.5), 60.4% selectivity towards 1,3-propanediol was achieved at 33.1% conversion of glycerol at 120 °C under 8 MPa H₂ after 12 h, whereas Ir/SiO₂ catalyst alone was almost inactive for glycerol hydrogenolysis. This indicates that the addition of ReO_x not only boosts the formation of 1,3-propanediol but also greatly improves the catalytic activity of Ir/SiO₂. In addition, ReO_x- and WO_x-modified Pt catalysts can also catalyze the selective cleavage of internal C–O bond to yield 1,3-propanediol [216–218].

The structure of Ir-ReO_x was proposed to involve a three-dimensional ReO_x clusters sitting on the surface of Ir nanoparticles based on catalyst

characterization results (Fig. 6a) [212,219,220]. Such a special configuration could provide an appropriate binding environment for hydride attack on the secondary carbon atom of glycerol, the kinetically-relevant step in the hydrogenolysis of glycerol to 1,3-propanediol (Fig. 6b). The reaction was proposed to proceed via a hydride attack mechanism analogous to that of THFA hydrogenolysis [214,220]. Glycerol first condenses with Re-OH species to form an adsorbed alkoxide intermediate, followed by heterolytic dissociation of H₂ to provide proton and hydride species. The latter attacks the secondary carbon atom of glycerol via a stable six-membered ring transition state, which induces the cleavage of secondary C–O bond to form an adsorbed 3-hydroxypropoxide intermediate. 1,3-propanediol is finally released by the hydrolysis of this intermediate accompanied by the regeneration of Re–OH species. Note that a distinct dehydration-hydrogenation mechanism was also proposed for the hydrogenolysis of glycerol into 1,3-propanediol in the presence of Pt-ReO_x and Pt-WO_x catalysts [216,221–223]. As indicated by kinetic results and catalyst characterization, Brønsted acid sites present on Pt-ReO_x and Pt-WO_x contribute to the hydrogenolysis of glycerol into 1,3-propanediol. The Brønsted acidity of Re–OH or W–OH species is believed to first dehydrate the secondary OH group in glycerol to form 3-hydroxypropionaldehyde or a secondary carbonium intermediate, followed by a hydrogenation step on Pt nanoparticles to yield 1,3-propanediol.

In contrast to the high selectivity of α,ω -diols obtained in the hydrogenolysis of furan-based alcohols and glycerol, the hydrogenolysis of complex polyols such as erythritol and sorbitol over Ir-ReO_x/SiO₂ usually affords diverse deoxygenated products with unsatisfactory selectivity towards desired α,ω -diols. For example, the hydrogenolysis of erythritol in the presence of Ir-ReO_x/SiO₂ (Ir/Re = 1) and H₂SO₄ at 100 °C after 24 h produced a mixture of monoalcohols, diols, and triols, mainly including 1,2,3-butanetriol (18% selectivity), 1,2,4-butanetriol (5% selectivity), 1,4-butanediol (33% selectivity), 1,3-butanediol (12% selectivity), 1-butanol (21% selectivity), and 2-butanol (6%

selectivity) [224]. The formation of desired product 1,4-butanediol, a high-value monomer, reached the highest selectivity (33%) at 24 h, and then declined with prolonging reaction time (Fig. 7a). The major product was shifted from 1,4-butanediol to 1-butanol at longer reaction

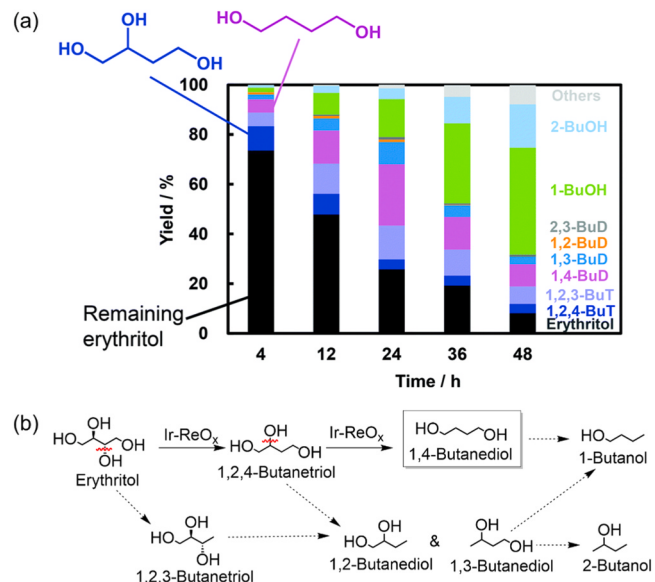


Fig. 7. (a) The evolution of product distributions for the hydrogenolysis of erythritol over Ir-ReO_x/SiO₂ (Ir/Re = 1) and H₂SO₄ at 100 °C under 8 MPa H₂; BuT = butanetriol, BuD = butanediol, BuOH = butanol; (b) Proposed reaction pathways for the selective hydrogenolysis of erythritol to 1,4-butanediol (solid arrow) and side reactions to other polyol products (dashed arrow). Adapted with permission from ref. [203 and 224].

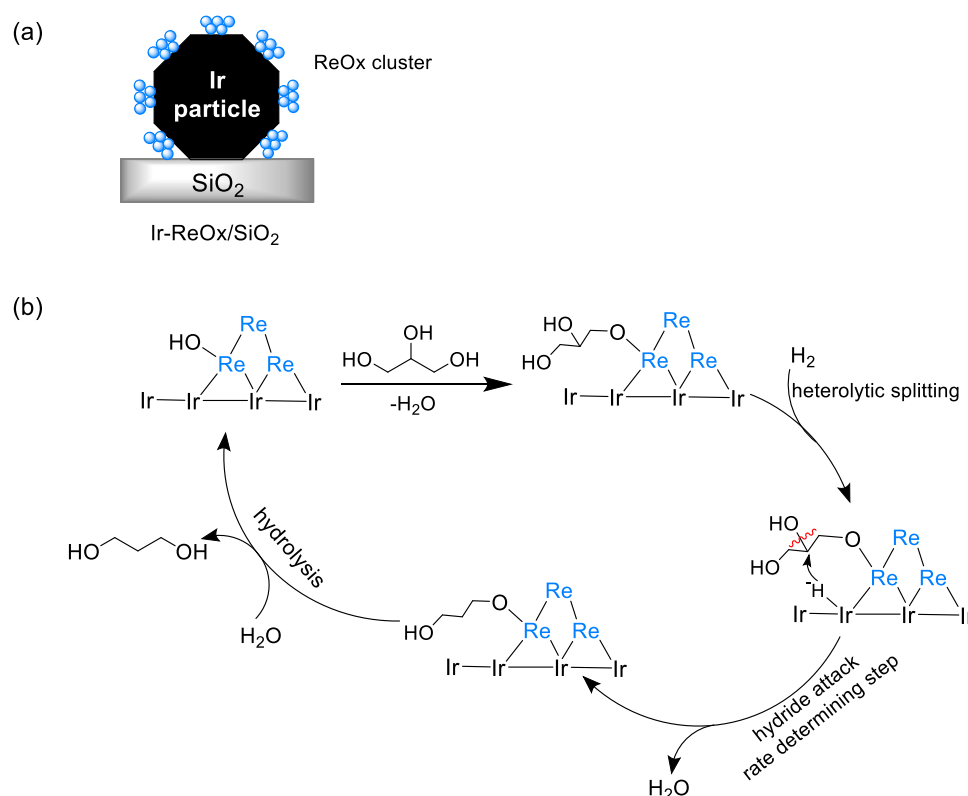


Fig. 6. (a) Proposed three-dimensional structures of ReO_x clusters dispersed on Ir nanoparticles in Ir-ReO_x/SiO₂; (b) Proposed mechanism for the selective cleavage of internal C–O bond in glycerol via a hydride attack mechanism over the interface of Ir nanoparticles and ReO_x clusters. Adapted with permission from ref. [214 and 219].

time (36 or 48 h), indicating the continuous C–O bond cleavage of 1,4-butanediol. A complex reaction network involving the tandem hydrogenolysis of C–O bonds in erythritol was proposed for the formation of monoalcohols, diols, and triols (Fig. 7b). The formation of 1,4-butanediol very likely arises from the successive secondary C–O bond cleavage reactions of erythritol via 1,2,4-butanetriol based on the aforementioned principle that the secondary C–O bond neighboring primary OH group is more easily to be cleaved. To improve the selectivity of 1,4-butanediol, competitive side reactions (e.g., overhydrogenoysis of 1,4-butanediol) need to be effectively suppressed either by tailoring catalyst structure/component or by tuning reaction conditions.

In the case of sorbitol, hexane (50.5% yield) was produced as the major product with minor amounts of 3-hexanol (35.6% yield) and 2-hexanol (7.7% yield) over $\text{Ir}-\text{ReO}_x/\text{SiO}_2$ at 140 °C after 75 h in water [184]. The total yield of hexanols (1-hexanol, 2-hexanol, 3-hexanol) could be improved to 60% by employing a biphasic medium (water-/decane) to inhibit the continuous hydrogenolysis [225]. Similarly, a wide spectrum of products including pentanols (1-pentanol, 2-pentanol, 3-pentanol), pentanediols (1,4-pentanediol, 1,3-pentanediol, 2,3-pentanediol), and pentanetriols were obtained when applying the internal C–O bond cleavage strategy to process xylitol in the presence of $\text{Pt}-\text{WO}_x/\text{SiO}_2$ [226]. Pentanols (1-pentanol, 2-pentanol, 3-pentanol) were generated as major products probably via the successive C–O bond cleavage of pentanetetraols, pentanetriols, and pentanediols. These complicated product distributions obtained from sorbitol and xylitol indicate that the hydrogenolysis reaction does not proceed as the expected selective cleavage of internal C–O bonds, probably due to the challenge of discriminating the targeted C–O bond among an ensemble of similar OH groups in sorbitol and xylitol.

In addition to the prevalent utilization of noble metals along with oxophilic metal oxides, non-noble metals (e.g., Ni) dispersed on strongly basic lanthanide oxides (La, Pr, Sm) have been demonstrated to facilitate the selective cleavage of internal C–O bonds in THFA [227,228]. For instance, Köckritz reported that Ni-La catalyst with a Ni/La ratio of 2.5 showed a high 1,5-pentanediol yield of up to 87.9% at 150 °C after 24 h in a batch reactor [228]. Under same reaction conditions, a similar high 1,5-pentanediol yield of 85.7% was also obtained over Ni-Pr, whereas Ni-Sm afforded a lower yield of 73.1%, probably due to its less basic sites (1144 vs. 1370 $\mu\text{mol/g}$). Moreover, Ni-La catalyst displayed excellent stability with maintained 1,5-propanediol yield at around 70% over 386 h on stream in a continuous flow reactor. The excellent performance of Ni-La catalyst was attributed to the bifunctional catalysis of basic sites on La hydroxides and H_2 activation sites on metallic Ni. As proposed in Scheme 28, basic sites promote the deprotonation of THFA to form an adsorbed alkoxide intermediate, which further undergoes hydride attack to trigger the selective cleavage of internal C–O bond. In contrast

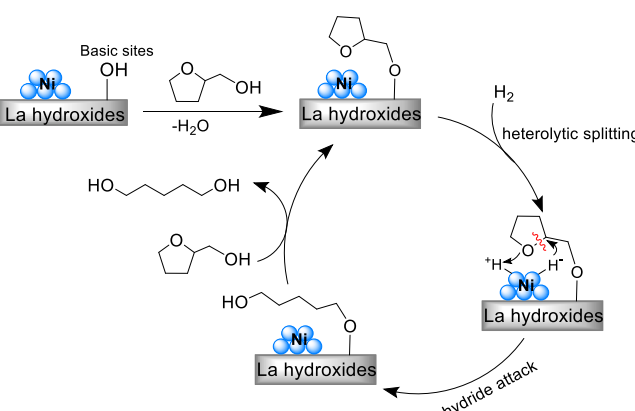
to the expensive and easily deactivated $\text{Ir}-\text{ReO}_x$ catalysts, the low cost and robust nature of Ni-La render it a very promising catalyst candidate for implementing the internal C–O bond cleavage strategy in practice.

It is important to mention that water is often employed as the solvent for aforementioned internal C–O bond cleavage reactions. Water seems to play roles in promoting the selective cleavage of internal C–O bond adjacent to primary OH group. For example, the hydrogenolysis of THFA over $\text{Ir}-\text{ReO}_x/\text{SiO}_2$ in water led to the exclusive formation of 1,5-pentanediol (97% selectivity) via breaking the internal C–O bond, whereas utilizing heptane as a solvent led to a lower 1,5-pentanediol selectivity of 50% with the formation of 1-pentanol (30% selectivity) [229]. Moreover, the hydrogenolysis reaction was retarded in heptane with a much slower reaction rate than that in water (2.4 vs. 28 $\text{mmol}_{\text{THFA}} \text{g}_{\text{cat}}^{-1} \text{h}^{-1}$). As mentioned above, the selective cleavage of internal C–O bonds was proposed to proceed via a hydride-attack mechanism involving H_2 heterolysis. The beneficial effect of using water as a solvent probably relates to the facilitated formation of proton and hydride species in water than non-polar alkane solvents, as discovered for the aqueous hydrogenolysis of carbonyl compounds [189,230,231]. This solvent-dependent reaction selectivity could be a result of the different adsorption configurations of THFA on $\text{Ir}-\text{ReO}_x/\text{SiO}_2$, that is, the preferential adsorption of primary OH group in water leads to the exclusive cleavage of internal C–O bonds, whereas in heptane THFA could be adsorbed at both primary OH group and cyclic O atom. Further mechanistic studies are required to clarify the beneficial effects of water in the hydrogenolysis of internal C–O bonds.

2.5. Summary of C–O bond cleavage strategies

Aforementioned four C–O bond cleavage strategies provide useful tools to depolymerize (hemi)cellulose, and more importantly, to tailor the oxygenated groups present in platform molecules towards targeted valuable products. In terms of reaction mechanism, both glycosidic bond hydrolysis and dehydration of OH groups simply utilize proton species as the catalytically active site to attack oxygen atoms, thus inducing the cleavage of C–O bonds. The reaction performance is primarily determined by the concentration of proton as well as the accessibility of OH group and glycosidic linkage. The latter factor is mirrored by the harsher reaction conditions applied for cellulose hydrolysis owing to the highly crystalline network of cellulose hampering the exposure of glycosidic linkage towards proton. As discussed above, the oxygen affinity (electrophilicity) of proton is considered as the key factor that leads to the cleavage of C–O bonds. However, the excellent oxygen affinity of proton enables the facile activation of both OH groups and glycosidic linkage without specificity in targeted groups. As a result, the hydrolysis of (hemi)cellulose, especially cellulose, is usually accompanied by the further dehydration of OH groups to form HMF. It remains a grand challenge to direct glycosidic bond hydrolysis and dehydration of OH groups towards targeted products by tuning the oxygen affinity of proton to differentiate specific oxygenated group (OH, glycosidic linkage). This is probably due to the similarly high reactivities of oxygenated groups to react with proton and also the lack of methods to regulate the oxygen affinity of proton. Therefore, by far the selectivity control of glycosidic bond hydrolysis and dehydration of OH groups is mainly realized by tuning reaction conditions (e.g., solvent, temperature, proton concentration), reactor design (flow-through reactor), and introducing stabilization reagents [232–234].

Mechanistically distinct from acid-catalyzed C–O bond cleavage strategies, both DODH and hydrogenolysis of internal C–O bond rely on the catalytic function of oxophilic metal oxides (ReO_x , WO_x , MoO_x) to bond OH groups for the activation/cleavage of specific C–O bond (Table 3). Unlike acid-catalyzed dehydration of OH groups showing poor selectivity control on reaction outcome, DODH is highly selective in removing adjacent OH groups to generate alkenes/dienes owing to the unique ability of oxophilic metal oxides to coordinate with paired OH groups. A prominent feature of DODH is that it can selectively



Scheme 28. Proposed reaction mechanism for the hydrogenolysis of THFA into 1,5-pentanediol over Ni-La catalysts. Adapted with permission from ref. [228].

Table 3

Comparison of different C–O bond cleavage strategies applicable to (hemi)cellulose and its derivatives.

	Bond type	Typical catalyst	Selectivity of bond cleavage	Typical product
Glycosidic bond hydrolysis		H ⁺	Non-specific	Sugar monomers
Dehydration of OH groups		H ⁺	Non-specific	Furanics
DODH of adjacent OH groups		ReO _x	Moiety specific	Alkenes, dienes, enol, furanics
Hydrogenolysis of internal C–O bond		M-MO _x	Moiety specific	α,ω-Diols

convert challenging feedstocks which contain a group of similar OH groups (e.g., polyols) into olefinic compounds. The reaction performance of DODH is mainly determined by the ability of oxophilic metal center to interact/abstract the oxygen atoms in diols, which can be tuned by optimizing the surrounding environments (e.g., ligands, supports) of metal center to reach appropriate electronic properties. Note that DODH typically necessitates a reductant (e.g., H₂, secondary alcohols) to promote the reduction of metal center. One issue related to the utilization of reductant is that it can compromise reaction selectivity toward alkenes by hydrogenating the double bond or etherifying with OH groups to form alkane or ethers, respectively.

Different from DODH, selective hydrogenolysis of internal C–O bond requires the synergistic catalysis of oxophilic metal sites and noble metals (M-MO_x). The former serves as a binding site for the terminal OH group to arrange the substrate adsorbed in a special configuration that facilitates the cleavage of C–O bond next to the terminal OH group. This C–O bond cleavage process is fulfilled by the active hydride species released from the heterolysis of H₂ over noble metals. Hence, the interface engineering of M-MO_x catalysts to have both OH-binding and H₂ activation sites is of pivotal importance for the selective hydrogenolysis of internal C–O bond. Despite displaying high specificity in breaking internal C–O bond to form α,ω-diols, the selective hydrogenolysis strategy is mainly applicable to simple polyols containing one internal C–O bond such as glycerol and furfuryl alcohol. It's still very challenging to realize the selective hydrodegenolysis of specific C–O bond in complex polyols containing multiple OH groups, which needs the development of novel catalysts/strategies to impose selectivity control in activating and breaking a cluster of similar C–O bonds (OH groups).

3. C–C bond cleavage strategies

The majority of (hemi)cellulose-derived C6/C5 platform molecules such as glucose, xylose, sorbitol, gluconic acid, and HMF bear a long carbon skeleton containing multiple C–C bonds. Catalytic upgrading of these platform molecules often involves an essential step of breaking their carbon skeletons, which can open the access to valuable short-chain chemicals such as ethylene glycol, butanediol, lactic acid, formic acid, etc. It should be noted that C–C bonds are inherently stable owing to the nonpolarized nature of C–C σ bonds. The bond dissociation energy of C–C connection is estimated to be as high as 305–330 kJ/mol [235]. In order to realize the efficient cleavage of robust C–C bonds, considerable effort has been devoted to the development of high-temperature fragmentation of (hemi)cellulose and its derivatives such as gasification and pyrolysis [236–238]. However, these thermochemical methods are limited by uncontrolled cleavage of C–C bonds thus giving complex product distributions. Notably, (hemi)cellulose-derived C6/C5 molecules contain multiple C–C bonds featuring very similar reactivities and chemical environments, which allow C–C bond cleavage occurring at multiple positions in the carbon backbone. Despite these challenges, pursuing reaction strategies capable of cleaving

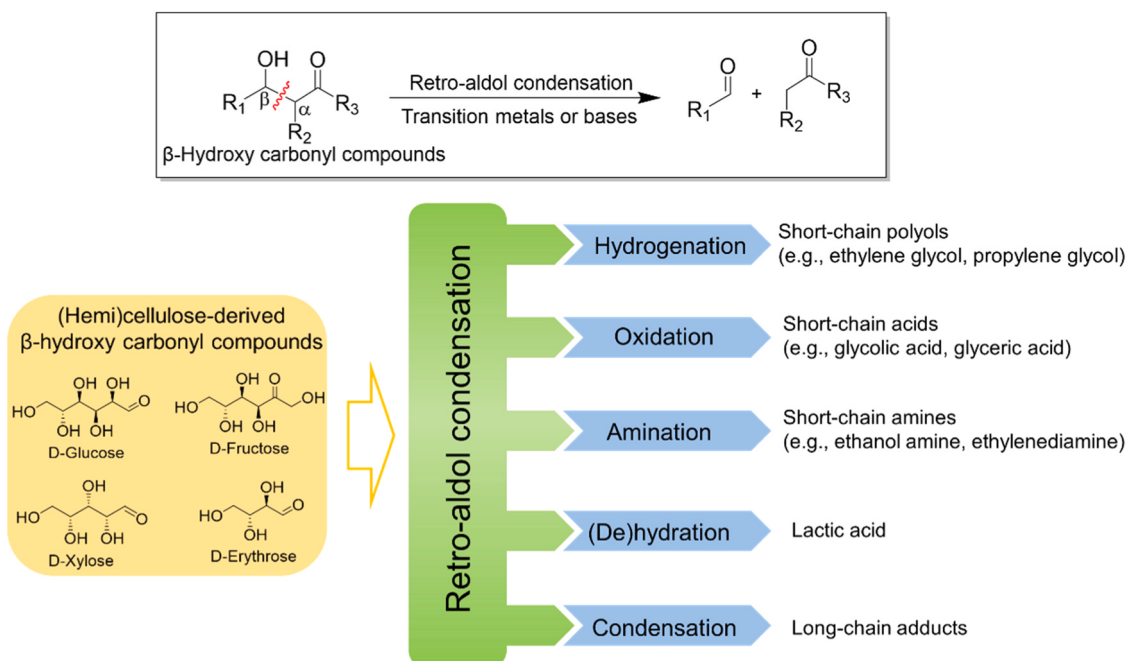
specific C–C bonds in a selective manner is a long-standing goal in the field of (hemi)cellulose valorization. So far, several reaction strategies based on reverse C–C coupling reaction, e.g., retro-aldol fragmentation, the elimination of leaving groups, e.g., decarbonylation/decarboxylation, as well as oxidative cleavage have been identified as effective methods for the selective cleavage of C–C bonds of (hemi)cellulose and its derivatives. Details of these methods and especially their broad applications in transforming (hemi)cellulose derivatives to small oxygenated molecules will be presented separately in the following sections.

3.1. Retro-aldol condensation

Retro-aldol condensation (RAC), also called retro-aldol fragmentation, literally refers to the backward reaction of aldol reaction, a classic C–C coupling reaction in organic chemistry. With the assistance of base or transition metal catalysts, RAC is able to break the carbon skeleton of β-hydroxy carbonyl compounds into small carbonyl compounds, e.g., ketones and aldehydes (Scheme 29). Notably, RAC can selectively break the specific C_α–C_β bond of β-hydroxy carbonyl compounds. Carbonyl and hydroxyl groups constitute the substructure of many biomass-derived molecules. Therefore, RAC is perceived as a very useful strategy to break the C–C bond of (hemi)cellulose-derived chemicals like sugars and sugar alcohols. Considerable attention has been paid to unlock the potential of RAC in the field of (hemi)cellulose valorization. However, the generated products from RAC, for example, glycolaldehyde and glyceraldehyde, bear highly active aldehyde groups, which are liable to undergo side reactions such as re-condensation and dehydration to form humins. To address this issue, RAC is usually coupled with other reactions including hydrogenation, oxidation, amination, (de)hydration, condensation to transform the in situ formed RAC products into corresponding stable molecules (Scheme 29). For instance, the hydrogenation of glycolaldehyde gives rise to relatively stable ethylene glycol, a commodity chemical for polymer industry [239,240]. Following this strategy, a number of bio-based synthesis routes relying on the combination of RAC with diverse reactions have been established targeting short-chain chemicals such as ethylene glycol, propylene glycol, butanediol, lactic acid, glycolic acid, erythrose, ethanol, ethanol amine, etc (Scheme 29).

3.1.1. RAC of sugar and sugar alcohol

Already before being considered as a selective C–C bond scission method, RAC had been proposed as one important reaction mechanism for the catalytic hydrogenolysis of sugar alcohols into small polyols (e.g., ethylene glycol, propylene glycol, butanediol) in the presence of supported metal catalysts and basic additives (e.g., Ca(OH)₂) [241–243]. This proposal was experimentally verified by Hawley et al., who employed a series of 1,3-diols bearing different moieties as model compounds for control experiments [244]. Molecular structures of the detected reaction intermediates and products from different 1,3-diols

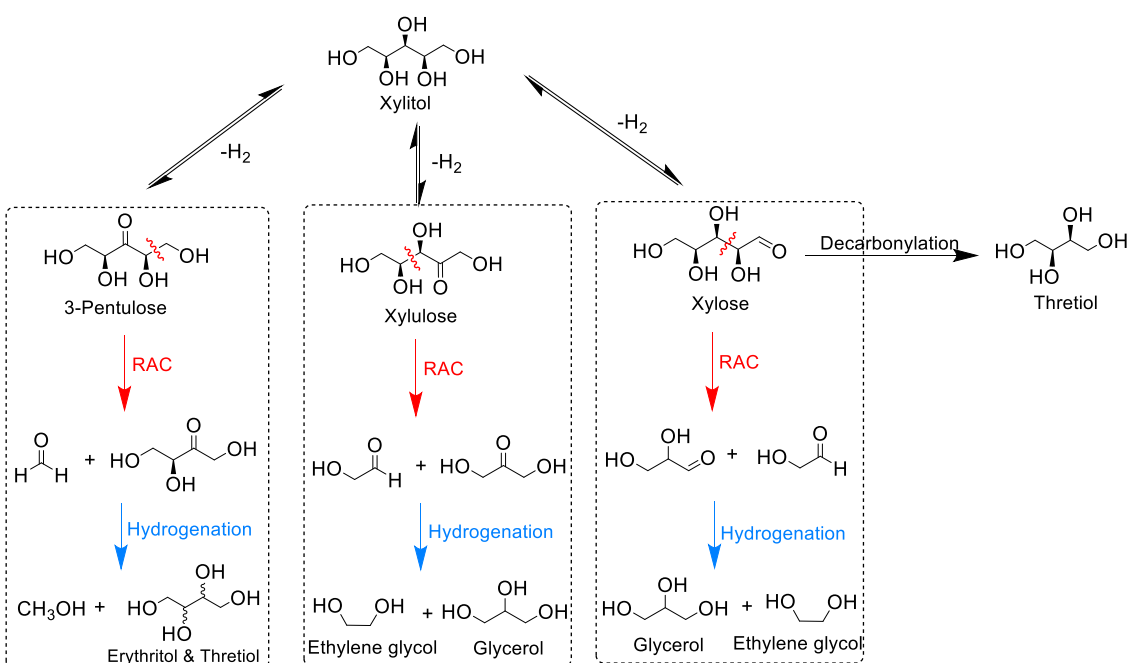


Scheme 29. Retro-aldol condensation and its combination with other reactions for the transformation of (hemi)cellulose derived sugars into various short-chain chemicals of high value.

are perfectly consistent with that predicted by RAC mechanism. Another important finding from this study is that the dehydrogenation of sugar alcohol is a necessary step prior to the occurrence of RAC, since sugar alcohol does not meet the structural demand of RAC, that is, the existence of carbonyl moiety. Hence, sugar alcohols hydrogenolysis under basic conditions is believed to proceed mainly via metal-catalyzed dehydrogenation followed by RAC on basic sites. Shanks and co-workers systematically investigated the catalytic hydrogenolysis of C3–C6 sugar alcohols at 240 °C in the presence of Ru catalysts and CaO [245]. The authors discovered that the obtained products are a mixture of polyols with carbon atoms ranging from one to six, despite RAC being

selective in breaking C–C bonds. This is mainly due to the concurrent occurrence of many competitive reactions such as dehydration, dehydrogenation, decarbonylation, isomerization. Among these reactions, decarbonylation offers another important method to break the terminal C–C bond linked to an aldehyde moiety (to be discussed later).

The dehydrogenation of OH groups at different carbon atoms determines the position of C–C bond cleavage during the RAC of sugar alcohols, thus generating various fragmented products. Taking xylitol as an example (Scheme 30), the initial dehydrogenation could in principle occur at three different carbon atoms, thus leading to three isomers including xylrose, xylulose, and 3-pentulose [246]. Terminal OH groups



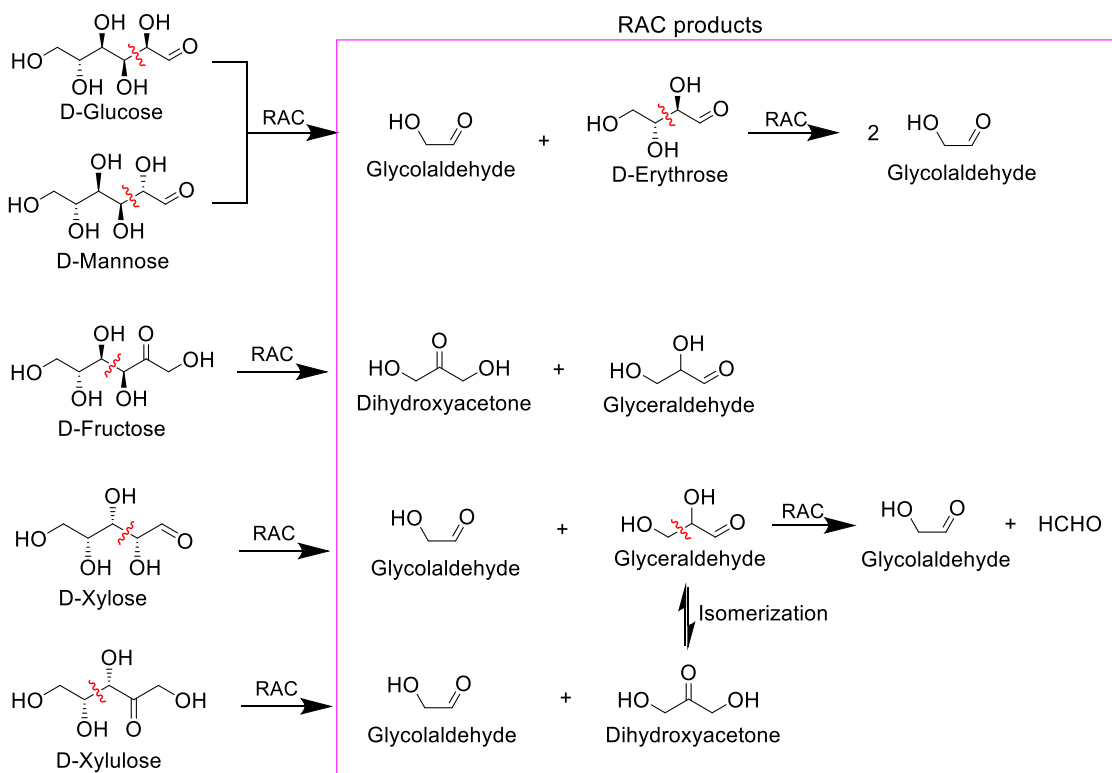
Scheme 30. Proposed reaction pathways for the hydrogenolysis of xylitol into short-chain polyol products via cascade dehydrogenation/RAC/hydrogenation reactions. Adapted with permission from ref. [246].

have been proven more liable to undergo dehydrogenation than inner OH groups. Xylitol dehydrogenation into xylose and xylulose are therefore more favorable than into 3-pentulose. Among these pentose isomers, xylose featuring a terminal carbonyl group can also undergo decarbonylation to yield a C4 sugar alcohol (i.e., threitol). According to the principle of RAC, three types of RAC reactions can theoretically occur considering the presence of three different carbonyl groups in these sugar intermediates. These RAC reactions can give rise to a series of carbonyl intermediates (i.e., C1/C4, C2/C3, C3/C2 fragments), which can be further reduced into corresponding short-chain polyol products (**Scheme 30**). The observed product composition is related to the kinetic competition of decarbonylation and RAC as well as the position of initial dehydrogenation, which in turn are determined by the employed reaction parameters, catalysts, and substrate structure. For example, the hydrogenolysis of sorbitol was found to occur mainly via decarbonylation over sulfur-modified Ru catalysts, whereas unmodified Ru catalysts favored the hydrogenolysis of sorbitol via RAC [242,245]. Generally, under neutral conditions the C–C bond scission of sugar alcohols prefers to proceed via decarbonylation, while RAC becomes predominant under basic conditions using, for example, calcium oxides as catalyst. For more details, the reader is referred to other studies focusing on sugar alcohols hydrogenolysis [247–254]. In short, RAC plays an important role in the C–C bond scission of sugar alcohols but unable to control product distribution owing to the complex reaction network.

In comparison to sugar alcohols, sugars appear as more suitable substrates for RAC, since the RAC of sugars can occur directly without the prior dehydrogenation step. Avoiding the dehydrogenation step reduces the chance of diverse RAC reaction routes (as depicted for xylitol in **Scheme 30**), thus leading to improved selectivity towards target C2 and C3 products. With regard to the application of RAC in converting sugars, considerable research attention has been focused on the C–C bond cleavage of glucose and xylose, two main sugar units in biomass. According to the rule of RAC, the C–C bond cleavage of glucose can only occur at the C2–C3 bond of glucose, affording glycolaldehyde as the C2

product and erythrose as the C4 product (**Scheme 31**). The latter may continue to undergo RAC reaction at the C2–C3 bond of erythrose, ultimately yielding two glycolaldehyde molecules. Therefore, one glucose molecule can in principle be fully converted into three glycolaldehyde molecules without the formation of other C–C bond cleavage products. Evidently, the RAC reaction of glucose is characterized by excellent atom economy and C2/C3 product selectivity. Note that the generated glycolaldehyde has recently been proposed as a novel C2 platform chemical that can open up new opportunities for the synthesis of C2 commodity chemicals from biomass [4]. The RAC of mannose, the epimer of glucose, follows an exactly same pathway as that of glucose, since the position of carbonyl moiety in glucose and mannose remains identical. The RAC of xylose, a C5 aldose, occurs at the C2–C3 bond, yielding equimolar C2 (glycolaldehyde) and C3 (glyceraldehyde) products. Glyceraldehyde can continue to undergo RAC leading to the production of glycolaldehyde and formaldehyde as the final products (**Scheme 31**). In addition, when applying RAC to convert fructose, a C6 ketose with an interior carbonyl group, the C3–C4 bond cleavage of fructose will occur, thus affording two C3 products of glyceraldehyde and dihydroxyacetone (**Scheme 31**). These two isomers are present in equilibrium and can be cracked into glycolaldehyde and formaldehyde by RAC. Similarly, the RAC of xylulose also follows the C3–C4 bond cleavage, but leads to the same C2 + C3 products (glycolaldehyde and dihydroxyacetone) as that of xylose (**Scheme 31**).

Generally, the RAC of glucose and xylose occurs under moderate reaction conditions (150–250 °C) in the presence of base or transition metal catalysts. Considering the fact that catalytic RAC is mostly utilized in combination with other reactions to constitute tandem protocols, the catalytic RAC of sugars will be discussed in the following sections dedicated to various reaction coupling processes. Notably, the RAC reaction of sugars can also proceed in the absence of catalysts. In this regard, many researches have highlighted the selection of subcritical or supercritical water as a beneficial medium to enable the non-catalytic RAC reaction (**Table 4**) [255–258]. For example, Sasaki et al. reported that the RAC of glucose assisted by supercritical water (450 °C, 35 MPa)



Scheme 31. The RAC of sugars into various C2/C3/C4 products.

Table 4

A summary of the non-catalytic RAC of glucose and xylose into oxygenated products.

Substrate	Reactor	Major Product	Reaction medium	Temp. (°C)	Time	Pressure	Yield (%)	Ref.
Glucose	Tubular	Glycolaldehyde	Supercritical water	450	0.25 s	350 bar	63.8	259
Glucose	Tubular	Glycolaldehyde	Supercritical water	400	20 s	230 bar	85	258
Glucose	Fluidized bed	Glycolaldehyde	Water vapor	525	1 s	N ₂ /1 bar	74	266
Glucose	Flask	Glycolaldehyde	Isosorbide dimethylether	250	30 min	N ₂ /1 bar	56	260
Xylose	Tubular	Glycolaldehyde	Supercritical water	450	0.96 s	350 bar	38.4	263
Xylose	Tubular	C1-C3 oxygenates ^a	Supercritical water	400	0.82 s	400 bar	46.6	262

^a a mixture of RAC products including glyceraldehyde, glycolaldehyde, dihydroxyacetone, pyruvaldehyde, formaldehyde and lactic acid.

in a continuous flow reactor afforded glycolaldehyde in a high selectivity of 64.2% [259]. Water density was proposed as the main factor to determine glycolaldehyde selectivity. A very low water density of 0.2 g/mL under supercritical conditions (450 °C, 35 MPa) was believed to promote the RAC of glucose. Moreover, it was found that other side reactions like the dehydration and isomerization of glucose were greatly suppressed at lower water density. The underlying reason for the promoting effect of decreased water density was attributed to the favorable formation of intramolecular hydrogen bonds within glucose molecules, an essential step proposed for the non-catalytic RAC of glucose, as shown in **Scheme 32**. The reduced water density would decrease the intermolecular hydrogen bonds between water and glucose, thus facilitating the formation of intramolecular hydrogen bonds within glucose molecules.

In addition to supercritical water, polyethers such as isosorbide dimethylether was discovered as an efficient medium for the non-catalytic RAC of glucose [260]. At a much lower temperature of 250 °C and atmospheric pressure, 56% yield of glycolaldehyde could be obtained in 30 min. Slightly lower yields (35–40%) were also obtained for other polyethers including tetraethyleneglycol dimethylether and 18-crown-6. This unique function of polyethers was attributed to the basicity of oxygen atoms in polyethers that can interact with OH groups of glucose through hydrogen bonding.

Unlike the high glycolaldehyde selectivity obtained for the RAC of glucose, the non-catalytic RAC of xylose under supercritical water conditions usually give rise to a mixture of glyceraldehyde, glycolaldehyde, and formaldehyde as the major RAC products [261–265]. In addition, two side products including furfural (dehydration) and xylulose (isomerization) were also observed. Similar to the finding for glucose, the product distribution of xylose is also strongly influenced by water density. Lower water densities are advantageous to the formation of RAC products, while high water densities favor the dehydration and isomerization of xylose to furfural and xylulose, respectively. For instance, Matsumura et al. reported that glycolaldehyde was dominated among all products in a yield of 38.4% at a low water density of 0.11 g/mL under supercritical conditions (450 °C, 35 MPa) [263]. By contrast, when performing the conversion of xylose under hydrothermal or subcritical conditions with water densities above 0.6 g/mL, furfural and xylulose were usually detected as major products.

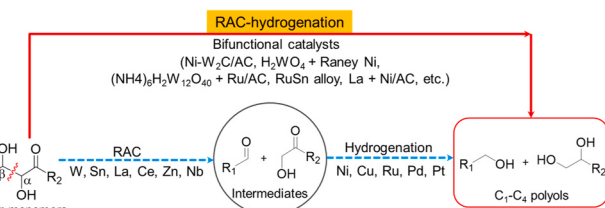
High-temperature cracking (i.e., pyrolysis) of glucose under atmospheric pressure represents another feasible approach to enable the non-catalytic RAC of sugars. For example, Schandl and coworkers reported a very efficient and selective continuous RAC process, wherein aqueous sugar solution was sprayed into a fluidized bed reactor loaded with glass beads under N₂ fluidization at 525 °C [266]. In the case of glucose solution, glycolaldehyde was generated following the pathway in **Scheme**

31 in a high yield of 74% in very short residence time (ca. 1 s). The carbon yield of all carbon-containing products in liquid phase can amount to 95% along with a small amount of other detected C2/C3 oxygenated products including glyoxal, formaldehyde, pyruvaldehyde, acetol, and acetic acid. Besides, this process holds great potential in terms of practical application, since it can deal with concentrated glucose solution up to 40 wt% while maintaining glycolaldehyde yields at around 70% for 90 h on stream.

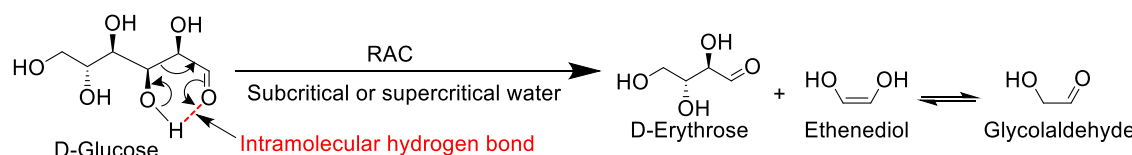
3.1.2. RAC coupled with various reactions

RAC-hydrogenation.

As aforementioned, the RAC products generated from sugars bear reactive hydroxyl and carbonyl moieties which tend to undergo various degradation or re-condensation. One straightforward option to address this issue concerns the instant hydrogenation of these reactive RAC products into stable polyol products under H₂ atmosphere. For instance, glycolaldehyde and glyceraldehyde, two representative RAC products of sugars, can be readily reduced into ethylene glycol and glycerol, respectively. Therefore, the combination of RAC with subsequent hydrogenation (RAC-hydrogenation) in one pot offers new routes to synthesize bio-based C2–C3 polyols directly from (hemi)cellulose and its derivatives (**Scheme 33**). The successful implementation of RAC-hydrogenation requires the design of bifunctional catalysts capable of promoting both RAC and hydrogenation reactions. Catalytic hydrogenation of RAC products primarily involves the reduction of their carbonyl groups, which can readily occur over commonly-used transition metal catalysts (i.e., Ni, Cu, Ru, Pt). In contrast, the first RAC step is more difficult in terms of reaction kinetics, as indicated by the higher apparent activation energy of the RAC of glucose (140–160 kJ/mol) than that of glycolaldehyde hydrogenation (35–45 kJ/mol) [267–269]. RAC is traditionally catalyzed by various base catalysts, mainly inorganic bases, e.g. Ca(OH)₂, NaOH, NH₄OH, and Ba(OH)₂ [250,270]. However, such basic reaction conditions are not compatible with the



Scheme 33. Selective fragmentation of sugar monomers into short-chain polyols by combining RAC with hydrogenation over bifunctional catalysts.



Scheme 32. Proposed reaction mechanism for the RAC of glucose in supercritical or subcritical water promoted by intramolecular hydrogen bonds. Adapted with permission from ref. [257].

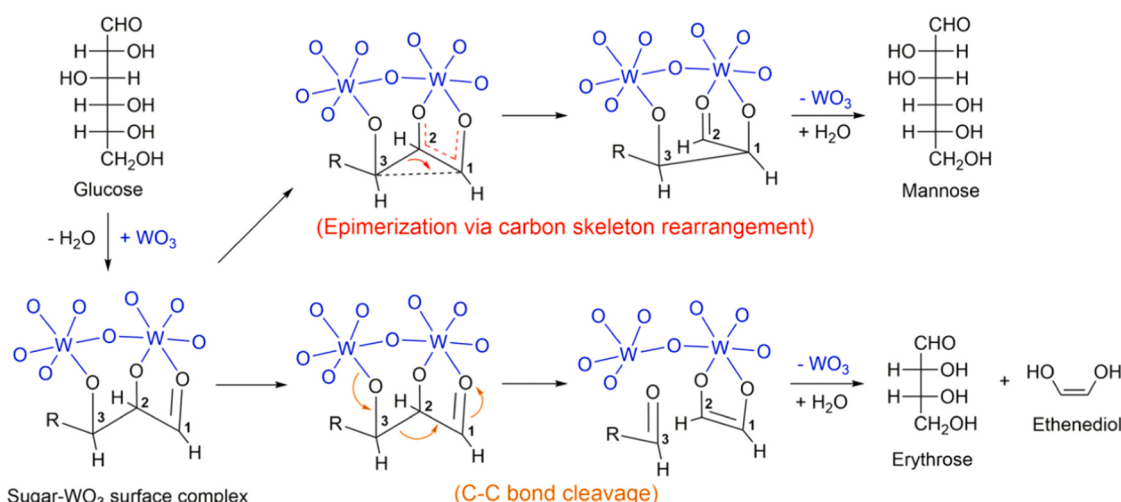
conventional biomass depolymerization processes, for example, acid-catalyzed hydrolysis of cellulose and hemicellulose. In addition, side reactions like glucose isomerization will be facilitated under basic conditions, further complicating the product distribution, as aforementioned for sugar alcohol hydrogenolysis.

In the last decade, significant advancements have been achieved in developing non-base RAC catalysts relying on transition metals. Pioneering work in this direction was done by Zhang and coworkers, who developed a series of tungsten-based catalysts for the RAC of glucose, fructose, and cellulose [271,272]. It was found that tungsten species is uniquely active for the RAC reaction of various sugars, irrespective of the type of tungsten compounds, i.e., tungsten oxides [273–275], tungsten carbide [19,276,277], tungsten phosphide [278], metallic tungsten [20,279], tungstates [280], tungstic acids [281,282]. These tungsten compounds were found to undergo in situ reduction by H_2 during the reaction to generate water-soluble tungsten bronze (H_xWO_3), a reduced form of tungsten oxide, as indicated by X-ray powder diffraction (XRD) [282]. The dissolved H_xWO_3 was proposed as the truly active species for the RAC reaction proceeding in a homogeneous manner. Despite the absence of a clear picture of tungsten-catalyzed reaction mechanism, it is widely believed that the reduced tungsten oxides featuring oxygen vacancies are able to activate and break glucose molecules (i.e., C2–C3 bond cleavage) probably by coordinating with the oxygen-containing moieties (hydroxyl and carbonyl) of glucose [283,284].

Based on spectroscopic results and kinetic analysis, Liu and coworkers recently proposed a key glucose- WO_3 intermediate, wherein the carbonyl and two adjacent OH groups of glucose bind with two vicinal W atoms (W-O-W sites) to form a tridentate glucose- WO_3 complex (Scheme 34) [273,285]. Within this complex, the C2–C3 bond of glucose is weakened and easily undergoes cleavage to form C2 and C4 products. It was found that glucose could also undergo epimerization (also known as the Bilik reaction) by shifting the position of C1 and C2 atoms to yield mannose in the presence of WO_3 . The epimerization step is believed to share the same tridentate glucose- WO_3 complex as the RAC of glucose (Scheme 34). It seems that there exists a close correlation between epimerization and RAC, since several transition metals capable of facilitating glucose epimerization including W, Mo, La, and Sn have been discovered as efficient catalysts for the RAC of glucose [279, 285–290]. Moreover, Liu and coworkers claimed that the C2–C3 bond cleavage of glucose does not conform to the widely-accepted RAC pathway [285]. This is based on the finding that glucose without α -OH group (2-deoxy-glucose) merely underwent hydrogenation to form 2-deoxy-sorbitol instead of fragmented products (ethanol and

erythritol). Likewise, only 3-deoxy-sorbitol was obtained when utilizing glucose without β -OH group (3-deoxy-glucose) as the substrate. Apparently, the C2–C3 bond cleavage of glucose over WO_3 entails the presence of both α - and β -OH groups, which is distinct from the classical RAC that generally requires the presence of β -OH group only. Conclusive evidences of monitoring the evolution of tungsten species and detecting tungsten-sugar complexes by in situ characterization techniques at a molecular level are needed to verify these mechanistic conjectures.

Since the disclosure of the unique activity of tungsten species towards RAC by Zhang and coworkers [19,20], tungsten-based catalysts have been intensively explored for RAC-hydrogenation (Table 5). Zhang et al. first reported the synergistic catalysis of tungsten-based catalysts with hydrogenation catalysts in converting cellulose and glucose into ethylene glycol [19]. They designed a bifunctional nickel-promoted tungsten carbide (Ni-W₂C/AC) catalyst for the direct conversion of lignocellulose into ethylene glycol (termed DLEG), giving a high ethylene glycol yield of 61% at 245 °C under 6 MPa H_2 . By contrast, using Ni/AC catalyst without tungsten species afforded a very low ethylene glycol yield of 5.8%, indicating the key role of tungsten in catalyzing the RAC of glucose. As shown in Scheme 35, this novel DLEG process is a three-step cascade reaction involving cellulose hydrolysis to glucose, glucose to glycolaldehyde via RAC, glycolaldehyde hydrogenation to ethylene glycol. The first hydrolysis step is fulfilled by the protons released from high temperature water and H_2 splitting over Ni. The second RAC step is catalyzed by W₂C, and Ni is responsible for the final hydrogenation of glycolaldehyde. This excellent selectivity towards ethylene glycol is attributed to the synergy catalysis of protons, W₂C, and Ni, leading to well-matched reaction kinetics of hydrolysis, RAC, and hydrogenation steps. Obviously, the successful implementation of RAC-hydrogenation strategy lies in the rational combination of hydrogenation and RAC catalysts. Following this pioneering work, intensive efforts have been dedicated to optimize tungsten-based catalysts by tailoring tungsten species, hydrogenation metals, supports, and trying other preparation methods [20,273,276,277,279,281,282, 291–298]. Some of these optimized tungsten catalysts exhibited improved performance with excellent ethylene glycol yields ranging from 70 to 89% [20,276,291,293,297]. Among these tungsten-based catalysts, there exist two promising examples for practical application, that is, H_2WO_4 + Raney Ni and ammonium metatungstate (AMT) + Ru/C (Table 5) [280,281]. The former can be reused up to 18 times for the RAC-hydrogenation of cellulose while maintaining ethylene glycol yield around 60% in a batch reactor [281]. The combination of AMT and Ru/C has been demonstrated to catalyze the RAC-hydrogenation of glucose to ethylene glycol (ca. 60% yield) in a semi-continuous batch

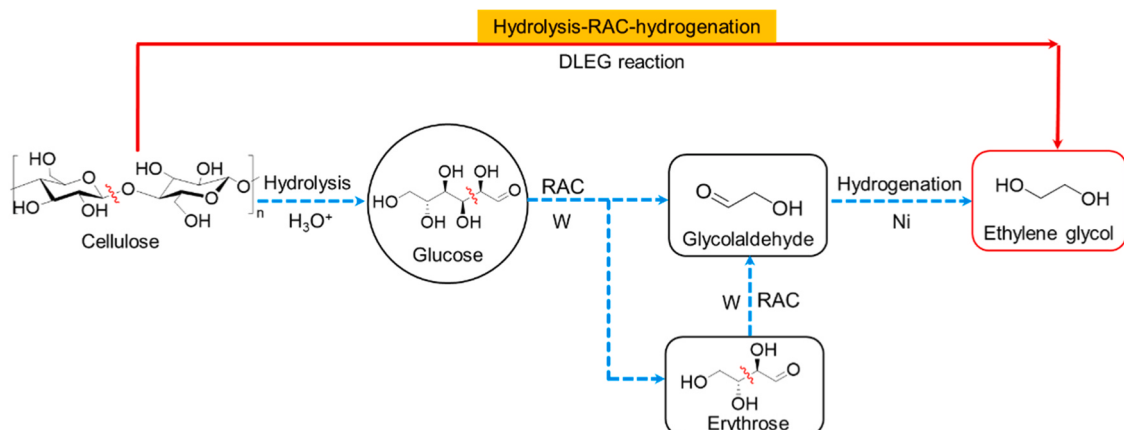


Scheme 34. Proposed reaction mechanism for WO_3 -catalyzed fragmentation and epimerization of glucose via a tridentate glucose- WO_3 complex. Reproduced with permission from ref. 285.

Table 5

Representative catalyst systems for the RAC-hydrogenation of sugars into ethylene glycol and 1,2-propylene glycol.

Substrate	Catalyst	Temp. (°C)	Time (min)	Pressure of H ₂ (bar)	Conv. (%)	Yield (%)		Ref.
						Ethylene glycol	1,2-Propylene glycol	
Cellulose	Ni-W ₂ C/AC	245	30	60	100	61	7.6	19
Cellulose	Ni-W/SBA-15	245	30	60	100	76.1	3.2	20
Cellulose	WO ₃ + Ru/C	205	30	60	23.4	12.1	1.6	273
Cellulose	H ₂ WO ₄ + Raney Ni	245	30	60	100	65.4	3.3	281
Glucose	AMT + Ru/C	240	40	50	100	60	6.9	280
Cellulose	Sn powder + Ni/AC	245	95	50	100	57.6	9.2	299
Cellulose	Ni-Ir/La ₂ O ₃	245	150	50	100	46.6	17.1	302
Glucose	RuSn/AC	240	10	50	100	26.9	25	300
Inulin	Ni-W ₂ C/AC	245	80	60	100	6.8	36.4	303
Glucose	Pd-WO _x /Al ₂ O ₃	180	—	40	92.2	5.3	56.1	307
Cellulose	Ni/ZnO	245	120	60	100	19.1	34.4	308

Scheme 35. Direct conversion of lignocellulose into ethylene glycol through a cascade hydrolysis/RAC/hydrogenation route over Ni-W₂C/AC.

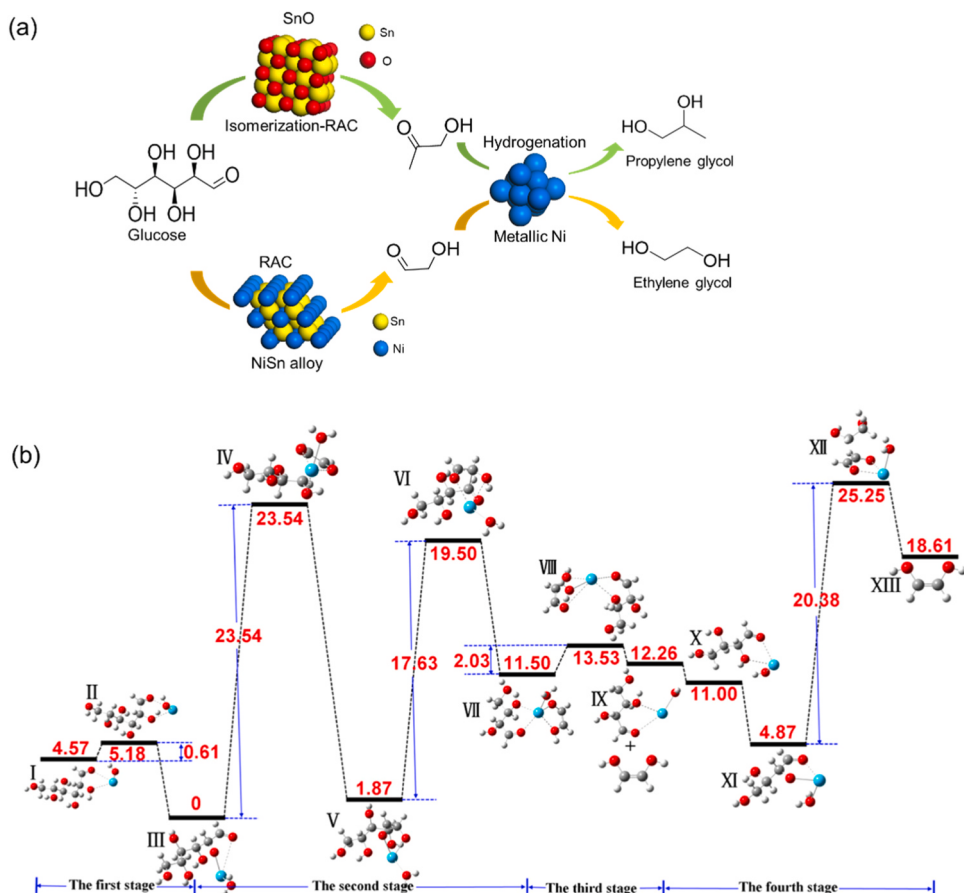
reactor which can handle concentrated glucose streams (10–50 wt%) [280].

Apart from tungsten-based catalysts, a number of non-tungsten catalysts relying on Sn, La, Ce, Nb and Zn, have been reported for the RAC-hydrogenation of cellulose into ethylene glycol and propylene glycol. Sun et al. reported a highly efficient AC-supported NiSn alloy catalyst containing NiSn alloy and metallic Ni nano-particles, affording a high ethylene glycol yield of 57.6% at 245 °C under 5 MPa H₂ in 95 min [299]. The slightly positively charged Sn species in NiSn alloy has been identified as the active site for the RAC of glucose into glycolaldehyde, while metallic Ni particles are responsible for the following hydrogenation, as shown in Scheme 36a. The authors also discovered the high activity of SnO together with Ni/AC for the RAC-hydrogenation of cellulose (Scheme 36a). However, this composite catalyst favored the formation of 1,2-propylene glycol (32.2% yield) rather than ethylene glycol (22.9% yield). It was revealed that Sn(II) species possesses dual catalytic functions, that is, glucose isomerization to fructose and RAC, which could account for the dominated formation of 1,2-propylene glycol via an isomerization-RAC-hydrogenation pathway (Scheme 36a). Analogous to Ni-Sn catalysts, Ru-Sn catalysts were reported to catalyze the RAC-hydrogenation of glucose into 1,2-propylene glycol (25% yield) and ethylene glycol (26.9% yield) at 245 °C in 10 min [300]. As indicated by RuSn catalyst characterization, most Sn components existed in the form of RuSn alloy, which was identified as the active sites for RAC and hydrogenation. The rest well-dispersed SnO₂ species was proposed to promote the isomerization of glucose to fructose. Wang et al. reported the selective conversion of cellulose to ethylene glycol and its mono-ether in an overall yield of 64% in methanol over a Ru-Ni/NbOPO₄ catalyst at 220 °C under 3 MPa H₂ in 20 h [301]. NbOPO₄ support was believed to provide catalytically active sites for the RAC of glucose, while Ru-Ni sites are responsible for the hydrogenation of

glycolaldehyde.

Sun and coworkers designed a Ni-La catalyst by dispersing Ni nanoparticles onto La₂O₃ for the RAC-hydrogenation of cellulose into ethylene glycol in a yield of 46.6% [302]. In addition, the physical combination of soluble La salts (e.g., La(NO₃)₃, La(OAc)₃) with Ni/AC showed similar activity as Ni/La₂O₃. The dissolved La(III) cations were therefore considered as the catalytically active sites for RAC, while Ni nanoparticles are responsible for the subsequent hydrogenation. A detailed mechanistic picture for La(III)-catalyzed RAC of glucose was gained based on DFT calculations and experimental results. As shown in Scheme 36b, La(III) cations are present in the form of La(III)-OH species owing to its easy hydrolysis in water. The complexation of La(III)-OH into glucose at C1 and C2 atoms leads to the first epimerization of glucose into mannose through a 1,2-intermolecular carbon shift. Subsequently, an intramolecular 2,3-hydride shift triggers the C2-C3 bond cleavage of mannose, yielding equivalent glycolaldehyde and erythrose. The latter could further undergo a direct C2-C3 bond cleavage to form two molecules of glycolaldehyde without the epimerization step. The epimerization of glucose to mannose is the rate-determining step for the whole reaction owing to the highest activation barrier of 23.54 kcal/mol.

In addition to glucose and cellulose, the selective breakage of fructose-enriched inulin was explored with Ni-W₂C/AC catalyst, generating 1,2-propylene glycol and glycerol instead of ethylene glycol as the major products [303]. At 245 °C under 6 MPa H₂, 1,2-propylene glycol and glycerol were obtained in a yield of 36.4% and 22.3%, respectively, whereas ethylene glycol was produced in a low yield of only 6.8%. Such a different product distribution is related to the special composition of inulin that bears a high fraction of fructose. As aforementioned, ethylene glycol arises from the RAC of glucose, while C3 polyols like glycerol and 1,2-propylene glycol arises from the RAC of fructose. Based on the

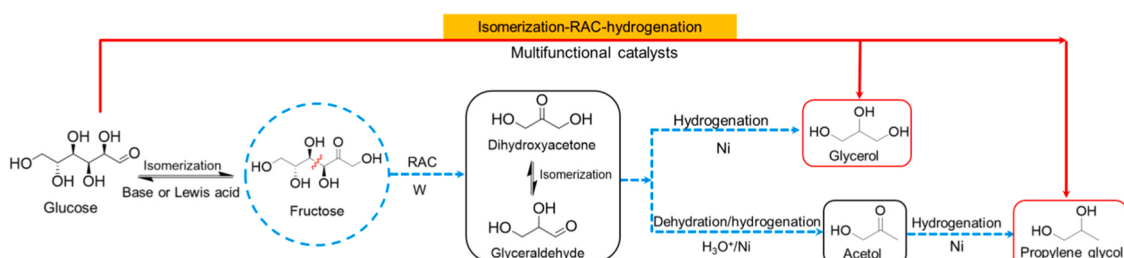


Scheme 36. (a) Selectivity-switchable fragmentation of glucose into ethylene glycol and propylene glycol over binary Ni-Sn catalysts; (b) Reaction mechanism and energy diagram calculated by DFT for La-catalyzed RAC of glucose to glycolaldehyde; La atoms in cyan, O atoms in red, C atoms in dark grey, H atoms in light grey. Reproduced with permission from ref. [299 and 302].

results of control experiments, reaction pathways towards glycerol and 1,2-propylene glycol were proposed in **Scheme 37**. Fructose first undergoes a C3-C4 bond cleavage via the RAC to yield glyceraldehyde and dihydroxyacetone as two major C3 fragments. Glyceraldehyde was proposed as the precursor to glycerol, since it can be readily hydrogenated to glycerol. The formation of 1,2-propylene glycol was believed to arise from the hydrogenation of acetol, a detected intermediate from the sequential dehydration and hydrogenation of glyceraldehyde/dihydroxyacetone.

As aforementioned for Sn-catalyzed RAC, 1,2-propylene glycol can also be produced directly from glucose by introducing an isomerization step to first transform glucose into fructose, following a cascaded isomerization-RAC-hydrogenation pathway (**Scheme 37**). In addition to RAC and hydrogenation catalysts, bases or Lewis acids, typically used to catalyze glucose isomerization [304–306], are needed to realize this multistep process. For example, ethylene glycol was obtained as the

major product (45% yield) over a composite catalyst of $\text{WO}_3/\text{Al}_2\text{O}_3 + \text{Ru/C}$ at 205 °C under 6 MPa H_2 in 30 min. Upon adding AC featuring basic sites to the reaction, the major product was switched to 1,2-propylene glycol (40.9% yield) [273]. In addition to the RAC function of W species, Li et al. disclosed that highly-dispersed WO_4 species on Al_2O_3 in an isolated configuration could serve as Lewis acidic sites for glucose isomerization [307]. In comparison, high WO_x loading (ca. 30 wt%) led to the formation of polymeric WO_x species presenting Brønsted acidic nature. Capitalizing on the Lewis acidic nature of highly-dispersed WO_4 , the authors designed a highly-selective $\text{Pd-WO}_x/\text{Al}_2\text{O}_3$ catalyst for the formation of 1,2-propylene glycol (60.8% selectivity) at 92.2% conversion of glucose at 180 °C under 4 MPa H_2 in a continuous flow reactor. The combination of ZnO with transition metals (Ru, Ni) has been identified as a selective catalyst for the isomerization-RAC-hydrogenation of cellulose/glucose into 1,2-propylene glycol. Both physical mixing such as $\text{Ru/C} + \text{ZnO}$ and $\text{Ni-W/H}\beta$



Scheme 37. Proposed reaction pathway for the direct conversion of glucose into propylene glycol and glycerol through cascade isomerization/RAC/hydrogenation reactions.

+ ZnO and supported catalysts such as Ni/ZnO could facilitate the dominant formation of 1,2-propylene glycol in 30–40% yields [308–312]. As indicated by control experiments, ZnO appears to promote the isomerization of glucose to fructose as well as subsequent RAC, while Ru and Ni are responsible for the hydrogenation of acetol to propylene glycol. The dual catalysis roles of ZnO are likely related to its amphoteric nature featuring both basic sites and Lewis acid sites. Further studies are needed to unravel the mechanism of ZnO-catalyzed isomerization and RAC.

The utility of RAC-hydrogenation strategy has been extended to the synthesis of ethanol directly from cellulose. Based on the well-established tungsten-catalyzed DLEG process, an innovative chemocatalytic route to synthesize bio-ethanol from cellulose in one pot was designed by Zhang and coworkers [313]. Central to this new route is the elaborate design of multifunctional Mo/Pt/WO_x catalysts, enabling the integration of cellulose to ethylene glycol and the subsequent ethylene glycol hydrogenolysis to ethanol in one pot. A high ethanol yield of 43.2% can be achieved over Mo/Pt/WO_x catalysts at 245 °C under 6 MPa H₂ in 2 h. As shown in Scheme 38, this one-pot process was proposed to involve four cascade reactions: (1) proton-catalyzed hydrolysis of cellulose to glucose, (2) the RAC of glucose to glycolaldehyde over WO_x sites, (3) the hydrogenation of glycolaldehyde to ethylene glycol over Pt sites, (4) the final hydrogenolysis of ethylene glycol to ethanol over Mo/Pt/WO_x. The last step was identified as the rate-determining step. The assembly of MoO_x sites and Pt particles in a special architecture, that is, isolated MoO_x species residing at the top of Pt nanoparticles anchored on WO_x support, has been proved to significantly promote the selective C–O bond cleavage (hydrogenolysis) of ethylene glycol to ethanol (Scheme 38). Following the idea of coupling RAC-hydrogenation with the hydrogenolysis of ethylene glycol, a series of tungsten-containing multifunctional catalysts for ethanol synthesis have recently been developed such as Ru-WO_x/HZSM-5, H₂WO₄ + Pt/ZrO₂, and Pd-Cu-WO_x/SiO₂, affording 53.7%, 32%, and 42.5% yields of ethanol, respectively [314–316]. Notably, one-pot conversion of cellulose into ethanol represents a typical example to show that advanced valorization routes of (hemi)cellulose can be designed by the rational combination of available C–C and C–O bond cleavage methods.

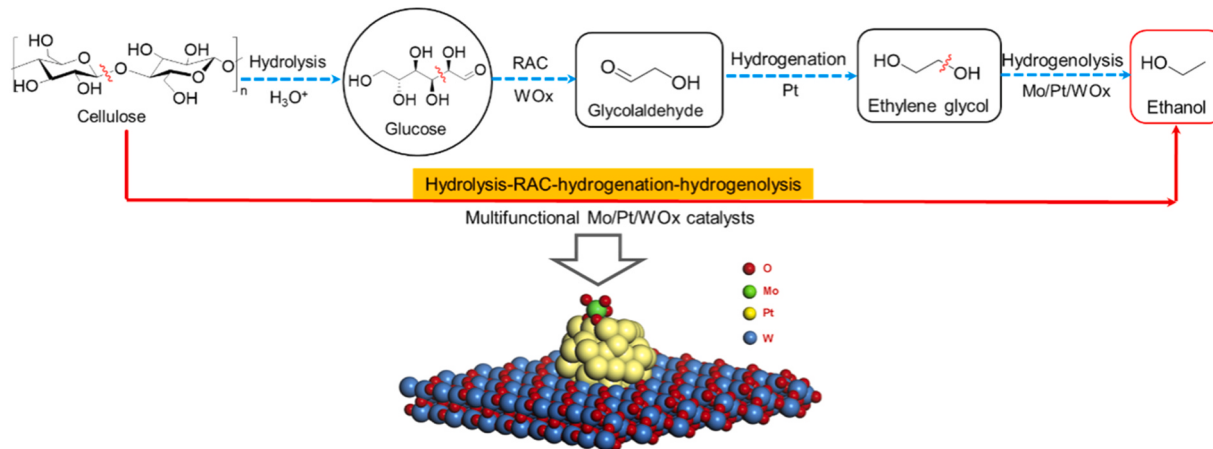
RAC-oxidation.

RAC products bearing aldehyde groups are apt to undergo oxidation to form carboxyl groups especially under O₂ atmosphere, for example, the oxidation of glycolaldehyde to glycolic acid. The oxidation of aldehyde groups is compatible with RAC in terms of reaction conditions. Hence, it can be conceived that the implementation of RAC reaction under O₂ atmosphere can provide a cascade reaction strategy, i.e., RAC-oxidation, to yield carboxyl acids as major products in one pot. The most

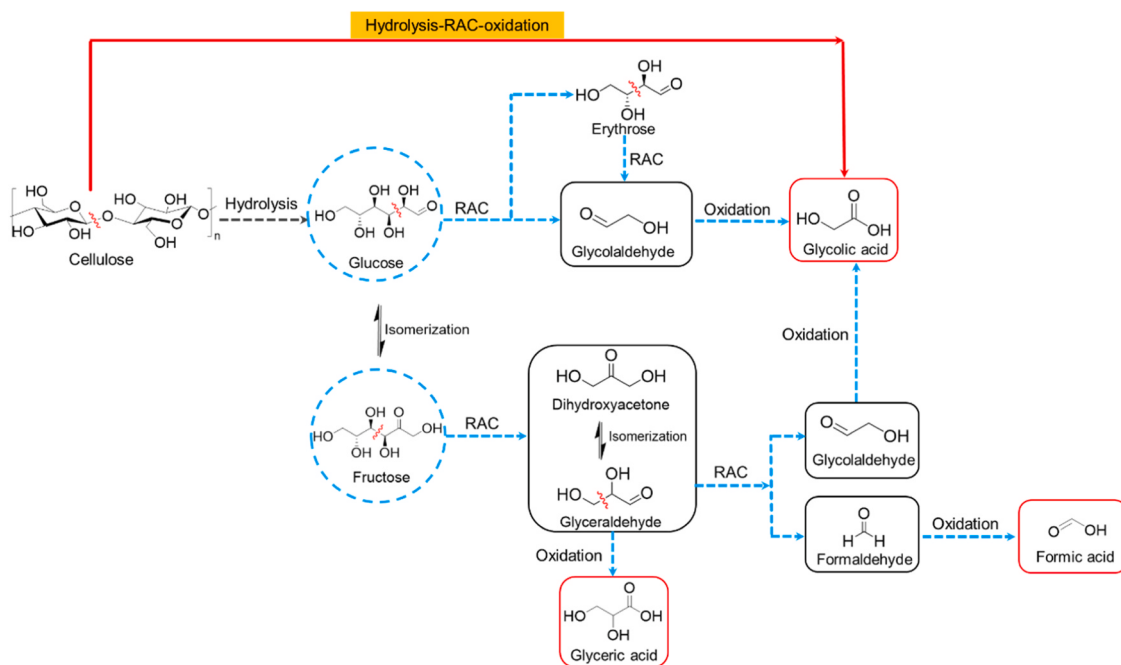
successful application of RAC-oxidation is the direct oxidation of cellulose to glycolic acid, which combines the RAC of cellulose to glycolaldehyde with the oxidation of glycolaldehyde to glycolic acid in one pot.

Han et al. first demonstrated the selective RAC-oxidation of cellulose over phosphomolybdcic acid (H₃PMo₁₂O₄₀), affording 49.3% yield of glycolic acid at 180 °C under 0.6 MPa O₂ after 1 h [317]. The utilization of H₃PMo₁₂O₄₀ as catalyst is of pivotal importance, since it can provide protons for cellulose hydrolysis, Lewis acidic MoO_x sites for RAC, and lattice oxygen atoms for oxidation. As depicted in Scheme 39, this reaction was believed to proceed via a three-step tandem reaction including cellulose hydrolysis to glucose, the RAC of glucose to glycolaldehyde, and the oxidation of glycolaldehyde to glycolic acid. The formed erythrose intermediate can also undergo RAC-oxidation to from two glycolic acid molecules. Apparently, the RAC-oxidation of cellulose is a very selective reaction with the exclusive formation of glycolic acid, similar to RAC-hydrogenation. However, in comparison to high ethylene glycol yields (up to 76%) obtained from RAC-hydrogenation, RAC-oxidation gave lower glycolic acid yields (below 50%), which is probably related to the facile degradation or over-oxidation of reaction intermediates and products under oxidative conditions. In addition to glycolic acid, other small organic acids including formic acid, glyceric acid, and acetic acid were also produced as side products in small amounts. Notably, when utilizing fructose as the reactant, the production of glyceric acid (23.3% yield) and formic acid (12.6% yield) were markedly enhanced. The authors therefore proposed that formic acid and glyceric acid were mainly generated from fructose arising from the isomerization of glucose. The RAC of fructose generates C3 intermediate glyceraldehyde, which undergoes a further RAC to form formaldehyde and glycolaldehyde followed by oxidation to generate formic acid and glycolic acid, respectively (Scheme 39). In parallel, the formed glyceraldehyde could undergo oxidation to from glyceric acid directly. Besides, it was reported that malonic acid can be produced as the major product through the over-oxidation of glyceraldehyde at 300 °C in aqueous NaOH [318]. Clearly, a number of C1 and C3 organic acids could be generated from the RAC products of fructose. Hence, in order to control the product distribution dominated by glycolic acid, the isomerization of glucose to fructose should be avoided as much as possible, since fructose can lead to diverse oxidation products.

The beneficial role of O₂ in promoting the RAC-oxidation of cellulose into glycolic acid was disclosed by Bayu et al., who discovered that the formation of glycolic acid is significantly accelerated upon switching the atmosphere from N₂ to O₂ over H₃PMo₁₂O₄₀ [319]. According to the observed color change of H₃PMo₁₂O₄₀ as well as the results of UV-Vis and FTIR, the authors suggested that the lattice oxygen atoms in



Scheme 38. Proposed reaction pathway for the direct conversion of cellulose into ethanol over a multifunctional Mo/Pt/WO_x catalyst. Adapted with permission from ref. [313].



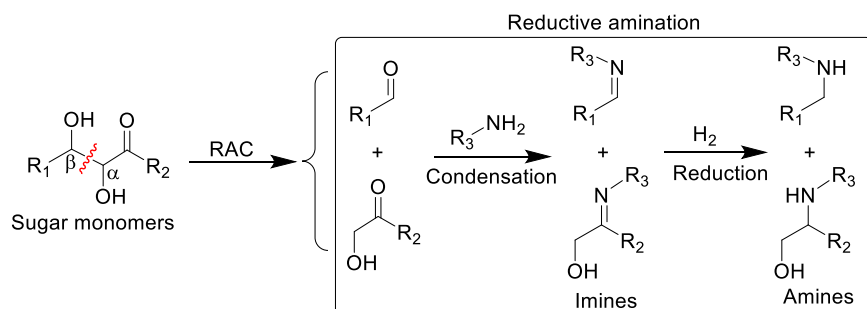
Scheme 39. Proposed reaction network for the one-pot RAC-oxidation of cellulose into glycolic acid, formic acid, and glyceric acid. Adapted with permission from ref. [317].

$\text{H}_3\text{PMo}_{12}\text{O}_{40}$ were involved in the oxidation of glycolaldehyde to glycolic acid accompanied by the oxidation of Mo(IV) to Mo(V). The consumed oxygen atoms could be replenished by reacting with O_2 to recover the oxidation activity of $\text{H}_3\text{PMo}_{12}\text{O}_{40}$. Besides, Han et al. reported that CuO catalysts can promote the RAC-oxidation of cellulose into oxalic acid in a yield of 41.5% in alkaline solutions [320]. The formation of oxalic acid was proposed to result from the continuous oxidation of glycolic acid over CuO.

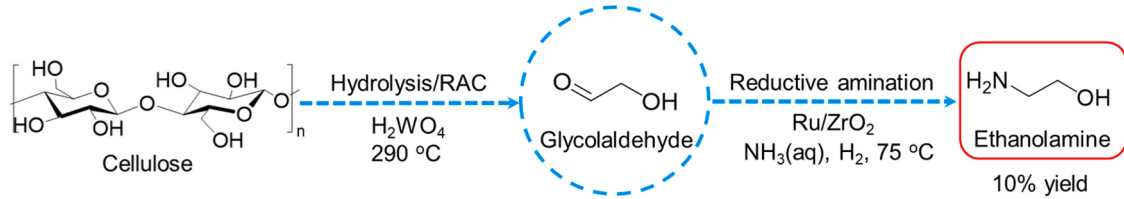
Tungsten catalysts have been explored for the RAC-oxidation of cellulose to glycolic acid by Zhang and co-workers [321]. The reaction was conducted in methanol instead of water, thus giving rise to methyl glycolate, a promising platform molecule to synthesize ethylene glycol and ethanol, as the final product. Among the examined tungsten compounds (e.g., carbide, oxide, heteropoly acid, salt), the physical combination of WO_x and mesoporous carbon CMK-3 gave the highest methyl glycolate yield of up to 57.7% at 240 °C under 1 MPa O_2 after 2 h. The conversion of cellulose to methyl glycolate follows the same reaction pathway as depicted in Scheme 39, except for the additional esterification of glycolic acid with methanol. Experimental and characterization results of the fresh and spent tungsten catalysts indicated that the in situ dissolved WO_x species in methanol likely served as the active sites for both RAC and oxidation reactions. This is consistent with the catalytic behaviors of tungsten species observed for RAC-hydrogenation.

RAC-amination.

The presence of both carbonyl and hydroxy groups in RAC products make them attractive substrates for reductive amination, a commonly-used approach to produce N-containing chemicals [322–324]. Especially for the reactive carbonyl groups, they can undergo nucleophilic addition with ammonia or amines followed by dehydration to form an imine intermediate (Schiff base), which can be further reduced into amines under H_2 (Scheme 40). Hence, a cascade RAC-amination protocol can be formulated by rationally integrating RAC with reductive amination, which offers a useful method to synthesize short-chain amines from biomass-derived sugars. The RAC-amination strategy has been applied for the catalytic upgrading of glucose and xylose into C2 monoamines and diamines such as ethanolamine, N, N-dimethylaminoethanol (DMAE), and N,N,N',N'-tetramethyl ethylenediamine (TMEDA). These reported examples are primarily based on the established RAC of sugars to glycolaldehyde followed by the reductive amination of glycolaldehyde with various amines. For example, Zhang et al. demonstrated the RAC-amination of cellulose to ethanolamine in a two-step manner including the first RAC of cellulose to glycolaldehyde followed by reductive amination to form ethanolamine (Scheme 41) [325]. The first RAC step was realized in water using H_2WO_4 as the catalyst at 290 °C, affording 20.6% yield of glycolaldehyde. The obtained aqueous glycolaldehyde solution was concentrated and then used for reductive amination to produce ethanolamine in a medium yield of 52% in the presence of aqueous ammonia over a



Scheme 40. Selective conversion of sugars into various amines via the combination of RAC with reductive amination (RAC-amination).



Scheme 41. Two-step conversion of cellulose into ethanolamine through glycolaldehyde.

Ru/ZrO₂ catalyst at 75 °C and 3 MPa H₂. Through this two-step process, an overall ethanolamine yield of 10% was achieved from cellulose. Characterization results indicated the presence of both Lewis acidic RuO₂ and metallic Ru sites on Ru/ZrO₂. Lewis acidic RuO₂ sites were proposed to contribute to the reaction of glycolaldehyde with ammonia to form imine intermediates by activating the carbonyl group in

glycolaldehyde, whereas metallic Ru sites catalyze the hydrogenation of imine. Despite these promising results, the one-pot RAC-amination of cellulose into amines has not yet been realized experimentally. The major challenge lies in the high reaction temperatures of RAC (above 150 °C) unfavorable for glycolaldehyde amination (below 100 °C), as well as unfavorable acid-catalyzed hydrolysis of cellulose in the

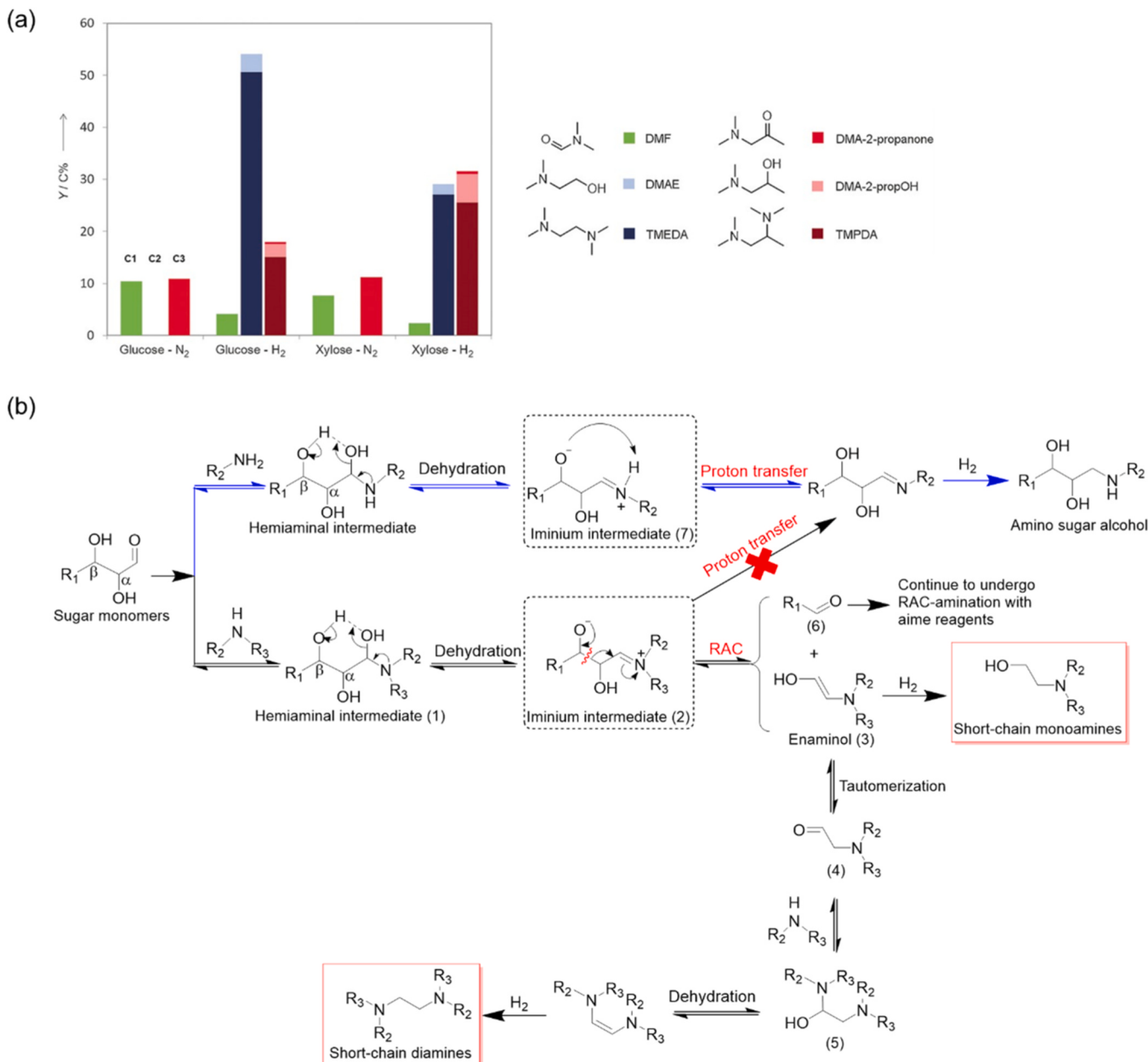


Fig. 8. (a) Product distribution for the one-pot RAC-amination of glucose and xylose over Ru/C at 125 °C under N₂ or H₂ atmosphere; (b) Proposed reaction mechanism for the amine-promoted RAC-amination of sugars into short-chain amine products (black arrows) and the conversion of sugars into amino sugar alcohol (blue arrows). Adapted with permission from ref. [326 and 327].

presence of ammonia.

To overcome the challenge of incompatible reaction temperatures for RAC and amination, Sels and coworkers proposed a new strategy relying on alkylated amine-facilitated RAC at low temperatures, analogous to aldolase-catalyzed RAC [326]. This strategy successfully realized the integration of RAC and reductive amination in one pot. In the presence of dimethylamine, glucose was directly converted into TMEDA in a high yield of 51% over Ru/C at a low temperature of 125 °C under 7.5 MPa H₂ (Fig. 8a). In contrast, under N₂ atmosphere, the production of amines was markedly inhibited giving a dark brown product solution due to Maillard and caramelization side reactions. A small amount of DMAE (4% yield) and 15% yield of *N,N,N',N'*-tetramethyl-1,2-propylene-diamine (TMPDA) were also formed as by-products. The formation of C3 diamine TMPDA probably resulted from the isomerization of glucose to fructose followed by RAC to form C3 intermediates, as mentioned above. In the case of xylose, both C2 amines (TMEDA and DMAE) and C3 diamines (TMPDA and *N,N*-dimethylamino-2-propanol) were produced as the major products in nearly equal yields of around 30% (Fig. 8a). This can be explained by the formation of equal moles of C2 and C3 intermediates from the RAC of xylose, as discussed above. Besides dimethylamine, other primary and secondary amines (e.g., ethanalamine, diethylamine, *N*-methylethanolamine) are also applicable for the RAC-amination of glucose, producing corresponding C2 diamines as products.

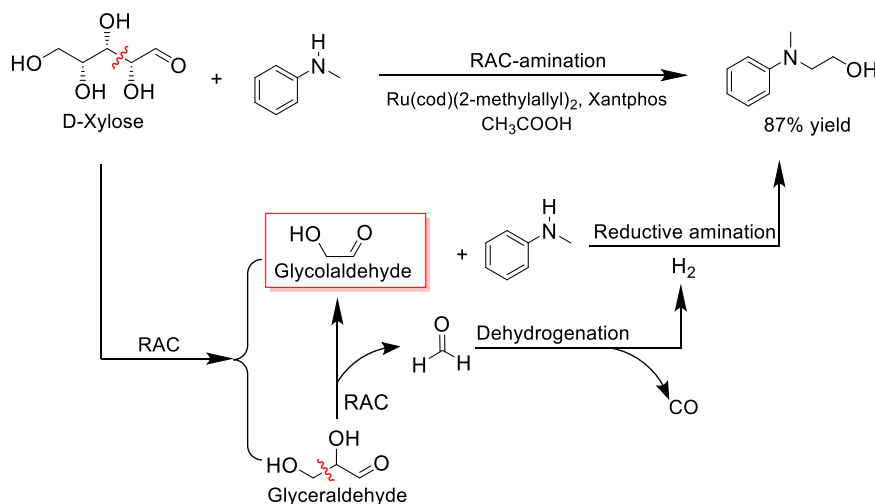
Note that reaction of glucose with amines featuring less alkyl groups (e.g., NH₃, primary amines) afforded lower yields towards diamines accompanied by the enhanced formation of amino sugar alcohol. This is attributed to the intramolecular proton transfer from the positive nitrogen ion to the negative oxygen ion in iminium intermediate (7), thus leading to facile reduction of the imine moiety rather than RAC (Fig. 8b). In the case of secondary amines, the intramolecular proton transfer step was blocked, thus favoring the RAC of glucose to form short-chain amines (Fig. 8b). Dimethylamine plays two pivotal roles in realizing this low-temperature RAC-amination, namely, as a promotor to facilitate the RAC of glucose and as an amine reagent to react with carbonyl groups. Different from aforementioned RAC reactions typically at temperatures above 150 °C, dimethylamine-promoted RAC follows a peculiar pathway analogous to the mechanism of aldolase-catalyzed RAC, thus enabling the occurrence of RAC at low temperatures (e.g., 125 °C). Based on kinetic analysis and DFT calculations, the authors proposed a reaction mechanism for the amine-promoted RAC [327]. As shown in Fig. 8b, the initial nucleophilic addition of an amine reagent with the carbonyl of sugar monomers gives a hemiaminal intermediate (1),

followed by a dehydration step to form a zwitterionic iminium intermediate (2). The intermediate (2) prefers to undergo RAC rather than intramolecular proton transfer owing to the absence of proton attached to the N atom, accounting for the high selectivity towards short-chain amines. Subsequently, the electron transfer from the negative oxygen ion to the C_β atom leads to the formation C_β=O bond, thus triggering the C_α-C_β bond scission (RAC). As a result, this zwitterionic iminium intermediate is fragmented into a C2 enaminol intermediate (3) along with a carbonyl fragment (6). The latter can continue to undergo RAC-amination with amine reagents, while the C2 enaminol (3) is either reduced into a monoamine product or subjected to keto-enol tautomerization into a carbonyl-containing intermediate (4). The intermediate (4) tends to react with a second amine reagent to form a hemiaminal intermediate (5), which readily undergoes sequential dehydration and hydrogenation steps to ultimately yield diamine as the main product.

Recently, Jia and coworkers claimed the RAC-amination of xylose into C2 alkanolamines using N-methylaniline as the N source in the presence of acetic acid and a ruthenium complex comprising Ru(cod)(2-methylallyl)₂ and Xantphos ligands (Scheme 42) [328]. A high yield of up to 87% was obtained for the target C2 alkanolamine at 150 °C after 16 h. As shown in Scheme 42, the formation of C2 alkanolamine was proposed to start with the RAC of xylose to generate equimolar glycolaldehyde and glyceraldehyde. Considering the high selectivity of C2 alkanolamine, glyceraldehyde was speculated to undergo a second RAC to form equimolar formaldehyde and glycolaldehyde. Therefore, one molecule of xylose can in principle generate two molecules of glycolaldehyde. The formed glycolaldehyde further reacts with N-methylaniline to form imine intermediates followed by Ru-catalyzed hydrogenation to yield C2 alkanolamine as the final product. Interestingly, Ru-catalyzed dehydrogenation of formaldehyde could provide in situ H₂ for the hydrogenation of imine intermediates. Detailed reaction pathways of RAC remain unclear and seem to follow the aforementioned mechanism of amine-promoted RAC.

RAC-(de)hydration.

C3 products obtained from RAC including glyceraldehyde and dihydroxyacetone, also called trioses, have been intensively discussed as ideal substrates for the synthesis of lactic acid [329–332], an important platform compound to synthesize various fine chemicals as well as biodegradable polylactide. It is widely accepted that lactic acid is formed through the sequential dehydration, hydration, and hydride shift of glyceraldehyde or dihydroxyacetone [333–335]. One major approach to synthesize these C3 trioses (rare in nature) is thorough the RAC of abundant C6/C5 sugars such as glucose, fructose, and xylose. Hence, the



Scheme 42.

Proposed reaction mechanism for Ru-catalyzed RAC-amination of xylose into C2 alkanolamines using N-methylaniline as the N source. Adapted with permission from ref. 328.

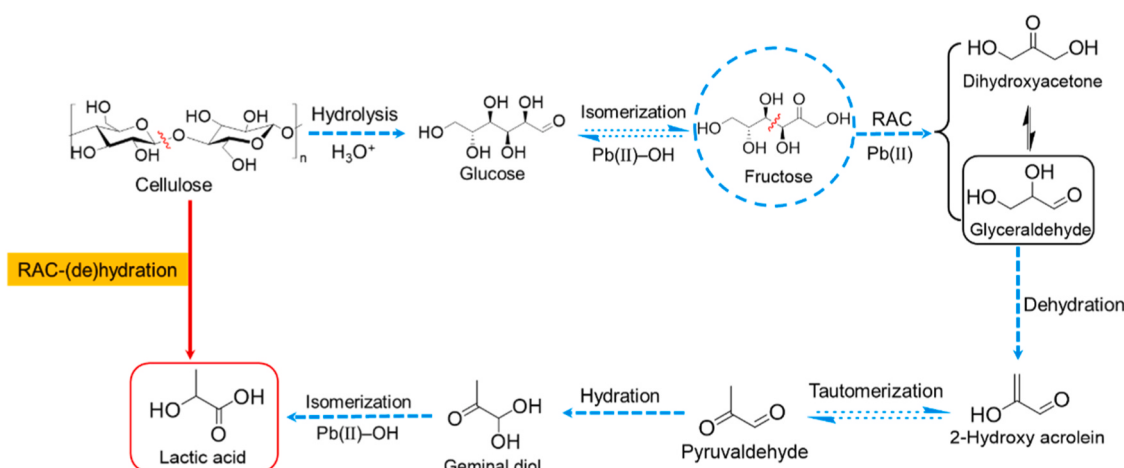
combination of RAC with (de)hydration and hydride shift steps (termed as RAC-(de)hydration) offers a cascade reaction strategy for the selective production of lactic acid directly from C6 sugars. As discussed above, the RAC of C6/C5 sugars, the rate-limiting step for lactic acid synthesis, is typically catalyzed by Lewis acidic transition metal species, whereas (de)hydration reactions can proceed in the presence of either Brønsted or Lewis acidic sites. The sole utilization of Lewis acids or combined with weakly acidic media (e.g., water) for RAC-(de)hydration is preferred considering that sugars and their RAC products are susceptible to degrade in the presence of strong Brønsted acids. In addition, an inert atmosphere (e.g., N_2) is usually employed for RAC-(de)hydration to inhibit undesirable oxidation reactions of reaction intermediates. Evidently, Lewis acidity is of pivotal importance for the selective formation of lactic acid from sugars via RAC-(de)hydration. As of now, numerous Lewis acidic catalysts have been developed including homogenous cations such as Pb(II),^[21] Al(III) + Sn(II)^[336], Zn(II)^[337, 338], In(III) + Sn(II)^[339], Y(III)^[340], Er(III)^[341,342], and heterogeneous Lewis acids such as tungstated zirconia^[343], Sn- β ^[344-347], ZrO_2 ^[348], Ga-Zn-HY^[349], and γ -Al₂O₃^[350-352]. Herein, several representative catalyst systems will be discussed to showcase the utility of RAC-(de)hydration in selectively transforming various sugars into lactic acid in one pot.

In contrast to the direct formation of C3 trioses via the RAC of xylose and fructose, the RAC of glucose typically gives C2 (glycolaldehyde) and C4 products (erythrose) that are not applicable to the synthesis of lactic acid. An isomerization step is therefore needed to first transform glucose into fructose. Accordingly, in addition to catalyzing RAC-(de)hydration, the employed catalysts should be active for glucose isomerization, which can also occur over Lewis acids. For example, Deng et al. reported that soluble Pb(II) species can serve as a highly selective Lewis acid catalyst to enable the one-pot conversion of cellulose into lactic acid in a high yield of 68% in water at 190 °C under N_2 ^[21]. Kinetic investigations indicated that the reaction proceeds through four sequential steps (**Scheme 43**): (a) cellulose hydrolysis to glucose, (b) the isomerization of glucose into fructose, (c) the RAC of fructose to glyceraldehyde and dihydroxyacetone, (d) the final (de)hydration and isomerization of glyceraldehyde to form lactic acid. The last step was proposed to involve the dehydration of trioses to 2-hydroxy acrolein in equilibrium with pyruvaldehyde followed by hydration to form a geminal diol intermediate. This diol intermediate is eventually isomerized into lactic acid via an intramolecular 1,2-hydride shift. Protons released from H_2O were believed to catalyze the first cellulose hydrolysis step as well as the dehydration step. As indicated by DFT calculations, the RAC of fructose was primarily catalyzed by Pb(II) ions, whereas glucose isomerization to fructose and geminal diol isomerization to lactic acid were catalyzed by the partially hydrolyzed Pb(II)-OH species following an intramolecular

hydride-shift mechanism. These catalytic functions of Pb(II) led to a remarkable decrease of the activation energies of RAC and isomerization by 10.4 and 8.9 kcal/mol, respectively, in comparison to that without Pb (II). Notably, such multiple catalytic roles of Lewis acidic Pb(II) species are able to tailor the complex reaction routes towards selective formation of lactic acid.

Apart from homogeneous metal cations, Sn-incorporated zeolites (e.g., Sn- β , Sn-MFI, Sn-MCM-41, Sn-SBA-15) present excellent heterogeneous catalysts for the heterogeneous RAC-(de)hydration of sugars into lactic acid. The most representative example is Sn- β catalyst, which has been demonstrated to convert diverse sugars (e.g., glucose, fructose, xylose) into lactic acid in excellent yields. For example, Sun et al. reported that glucose can be efficiently converted into lactic acid over a mesoporous Sn- β catalyst in a high yield of up to 57.9% at 200 °C within 30 min^[347]. By contrast, at a lower reaction temperature of 130 °C, fructose was generated as the main product (47.6% yield) accompanied by a low lactic acid yield of 20.1%, indicating the excellent isomerization capability of Sn- β catalysts. For the RAC-(de)hydration of fructose and xylose over Sn- β catalysts, high lactic acid yields up to 58.4% and 67.1% could be also obtained, respectively. The similar lactic acid yields achieved for glucose and fructose further supported the proposed reaction route via a fructose intermediate for the conversion of cellulose-/glucose into lactic acid. Followed by glucose isomerization, fructose is further converted into lactic acid through sequential RAC, dehydration, hydration, and 1,2-hydride shift steps, as previously described in **Scheme 43**. The superb activity of Sn- β catalysts towards these reactions is attributed to the presence of isolated Sn sites embedded in the framework of β zeolites. Under hydrothermal conditions, these isolated Sn species likely exist in an open coordination structure (partially hydrolyzed $(SiO_3)SnOH$) possessing strong Lewis acidity^[289,353-355]. The Lewis acidity of Sn has been demonstrated to promote two key reaction steps, that is, glucose isomerization to fructose via a 1,2-hydride shift mechanism and the RAC of sugars, while weak Brønsted acidity arising from silanol groups is beneficial to dehydration/hydration steps^[344,347]. Moreover, the three-dimensional large pore system of β zeolites also contributes to the excellent performances of Sn- β catalysts by facilitating the diffusion of large sugar molecules.

Commercial γ -Al₂O₃ has been reported as an efficient heterogeneous catalyst for the RAC-(de)hydration of xylose into lactic acid. At 170 °C and 15 bar N_2 , a high lactic acid yield of 63% was achieved over γ -Al₂O₃ featuring abundant Lewis acid sites^[352]. In contrast, HZSM-5 zeolites with rich Brønsted acidities afforded furfural (42.4% yield) as the major product with only 3.1% yield of lactic acid, owing to the favorable dehydration of xylose into furfural over Brønsted acid sites. A calcination treatment of γ -Al₂O₃ at 1100 °C significantly reduced the number of Lewis acid sites from 0.34 to 0.05 mmol/g, which led to a pronounced



Scheme 43. Proposed reaction mechanism for Pb-catalyzed conversion of cellulose to lactic acid. Adapted with permission from ref. [21].

decrease of lactic acid yield from 63% to 30.9%. These results clearly indicated the crucial role of Lewis acidic Al sites in directing the reaction pathway towards lactic acid. As revealed by DFT calculations, the isomerization of xylose into xylulose, the RAC of xylose/xylulose, and the isomerization of triose to lactic acid can all be facilitated by Lewis acidic Al sites, while the dehydration and hydration steps were likely promoted by the hydroxylated Al sites (i.e., Al-OH) featuring weak Brønsted acidity [352,356].

In principle, the conversion of xylose into lactic acid can proceed either with or without the initial isomerization step, but they can all lead to same trioses and finally produce lactic acid. As aforementioned in **Scheme 31**, the RAC of pentoses always gives rise to a C2 intermediate glycolaldehyde and a triose (glyceraldehyde from xylose or dihydroxyacetone from xylulose) irrespective of the structure of pentoses. The facile interconversion of glyceraldehyde and dihydroxyacetone typically leads to a mixture of these two isomers, and both of them can be evolved into lactic acid via a series of sequential reactions including dehydration, hydration, and 1,2-hydride shift, as mentioned above. Generally, the generated C2 intermediate glycolaldehyde is considered not to contribute to the formation of lactic acid directly. Therefore, the carbon yield of lactic acid from pentoses should not exceed 60% theoretically. However, lactic acid yields higher than 60% have been reported in recent studies [344,347]. For example, Zhang et al. claimed a high lactic acid yield of up to 70% in the presence of Sn- β catalysts at 200 °C and 40 bar N₂ [344]. In parallel to the widely-accepted pathway via trioses, the authors proposed another possible pathway to produce lactic acid via glycolaldehyde based on the detected erythrose through ¹³C NMR studies. As shown in **Scheme 44**, this new reaction route starts with the self-condensation of glycolaldehyde to form erythrose followed by sequential dehydration and keto-enol tautomerization to yield 2-carbonyl-4-hydroxybutyraldehyde [344,357]. This C4 intermediate can be cleaved into a C3 intermediate pyruvaldehyde and formaldehyde via RAC followed by rehydration and isomerization to eventually yield lactic acid. The obtained high lactic acid yields could be explained by the concurrence of both pathways.

RAC-condensation.

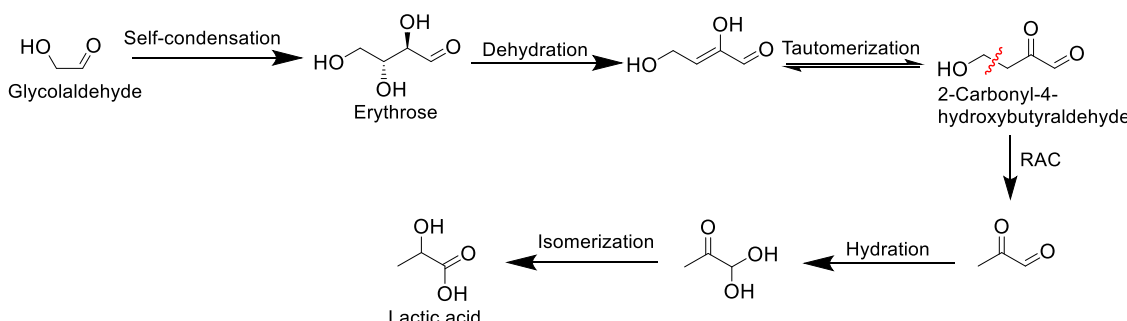
RAC-condensation refers to a cascade reaction comprising the RAC of sugars into carbonyl intermediates followed by aldol condensation with another carbonyl compound. This cascade reaction combines C-C bond cleavage with C-C bond formation reactions, thus providing an efficient approach to construct carbon-increasing molecules. For example, Zhang and coworkers described the one-pot transformation of glucose into two complex furanic compounds, namely 2-methyl-3-acetyl furan (MAF) and 1-(5-(1,2-dihydroxyethyl)-2methylfuran-3-yl)ethan-1-one (DMAF) [358]. In the presence of acetylacetone (acac) as the condensation reagent, 66% yield of MAF was obtained over H₂MoO₄ at 220 °C and 2.5 MPa N₂, whereas the production of DMAF is maximized in a yield of 42% at a low temperature of 80 °C. As depicted in **Scheme 45**, the formation of MAF from glucose and acac was proposed to follow the RAC-condensation pathway involving the first Mo-catalyzed RAC of glucose to form glycolaldehyde and erythrose. The subsequent

condensation of glycolaldehyde with acac, a reactive nucleophile, gives rise to a C7 adduct, which is eventually evolved into MAF via a tandem dehydration/keto-enol tautomerization/etherification reaction sequence promoted by the protons in H₂MoO₄. The formation of DMAF arises from the condensation of erythrose and acac following a similar reaction pathway as that of MAF. In addition to catalyzing RAC, H₂MoO₄ is also known as an epimerization catalyst to transform glucose into mannose. The formed mannose can also be converted into MAF and DMAF through the same RAC-condensation pathway as that of glucose, owing to the identical carbonyl position in glucose and mannose.

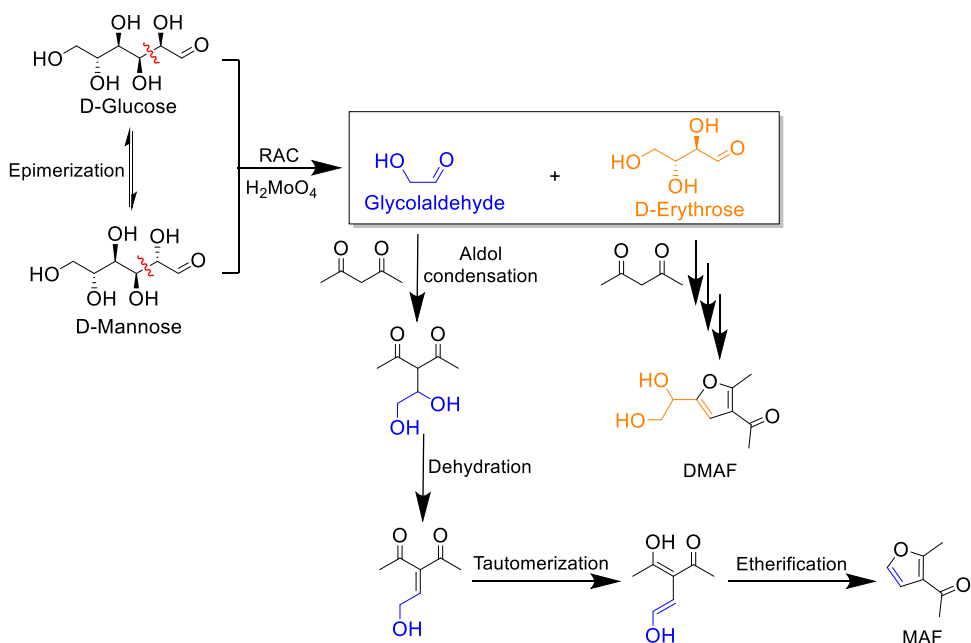
3.2. Oxidative cleavage

Oxidative cleavage herein specifically refers to the rupture of the C-C bond between a carbonyl moiety and a carbon atom containing an OH group (α -hydroxy carbonyl motif) in the presence of H₂O₂ as the oxidant (**Scheme 46**). This reaction is analogous to periodate oxidation, a classical bond cleavage method in carbohydrate chemistry [359,360]. The utilization of oxidative cleavage strategy can realize the complete breakage of the carbon skeleton bearing carbonyl and OH groups, for example, aldoses and ketoses, accompanied by the oxidation of carbonyl and OH groups into formic acid as the major product.

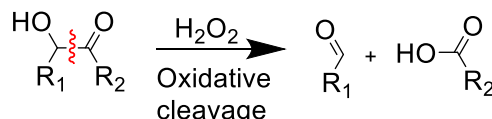
Jin et al. described the oxidative cleavage of glucose into formic acid in the presence of excess H₂O₂ and alkalis (e.g., NaOH), giving a high formic acid yield of 75% at 250 °C in 60 s [361]. By contrast, the sole utilization of H₂O₂ without alkali catalysts only led to 24% yield of formic acid, owing to the significant decomposition of formic acid at such high temperatures. Clearly, the addition of NaOH effectively suppresses the decomposition of formic acid. The decomposition of formic acid can also be inhibited by lowering the reaction temperature to room temperature with a longer reaction time of 8 h. Under room temperature and excess amounts of H₂O₂ and LiOH, formic acid could be directly produced from glucose in a record-high yield of 91.3% [362]. In addition to inhibiting formic acid decomposition, the addition of alkalis was believed to enhance the oxidation capability of H₂O₂ by transforming H₂O₂ into HOO⁻ (**Scheme 47a**), a strong oxidative species enabling room temperature oxidation of glucose into formic acid [363,364]. The synergy between H₂O₂ and alkalis contributes to the excellent yield of formic acid. To probe the reaction pathway, other sugars were examined for the oxidative cleavage reaction. Xylose and glycolaldehyde led to comparable high formic acid yields (around 90%) as that of glucose [362]. These results indicated that xylose and glycolaldehyde are potential reaction intermediates for the oxidative cleavage of glucose into formic acid. According to experimental results, a tentative pathway for the oxidative cleavage of glucose into formic acid was depicted in **Scheme 47b**. H₂O₂-promoted oxidative cleavage of glucose was proposed to follow the α scission at the C-C bond of carbonyl and OH groups [361,365]. Initially, the C1-C2 bond of glucose is cleaved by the reaction of highly-active HOO⁻ species attacking the aldehyde group, accompanied by the oxidation of aldehyde moiety into formic acid and the formation of a C5 aldose intermediate. Meanwhile, the hydroxyl ion



Scheme 44. Proposed reaction pathway for the conversion of glycolaldehyde to lactic acid. Adapted with permission from ref. [344].



Scheme 45. Proposed reaction pathway for the conversion of glucose to MAF and DMAF via RAC-condensation. Adapted with permission from ref. [358].



Scheme 46. H_2O_2 -promoted oxidative cleavage of sugar monomers into acids and carbonyl compounds.

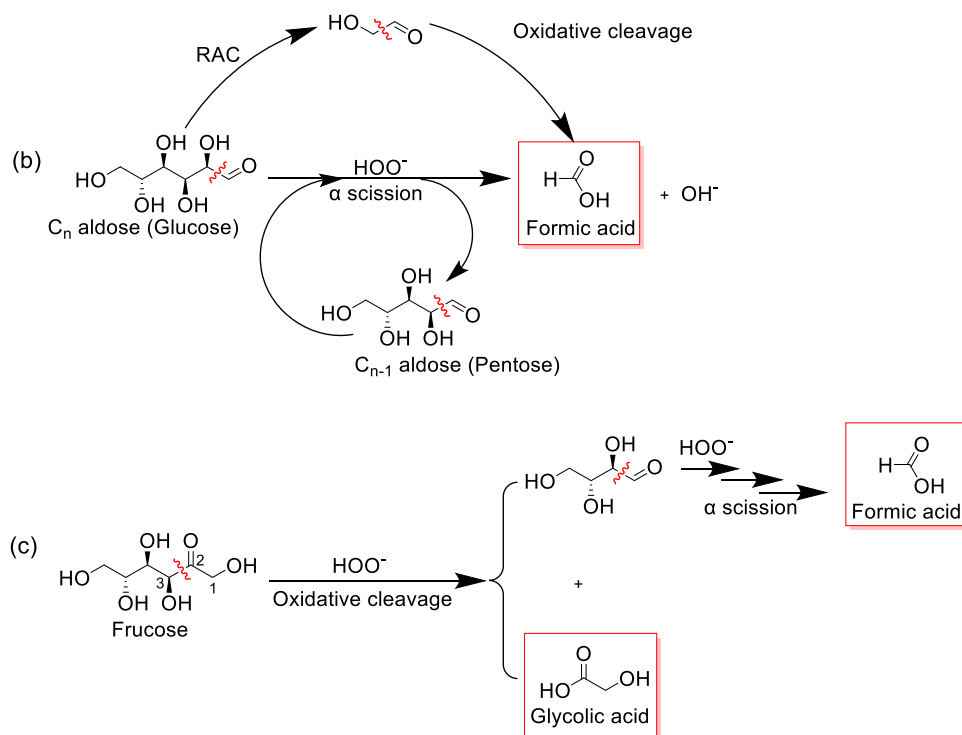
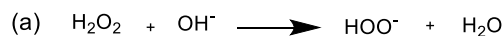
is regenerated to enter the next cycle of H_2O_2 activation. Repetition of this α scission step over HOO^- species results in the stepwise conversion of aldoses into a chain-shortened aldose and formic acid. Following this mechanism, all carbon atoms in glucose can be theoretically converted into formic acid, accounting for the obtained high yields of formic acid close to 100%. Alternatively, formic acid could be also generated from the oxidation of glycolaldehyde which results from the RAC of glucose. In contrast to the high formic acid selectivity obtained for glucose, the oxidative cleavage of ketoses like fructose affording a lower formic acid yield of 58.3% along with the considerable formation of glycolic acid (21%) and unknown products [362]. The formation of glycolic acid indicates a distinct pathway for the oxidative cleavage of fructose. Unlike glucose, the initial oxidative cleavage occurs preferentially at the C2–C3 bond of fructose, thus leading to the formation of glycolic acid and C4 aldose. The latter probably continues to undergo the α scission oxidation to ultimately yield formic acid (Scheme 47c).

Notably, the combination of oxidative cleavage and RAC can also enable the selective fragmentation of sugars into formic acid. For example, VOSO_4 was reported as an efficient catalyst for the oxidative conversion of glucose into formic acid (53% yield) in the presence of O_2 as the oxidant at 140°C [366]. Time-course monitoring of the reaction progress indicated that fructose, trioses (i.e., glyceraldehyde/dihydroxyacetone), glycolic acid, and glyceric acid were formed as reaction intermediates. Hence, the formation of formic acid was proposed to arise from the isomerization of glucose into fructose followed by RAC to generate C3 intermediates (glyceraldehyde/dihydroxyacetone). These C3 intermediates subsequently undergo oxidative cleavage to yield formic acid probably via glycolic and glyceric acids intermediates (Scheme 48). The oxidative cleavage of glyceraldehyde/dihydroxyacetone into formic acid over a VOSO_4 catalyst follows the same principle as aforementioned for H_2O_2 -promoted oxidative cleavage, that

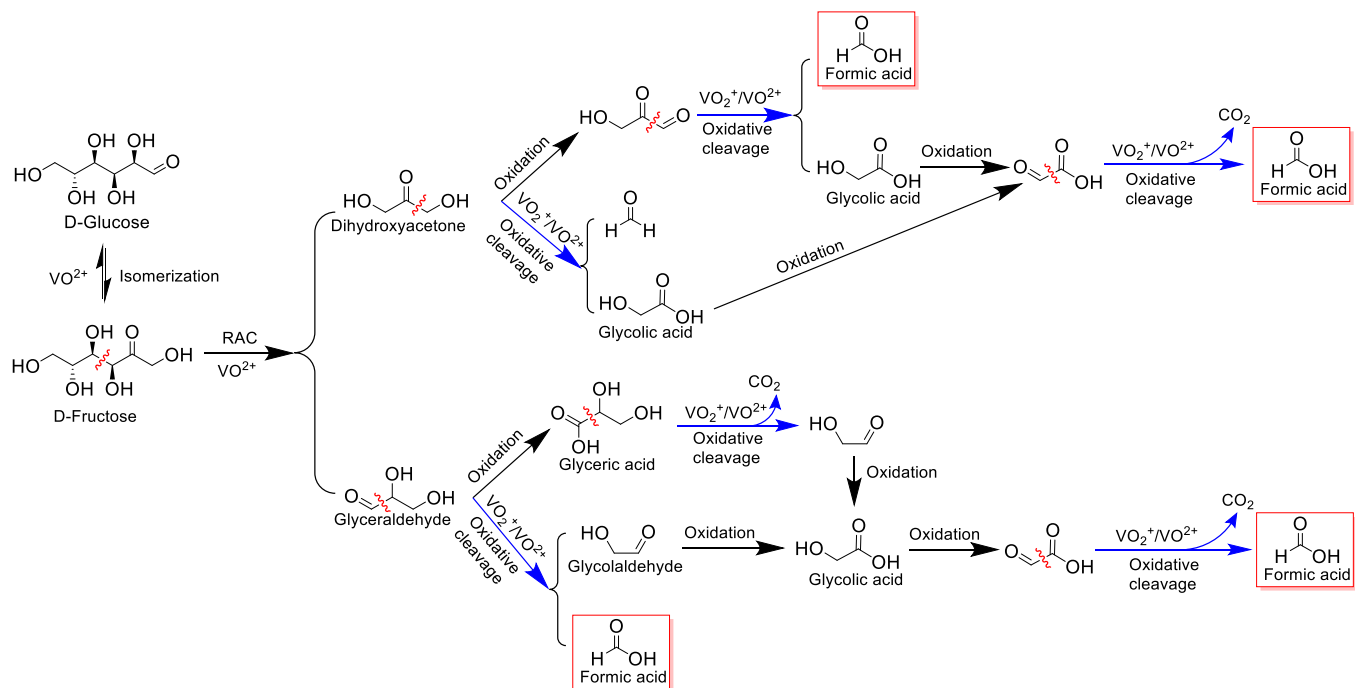
is, the cleavage of the C–C bond at α position. The carbonyl group is oxidized into formic acid or a carboxyl group, and the other C–OH moiety is oxidized into a carbonyl group (Scheme 48). In addition, a considerable amount of CO_2 was also detected in this reaction, which was ascribed to the oxidative cleavage (decarboxylation) of glycolic and glyceric acid intermediates. As indicated by electron spin resonance (ESR) and ^{51}V NMR studies, $\text{VO}_2^+/\text{VO}^{2+}$ redox couple was identified as the active site for the oxidative cleavage reaction of C3 intermediates into formic acid via an electron transfer coupled with oxygen transfer mechanism. Moreover, The Lewis acidity of V(IV) species is able to facilitate glucose isomerization and RAC. Such multiple catalytic roles of V species guarantee all reactions occurring in a sequential manner to eventually yield formic acid and CO_2 .

3.3. Decarboxylation

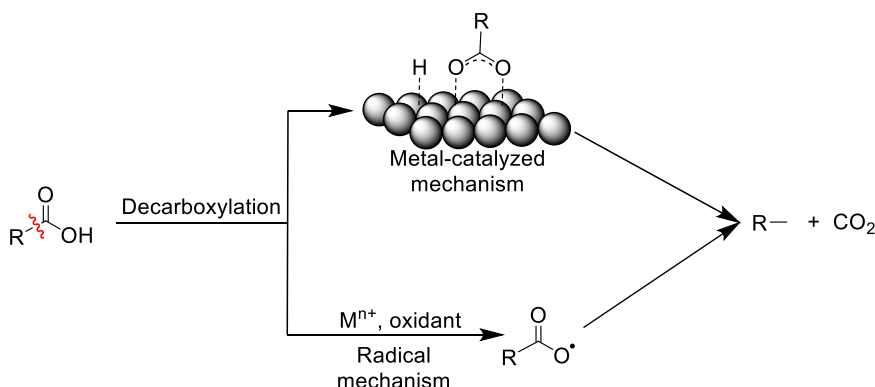
Decarboxylation literally means the removal of a carboxyl group typically from a carboxyl acid or its derivatives accompanied by the release of CO_2 . The rest part of carboxyl acids is generally retained in corresponding products. This reaction typically enables the cleavage of terminal C–C bonds connected to carboxyl groups. Obviously, the substrate scope of decarboxylation is limited to carboxyl acids or their derivatives like esters. As a C–C bond cleavage method, decarboxylation has found important applications in valorizing bio-derived acids principally including fatty acids, amino acids, and small organic acids. The last two classes of acids can be generated from (hemi)cellulose via chemo-catalytic or enzymatic methods. Fatty acids are beyond the scope of this review, although the decarboxylation of fatty acids into fuel-like hydrocarbons have been actively studied. The reader is referred to specialized literature on this topic [367–370]. The decarboxylation of (hemi)cellulose derived amino and organic acids, e.g., glycine, lysine, levulinic, itaconic, glucaric, and furoic acids, can eliminate their carboxyl moieties, thus leading to various value-added fine chemicals such as amine, furan, butene, methacrylic acid, and ketone. In principle, decarboxylation can occur spontaneously at high temperatures (above 300°C), for example, during biomass pyrolysis/liquefaction, but usually leading to uncontrollable product distributions [371,372]. Alternatively, decarboxylation can be implemented in the presence of homogeneous or heterogeneous catalysts at moderate temperatures under inert atmosphere. The catalytic decarboxylation mostly follows a



Scheme 47. (a) Formation of active HOO^- species by the reaction of H_2O_2 and alkalis; (b) Proposed reaction pathway for the oxidative cleavage of glucose exclusively into formic acid following the α scission mode; (c) Proposed reaction pathway for the oxidative cleavage of fructose into formic and glycolic acids. Adapted with permission from ref. [361–363].



Scheme 48. Proposed reaction pathway for VOSO_4 -catalyzed conversion of glucose into formic acid and CO_2 through RAC and oxidative cleavage reactions. Adapted with permission from ref. [366].



Scheme 49. Catalytic decarboxylation via a radical mechanism or a metal-catalyzed mechanism.

metal-catalyzed mechanism or a radical mechanism (Scheme 49) [373, 374]. The former is based on the adsorption and activation of carboxyl groups on transition metals, while the latter relies on the formation of carboxyl radicals via catalytic oxidation in the presence of redox-active sites and oxidants.

3.3.1. Decarboxylation of (hemi)cellulose derived organic acids

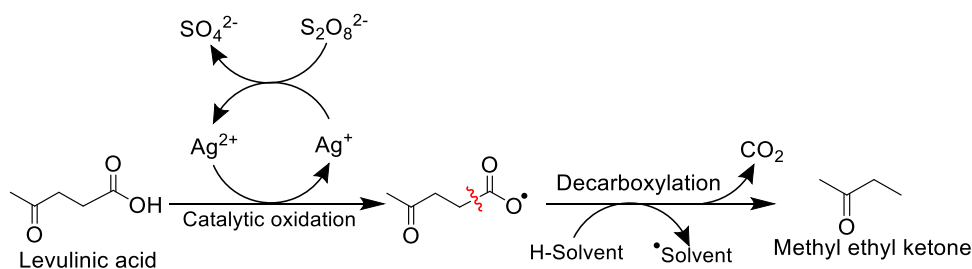
Oxidative decarboxylation promoted by redox-active metal species and oxidants presents a selective strategy to convert glucose-derived levulinic acid into methyl ethyl ketone (MEK) [375]. Amongst the examined metal species (e.g., cobalt nitrate, ferrous chloride, manganese chloride, silver nitrate), the utilization of silver nitrate as catalyst and sodium peroxydisulphate as oxidation agent afforded the highest yield of MEK (44.2%) at 160 °C in a buffer solution (pH = 5) containing NaOH-KH₂PO₄. The authors proposed that the in situ formed Ag(II) species from the oxidation of Ag(I) species by sodium peroxydisulphate serve as the catalytically active sites for decarboxylation. The reaction was believed to proceed likely via the oxidation of the carboxyl group in levulinic acid by Ag(II) species into a labile carboxyl radical, which tends to fragment into equimolar CO₂ and MEK (Scheme 50). This is accompanied with simultaneous reduction of Ag(II) back to Ag(I) species which can reenter the catalytic cycle.

In addition to oxidative decarboxylation of levulinic acid, metal-catalyzed hydrogenative decarboxylation has been applied to transform levulinic acid into 2-butanol in high yields (Table 6) [376–379]. Among many different transition metals and oxide supports, the combination of Ru nanoparticles with CeO₂ was discovered to show superior catalytic activity for the production of 2-butanol in water in a high yield of 85% at 150 °C under 3 MPa H₂ [376]. Methane is the only product detected in gas phase, indicating the likely occurrence of CO/CO₂ methanation. Catalyst characterization results indicated that CeO₂ was in situ reduced to Ce(OH)₃ during the reaction and Ru nanoparticles (3 nm) were highly dispersed on Ce(OH)₃ in metallic state. As depicted in Scheme 51a, the authors speculated that the hydrogenative decarboxylation of levulinic acid likely follows a hydrogenation-decarboxylation pathway. Metallic Ru nanoparticles

were proposed to catalyze a series of reactions including the reduction of carbonyl and carboxyl to hydroxyl and aldehyde, the decarbonylation of 4-hydroxypentanal to 2-butanol, the (de)hydrogenation between 4-hydroxypentanal and 1,4-pentanediol, and CO reduction to methane. The basicity of Ce(OH)₃ was believed to promote the reduction of carboxyl to aldehyde, the hydrolysis of GVL to 4-hydroxypentanoic acid, and the (de)hydrogenation of 1,4-pentanediol to 4-hydroxypentanal. Therefore, the synergistic catalysis of Ru nanoparticles and Ce(OH)₃ accounts for the excellent yields of 2-butanol.

Chen and coworkers reported that the modification of Ru nanoparticles with MnO_x could significantly improve catalytic performance, affording a high 2-butanol yield of up to 98.8% with a high turnover frequency of 1990000 h⁻¹ [380]. The excellent performance of Ru-MnO_x catalyst was ascribed to the interaction between Ru and MnO_x that leads to the formation of Ru⁰ and Mn²⁺ as the catalytically active sites. This was evidenced by the linear correlation between 2-butanol yield and the concentration of Ru⁰ and Mn²⁺ (Scheme 51c). Ru⁰ serves as the hydrogenation sites and Mn²⁺ offers binding sites (Lewis acid sites) to promote the adsorption of 1,4-pentanediol. The authors proposed that the hydrogenative decarboxylation of levulinic acid to 2-butanol follows a distinct hydrogenation-dehydroxymethylation pathway via an intermediate of 1,4-pentanediol (Scheme 51b). Levulinic acid is first reduced to GVL followed by further reduction and ring open to form 1,4-pentanediol. Moreover, 2-butanol is generated by the dehydroxymethylation of primary OH group of 1,4-pentanediol. Finally, 2-butanol is generated by the dehydroxymethylation of primary OH group of 1,4-pentanediol. Moreover, the same group developed non-noble bimetallic catalysts of NiMn/Al₂O₃ for the hydrogenative decarboxylation of levulinic acid to 2-butanol in a yield of 84.5%, comparable to that of Ru catalysts [379]. Similar to Ru-MnO_x catalyst, the excellent performance of NiMn was ascribed to the synergistic effect between Mn²⁺ and Ni⁰, which could promote the adsorption of levulinic acid/4-hydroxypentanoic acid and the reduction of carbonyl/carboxyl, respectively.

The decarboxylation of GVL, a hydrogenation product of levulinic acid, has been reported to produce butenes as major products in the presence of SiO₂/Al₂O₃ catalysts [381]. A high butene yield of up to 93% can be obtained at 375 °C and a low weight hourly space velocity of

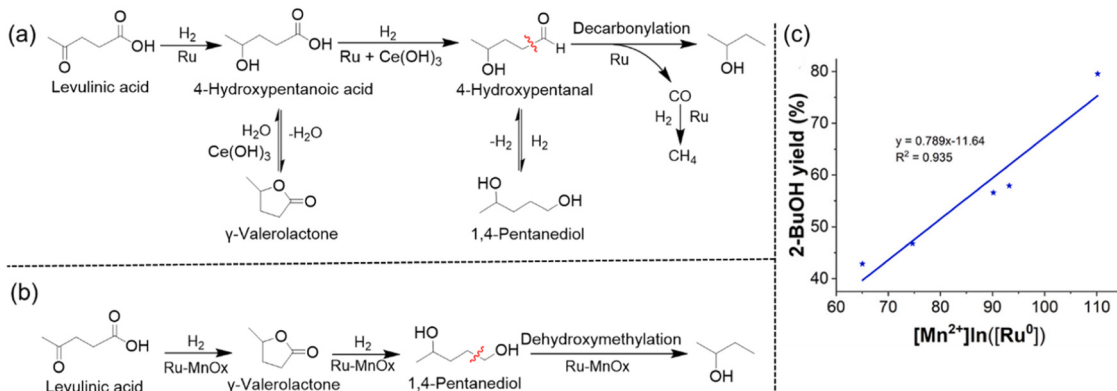
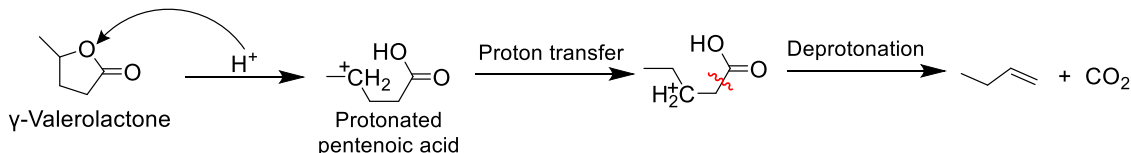


Scheme 50. Proposed reaction mechanism for the decarboxylation of levulinic acid through a radical intermediate in the presence of catalytic Ag(I) species and sodium peroxydisulphate. Adapted with permission from ref. [375].

Table 6

Representative catalysts for the decarboxylation of (hemi)cellulose derived organic acids.

Substrate	Catalyst	Product	Conv. (%)	Temp. (°C)	Time (h)	Atmosphere	Yield (%)	Ref.
Levulinic acid	AgNO ₃	MEK	70	160	0.5	–	44.2	375
	Ru-Ce(OH) ₃	2-Butanol	99	150	12	30 bar H ₂	85	376
	Ru-MnO _x /Al ₂ O ₃	2-Butanol	100	200	4	50 bar H ₂	98.8	380
	Nanoporous Ru	2-Butanol	100	140	20	60 bar H ₂	63.6	378
	NiMn/Al ₂ O ₃	2-Butanol	100	250	5	50 bar H ₂	84.5	379
	GVL	Butene	100	375	–	36 bar He	93	381
Itaconic acid	Pd/C + NaOH	MAA	86	250	1	1 bar Ar	65	382
Itaconic acid	Ba-hexaaluminate	MAA	17	250	3	20 bar N ₂	50	384
Glucaric acid	SnCl ₄	Furan	100	200	2	7 bar N ₂	80	385

**Scheme 51.** Proposed reaction pathways for the hydrogenative decarboxylation of levulinic acid into 2-butanol over (a) Ru-Ce(OH)₃ and (b) Ru-MnO_x; (c) Correlation between 2-butanol yield and the concentration of Ru⁰ and Mn²⁺ for Ru-MnO_x catalyst. Adapted with permission from ref. [376 and 380].**Scheme 52.** Proposed reaction mechanism for proton-catalyzed decarboxylation of gamma-valerolactone into butene. Adapted with permission from ref. [381].

0.18 h⁻¹ under 36 bar He. This decarboxylation process actually involves two cascaded reaction steps, that is, the ring opening of GVL to form protonated pentenoic acid isomers followed by the decarboxylation to form equimolar butenes and CO₂ (Scheme 52). Brønsted acid sites present on SiO₂/Al₂O₃ catalysts play a key role in promoting ring opening and decarboxylation reactions. Protonation at the ring oxygen atom of GVL can trigger the scission of the lactone linkage. The subsequent proton transfer and deprotonation steps lead to the elimination of carboxyl group.

Decarboxylation offers a promising approach to upgrade sugar-derived itaconic acid into bio-based methacrylic acid (MAA), a key monomer in polymer industry. Haveren and coworkers reported that Pd/C catalyst is highly selective for the decarboxylation of itaconic acid into MAA in a high yield of 65% at 250 °C under Ar in the presence of NaOH [382]. The amount of base was identified as a key factor to affect the yield of methacrylic acid (Fig. 9). In the absence of base, the yield of MAA markedly decreased to 13%. The addition of excess base (above two equivalents) led to a very low MAA yield of below 10%. The highest yield of MAA was obtained at around one equivalent of NaOH, which can deprotonate itaconic acid to generate itaconate in a monoanion form. This partially deprotonated species was discovered to possess high reactivity towards decarboxylation than the fully deprotonated itaconate in a dianion form and pristine itaconic acid [383]. The decarboxylation of itaconic acid was proposed to proceed by eliminating the non-conjugated carboxyl group, as the remaining carboxyl group and

double bond can form a stabilized cyclic intermediate in a conjugated configuration (Fig. 9). The adsorption/activation of carboxyl group and double bond on Pd sites is of pivotal importance in enabling itaconic acid decarboxylation. However, a detailed catalytic decarboxylation mechanism on Pd sites remains unclear.

Recently, non-noble metal catalysts based on hexaaluminates were reported to be active for the decarboxylation of itaconic acid into MAA without any base additives [384]. Four hexaaluminates containing La (III), Ba(II), Ca(II), and Mg(II) cations featuring different basic properties were synthesized and examined. The decarboxylation activities of these hexaaluminate catalysts were found to depend on the number of their basic sites. Ba(II) hexaaluminate with a medium amount of basic sites (3 μmol/g) afforded the highest yield of MAA (50%) at 250 °C and 20 bar N₂ in water. By contrast, Ca(II) hexaaluminate with a higher number of basic sites (4.1 μmol/g) and La(III) hexaaluminate with less basic sites (1.7 μmol/g) gave 22% and 12% yields of MAA, respectively. By monitoring the reaction progress and identifying reaction intermediates, a plausible reaction network for the decarboxylation of itaconic acid into MAA and associated side reactions was proposed in Scheme 53. Itaconic acid is actually in equilibrium with citraconic and mesaconic acids due to the fast isomerization among them. Upon the adsorption of itaconic acid on hexaaluminates, their basic sites can deprotonate the non-conjugated carboxyl group to form a reactive intermediate itaconate monoanion followed by the extrusion of CO₂ to from MAA. Possible competitive reactions include the further

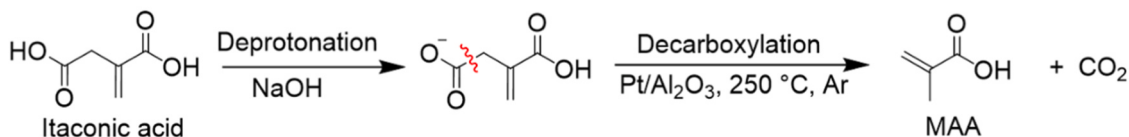
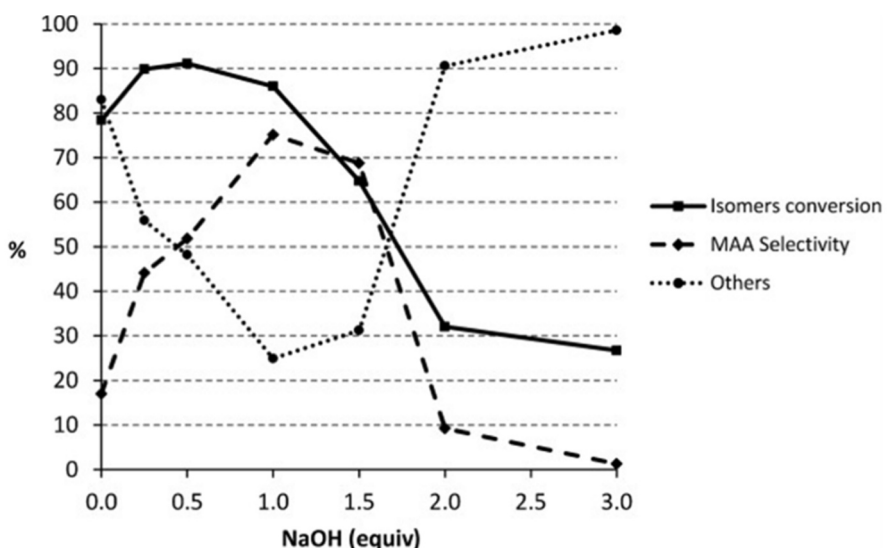
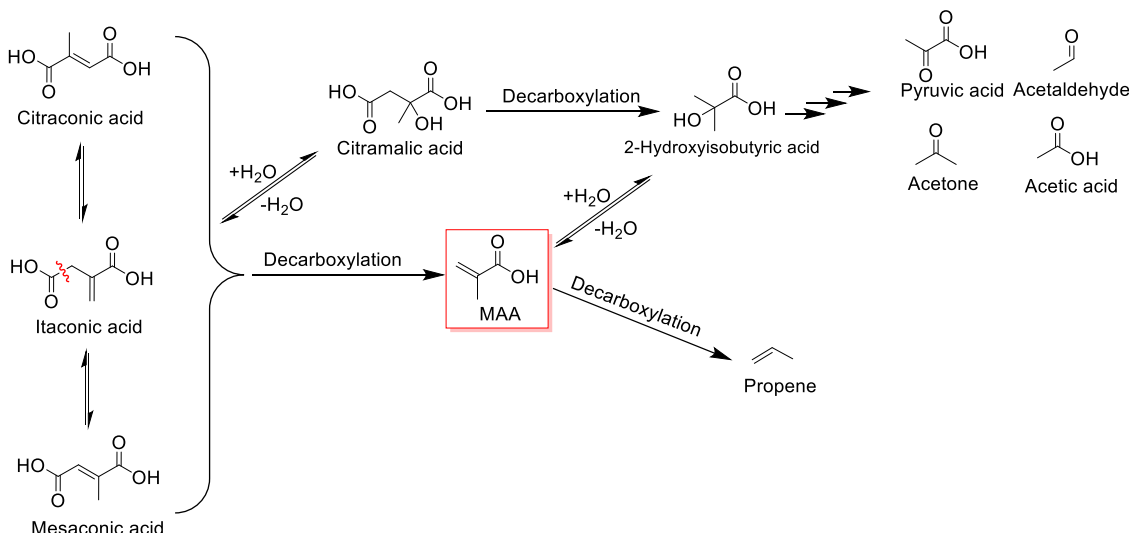
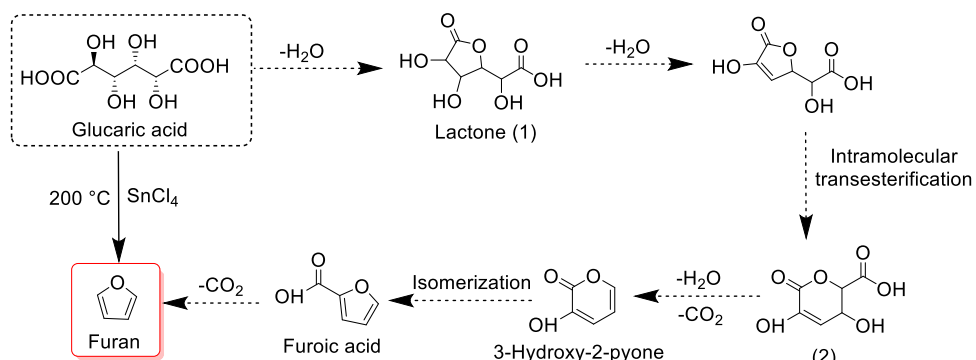


Fig. 9. Effect of the equivalent of NaOH on the decarboxylation of itaconic acid into MAA. Adapted with permission from ref. [382].



Scheme 53. Proposed reaction network for the decarboxylation of itaconic acid into MAA. Adapted with permission from ref. [384].



Scheme 54. Proposed reaction pathway for SnCl_4 -catalyzed conversion of glucaric acid into furan. Adapted with permission from ref. [385].

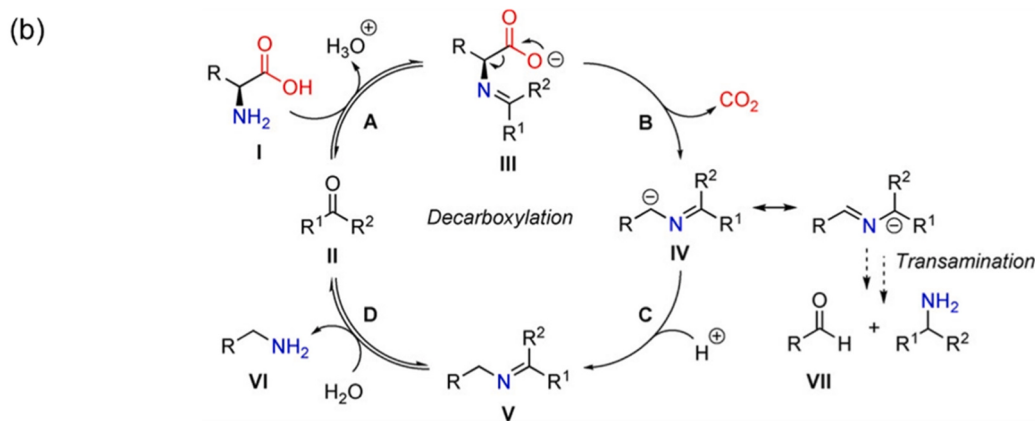
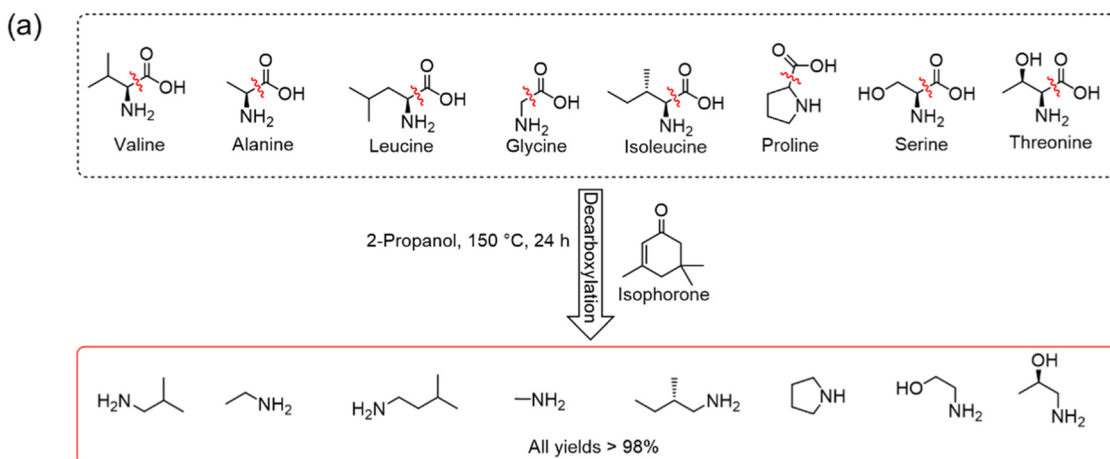
decarboxylation of MAA into propene as well as the hydration of itaconic acid and MAA into 2-hydroxyisobutyric acid which tends to undergo radical fragmentation to form C2-C3 acids, aldehydes, and ketones.

In addition, decarboxylation has been applied for the synthesis of furan from sugar-derived glucaric and furoic acids. For example, Li et al. described a tandem reaction strategy relying on the dehydration and decarboxylation of glucaric acid, giving a high furan yield of ca. 80% in a water/toluene biphasic system using SnCl_4 as the catalyst at 200 °C in 2 h [385]. Furoic acid and 3-hydroxy-2-pyone (3-HP) were identified as key intermediates by monitoring the reaction progress. As shown in Scheme 54, glucaric acid conversion to furan was proposed to be initiated by the intramolecular esterification to form a lactone intermediate (1), which can further undergo dehydration and intramolecular trans-esterification to generate an unsaturated lactone intermediate (2). Subsequently, the concerted dehydration-decarboxylation of compound (2) gives rise to 3-hydroxy-2-pyone followed by isomerization to form furoic acid. Furan is eventually obtained by a second decarboxylation of furoic acid, the rate-determining step for the whole reaction. The Lewis acidity of Sn(IV) was proposed to play two important catalytic roles, that is, promoting dehydration/esterification steps and facilitating the concerted dehydration-decarboxylation of intermediate (2) to 3-hydroxy-2-pyone by coordinating with hydroxyl and carboxyl groups simultaneously. In addition, protons and chloride ions present in aqueous SnCl_4 solution have been proven beneficial to the decarboxylation of furoic acid.

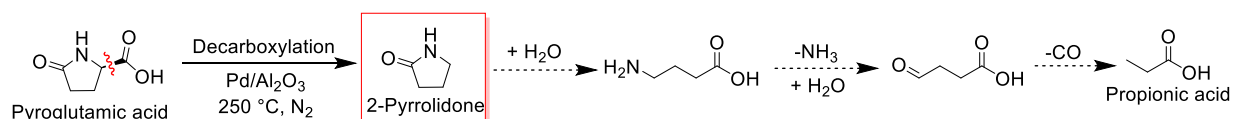
3.3.2. Decarboxylation of amino acids

Decarboxylation of amino acids, available from carbohydrates fermentation, could selectively remove their carboxyl moieties, thus providing an attractive and straightforward method to synthesize amines from renewable resources. Organocatalysts and heterogeneous noble metal catalysts have been demonstrated to facilitate the decarboxylation of amino acids into amines. For example, isophorone has been identified as an excellent organocatalyst for the decarboxylation of numerous amino acids such as valine, alanine, leucine, glycine, isoleucine, proline, serine, threonine, and norleucine into corresponding primary and secondary amines in high yields of above 90% at 150 °C using 2-propanol as solvent (Scheme 55a) [386]. A reaction mechanism based on Schiff base reaction was proposed in Scheme 55b. The condensation of amino acids with the ketone moiety of isophorone generates Schiff base adduct III, wherein the terminal C-C bond readily cleaves with the elimination of CO_2 and the formation of intermediate IV. Subsequent hydrolysis of Schiff base adduct V releases the amine product accompanied by the regeneration of isophorone catalyst. The high catalytic activity of isophorone is attributed to its α,β -unsaturated conjugated structure and six-membered ring, which can stabilize the reaction intermediate IV via electron delocalization (resonance stabilization).

Heterogeneously catalytic decarboxylation of amino acids has been demonstrated over several noble metal catalysts primarily based on Pd and Ru. Schouwer et al. reported that Pd/ Al_2O_3 catalyst can enable the decarboxylation of pyroglutamic acid into 2-pyrrolidone in a high yield of 70% at 250 °C in water under 6 bar N_2 (Scheme 56) [387]. Propionic acid was detected as the main byproduct (ca. 9% yield), likely resulting from the consecutive hydrolysis/deamination/decarbonylation of



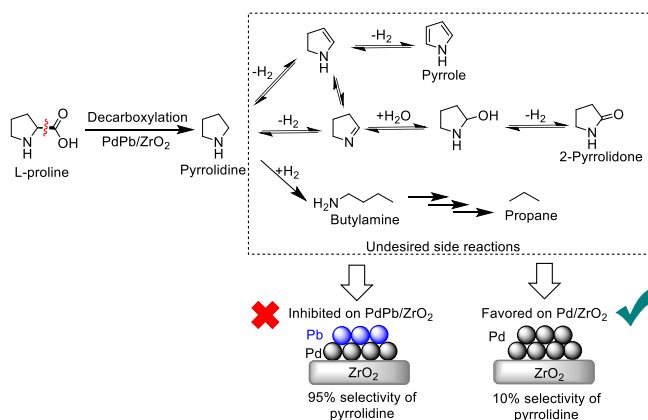
Scheme 55. (a) Isophorone-catalyzed decarboxylation of amino acids into amines; (b) Proposed reaction mechanism for isophorone-catalyzed decarboxylation of amino acids mainly including A condensation, B decarboxylation, C protonation, D hydrolysis. Adapted with permission from ref. [386].



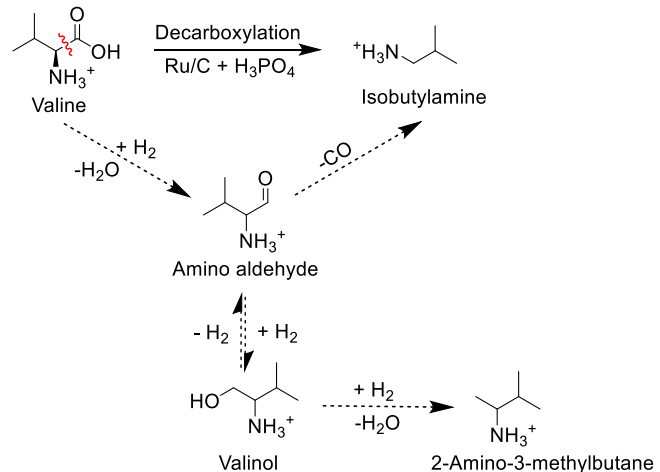
Scheme 56. Pd-catalyzed decarboxylation of pyroglutamic acid into 2-pyrrolidone.

2-pyrrolidone. Among the screened supports, Al_2O_3 displayed the highest yield of 2-pyrrolidone. This is probably related to the electrostatic attraction between Al_2O_3 surface and acidic carboxyl groups, leading to the high surface coverage of amino acids over $\text{Pd}/\text{Al}_2\text{O}_3$ catalysts available for decarboxylation. In the case of catalytic decarboxylation of L-proline into pyrrolidine, common Pd catalysts such as Pd/C , $\text{Pd}/\text{Al}_2\text{O}_3$, and Pd/ZrO_2 all displayed very poor selectivities (below 20%) towards pyrrolidine at 99% conversion of L-proline at 225 °C in water under 6 bar N_2 (Scheme 57) [388]. This is related to the high reactivity of pyrrolidine, which is apt to undergo two main side reactions including dehydrogenation to generate pyrrole or 2-pyrrolidone and ring-opening hydrogenolysis to generate butylamine or propane (Scheme 57). Covering Pd sites by Pb species has been proven effective in inhibiting these side reactions. The Pb-modified Pd/ZrO_2 catalyst showed a markedly improved pyrrolidine selectivity of up to 95% at 58% conversion of L-proline under 4 bar H_2 and 2 bar N_2 . The formation of electron-rich Pd sites in the presence of Pb was speculated to weaken the adsorption of pyrrolidine on Pd sites, thus reducing the chance of undesired side reactions (ring opening, hydrogenolysis, dehydrogenation) [389]. Besides, conducting the reaction under H_2 atmosphere is helpful to suppress the successive dehydrogenation of pyrrolidine.

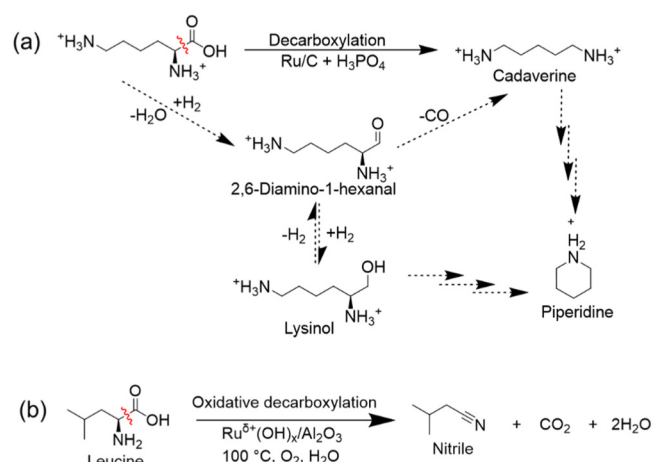
The combination of Ru/C with H_3PO_4 has been reported as an efficient catalyst system for the indirect decarboxylation (hydrogenation-decarbonylation mechanism) of amino acids at mild temperatures. For example, L-valine could be transformed into isobutylamine in a high yield of 87% at 150 °C and 40 bar H_2 in the presence of Ru/C and 1.2 equiv. of H_3PO_4 [390]. Kinetic studies indicated that the decarboxylation of L-valine follows a hydrogenation-decarbonylation mechanism via an amino alcohol intermediate. As shown in Scheme 58, L-valine first undergoes hydrogenation to form valinol via an amino aldehyde intermediate followed by decarbonylation to form isobutylamine as the main product. Adding H_3PO_4 as the co-catalyst is of crucial importance in achieving high yields of isobutylamine. An acidic environment was believed to not only accelerate the hydrogenation of amino acids but also prevent isobutylamine from undergoing side reactions like dehydrogenation, condensation, and hydrolysis. Note that an excessive amount of H_3PO_4 would result in the dehydration-hydrogenation of valinol into 2-amino-3-methylbutane, and the optimal dosage of H_3PO_4



Scheme 57. Proposed reaction network for Pd-catalyzed decarboxylation of L-proline into pyrrolidine as well as associated side reactions of pyrrolidine. Adapted with permission from ref. [388].

Scheme 58. Decarboxylation of L-valine into isobutylamine following a hydrogenation-decarbonylation mechanism in the presence of Ru/C and H_3PO_4 . Adapted with permission from ref. [390].

is 1.2 equiv. Very recently, Xie et al. reported that the combination of Ru/C and H_3PO_4 is able to realize the decarboxylation of lysine into cadaverine, a key monomer for nylon industry, in a yield of 46.6% at 200 °C for 2 h [391]. By contrast, in the absence of H_3PO_4 , lysine deamination became dominant over Ru/C , affording 6-aminocaproic acid and 2-aminohexanoic acid as main products. Obviously, the addition of H_3PO_4 effectively blocked undesired lysine deamination, owing to the enhanced stability of the fully protonated amino groups. As depicted in Scheme 59a, the decarboxylation of lysine also follows the hydrogenation-decarbonylation mechanism via a 2,6-diamino-1-hexanal intermediate, which can undergo either decarbonylation to yield cadaverine or hydrogenation to yield lysinol. In addition to cadaverine, a considerable amount of piperidine was detected (ca. 38.6% yield), probably resulting from multistep degradation (e.g., deamination,

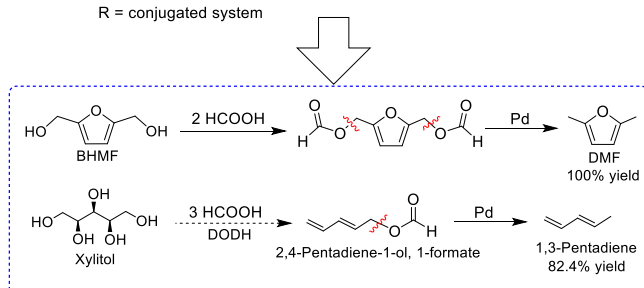
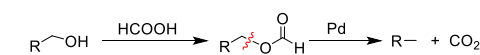
Scheme 59. (a) Decarboxylation of lysine into cadaverine following a hydrogenation-decarbonylation mechanism in the presence of Ru/C and H_3PO_4 ; (b) Oxidative decarboxylation of leucine into nitrile catalyzed by $\text{Ru}^{\delta+}(\text{OH})/\text{Al}_2\text{O}_3$. Adapted with permission from ref. [391 and 392].

decarbonylation, dehydrogenation, isomerization) of lysinol or cadaverine.

The integration of decarboxylation with amine oxidation, namely oxidative decarboxylation, provides an alternative approach to synthesize nitriles directly from amino acids. Laurens and coworkers reported that various Ru catalysts were highly active for the aerobic oxidative decarboxylation of amino acids into nitriles [392]. Taking leucine as the model substrate (Scheme 59b), both homogeneous and heterogeneous Ru catalysts, for example, RuCl₃, Ru(acac)₃, and Ru hydroxides dispersed on various metal oxides, exhibited high selectivities (60–90%) towards nitrile at nearly full leucine conversion at 100 °C in water under 30 bar O₂ after 24 h. For the supported Ru catalysts, ionic Ru^{δ+}(OH) species was identified as the active sites for decarboxylation and also the oxidation of amine into nitrile, whereas metallic Ru species led to poor nitrile selectivity (14%) with the formation of fragmented oxidation products. The same team also developed the hypobromite-mediated oxidative decarboxylation of amino acid into nitrile using layered double hydroxide-supported peroxotungstate (LDH-WO₆) as catalyst and H₂O₂ as oxidant [393]. When using phenylalanine as the substrate, 88% yield of phenylacetonitrile was obtained at room temperature in the presence of LDH-WO₆, H₂O₂, and NH₄Br. As depicted in Scheme 60a, tungstate species immobilized on LDH is oxidized by H₂O₂ to form active peroxotungstate species, which in turn promotes the oxidation of bromide to form hypobromite. The in situ formed hypobromite species was proposed as the key species that directly participates in the oxidative decarboxylation of amino acids. The electrostatic interaction between amino acid and positively-charged LDH brings amino acid in close proximity to hypobromite species for oxidative decarboxylation. Hypobromite-mediated reaction mechanism was speculated to be initiated by the bromination of amino acid with hypobromite to form a N-bromo amino acid intermediate (Scheme 60b). Under neutral or slightly acidic conditions, this N-bromo amino acid tends to undergo a second bromination to give a N,N-dibromo amino acid intermediate. This is followed by the successive elimination of two HBr molecules and one CO₂ molecule to finally yield nitriles. By contrast, under alkaline conditions, the N-bromo amino acid prefers to undergo HBr elimination to yield aldehydes through an imino acid intermediate.

3.3.3. Formic acid-mediated decarboxylation

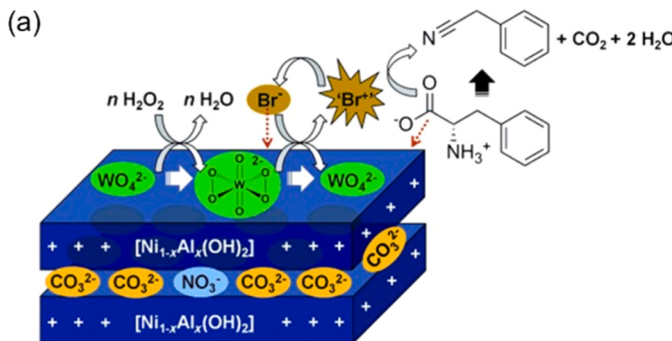
As a special case of decarboxylation, formic acid-mediated decarboxylation can lead to the cleavage of C–O rather than C–C bonds. As mentioned in Section 2.2.2.2, formic acid has been utilized as a deoxygenation agent to enable the cleavage of paired OH groups in the DODH of vicinal diols. This unique function of formic acid has been further utilized to assist the cleavage of single OH group catalyzed by Pd catalysts. To be specific, the esterification of OH group with formic acid first generates a formate ester intermediate, which subsequently undergoes C–O bond cleavage over Pd sites to generate corresponding



Scheme 61. Selective C–O bond cleavage of the esterified OH group via formic acid-mediated decarboxylation over Pd catalysts.

deoxygenated products by extruding one molecule of CO₂ (Scheme 61). The transformation of OH group to its formate ester plays a key role in facilitating the cleavage of C–O bonds, since formate ester is known as a labile moiety that can be easily eliminated in the form of CO₂. Hence, this C–O bond cleavage process can be actually viewed as a formic acid-mediated decarboxylation reaction, which is especially effective to remove the OH group connected to a conjugated system such as biomass-derived bis(hydroxymethyl)furan (BHMF) and pentadien-1-ol. For these conjugated chemicals, their formate esters are more liable to undergo decarboxylation rather than competitive decarbonylation, thus leading to selective C–O bond cleavage.

Thananathanachon et al. reported double C–O bond cleavage of BHMF into 2,5-dimethylfuran (DMF) over Pd/C via formic acid-mediated decarboxylation [394]. At a mild temperature (refluxing THF), the diformate ester of BHMF could be selectively converted into DMF in a quantitative yield of up to 100% over Pd/C (Scheme 61). By integrating Pd-catalyzed hydrogenation of HMF to BHMF with formic acid-mediated decarboxylation, HMF was smoothly converted to DMF (> 95% yield) in one pot in the presence of formic acid, H₂SO₄ and Pd/C. This high DMF yield was ascribed to two important roles of formic acid: a hydrogen donor for HMF reduction and a deoxygenation agent for C–O bond cleavage. In contrast, the C–O bond cleavage of HMF/BHMF to DMF via catalytic hydrogenolysis usually occurs at higher temperatures (100–250 °C) accompanied by many side reactions like furan ring hydrogenation, partial deoxygenation and decarbonylation. In addition, Zhang and coworkers demonstrated that formic acid-mediated decarboxylation can be applied to break the C–O bond within the formate ester of 2,4-pentadien-1-ol, produced from the DODH of xylitol (Scheme 61) [126]. Eliminating the formate moiety led to the exclusive formation of 1,3-pentadiene in a high yield of 82.4% over Pd/C at 80 °C. Clearly, these two examples manifest the unique function of formic acid in assisting the selective cleavage of C–O bonds for OH-containing



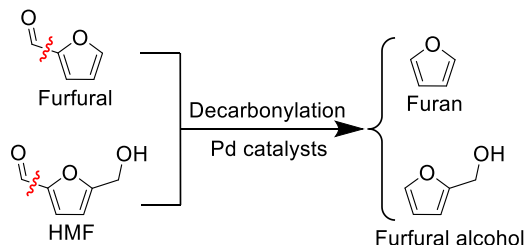
Scheme 60. (a) Peroxotungstate immobilized on a LDH support for hypobromite-mediated oxidative decarboxylation of phenylalanine to phenylacetonitrile; (b) Proposed reaction mechanism for hypobromite-mediated oxidative decarboxylation of amino acids to nitriles and aldehydes. Reproduced with permission from ref. [393].

conjugated molecules derived from (hemi)cellulose at low temperatures.

3.4. Decarbonylation

Decarbonylation is known as a carbonyl-removal reaction that is frequently encountered in the conversion of carbonyl compounds including aldehydes, acids, and metal carbonyls. In the case of aldehyde decarbonylation, the terminal C–C bond connected to carbonyl group in aldehyde needs to be cleaved, thus leading to the elimination of carbonyl groups in the form of CO. The rest moieties of aldehyde remain unchanged. This feature renders decarbonylation a useful method to selectively break the terminal C–C bond of (hemi)cellulose derivatives containing aldehyde groups such as aldoses, furfural, and HMF. In view of the strong affinity of noble metals towards carbonyl group, heterogeneous or molecular catalysts based on noble metals (e.g., Pd, Ru, Rh, Ir) are usually employed to facilitate the decarbonylation of these bio-based carbonyl compounds.

The decarbonylation of HMF and furfural could lead to the formation of furfuryl alcohol and furan, respectively (Scheme 62). Heterogeneous and molecular catalysts reported for HMF and furfural decarbonylation primarily containing Pd as the catalytically active component [147, 395]. For example, a commercial Pd/C catalyst was reported to catalyze the decarbonylation of HMF into furfuryl alcohol in a high yield of 90% at 120 °C using dioxane as solvent under reflux conditions [396]. Huang et al. examined the effect of utilizing different oxide supports (e.g., MgO, SiO₂, ZrO₂, TiO₂, HZSM-5) to prepare Pd catalysts on HMF decarbonylation [397]. It was found that well-dispersed Pd nanoparticles on SBA-15 (Pd/SBA-15) displayed the highest furfuryl alcohol yield of up to 96% at 130 °C using cyclohexane as solvent in the presence of molecular sieves. The role of molecular sieves is to keep the reaction system anhydrous, since a trace amount of water was found to deteriorate the formation of furfuryl alcohol. Likewise, furfural could be selectively decarbonylated into furan in a high yield of 96% at 150 °C in the presence of Pd/SBA-15 and molecular sieves. The superior activity of Pd/SBA-15 over other supported catalysts was attributed to the large specific surface area of SBA-15 conducive to the formation of small-sized Pd nanoparticles (about 4–6 nm) and the absence of acid or basic sites on SBA-15. Hence, acid- or base-catalyzed decomposition/condensation of HMF was effectively suppressed. Li et al. reported that the addition of alkaline Sr species to Pd/Al₂O₃ could improve the furan yield up to 92.3% [398]. Doping Sr markedly reduced the acidity of Pd/Al₂O₃ catalysts thus suppressing acid-catalyzed side reactions. On the other hand, the electron donation effect of Sr favoring the adsorption of HMF on Pd atoms instead of Al₂O₃ in a $\eta^2(\text{C},\text{O})$ configuration which is considered as a key adsorption mode for HMF decarbonylation [399, 400]. Besides, introducing compressed carbon dioxide to the reaction medium has been demonstrated to promote the decarbonylation of HMF. Under 6 MPa CO₂, a high furfuryl alcohol yield of up to 99% was achieved at 145 °C for 4 h over a commercial Pd/Al₂O₃ catalyst [401]. Same promotion effect was also observed for Ir complex-catalyzed HMF decarbonylation in an expanded liquid medium comprising pressurized CO₂ and dioxane [402]. The benefit of introducing compressed CO₂ is presumably related to the altered physicochemical properties of the



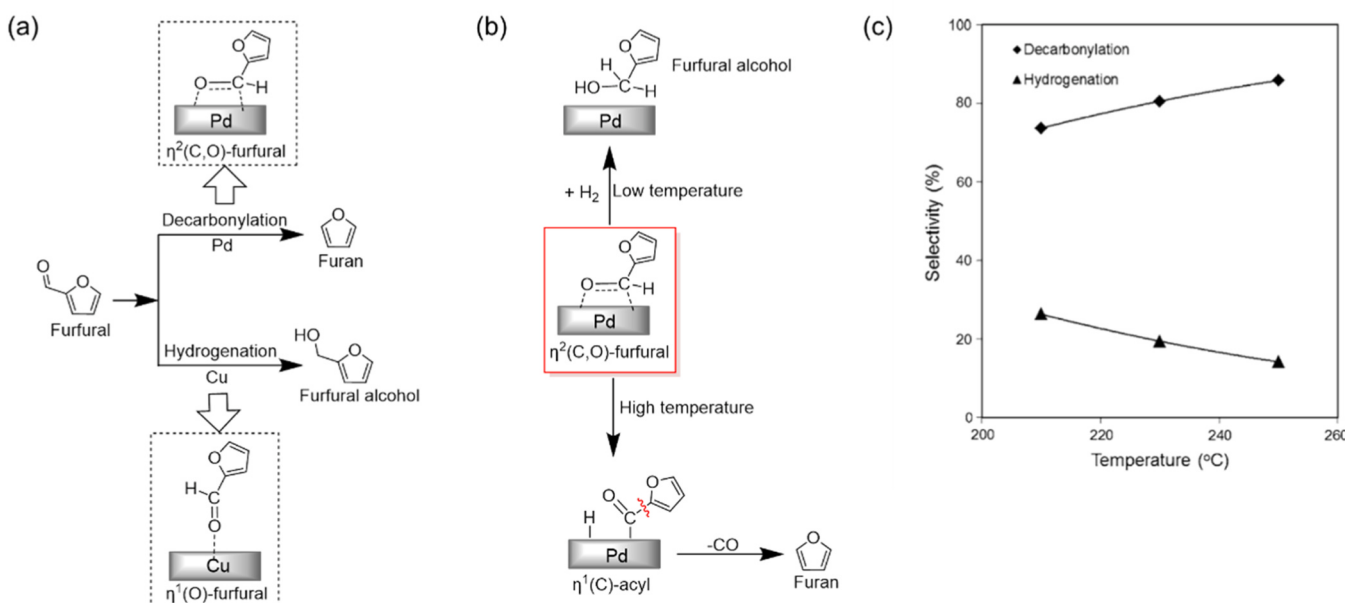
Scheme 62. Decarbonylation of HMF and furfural into furfuryl alcohol and furan over Pd catalysts.

reaction medium that promotes the dissolution and diffusion of HMF.

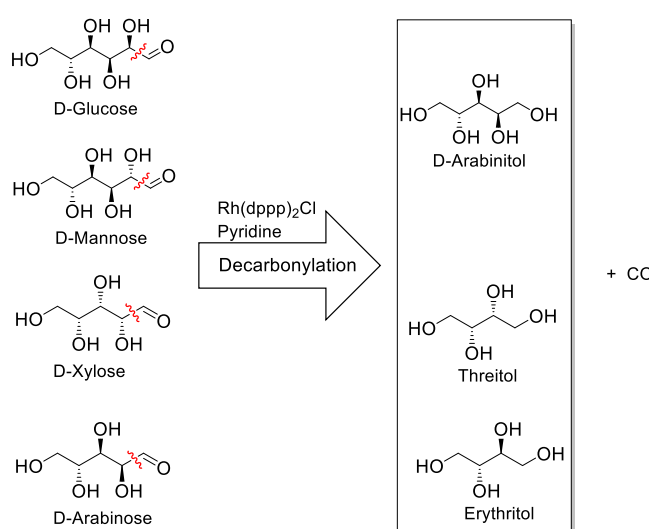
Catalytic behaviors of different metal catalysts in furfural conversion were studied by Sitthisa [403]. Under 1 bar H₂, furfural still preferred to undergo decarbonylation into furan (59% yield) over hydrogenation into furfuryl alcohol (9% yield) in the presence of Pd/SiO₂ at 250 °C. By contrast, furfural was almost exclusively reduced into furfuryl alcohol over Cu/SiO₂ under similar reaction conditions. These results indicate that Pd is intrinsically more active in furfural decarbonylation, whereas Cu appears more selective for the hydrogenation of aldehyde group. These distinct catalytic behaviors are related to the different adsorption modes of furfural on Pd and Cu atoms, as proposed in Scheme 63a. According to DFT calculations and spectroscopic studies, furfural is suggested to adsorb on Pd atoms with its carbonyl group to form a $\eta^2(\text{C},\text{O})$ -carbonyl intermediate with both oxygen and carbon atoms bonding to Pd atoms [404–406]. At low temperatures, this $\eta^2(\text{C},\text{O})$ intermediate is proposed to undergo hydrogenation to form furfuryl alcohol (Scheme 63b). However, with increasing temperatures, this $\eta^2(\text{C},\text{O})$ intermediate prefers to undergo further conversion to form an acyl intermediate in a $\eta^1(\text{C})$ configuration followed by exocyclic C–C bond cleavage to yield furan and CO. These speculations are supported by the observed temperature-dependent selectivity towards decarbonylation and hydrogenation products, as shown in Scheme 63c. The same $\eta^2(\text{C},\text{O})$ adsorption mode of furfural was also found for Ni catalysts which favor furfural decarbonylation to furan as well [407,408].

In the case of Cu-based catalysts, the preferred adsorption mode of furfural was proposed as the $\eta^1(\text{O})$ -carbonyl configuration, wherein the oxygen atom of carbonyl group is bonded to Cu atoms (Scheme 63a) [409–411]. This relatively weak interaction favors the selective hydrogenation of carbonyl group (not enough to break exocyclic C–C bond), thus accounting for the dominant formation of furfuryl alcohol on Cu/SiO₂. The presence of H₂ was found to be advantageous to the decarbonylation of furfural despite H₂ is not stoichiometrically needed, whereas high H₂ coverages favor furfural hydrogenation over decarbonylation [412–414]. This is probably related to different configurations of furfural adsorbed on Pd atoms under H₂ atmosphere, as revealed by DFT simulations [412,414]. At low H₂ coverages, furfural is proposed to adsorb flat on Pd atoms with both furan and aldehyde group interacting with Pd atoms. The flat adsorption enabling strong interaction between furfural and Pd atoms is beneficial to decarbonylation. At high H₂ coverages, furfural tends to adsorb in a tilted configuration with its aldehyde group interacting with Pd atoms, thus leading to furfuryl alcohol. Moreover, Pd atomicity was found to strongly affect furfural decarbonylation [415]. Decreasing the size of ZrO₂-supported Pd nanoparticles led to improved decarbonylation activity. The highest activity was achieved over Pd clusters containing several Pd atoms affording a high furan yield of 98% at 140 °C under N₂. In contrast, single Pd atom stabilized by CeO₂ gave a furan yield of 81%. As aforementioned, decarbonylation requires furfural adsorbing preferentially in a $\eta^2(\text{C},\text{O})$ or a flat configuration. Both configurations are allowed on Pd clusters thus accounting for its superior activity.

The decarbonylation of (hemi)cellulose derived aldoses enables the removal of their aldehyde groups and thus generates corresponding sugar alcohols with one less carbon atom, for example, the decarbonylation of hexoses and pentoses into pentitols and tetritol, respectively. Hence, decarbonylation offers an attractive approach to synthesize alditols such as pentitols and tetritol directly from easily-available sugars. However, owing to the presence of highly reactive aldehyde and hydroxyl groups in aldoses, the selective removal of carbonyl group without the occurrence of side reactions (e.g., dehydration, condensation) is very challenging. There exist only a few examples on the decarbonylation of aldoses with acceptable yields towards sugar alcohols. For instance, Nygaard et al. reported a highly active and selective Rh complex consisting of a bidentate phosphine ligand (1,3-bis(diphenylphosphino)propane = dppp) for the decarbonylation of C5 and C6 aldoses [416]. When using D-glucose as the substrate, D-arabinitol was produced in a high yield of 71% at 162 °C for 9 h using a mixture of



Scheme 63. (a) Proposed adsorption modes of furfural on Pd and Cu atoms; (b) Proposed transformation pathways of the $\eta^2(\text{C},\text{O})$ -furfural intermediate over Pd catalysts; (c) Selectivity of products from decarbonylation (furan and tetrahydrofuran) and hydrogenation (furfuryl alcohol and tetrahydrofurfuryl alcohol) reactions at different temperatures. Adapted with permission from ref. [403 and 407].



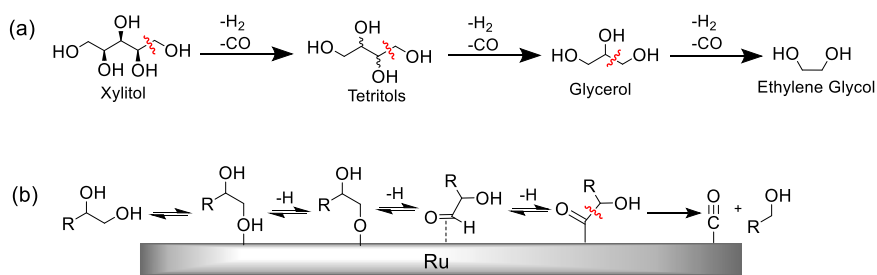
Scheme 64. Rh-catalyzed decarbonylation of C5/C6 aldoses into corresponding sugar alcohols.

diglyme and N,N-dimethylacetamide as solvent (Scheme 64). D-mannose gave similar yields of D-arabinitol as D-glucose. The reaction time can be shortened to 8 h by adding pyridine, a basic additive capable of promoting the mutarotation of glucose towards an open-chain form bearing a free aldehyde group for decarbonylation. This Rh complex also exhibited high catalytic activity in the decarbonylation of D-xylose and D-arabinose, affording 74% yield of threitol and 70% yield of erythritol, respectively. Bitter and coworkers reported a heterogeneous Ru/C catalyst for the aqueous-phase decarbonylation of D-xylose, affording a mixture of threitol and erythritol in a lower yield of 24% at 138 °C under 6 bar H₂ in 24 h [417]. As indicated by the product evolution over time, xylose preferred to first undergo hydrogenation to form xylitol as the major product at the beginning of the reaction (1 h). The formed xylitol can be transformed into other C5 alditols (arabinitol and adonitol) via epimerization. After the initial hydrogenation stage, the yields of

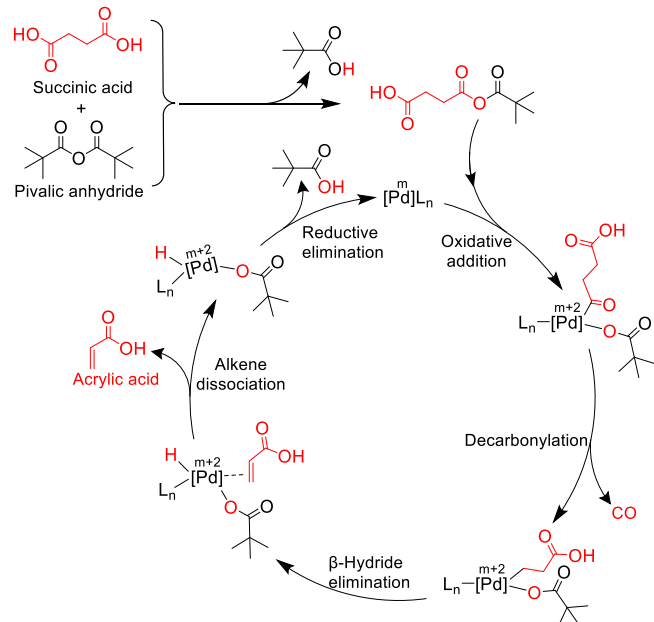
threitol and erythritol started to increase gradually accompanied by the consumption of C5 alditols. According to these results, the formation of threitol was proposed to proceed via the dehydrogenation of xylitol into xylose followed by decarbonylation rather than directly from xylose decarbonylation. The appearance of erythritol, an isomer of threitol, was speculated to arise from the epimerization of threitol or the decarbonylation of arabinose from arabinitol dehydrogenation.

In addition to aldoses, sugar alcohols can be selectively fragmented via decarbonylation to generate short-chain polyols. In fact, decarbonylation and aforementioned RAC are regarded as two major C–C bond cleavage reactions for the hydrogenolysis of sorbitol and xylitol. Under neutral conditions without basic additives, the C–C bond cleavage of sorbitol and xylitol prefers to follow a decarbonylation mechanism instead of RAC [246,418,419]. Note that the decarbonylation of sorbitol and xylitol usually proceed in a consecutive way, that is, the formed polyol products can continue to undergo decarbonylation with the stepwise elimination of CH₂OH moieties [418]. Hence, a complicated product distribution was usually obtained for sugar alcohol decarbonylation. Hausoul et al. demonstrated the consecutive decarbonylation of sorbitol in the presence of Ru/C at 160 °C under 6 MPa H₂, affording a series of polyols including pentitols, tetratols, and glycerol [248]. Similarly, the decarbonylation of xylitol led to the successive generation of tetratols, glycerol, and ethylene glycol (Scheme 65a) [246]. Among these polyol products, pentitols and tetratols were dominantly generated in yields around 20% for the decarbonylation of sorbitol and xylitol, respectively. As depicted in Scheme 65b, the decarbonylation of sugar alcohols was proposed to involve an initial dehydrogenation to form an aldoose attached to Ru sites, subsequent elimination of the aldehydic proton to give an adsorbed acyl intermediate, and a C–C bond scission reaction to yield adsorbed CO and C_{n-1} polyol [418].

Note that decarbonylation is also applicable to eliminating the carboxyl group of (hemi)cellulose-derived organic acids to form terminal alkenes and CO. For example, succinate, available from the fermentation of sugars, could be selectively transformed to acrylate through decarbonylation [420]. In the presence of homogeneous phosphine-ligated Pd catalysts, acrylate was generated in 62% yield by the decarbonylation of succinate at 190 °C using one equivalent of pivalic anhydride as a sacrificial agent to activate succinate. The C–C bond cleavage mechanism was proposed to follow a typical Pd-catalyzed



Scheme 65. (a) Stepwise decarbonylation of xylitol into a series of polyols in the presence of Ru/C under H_2 ; (b) Proposed reaction mechanism for the decarbonylation of sugar alcohols over Ru catalysts. Adapted with permission from ref. [246 and 418].



Scheme 66. Proposed reaction mechanism for Pd-catalyzed decarbonylation of succinic acid into acrylic acid in the presence of pivalic anhydride as a sacrificial agent. Adapted with permission from ref. 421.

decarbonylation pathway [421]. Initially, succinate was in situ transformed into a mixed anhydride intermediate by reacting with pivalic anhydride (Scheme 66). This mixed anhydride intermediate undergoes a series of reaction steps in sequence including oxidative addition on the Pd center to form a Pd-acyl complex, decarbonylation, β -hydride elimination to form a Pd-alkene complex, alkene dissociation, and final reductive elimination to regenerate the Pd complex. Benjamin et al. reported the decarbonylation of lactic acid to acetaldehyde and CO over silica-supported heteropolyacid catalysts [422]. Among various Mo- and W-containing heteropolyacids, silicotungstic acid exhibited a high acetaldehyde selectivity of 98% at 85% conversion of lactic acid at 275 °C. The superior selectivity of silicotungstic acid is probably related to the well-dispersed WO_x species featuring Lewis acidic sites to activate the carboxyl group. Further studies are needed to unravel the catalytic mechanism of WO_x -promoted decarbonylation of lactic acid.

3.5. Summary of C–C bond cleavage strategies

Breaking C–C bond is an essential process when targeting the production of short-chain molecules from (hemi)cellulose and its derivatives. However, the cleavage of C–C bond is more challenging than C–O bond owing to its recalcitrant nature. Moreover, the prevalence of multiple C–C bonds featuring similar properties renders the selective cleavage at specific position even more challenging.

As shown in Table 7, a common feature of the C–C bond cleavage

Table 7

Comparison of different C–C bond cleavage strategies applicable to (hemi)cellulose and its derivatives.

Bond type	Typical catalyst	Selectivity of bond cleavage	Typical product
RAC	H_2WO_4 , WO_3	Specific	C2–C4 sugar monomers
Decarboxylation	Pd, Ru	Specific	Ketones, alkenes, amines
Decarbonylation	Pd, Rh	Specific	Sugar alcohol, furanics
Oxidative cleavage	Non-catalytic	-	Formic acid

strategies discussed herein lies in the structural requirements for substrates. RAC and oxidative cleavage typically requires the presence of β -hydroxy carbonyl and α -hydroxy carbonyl motifs in substrates, respectively. Decarboxylation and decarbonylation are only applicable to substrates containing carboxyl and carbonyl moieties, respectively. Interestingly, these oxygenated moieties (hydroxyl, carbonyl, carboxyl) seemingly play important roles in breaking C–C bond. As indicated by aforementioned C–C bond cleavage mechanism, these oxygenated moieties largely serve as binding sites for the adsorption and activation of substrates on metal catalysts, thus leading to the selective cleavage of C–C bond. In a sense, the role of oxygenated moieties resembles a useful “handle” that could be turned by appropriate metal catalysts to enable the cleavage of C–C bond in substrates. Obviously, one should consider how to make good use of the “handle” function of relevant oxygenated moieties attached to C–C bonds when developing effective bond cleavage methods/strategies.

C–C bond cleavage strategies (RAC, decarboxylation and decarbonylation) mostly rely on the catalytic roles of metal species to interact with oxygenated moieties with the exception of non-catalytic oxidative cleavage which requires stoichiometric oxidation agents (e.g., H_2O_2) to break C–C bond. The strong oxidation capacity of superoxide anion can oxidize hydroxyl and carbonyl into acid accompanied by the complete cleavage of carbon skeleton into formic acid. Regardless of the type of substrates, the major product of oxidative cleavage is usually fixed as formic acid.

In contrast to decarboxylation/decarbonylation, RAC has shown much broader applications as it can selectively break the specific C–C bond of various sugar monomers, readily available from (hemi)cellulose but very challenging for C–C bond cleavage. The specificity of RAC in breaking C–C bond is a result of the unique complexation ability of WO_3

to bond both hydroxyl and carbonyl with the formation of a reactive complex of sugar-WO₃, which is susceptible to C–C bond cleavage reaction. Amongst transition metal catalysts, tungsten oxides have been identified as the most active RAC catalysts owing to their peculiar oxophilic properties (the ability to interact with oxygenated moieties). The chemical properties of molybdenum are very close to that of tungsten, since both of them belong to the chromium group. The RAC performance of molybdenum oxide appears sensitive to the reaction atmosphere. Unlike tungsten oxide that can catalyze RAC under both oxidative and reductive conditions (i.e., RAC-hydrogenation and RAC-oxidation), molybdenum oxide was reported to mainly catalyze the RAC under non-reductive conditions (i.e., RAC-oxidation and RAC-condensation). The poor activity of molybdenum oxide for RAC-hydrogenation is probably related to the easy formation of reduced molybdenum species featuring low RAC activity under reductive conditions. Similar to tungsten and molybdenum oxides, rhenium oxides also feature strong oxophilicity to react with OH groups. Nevertheless, rhenium oxides have been demonstrated to serve as efficient catalysts for DODH instead of RAC. On the contrary, tungsten oxides are almost inactive for DODH, but exhibit very high activity towards RAC. Such distinct catalytic behaviors are speculated to relate to the different oxophilicities of rhenium and tungsten oxides, which could affect the preferential cleavage of C–O bond (DODH) or C–C bond (RAC). The type of sugar monomers (e.g., aldose or ketose) affects the C–C bond to be cleaved. By changing the position of carbonyl in sugar monomers, for example, by the isomerization of glucose into fructose, one can regulate the selectivity of fragmented products. Note that RAC is mostly implemented in combination with other reactions in order to transform the *in situ* formed carbonyl-containing products into a stabilized form.

Both decarboxylation and decarbonylation are based on the fact that carboxyl and aldehyde moieties are apt to undergo elimination over metal catalysts, which can lead to the cleavage of related C–C bond. Similar to RAC, the activation of carboxyl and aldehyde moieties on metal catalysts is key to realizing the selective elimination. Noble metals are widely employed to catalyze decarboxylation and decarbonylation owing to their high affinity towards carboxyl and aldehyde moieties. One issue related to decarboxylation and decarbonylation is that they can only cleave the terminal C–C bond of substrates to obtain products with almost unchanged carbon chain. This is distinct from RAC capable of breaking the carbon chain at the middle C–C bond to obtain fragmented products.

4. Conclusions and outlook

As the major component of lignocellulose, (hemi)cellulose has attracted tremendous interest as a renewable carbon feedstock for the manufacture of drop-in and novel fuels and chemicals with advantaged carbon-neutrality. Valorizing (hemi)cellulose towards valuable chemicals and fuels typically involves the depolymerization of its polymeric structure into sugars or platform molecules followed by further upgrading through various chemo-catalytic conversion routes. The initial depolymerization along with downstream upgrading processes generally entail the cleavage of various C–C and C–O linkages present in (hemi)cellulose and its derivatives. In particular, the precise and selective cleavage of specific C–C and C–O bonds is of paramount importance, which lays the foundation for the selective transformation of (hemi)cellulose into desired products. Among the vast number of conversion methods/pathways reported for (hemi)cellulose, we have tried to generalize the common bond cleavage strategies featuring wide utility in selectively breaking specific C–C/C–O bonds of (hemi)cellulose and its derivatives. The present review has summarized several commonly-used C–O bond cleavage strategies including glycosidic bond hydrolysis, dehydration of hydroxyl groups, DODH of adjacent hydroxyl groups, and hydrogenolysis of internal C–O bond, as well as C–C bond cleavage strategies including RAC, oxidative cleavage, decarbonylation, and decarboxylation. For each strategy, bond cleavage mechanism, typical

catalysts, important applications have been adequately discussed with representative examples for the upgrading of (hemi)cellulose and its derivatives.

Among the four C–O bond cleavage strategies, glycosidic bond hydrolysis and dehydration of hydroxyl groups are actually intertwined in most cases, since both of them employ similar Brønsted acid catalysts and reaction temperatures. As a result, the application of these two methods presents an issue in controlling C–O bond cleavage towards dehydration or hydrolysis products. For instance, the concurrent formation of HMF (a dehydration product of glucose) is frequently observed during the hydrolysis of cellulose to glucose. Potential solutions to decouple these two reactions include tuning reaction parameters (temperature, solvent), adding protection agents, or tailoring acidic properties. By contrast, DODH of adjacent hydroxyl groups and hydrogenolysis of internal C–O bond are moiety-specific and particular selective towards eliminating paired OH groups and the secondary OH group adjacent to primary OH group, respectively. These two strategies rely on metal catalysis (e.g., ReO_x, Ir-ReO_x) instead of Brønsted acid catalysis. The abilities of these metal sites to bind and activate specific moieties might account for the selective C–O bond cleavage to deliver superior selectivity of desired products. Among the four C–C bond cleavage strategies, oxidative cleavage is a non-catalytic reaction requiring stoichiometric oxidants, usually leading to the most stable oxidized product (primarily formic acid) irrespective of the sugar substrates. RAC, decarbonylation, and decarboxylation present high selectivity in breaking specific C–C bonds related to β-hydroxy carbonyl, aldehyde, and carboxyl moieties, respectively. These strategies all necessitate the participation of metal catalysts and appropriate reaction conditions. In terms of product diversity, RAC is able to split the carbon chain of sugars into C₂/C₃/C₄ oxygenates depending on the position of carbonyl group in sugar substrates, while decarbonylation and decarboxylation usually enable the removal of terminal carbon atom with preserved substrate structure. Hence, RAC is actually more useful in the valorization of (hemi)cellulose into short-chain valuable oxygenates, and, in particular, its utility can be significantly expanded when combined with other reactions, as discussed above. Overall, these summarized bond cleavage strategies we showcase herein provide a powerful toolbox for chemists to precisely tailor the molecular structure of (hemi)cellulose derivatives towards specific products.

By leveraging these bond cleavage strategies, significant advancements have been achieved in realizing the precise conversion of (hemi)cellulose and its derivatives into specific products with maximized selectivity. Despite ongoing progress, there remain several challenges/opportunities related to the development of selective bond cleavage strategies to ultimately establish a target-product-oriented biorefinery.

- (1) Despite the hydrogenolysis of internal C–O bond strategy being selective in converting simple furan-based molecules, poor selectivity was achieved in processing complex molecules like xylitol and sorbitol. As stated above, acid-catalyzed glycosidic bond hydrolysis and dehydration proceed concurrently due to the strong affinity of protons towards both glycosidic and OH moieties without specificity. Therefore, the capability of C–O/C–C bond cleavage strategies to discriminate and identify specific moieties in a complex substrate containing multiple similar functional groups needs to be improved, which in turn calls for the design of advanced catalytic systems. In this regard, biological catalysts such as glycoside hydrolases, decarboxylases, and dehydratases known for their high regioselectivity, stereoselectivity, and chemoselectivity for specific moieties offer potential examples that can inspire or guide the rational design of chemo-catalysts with improved selectivity.
- (2) Most bond cleavage strategies are currently facilitated by scarce and expensive noble metal catalysts containing ReO_x, Ir-ReO_x, Pd, Pt, and Ru as active sites. In addition, DODH reaction and RAC are still dominated by homogeneous catalysts comprising Re

and W species, respectively. Their heterogeneous counterparts (i.e., immobilized or supported W and Re catalyst) often suffer from serious stability issues owing to the prevalent usage of high-temperature aqueous or organic phase conditions. Hence, more attentions should be devoted to developing robust, recyclable, and low-cost catalysts (preferably based on non-noble metals) that are more attractive for practical implementation. To this end, deep understanding of the metal-catalyzed bond cleavage mechanism and unravelling the key structural and electronic features of metal sites that govern their catalytic activities and stabilities are of pivotal importance.

- (3) As mentioned above, valorizing (hemi)cellulose into end products generally comprises a cascade of bond-breaking as well as bond-forming processes, depending on the molecular/functional complexity of target products. The rational combination of bond cleavage strategies with diverse bond-forming reactions (e.g., aldol condensation, hydrogenation, amination) deserve further exploration, since such combinations can further broaden the portfolio of attainable products and also bring new opportunities to synthesize molecules of increased value and functionalities. In particular, it is desired that different bond-breaking and bond-forming reactions can be integrated in one pot and proceed in sequence, thus circumventing complex isolation/purification procedures of reaction intermediates and potentially realizing the production of end products directly from (hemi)cellulose. To this end, reaction compatibility (solvent, temperature, atmosphere, reactor) optimizations as well as bifunctional or multifunctional catalyst engineering are needed to ensure the smooth occurrence of each reaction step.
- (4) Note that oxidative cleavage and DODH, two frequently-used protocols in organic and carbohydrate chemistry, have found important applications in the selective valorization of (hemi)cellulose. Hence, the toolbox of selective bond cleavage strategies can be expected to be diversified by referring to relevant C–C and C–O bond cleavage methods already known in organic or carbohydrate chemistry. For example, retro-allylation, a protocol to break the C–C bond between OH group and double bond [423], appears as a potential method to break the carbon chain of (hemi)cellulose-derived unsaturated molecules.
- (5) In addition to catalyst innovation, the greenness of each bond cleavage strategy (e.g., solvent, additive, side products) need to be taken into account. Stoichiometric reductants/oxidants and non-aqueous solvent are frequently employed for these C–C/C–O bond cleavage reactions, which can result in adverse environmental effects and reduce process sustainability. Further efforts should be focused on the recycle/regeneration of additives and non-aqueous solvents or the application of potential green alternatives (e.g., bio-based solvents, green hydrogen donors) with less environmental footprint.

CRDiT authorship contribution statement

Zheng Mingyuan: Conceptualization, Funding acquisition, Writing – review & editing. **Zhu Ning:** Writing – review & editing. **Fang Zheng:** Writing – review & editing. **Yang Cui:** Writing – original draft, Writing – review & editing. **Sun Ruiyan:** Writing – original draft, Writing – review & editing. **Zhang Tao:** Conceptualization, Funding acquisition, Writing – review & editing. **Guo Kai:** Conceptualization, Funding acquisition, Writing – review & editing.

Declaration of Competing Interest

The authors declare that they have no known competing financial interests or personal relationships that could have appeared to influence the work reported in this paper.

Data availability

All data in this Review was reproduced from relevant literature with permission.

Acknowledgements

Financial support of the Strategic Priority Research Program of the Chinese Academy of Sciences (No. XDA 21060200), Natural Science Foundation of Jiangsu Province (No. BK20220347), and National Natural Science Foundation of China (No. 22208142, No. 22278221) are acknowledged.

References

- [1] R. Kumar, S. Singh, O.V. Singh, Bioconversion of lignocellulosic biomass: biochemical and molecular perspectives, *J. Ind. Microbiol. Biotechnol.* 35 (2008) 377–391, <https://doi.org/10.1007/s10295-008-0327-8>.
- [2] L.T. Mika, E. Cséfalvay, Á. Németh, Catalytic conversion of carbohydrates to initial platform chemicals: chemistry and sustainability, *Chem. Rev.* 118 (2018) 505–613, <https://doi.org/10.1021/acs.chemrev.7b00395>.
- [3] J. Sherwood, The significance of biomass in a circular economy, *Bioresour. Technol.* 300 (2020), 122755, <https://doi.org/10.1016/j.biortech.2020.122755>.
- [4] W.H. Faveere, S. Van Praet, B. Vermeeren, K.N.R. Dumoleijn, K. Moonen, E. Taarning, B.F. Sels, Toward replacing ethylene oxide in a sustainable world: glycolaldehyde as a bio-based C2 platform molecule, *Angew. Chem., Int. Ed.* 60 (2021) 12204–12223, <https://doi.org/10.1002/anie.202009811>.
- [5] S.S. Wong, R. Shu, J. Zhang, H. Liu, N. Yan, Downstream processing of lignin derived feedstock into end products, *Chem. Soc. Rev.* 49 (2020) 5510–5560, <https://doi.org/10.1039/D0CS00134A>.
- [6] S. Shylesh, A.A. Gokhale, C.R. Ho, A.T. Bell, Novel strategies for the production of fuels, lubricants, and chemicals from biomass, *Acc. Chem. Res.* 50 (2017) 2589–2597, <https://doi.org/10.1021/acs.accounts.7b00354>.
- [7] F.H. Isikgor, C.R. Becer, Lignocellulosic biomass: a sustainable platform for the production of bio-based chemicals and polymers, *Polym. Chem.* 6 (2015) 4497–4559, <https://doi.org/10.1039/C5PY00263J>.
- [8] G.W. Huber, S. Iborra, A. Corma, Synthesis of transportation fuels from biomass: chemistry, catalysts, and engineering, *Chem. Rev.* 106 (2006) 4044–4098, <https://doi.org/10.1021/cr068360d>.
- [9] D.M. Alonso, S.G. Wettstein, J.A. Dumesic, Bimetallic catalysts for upgrading of biomass to fuels and chemicals, *Chem. Soc. Rev.* 41 (2012) 8075–8098, <https://doi.org/10.1039/C2CS35188A>.
- [10] B.M. Stadler, C. Wulf, T. Werner, S. Tin, J.G. de Vries, Catalytic approaches to monomers for polymers based on renewables, *ACS Catal.* 9 (2019) 8012–8067, <https://doi.org/10.1021/acscatal.9b01665>.
- [11] J. Cai, Y. He, X. Yu, S.W. Banks, Y. Yang, X. Zhang, Y. Yu, R. Liu, A.V. Bridgwater, Review of physicochemical properties and analytical characterization of lignocellulosic biomass, *Renew. Sust. Energ. Rev.* 76 (2017) 309–322, <https://doi.org/10.1016/j.rser.2017.03.072>.
- [12] X. Zhao, L. Zhang, D. Liu, Biomass recalcitrance. Part I: the chemical compositions and physical structures affecting the enzymatic hydrolysis of lignocellulose, *Biofuels Bioprod. Biorefin.* 6 (2012) 465–482, <https://doi.org/10.1002/bbb.1331>.
- [13] R.A. Sheldon, Green and sustainable manufacture of chemicals from biomass: state of the art, *Green. Chem.* 16 (2014) 950–963, <https://doi.org/10.1039/C3GC41935E>.
- [14] R. Rinaldi, R. Jastrzebski, M.T. Clough, J. Ralph, M. Kennema, P.C.A. Bruijnincx, B.M. Weckhuysen, Paving the Way for Lignin Valorisation: Recent Advances in Bioengineering, Biorefining and Catalysis, *Angew. Chem., Int. Ed.* 55 (2016) 8164–8215, <https://doi.org/10.1002/anie.201510351>.
- [15] P. Gallezot, Conversion of biomass to selected chemical products, *Chem. Soc. Rev.* 41 (2012) 1538–1558, <https://doi.org/10.1039/C1CS15147A>.
- [16] C. Xu, E. Paone, D. Rodríguez-Padrón, R. Luque, F. Mauriello, Recent catalytic routes for the preparation and the upgrading of biomass derived furfural and 5-hydroxymethylfurfural, *Chem. Soc. Rev.* 49 (2020) 4273–4306, <https://doi.org/10.1039/D0CS00041H>.
- [17] D.A. Bulushev, J.R.H. Ross, Catalysis for conversion of biomass to fuels via pyrolysis and gasification: a review, *Catal. Today* 171 (2011) 1–13, <https://doi.org/10.1016/j.cattod.2011.02.005>.
- [18] Y. Liu, Y. Nie, X. Lu, X. Zhang, H. He, F. Pan, L. Zhou, X. Liu, X. Ji, S. Zhang, Cascade utilization of lignocellulosic biomass to high-value products, *Green. Chem.* 21 (2019) 3499–3535, <https://doi.org/10.1039/C9GC00473D>.
- [19] N. Ji, T. Zhang, M. Zheng, A. Wang, H. Wang, X. Wang, J.G. Chen, Direct catalytic conversion of cellulose into ethylene glycol using nickel-promoted tungsten carbide catalysts, *Angew. Chem., Int. Ed.* 47 (2008) 8510–8513, <https://doi.org/10.1002/anie.200803233>.
- [20] M.-Y. Zheng, A.-Q. Wang, N. Ji, J.-F. Pang, X.-D. Wang, T. Zhang, Transition Metal-Tungsten bimetallic catalysts for the conversion of cellulose into ethylene glycol, *ChemSusChem* 3 (2010) 63–66, <https://doi.org/10.1002/cssc.200900197>.
- [21] Y. Wang, W. Deng, B. Wang, Q. Zhang, X. Wan, Z. Tang, Y. Wang, C. Zhu, Z. Cao, G. Wang, H. Wan, Chemical synthesis of lactic acid from cellulose catalysed by

lead(II) ions in water, *Nat. Commun.* 4 (2013), 2141, <https://doi.org/10.1038/ncomms3141>.

[22] D.M. Alonso, J.Q. Bond, J.A. Dumesic, Catalytic conversion of biomass to biofuels, *Green. Chem.* 12 (2010) 1493–1513, <https://doi.org/10.1039/C004654J>.

[23] M.J. Climent, A. Corma, S. Iborra, Conversion of biomass platform molecules into fuel additives and liquid hydrocarbon fuels, *Green. Chem.* 16 (2014) 516–547, <https://doi.org/10.1039/C3GC41492B>.

[24] W. Deng, Q. Zhang, Y. Wang, Catalytic transformation of cellulose and its derived carbohydrates into chemicals involving CC bond cleavage, *J. Energy Chem.* 24 (2015) 595–607, <https://doi.org/10.1016/j.jechem.2015.08.016>.

[25] W. Deng, H. Zhang, L. Xue, Q. Zhang, Y. Wang, Selective activation of the C–O bonds in lignocellulosic biomass for the efficient production of chemicals, *Chin. J. Cata.* 36 (2015) 1440–1460, [https://doi.org/10.1016/S1872-2067\(15\)60923-8](https://doi.org/10.1016/S1872-2067(15)60923-8).

[26] S. Li, W. Deng, S. Wang, P. Wang, D. An, Y. Li, Q. Zhang, Y. Wang, Catalytic transformation of cellulose and its derivatives into functionalized organic acids, *ChemSusChem* 11 (2018) 1995–2028, <https://doi.org/10.1002/cscs.201800440>.

[27] M. Wang, J. Ma, H. Liu, N. Luo, Z. Zhao, F. Wang, Sustainable productions of organic acids and their derivatives from biomass via selective oxidative cleavage of C–C bond, *ACS Catal.* 8 (2018) 2129–2165, <https://doi.org/10.1021/acscatal.7b03790>.

[28] Z. Zhang, G.W. Huber, Catalytic oxidation of carbohydrates into organic acids and furan chemicals, *Chem. Soc. Rev.* 47 (2018) 1351–1390, <https://doi.org/10.1039/C7CS00213K>.

[29] S. Kim, E.E. Kwon, Y.T. Kim, S. Jung, H.J. Kim, G.W. Huber, J. Lee, Recent advances in hydrodeoxygenation of biomass-derived oxygenates over heterogeneous catalysts, *Green. Chem.* 21 (2019) 3715–3743, <https://doi.org/10.1039/C9GC01210A>.

[30] A.N. Marchesan, M.P. Oncken, R. Maciel Filho, M.R. Wolf Maciel, A roadmap for renewable C2–C3 glycols production: a process engineering approach, *Green. Chem.* 21 (2019) 5168–5194, <https://doi.org/10.1039/C9GC02949D>.

[31] Y. Wan, J.-M. Lee, Toward value-added dicarboxylic acids from biomass derivatives via thermocatalytic conversion, *ACS Catal.* 11 (2021) 2524–2560, <https://doi.org/10.1021/acscatal.0c05419>.

[32] T.A. Bender, J.A. Dabrowski, M.R. Gagné, Homogeneous catalysis for the production of low-volume, high-value chemicals from biomass, *Nat. Rev. Chem.* 2 (2018) 35–46, <https://doi.org/10.1038/s41570-018-0005-y>.

[33] H. Li, A. Riisager, S. Saravananurugan, A. Pandey, R.S. Sangwan, S. Yang, R. Luque, Carbon-increasing catalytic strategies for upgrading biomass into energy-intensive fuels and chemicals, *ACS Catal.* 8 (2018) 148–187, <https://doi.org/10.1021/acscatal.7b02577>.

[34] L. Wu, T. Moteki, Amit A. Gokhale, David W. Flaherty, F.D. Toste, Production of fuels and chemicals from biomass: condensation reactions and beyond, *Chem* 1 (2016) 32–58, <https://doi.org/10.1016/j.chempr.2016.05.002>.

[35] D.E. Resasco, B. Wang, S. Crossley, Zeolite-catalysed C–C bond forming reactions for biomass conversion to fuels and chemicals, *Catal. Sci. Technol.* 6 (2016) 2543–2559, <https://doi.org/10.1039/C5CY02271A>.

[36] Y. Jing, Y. Guo, Q. Xia, X. Liu, Y. Wang, Catalytic production of value-added chemicals and liquid fuels from lignocellulosic biomass, *Chem* 5 (2019) 2520–2546, <https://doi.org/10.1016/j.chempr.2019.05.022>.

[37] Z. Sun, K. Barta, Cleave and couple: toward fully sustainable catalytic conversion of lignocellulose to value added building blocks and fuels, *Chem. Commun.* 54 (2018) 7725–7745, <https://doi.org/10.1039/C8CC02937G>.

[38] S. Gazi, Valorization of wood biomass-lignin via selective bond scission: a minireview, *Appl. Catal. B: Environ.* 257 (2019), 117936, <https://doi.org/10.1016/j.apcatb.2019.117936>.

[39] X. Shen, Y. Xin, H. Liu, B. Han, Product-oriented direct cleavage of chemical linkages in lignin: A review, *ChemSusChem* 13 (2020) 4367–4381, <https://doi.org/10.1002/cssc.202001025>.

[40] P.J. Deuss, K. Barta, From models to lignin: Transition metal catalysis for selective bond cleavage reactions, *Coord. Chem. Rev.* 306 (2016) 510–532, <https://doi.org/10.1016/j.ccr.2015.02.004>.

[41] S. Guadix-Montero, M. Sankar, Review on Catalytic Cleavage of C–C Inter-unit Linkages in Lignin Model Compounds: Towards Lignin Depolymerisation, *Top. Catal.* 61 (2018) 183–198, <https://doi.org/10.1007/s11244-018-0909-2>.

[42] P. Mäki-Arvela, T. Salmi, B. Holmbom, S. Willför, D.Y. Murzin, Synthesis of Sugars by Hydrolysis of Hemicelluloses- A Review, *Chem. Rev.* 111 (2011) 5638–5666, <https://doi.org/10.1021/cr2000042>.

[43] M. Zeng, X. Pan, Insights into solid acid catalysts for efficient cellulose hydrolysis to glucose: progress, challenges, and future opportunities, *Catal. Rev.* 64 (2022) 445–490, <https://doi.org/10.1080/01614940.2020.1819936>.

[44] R. Rinaldi, F. Schüth, Acid hydrolysis of cellulose as the entry point into biorefinery schemes, *ChemSusChem* 2 (2009) 1096–1107, <https://doi.org/10.1002/cssc.200900188>.

[45] C. Loerbroks, R. Rinaldi, W. Thiel, The Electronic Nature of the 1,4- β -Glycosidic Bond and Its Chemical Environment: DFT Insights into Cellulose Chemistry, *Chem. Eur. J.* 19 (2013) 16282–16294, <https://doi.org/10.1002/chem.201301366>.

[46] J.L. Liras, E.V. Anslyn, Exocyclic and endocyclic cleavage of pyranosides in both methanol and water detected by a novel probe, *J. Am. Chem. Soc.* 116 (1994) 2645–2646, <https://doi.org/10.1021/ja00085a065>.

[47] T.P. Nevell, W.R. Upton, The hydrolysis of cotton cellulose by hydrochloric acid in benzene, *Carbohydr. Res.* 49 (1976) 163–174, [https://doi.org/10.1016/S0008-6215\(00\)83134-1](https://doi.org/10.1016/S0008-6215(00)83134-1).

[48] H. Kobayashi, T. Komanoya, K. Hara, A. Fukuoka, Water-Tolerant Mesoporous-Carbon-Supported Ruthenium Catalysts for the Hydrolysis of Cellulose to Glucose, *ChemSusChem* 3 (2010) 440–443, <https://doi.org/10.1002/cssc.200900296>.

[49] Shimizu, H. Furukawa, N. Kobayashi, Y. Itaya, A. Satsuma, Effects of Brønsted and Lewis acidities on activity and selectivity of heteropolyacid-based catalysts for hydrolysis of cellobiose and cellulose, *Green. Chem.* 11 (2009) 1627–1632, <https://doi.org/10.1039/B913737H>.

[50] V.L. Sushkevich, P.A. Kots, Y.G. Kolyagin, A.V. Yakimov, A.V. Marikutsa, I. I. Ivanova, Origin of water-induced Brønsted acid sites in Sn-BEA zeolites, *J. Phys. Chem. C.* 123 (2019) 5540–5548, <https://doi.org/10.1021/acs.jpcc.8b12462>.

[51] E. Peeters, S. Calderon-Ardila, I. Hermans, M. Dusselier, B.F. Sels, Toward industrially relevant Sn-BETA zeolites: synthesis, activity, stability, and regeneration, *ACS Catal.* 12 (2022) 9559–9569, <https://doi.org/10.1021/acscatal.2c02527>.

[52] A. Shrotri, H. Kobayashi, A. Fukuoka, Cellulose depolymerization over heterogeneous catalysts, *Acc. Chem. Res.* 51 (2018) 761–768, <https://doi.org/10.1021/acs.accounts.7b00614>.

[53] Y.-B. Huang, Y. Fu, Hydrolysis of cellulose to glucose by solid acid catalysts, *Green. Chem.* 15 (2013) 1095–1111, <https://doi.org/10.1039/C3GC40136G>.

[54] F. Bergius, Conversion of wood to carbohydrates, *Ind. Eng. Chem.* 29 (1937) 247–253, <https://doi.org/10.1021/ie50327a002>.

[55] A.J. Stern, X.—Contributions to the chemistry of cellulose. I. Cellulose-sulphuric acid, and the products of its hydrolysis, *J. Chem. Soc., Trans.* 67 (1895) 74–90, <https://doi.org/10.1039/CT89567000074>.

[56] N.S. Mosier, C.M. Ladisch, M.R. Ladisch, Characterization of acid catalytic domains for cellulose hydrolysis and glucose degradation, *Biotechnol. Bioeng.* 79 (2002) 610–618, <https://doi.org/10.1002/bit.10316>.

[57] T. vom Stein, P.M. Grande, H. Kayser, F. Sibilla, W. Leitner, P. Domínguez de María, From biomass to feedstock: one-step fractionation of lignocellulose components by the selective organic acid-catalyzed depolymerization of hemicellulose in a biphasic system, *Green. Chem.* 13 (2011) 1772–1777, <https://doi.org/10.1039/C1GC00002K>.

[58] Y. Lu, N.S. Mosier, Biomimetic Catalysis for Hemicellulose Hydrolysis in Corn Stover, *Biotechnol. Prog.* 23 (2007) 116–123, <https://doi.org/10.1021/bp060223e>.

[59] L. Vanoye, M. Fanselow, J.D. Holbrey, M.P. Atkins, K.R. Seddon, Kinetic model for the hydrolysis of lignocellulosic biomass in the ionic liquid, 1-ethyl-3-methylimidazolium chloride, *Green. Chem.* 11 (2009) 390–396, <https://doi.org/10.1039/B817882H>.

[60] R. Rinaldi, N. Meine, J. vomStein, R. Palkovits, F. Schüth, Which controls the depolymerization of cellulose in ionic liquids: the solid acid catalyst or cellulose? *ChemSusChem* 3 (2010) 266–276, <https://doi.org/10.1002/cssc.200900281>.

[61] L.-Q. Jin, N. Zhao, Z.-Q. Liu, C.-J. Liao, X.-Y. Zheng, Y.-G. Zheng, Enhanced production of xylose from corncobs hydrolysis with oxalic acid as catalyst, *Bioprocess Biosyst. Eng.* 41 (2018) 57–64, <https://doi.org/10.1007/s00449-017-1843-6>.

[62] H. Cai, C. Li, A. Wang, G. Xu, T. Zhang, Zeolite-promoted hydrolysis of cellulose in ionic liquid, insight into the mutual behavior of zeolite, cellulose and ionic liquid, *Appl. Catal. B: Environ.* 123–124 (2012) 333–338, <https://doi.org/10.1016/j.apcatb.2012.04.041>.

[63] M. Lara-Serrano, S. Morales-delaRosa, J.M. Campos-Martín, J.L.G. Fierro, High enhancement of the hydrolysis rate of cellulose after pretreatment with inorganic salt hydrates, *Green. Chem.* 22 (2020) 3860–3866, <https://doi.org/10.1039/DGOC01066A>.

[64] R. Rinaldi, R. Palkovits, F. Schüth, Depolymerization of cellulose using solid catalysts in ionic liquids, *Angew. Chem., Int. Ed.* 47 (2008) 8047–8050, <https://doi.org/10.1002/anie.200802879>.

[65] Q. Xu, C. Chen, K. Rosswurm, T. Yao, S. Janaswamy, A facile route to prepare cellulose-based films, *Carbohydr. Polym.* 149 (2016) 274–281, <https://doi.org/10.1016/j.carbpol.2016.04.114>.

[66] I. Bodachivskyi, U. Kuzhiumparambil, D.B.G. Williams, The role of the molecular formula of $ZnCl_2 \cdot nH_2O$ on its catalyst activity: a systematic study of zinc chloride hydrates in the catalytic valorisation of cellulosic biomass, *Catal. Sci. Technol.* 9 (2019) 4693–4701, <https://doi.org/10.1039/C9CY00846B>.

[67] L. Hu, L. Lin, Z. Wu, S. Zhou, S. Liu, Chemocatalytic hydrolysis of cellulose into glucose over solid acid catalysts, *Appl. Catal. B: Environ.* 174–175 (2015) 225–243, <https://doi.org/10.1016/j.apcatb.2015.03.003>.

[68] A. Galadima, A. Masudi, O. Muraza, Conversion of cellulose to glucose and further transformation into fuels over solid acid catalysts: A mini review, *Microporous Mesoporous Mater.* 336 (2022), 111846, <https://doi.org/10.1016/j.micromeso.2022.111846>.

[69] L. Vilcocq, P.C. Castilho, F. Carvalheiro, L.C. Duarte, Hydrolysis of oligosaccharides over solid acid catalysts: a review, *ChemSusChem* 7 (2014) 1010–1019, <https://doi.org/10.1002/cssc.201300720>.

[70] Z. Zhou, D. Liu, X. Zhao, Conversion of lignocellulose to biofuels and chemicals via sugar platform: An updated review on chemistry and mechanisms of acid hydrolysis of lignocellulose, *Renew. Sust. Energ. Rev.* 146 (2021), 111169, <https://doi.org/10.1016/j.rser.2021.111169>.

[71] Q. Yang, X. Pan, Bifunctional porous polymers bearing boronic and sulfonic acids for hydrolysis of cellulose, *ACS Sustain. Chem. Eng.* 4 (2016) 4824–4830, <https://doi.org/10.1021/acssuschemeng.6b01102>.

[72] S. Yuan, T. Li, Y. Wang, B. Cai, X. Wen, S. Shen, X. Peng, Y. Li, Double-adsorption functional carbon based solid acids derived from pyrolysis of PVC and PE for cellulose hydrolysis, *Fuel* 237 (2019) 895–902, <https://doi.org/10.1016/j.fuel.2018.10.088>.

[73] M. Kitano, D. Yamaguchi, S. Suganuma, K. Nakajima, H. Kato, S. Hayashi, M. Hara, Adsorption-Enhanced Hydrolysis of β -1,4-Glucan on Graphene-Based

Amorphous Carbon Bearing SO₃H, COOH, and OH Groups, *Langmuir* 25 (2009) 5068–5075, <https://doi.org/10.1021/la8040506>.

[74] L. Shuai, X. Pan, Hydrolysis of cellulose by cellulase-mimetic solid catalyst, *Energy Environ. Sci.* 5 (2012) 6889–6894, <https://doi.org/10.1039/C2EE03373A>.

[75] M. Yabushita, H. Kobayashi, J.-y Hasegawa, K. Hara, A. Fukuoka, Entropically favored adsorption of cellulosic molecules onto carbon materials through hydrophobic functionalities, *ChemSusChem* 7 (2014) 1443–1450, <https://doi.org/10.1002/cssc.201301296>.

[76] P.-W. Chung, A. Charmot, O.M. Gazit, A. Katz, Glucan adsorption on mesoporous carbon nanoparticles: effect of chain length and internal surface, *Langmuir* 28 (2012) 15222–15232, <https://doi.org/10.1021/la3030364>.

[77] G.S. Foo, C. Sievers, Synergistic effect between defect sites and functional groups on the hydrolysis of cellulose over activated carbon, *ChemSusChem* 8 (2015) 534–543, <https://doi.org/10.1002/cssc.201402928>.

[78] F. Liu, K. Huang, A. Zheng, F.-S. Xiao, S. Dai, Hydrophobic solid acids and their catalytic applications in green and sustainable chemistry, *ACS Catal.* 8 (2018) 372–391, <https://doi.org/10.1021/acscatal.7b03369>.

[79] H. Xiong, H.N. Pham, A.K. Datye, Hydrothermally stable heterogeneous catalysts for conversion of bio renewables, *Green. Chem.* 16 (2014) 4627–4643, <https://doi.org/10.1039/C4GC01152J>.

[80] Y. Liao, B.O. de Beeck, K. Thielemans, T. Ennaert, J. Snelders, M. Dusselier, C. M. Courtin, B.F. Sels, The role of pretreatment in the catalytic valorization of cellulose, *Mol. Catal.* 487 (2020), 110883, <https://doi.org/10.1016/j.mcat.2020.110883>.

[81] H. Chen, J. Liu, X. Chang, D. Chen, Y. Xue, P. Liu, H. Lin, S. Han, A review on the pretreatment of lignocellulose for high-value chemicals, *Fuel Process. Technol.* 160 (2017) 196–206, <https://doi.org/10.1016/j.fuproc.2016.12.007>.

[82] N. Akhtar, K. Gupta, D. Goyal, A. Goyal, Recent advances in pretreatment technologies for efficient hydrolysis of lignocellulosic biomass, *Environ. Prog. Sustain.* 35 (2016) 489–511, <https://doi.org/10.1002/ep.12257>.

[83] A. Fukuoka, P.L. Dhepe, Catalytic conversion of cellulose into sugar alcohols, *Angew. Chem., Int. Ed.* 45 (2006) 5161–5163, <https://doi.org/10.1002/anie.200601921>.

[84] J. Geboers, S. Van de Vyver, K. Carpentier, K. de Blochouse, P. Jacobs, B. Sels, Efficient catalytic conversion of concentrated cellulose feeds to hexitols with heteropoly acids and Ru on carbon, *Chem. Commun.* 46 (2010) 3577–3579, <https://doi.org/10.1039/C001096K>.

[85] L.-N. Ding, A.-Q. Wang, M.-Y. Zheng, T. Zhang, Selective transformation of cellulose into sorbitol by using a bifunctional nickel phosphide catalyst, *ChemSusChem* 3 (2010) 818–821, <https://doi.org/10.1002/cssc.201000092>.

[86] S. Van de Vyver, J. Geboers, W. Schutyser, M. Dusselier, P. Eloy, E. Dornez, J. W. Seo, C.M. Courtin, E.M. Gaigneaux, P.A. Jacobs, B.F. Sels, Tuning the acid/metal balance of carbon nanofiber-supported nickel catalysts for hydrolytic hydrogenation of cellulose, *ChemSusChem* 5 (2012) 1549–1558, <https://doi.org/10.1002/cssc.201100782>.

[87] Y. Delgado Arcano, O.D. Valmaña García, D. Mandelli, W.A. Carvalho, L. A. Magalhães Pontes, Xylitol: a review on the progress and challenges of its production by chemical route, *Catal. Today* 344 (2020) 2–14, <https://doi.org/10.1016/j.cattod.2018.07.060>.

[88] G. Yi, Y. Zhang, One-Pot Selective Conversion of Hemicellulose (Xylan) to Xylitol under Mild Conditions, *ChemSusChem* 5 (2012) 1383–1387, <https://doi.org/10.1002/cssc.201200290>.

[89] A. Yamaguchi, N. Mimura, M. Shirai, O. Sato, Cascade Utilization of Biomass: Strategy for Conversion of Cellulose, Hemicellulose, and Lignin into Useful Chemicals, *ACS Sustain. Chem. Eng.* 7 (2019) 10445–10451, <https://doi.org/10.1021/acssuschemeng.9b00786>.

[90] D. An, A. Ye, W. Deng, Q. Zhang, Y. Wang, Selective conversion of cellobiose and cellulose into gluconic acid in water in the presence of oxygen, catalyzed by polyoxometalate-supported gold nanoparticles, *Chem. Eur. J.* 18 (2012) 2938–2947, <https://doi.org/10.1002/chem.201103262>.

[91] M. Hernández, E. Lima, A. Guzmán, M. Vera, O. Novelo, V. Lara, A small change in the surface polarity of cellulose causes a significant improvement in its conversion to glucose and subsequent catalytic oxidation, *Appl. Catal. B: Environ.* 144 (2014) 528–537, <https://doi.org/10.1016/j.apcatb.2013.07.061>.

[92] H. Zhang, N. Li, X. Pan, S. Wu, J. Xie, Direct transformation of cellulose to gluconic acid in a concentrated iron(III) chloride solution under mild conditions, *ACS Sustain. Chem. Eng.* 5 (2017) 4066–4072, <https://doi.org/10.1021/acssuschemeng.7b00060>.

[93] P. Sun, X. Long, H. He, C. Xia, F. Li, Conversion of Cellulose into Isosorbide over Bifunctional Ruthenium Nanoparticles Supported on Niobium Phosphate, *ChemSusChem* 6 (2013) 2190–2197, <https://doi.org/10.1002/cssc.201300701>.

[94] G. Liang, C. Wu, L. He, J. Ming, H. Cheng, L. Zhuo, F. Zhao, Selective conversion of concentrated microcrystalline cellulose to isosorbide over Ru/C catalyst, *Green. Chem.* 13 (2011) 839–842, <https://doi.org/10.1039/C1GC15098G>.

[95] B. OpdeBeeck, J. Geboers, S. VandeVyver, J. VanLishout, J. Snelders, W.J. J. Huijgen, C.M. Courtin, P.A. Jacobs, B.F. Sels, Conversion of (Ligno)Cellulose Feeds to Isosorbide with Heteropoly Acids and Ru on Carbon, *ChemSusChem* 6 (2013) 199–208, <https://doi.org/10.1002/cssc.201200610>.

[96] E. Arceo, P. Marsden, R.G. Bergman, J.A. Ellman, An efficient didehydroxylation method for the biomass-derived polyols glycerol and erythritol. Mechanistic studies of a formic acid-mediated deoxygenation, *Chem. Commun.* (2009) 3357–3359, <https://doi.org/10.1039/B907746D>.

[97] G. Crank, F. Eastwood, Derivatives of orthoacids. II. The preparation of olefins from 1,2-diols, *Aust. J. Chem.* 17 (1964) 1392–1398, <https://doi.org/10.1071/CH9641392>.

[98] J.R. Dethlefsen, P. Fristrup, Rhenium-Catalyzed Deoxydehydration of Diols and Polyols, *ChemSusChem* 8 (2015) 767–775, <https://doi.org/10.1002/cssc.201402987>.

[99] G.K. Cook, M.A. Andrews, Toward nonoxidative routes to oxygenated organics: stereospecific deoxydehydration of diols and polyols to alkenes and allylic alcohols catalyzed by the metal oxo complex (C5Me5)ReO₃, *J. Am. Chem. Soc.* 118 (1996) 9448–9449, <https://doi.org/10.1021/ja9620604>.

[100] J. Michael McClain, K.M. Nicholas, Elemental reductants for the deoxydehydration of glycols, *ACS Catal.* 4 (2014) 2109–2112, <https://doi.org/10.1021/cs500461v>.

[101] G. Chapman, K.M. Nicholas, Vanadium-catalyzed deoxydehydration of glycols, *Chem. Commun.* 49 (2013) 8199–8201, <https://doi.org/10.1039/C3CC44656E>.

[102] S. Raju, M.-E. Moret, R.J.M. Klein Gebbink, Rhenium-catalyzed dehydration and deoxydehydration of alcohols and polyols: opportunities for the formation of olefins from biomass, *ACS Catal.* 5 (2015) 281–300, <https://doi.org/10.1021/cs501511x>.

[103] A.R. Petersen, P. Fristrup, New Motifs in deoxydehydration: beyond the realms of rhenium, *Chem. Eur. J.* 23 (2017) 10235–10243, <https://doi.org/10.1002/chem.201701153>.

[104] N.T. Tshibalonza, J.-C.M. Monbaliu, The deoxydehydration (DODH) reaction: a versatile technology for accessing olefins from bio-based polyols, *Green. Chem.* 22 (2020) 4801–4848, <https://doi.org/10.1039/D0GC00689K>.

[105] C. Muzyka, J.-C.M. Monbaliu, Perspectives for the upgrading of bio-based vicinal diols within the developing European bioeconomy, *ChemSusChem* 15 (2022), e202102391, <https://doi.org/10.1002/cssc.202102391>.

[106] S. Vukuturi, G. Chapman, I. Ahmad, K.M. Nicholas, Rhenium-Catalyzed Deoxydehydration of Glycols by Sulfite, *Inorg. Chem.* 49 (2010) 4744–4746, <https://doi.org/10.1021/ic100467p>.

[107] M. Shiramizu, F.D. Toste, Deoxygenation of biomass-derived feedstocks: oxorhenium-catalyzed deoxydehydration of sugars and sugar alcohols, *Angew. Chem., Int. Ed.* 51 (2012) 8082–8086, <https://doi.org/10.1002/anie.201203877>.

[108] J. Yi, S. Liu, M.M. Abu-Omar, Rhenium-catalyzed transfer hydrogenation and deoxygenation of biomass-derived polyols to small and useful organics, *ChemSusChem* 5 (2012) 1401–1404, <https://doi.org/10.1002/cssc.201200138>.

[109] S. Qu, Y. Dang, M. Wen, Z.-X. Wang, Mechanism of the methyltrioxorhenium-catalyzed deoxydehydration of polyols: a new pathway revealed, *Chem. Eur. J.* 19 (2013) 3827–3832, <https://doi.org/10.1002/chem.201204001>.

[110] M. Shiramizu, F.D. Toste, Expanding the scope of biomass-derived chemicals through tandem reactions based on oxorhenium-catalyzed deoxydehydration, *Angew. Chem., Int. Ed.* 52 (2013) 12905–12909, <https://doi.org/10.1002/anie.201307564>.

[111] B. Hočvar, A. Prašnikar, M. Hus, M. Grilc, B. Likozar, H₂-free Re-based catalytic dehydroxylation of aldaric acid to muconic and adipic acid esters, *Angew. Chem., Int. Ed.* 60 (2021) 1244–1253. (<https://onlinelibrary.wiley.com/doi/abs/10.1002/anie.202010035>).

[112] W. Deng, L. Yan, B. Wang, Q. Zhang, H. Song, S. Wang, Q. Zhang, Y. Wang, Efficient Catalysts for Green Synthesis of Adipic Acid from Biomass, *Angew. Chem., Int. Ed.* 60 (2021) 4712–4719, <https://doi.org/10.1002/anie.202013843>.

[113] J. Li, M. Lutz, M. Otte, R.J.M. Klein Gebbink, A Cptt-Based Trioxo-Rhenium Catalyst for the Deoxydehydration of Diols and Polyols, *ChemCatChem* 10 (2018) 4755–4760, <https://doi.org/10.1002/cctc.201801151>.

[114] M. Tamura, N. Yuasa, J. Cao, Y. Nakagawa, K. Tomishige, Transformation of Sugars into Chiral Polyols over a Heterogeneous Catalyst, *Angew. Chem., Int. Ed.* 57 (2018) 8058–8062. (<https://onlinelibrary.wiley.com/doi/abs/10.1002/anie.201803043>).

[115] J. Cao, M. Tamura, Y. Nakagawa, K. Tomishige, Direct synthesis of unsaturated sugars from methyl glycosides, *ACS Catal.* 9 (2019) 3725–3729, <https://doi.org/10.1021/acscatal.9b00589>.

[116] S.H. Krishna, J. Cao, M. Tamura, Y. Nakagawa, M. De Bruyn, G.S. Jacobson, B. M. Weckhuysen, J.A. Dumesic, K. Tomishige, G.W. Huber, Synthesis of Hexane-Tetrols and -Triols with Fixed Hydroxyl Group Positions and Stereochemistry from Methyl Glycosides over Supported Metal Catalysts, *ACS Sustain. Chem. Eng.* 8 (2020) 800–805, <https://doi.org/10.1021/acssuschemeng.9b04634>.

[117] C. Boucher-Jacobs, K.M. Nicholas, Oxo-rhenium-catalyzed deoxydehydration of polyols with hydroaromatic reductants, *Organometallics* 34 (2015) 1985–1990, <https://doi.org/10.1021/acs.organomet.5b00226>.

[118] S. Raju, J.T.B.H. Jastrzebski, M. Lutz, R.J.M. Klein Gebbink, Catalytic Deoxydehydration of Diols to Olefins by using a Bulky Cyclopentadiene-based Trioxorhenium Catalyst, *ChemSusChem* 6 (2013) 1673–1680, <https://doi.org/10.1002/cssc.201300364>.

[119] I. Ahmad, G. Chapman, K.M. Nicholas, Sulfite-Driven, Oxorhenium-Catalyzed Deoxydehydration of Glycols, *Organometallics* 30 (2011) 2810–2818, <https://doi.org/10.1021/om2001662>.

[120] S. Tazawa, N. Ota, M. Tamura, Y. Nakagawa, K. Okumura, K. Tomishige, Deoxydehydration with Molecular Hydrogen over Ceria-Supported Rhenium Catalyst with Gold Promoter, *ACS Catal.* 6 (2016) 6393–6397, <https://doi.org/10.1021/acscatal.6b01864>.

[121] K. Yamaguchi, J. Cao, M. Betchaku, Y. Nakagawa, M. Tamura, A. Nakayama, M. Yabushita, K. Tomishige, Deoxydehydration of Biomass-Derived Polyols Over Silver-Modified Ceria-Supported Rhenium Catalyst with Molecular Hydrogen, *ChemSusChem* 15 (2022), e202102663, <https://doi.org/10.1002/cssc.202102663>.

[122] J.H. Jang, H. Sohn, J. Camacho-Bunquin, D. Yang, C.Y. Park, M. Delferro, M. M. Abu-Omar, Deoxydehydration of Biomass-Derived Polyols with a Reusable Unsupported Rhenium Nanoparticles Catalyst, *ACS Sustain. Chem. Eng.* 7 (2019) 11438–11447, <https://doi.org/10.1021/acssuschemeng.9b01253>.

[123] E. Arceo, J.A. Ellman, R.G. Bergman, Rhenium-Catalyzed Didehydroxylation of Vicinal Diols to Alkenes Using a Simple Alcohol as a Reducing Agent, *J. Am. Chem. Soc.* 132 (2010) 11408–11409, <https://doi.org/10.1021/ja103436v>.

[124] N.N. Tshibalonza, R. Gérard, Z. Alsafrà, G. Eppe, J.-C.M. Monbaliu, A versatile biobased continuous flow strategy for the production of 3-butene-1,2-diol and vinyl ethylene carbonate from erythritol, *Green. Chem.* 20 (2018) 5147–5157, <https://doi.org/10.1039/C8GC02468E>.

[125] G. Crank, F. Eastwood, Derivatives of orthoacids. I. Bicyclic orthoesters, *Aust. J. Chem.* 17 (1964) 1385–1391, <https://doi.org/10.1071/CH9641385>.

[126] R. Sun, M. Zheng, X. Li, J. Pang, A. Wang, X. Wang, T. Zhang, Production of renewable 1,3-pentadiene from xylitol via formic acid-mediated deoxydehydration and palladium-catalyzed deoxygenation reactions, *Green. Chem.* 19 (2017) 638–642, <https://doi.org/10.1039/C6GC02868C>.

[127] N.N. Tshibalonza, J.-C.M. Monbaliu, Revisiting the deoxydehydration of glycerol towards allyl alcohol under continuous-flow conditions, *Green. Chem.* 19 (2017) 3006–3013, <https://doi.org/10.1039/C7GC00657H>.

[128] B. Wozniak, Y. Li, S. Tin, J.G. de Vries, Rhenium-catalyzed deoxydehydration of renewable triols derived from sugars, *Green. Chem.* 20 (2018) 4433–4437, <https://doi.org/10.1039/C8GC02387E>.

[129] R.T. Larson, A. Samant, J. Chen, W. Lee, M.A. Bohn, D.M. Ohlmann, S.J. Zuend, F. D. Toste, Hydrogen gas-mediated deoxydehydration/hydrogenation of sugar acids: catalytic conversion of glucarates to adipates, *J. Am. Chem. Soc.* 139 (2017) 14001–14004, <https://doi.org/10.1021/jacs.7b07801>.

[130] X. Li, D. Wu, T. Lu, G. Yi, H. Su, Y. Zhang, Highly efficient chemical process to convert mucic acid into adipic acid and DFT studies of the mechanism of the rhenium-catalyzed deoxydehydration, *Angew. Chem., Int. Ed.* 53 (2014) 1–6, <https://doi.org/10.1002/anie.201310991>.

[131] H. Zhang, X. Li, X. Su, E.L. Ang, Y. Zhang, H. Zhao, Production of adipic acid from sugar beet residue by combined biological and chemical catalysis, *ChemCatChem* 8 (2016) 1500–1506, <https://doi.org/10.1002/cctc.201600069>.

[132] J.H. Jang, I. Ro, P. Christopher, M.M. Abu-Omar, A Heterogeneous Pt-ReO_x/C Catalyst for Making Renewable Adipates in One Step from Sugar Acids, *ACS Catal.* 11 (2021) 95–109, <https://doi.org/10.1021/acscatal.0c04158>.

[133] J. Lin, H. Song, X. Shen, B. Wang, S. Xie, W. Deng, D. Wu, Q. Zhang, Y. Wang, Zirconia-supported rhenium oxide as an efficient catalyst for the synthesis of biomass-based adipic acid ester, *Chem. Commun.* 55 (2019) 11017–11020, <https://doi.org/10.1039/C9CC05413H>.

[134] Y. Onal, S. Schimpff, P. Claus, Structure sensitivity and kinetics of d-glucose oxidation to d-gluconic acid over carbon-supported gold catalysts, *J. Catal.* 223 (2004) 122–133, <https://doi.org/10.1016/j.jcat.2004.01.010>.

[135] O.V. Singh, R. Kumar, Biotechnological production of gluconic acid: future implications, *Appl. Microbiol. Biotechnol.* 75 (2007) 713–722, <https://doi.org/10.1007/s00253-007-0851-x>.

[136] X. Li, Y. Zhang, Highly Selective Deoxydehydration of Tartaric Acid over Supported and Unsupported Rhenium Catalysts with Modified Acidities, *ChemSusChem* 9 (2016) 2774–2778, <https://doi.org/10.1002/cssc.201600865>.

[137] H. Jiang, R. Lu, X. Si, X. Luo, J. Xu, F. Lu, Single-Site Molybdenum Catalyst for the Synthesis of Fumarate, *ChemCatChem* 11 (2019) 4291–4296, <https://doi.org/10.1002/cctc.201900332>.

[138] N. Ota, M. Tamura, Y. Nakagawa, K. Okumura, K. Tomishige, Hydrodeoxygenation of Vicinal OH Groups over Heterogeneous Rhenium Catalyst Promoted by Palladium and Ceria Support, *Angew. Chem., Int. Ed.* 54 (2015) 1897–1900, <https://doi.org/10.1002/anie.201410352>.

[139] T. Wang, S. Liu, M. Tamura, Y. Nakagawa, N. Hiyoshi, K. Tomishige, One-pot catalytic selective synthesis of 1,4-butanediol from 1,4-anhydroerythritol and hydrogen, *Green. Chem.* 20 (2018) 2547–2557, <https://doi.org/10.1039/C8GC00574E>.

[140] T. Wang, M. Tamura, Y. Nakagawa, K. Tomishige, Preparation of highly active monometallic rhenium catalysts for selective synthesis of 1,4-butanediol from 1,4-anhydroerythritol, *ChemSusChem* 12 (2019) 3615–3626, <https://doi.org/10.1002/cssc.201900900>.

[141] A.E. Settle, L. Berstis, N.A. Rorrer, Y. Roman-Leshkóv, G.T. Beckham, R. M. Richards, D.R. Vardon, Heterogeneous Diels–Alder catalysis for biomass-derived aromatic compounds, *Green. Chem.* 19 (2017) 3468–3492, <https://doi.org/10.1039/C7GC00992E>.

[142] B. Briou, B. Améduri, B. Boutevin, Trends in the Diels–Alder reaction in polymer chemistry, *Chem. Soc. Rev.* 50 (2021) 11055–11097, <https://doi.org/10.1039/D0CS01382J>.

[143] R. Lu, F. Lu, J. Chen, W. Yu, Q. Huang, J. Zhang, J. Xu, Production of diethyl terephthalate from biomass-derived muconic acid, *Angew. Chem., Int. Ed.* 55 (2016) 249–253, <https://doi.org/10.1002/anie.201509149>.

[144] J.W. Frost, A. Miermont, D. Schweitzer, V. Bui, Preparation of trans, trans muconic acid and trans, trans muconates, 2013, US 8426639 B2, United States.

[145] E. Arceo, J.A. Ellman, R.G. Bergman, A direct, biomass-based synthesis of benzoic acid: formic acid-mediated deoxygenation of the glucose-derived materials quinic acid and shikimic acid, *ChemSusChem* 3 (2010) 811–813, <https://doi.org/10.1002/cssc.201000111>.

[146] J. Zhu, G. Yin, Catalytic transformation of the furfural platform into bifunctionalized monomers for polymer synthesis, *ACS Catal.* 11 (2021) 10058–10083, <https://doi.org/10.1021/acscatal.1c01989>.

[147] K. Gupta, R.K. Rai, S.K. Singh, Metal catalysts for the efficient transformation of biomass-derived hmf and furfural to value added chemicals, *ChemCatChem* 10 (2018) 2326–2349, <https://doi.org/10.1002/cctc.201701754>.

[148] R. Mariscal, P. Maireles-Torres, M. Ojeda, I. Sádaba, M. López Granados, Furfural: a renewable and versatile platform molecule for the synthesis of chemicals and fuels, *Energy Environ. Sci.* 9 (2016) 1144–1189, <https://doi.org/10.1039/C5EE02666K>.

[149] F. Chacón-Huete, C. Messina, B. Cigana, P. Forgione, Diverse applications of biomass-derived 5-hydroxymethylfurfural and derivatives as renewable starting materials, *ChemSusChem* 15 (2022), e202200328, <https://doi.org/10.1002/cssc.202200328>.

[150] X. Yue, Y. Queneau, 5-hydroxymethylfurfural and furfural chemistry toward biobased surfactants, *ChemSusChem* 15 (2022), e202102660, <https://doi.org/10.1002/cssc.202102660>.

[151] G. Shen, B. Andrioletti, Y. Queneau, Furfural and 5-(hydroxymethyl)furfural: Two pivotal intermediates for bio-based chemistry, *Curr. Opin. Green. Sustain. Chem.* 26 (2020), 100384, <https://doi.org/10.1016/j.cogsc.2020.100384>.

[152] R.J. van Putten, J.C. van der Waal, E. de Jong, C.B. Rasrendra, H.J. Heeres, J. G. de Vries, Hydroxymethylfurfural, A Versatile Platform Chemical Made from Renewable Resources, *Chem. Rev.* 113 (2013) 1499–1597, <https://doi.org/10.1021/cr300182k>.

[153] A. Jaswal, P.P. Singh, T. Mondal, Furfural – a versatile, biomass-derived platform chemical for the production of renewable chemicals, *Green. Chem.* 24 (2022) 510–551, <https://doi.org/10.1039/D1GC03278J>.

[154] Q. Hou, X. Qi, M. Chen, H. Qian, Y. Nie, C. Bai, S. Zhang, X. Bai, M. Ju, Biorefinery roadmap based on catalytic production and upgrading 5-hydroxymethylfurfural, *Green. Chem.* 23 (2021) 119–231, <https://doi.org/10.1039/D0GC02770G>.

[155] B.R. Caes, R.E. Teixeira, K.G. Knapp, R.T. Raines, Biomass to Furans: Renewable Routes to Chemicals and Fuels, *ACS Sustain. Chem. Eng.* 3 (2015) 2591–2605, <https://doi.org/10.1021/acssuschemeng.5b00473>.

[156] H. Wang, C. Zhu, D. Li, Q. Liu, J. Tan, C. Wang, C. Cai, L. Ma, Recent advances in catalytic conversion of biomass to 5-hydroxymethylfurfural and 2, 5-dimethylfurfur, *Renew. Sust. Energ. Rev.* 103 (2019) 227–247, <https://doi.org/10.1016/j.rser.2018.12.010>.

[157] I. Agirre-Zabal-Telleria, I. Gandarias, P.L. Arias, Heterogeneous acid-catalysts for the production of furan-derived compounds (furfural and hydroxymethylfurfural) from renewable carbohydrates: A review, *Catal. Today* 234 (2014) 42–58, <https://doi.org/10.1016/j.cattod.2013.11.027>.

[158] J. Slak, B. Pomeroy, A. Kostyniuk, M. Grile, B. Likozar, A review of bio-refining process intensification in catalytic conversion reactions, separations and purifications of hydroxymethylfurfural (HMF) and furfural, *Chem. Eng. J.* 429 (2022), 132325, <https://doi.org/10.1016/j.cej.2021.132325>.

[159] Y. Zhao, K. Lu, H. Xu, L. Zhu, S. Wang, A critical review of recent advances in the production of furfural and 5-hydroxymethylfurfural from lignocellulosic biomass through homogeneous catalytic hydrothermal conversion, *Renew. Sust. Energ. Rev.* 139 (2021), 110706, <https://doi.org/10.1016/j.rser.2021.110706>.

[160] T. Wang, M.W. Nolte, B.H. Shanks, Catalytic dehydration of C6 carbohydrates for the production of hydroxymethylfurfural (HMF) as a versatile platform chemical, *Green. Chem.* 16 (2014) 548–572, <https://doi.org/10.1039/C3GC41365A>.

[161] L. Ricciardi, W. Verboom, J.-P. Lange, J. Huskens, Production of furans from C5 and C6 sugars in the presence of polar organic solvents, *Sustain. Energy Fuels* 6 (2022) 11–28, <https://doi.org/10.1039/D1SE01572A>.

[162] Y. Shao, Y. Ding, J. Dai, Y. Long, Z.-T. Hu, Synthesis of 5-hydroxymethylfurfural from dehydration of biomass-derived glucose and fructose using supported metal catalysts, *Green. Synth. Catal.* 2 (2021) 187–197, <https://doi.org/10.1016/j.gresc.2021.01.006>.

[163] L. Yang, G. Tsilomelekis, S. Caratzoulas, D.G. Vlachos, Mechanism of Brønsted Acid-Catalyzed Glucose Dehydration, *ChemSusChem* 8 (2015) 1334–1341, <https://doi.org/10.1002/cssc.201403264>.

[164] G.R. Akien, L. Qi, I.T. Horváth, Molecular mapping of the acid catalysed dehydration of fructose, *Chem. Commun.* 48 (2012) 5850–5852, <https://doi.org/10.1039/C2CC31689G>.

[165] J. Zhang, E. Weitz, An In Situ NMR Study of the Mechanism for the Catalytic Conversion of Fructose to 5-Hydroxymethylfurfural and then to Levulinic Acid Using ¹³C Labeled d-Fructose, *ACS Catal.* 2 (2012) 1211–1218, <https://doi.org/10.1021/cs300045r>.

[166] C. Moreau, R. Durand, S. Razigade, J. Duhamet, P. Faugeras, P. Rivalier, P. Ros, G. Avignon, Dehydration of fructose to 5-hydroxymethylfurfural over H-mordenites, *Appl. Catal., A* 145 (1996) 211–224, [https://doi.org/10.1016/0926-860X\(96\)00136-6](https://doi.org/10.1016/0926-860X(96)00136-6).

[167] J. Zhang, A. Das, R.S. Assary, L.A. Curtiss, E. Weitz, A combined experimental and computational study of the mechanism of fructose dehydration to 5-hydroxymethylfurfural in dimethylsulfoxide using Amberlyst 70, PO43–/niobic acid, or sulfuric acid catalysts, *Appl. Catal. B: Environ.* 181 (2016) 874–887, <https://doi.org/10.1016/j.apcatb.2014.10.056>.

[168] B. Danon, G. Marcotullio, W. de Jong, Mechanistic and kinetic aspects of pentose dehydration towards furfural in aqueous media employing homogeneous catalysis, *Green. Chem.* 16 (2014) 39–54, <https://doi.org/10.1039/C3GC41351A>.

[169] G. Marcotullio, W. de Jong, Furfural formation from d-xylene: the use of different halides in dilute aqueous acidic solutions allows for exceptionally high yields, *Carbohydr. Res.* 346 (2011) 1291–1293, <https://doi.org/10.1016/j.carres.2011.04.036>.

[170] M.J. Antal, W.S.L. Mok, G.N. Richards, Mechanism of formation of 5-(hydroxymethyl)-2-furaldehyde from d-fructose and sucrose, *Carbohydr. Res.* 199 (1990) 91–109, [https://doi.org/10.1016/0008-6215\(90\)84096-D](https://doi.org/10.1016/0008-6215(90)84096-D).

[171] I. Delidovich, R. Palkovits, Catalytic isomerization of biomass-derived aldehydes: a review, *ChemSusChem* 9 (2016) 547–561, <https://doi.org/10.1002/cssc.201501577>.

[172] H. Li, S. Yang, S. Saravanamurugan, A. Riisager, Glucose isomerization by enzymes and chemo-catalysts: status and current advances, *ACS Catal.* 7 (2017) 3010–3029, <https://doi.org/10.1021/acscatal.6b03625>.

[173] M.R. Nimlos, X. Qian, M. Davis, M.E. Himmel, D.K. Johnson, Energetics of xylose decomposition as determined using quantum mechanics modeling, *J. Phys. Chem. A* 110 (2006) 11824–11838, <https://doi.org/10.1021/jp0626770>.

[174] F. Delbecq, Y. Wang, A. Muralidhara, K. El Ouardi, G. Marlair, C. Len, Hydrolysis of Hemicellulose and Derivatives—A Review of Recent Advances in the Production of Furfural, *Front. Chem.* 6 (2018), <https://doi.org/10.3389/fchem.2018.00146>.

[175] L. Shuai, J. Luterbacher, Organic solvent effects in biomass conversion reactions, *ChemSusChem* 9 (2016) 133–155, <https://doi.org/10.1002/cssc.201501148>.

[176] M.E. Zakrzewska, E. Bogel-Lukasik, R. Bogel-Lukasik, Ionic liquid-mediated formation of 5-hydroxymethylfurfural—promising biomass-derived building block, *Chem. Rev.* 111 (2011) 397–417, <https://doi.org/10.1021/cr100171a>.

[177] Y. Kim, A. Mittal, D.J. Robichaud, H.M. Pilath, B.D. Etz, P.C. St. John, D. K. Johnson, S. Kim, Prediction of Hydroxymethylfurfural Yield in Glucose Conversion through Investigation of Lewis Acid and Organic Solvent Effects, *ACS Catal.* 10 (2020) 14707–14721, <https://doi.org/10.1021/acscatal.0c04245>.

[178] T. Ståhlberg, W. Fu, J.M. Woodley, A. Riisager, Synthesis of 5-(Hydroxymethyl)furfural in Ionic Liquids: Paving the Way to Renewable Chemicals, *ChemSusChem* 4 (2011) 451–458, <https://doi.org/10.1002/cssc.201000374>.

[179] L. Chen, Y. Xiong, H. Qin, Z. Qi, Advances of Ionic Liquids and Deep Eutectic Solvents in Green Processes of Biomass-Derived 5-Hydroxymethylfurfural, *ChemSusChem* 15 (2022), e202102635, <https://doi.org/10.1002/cssc.202102635>.

[180] H. Rasmussen, H.R. Sørensen, A.S. Meyer, Formation of degradation compounds from lignocellulosic biomass in the biorefinery: sugar reaction mechanisms, *Carbohydr. Res.* 385 (2014) 45–57, <https://doi.org/10.1016/j.carres.2013.08.029>.

[181] X. Qian, M.R. Nimlos, M. Davis, D.K. Johnson, M.E. Himmel, Ab initio molecular dynamics simulations of β -d-glucose and β -d-xylose degradation mechanisms in acidic aqueous solution, *Carbohydr. Res.* 340 (2005) 2319–2327, <https://doi.org/10.1016/j.carres.2005.07.021>.

[182] J. tenDam, U. Hanefeld, Renewable Chemicals: Dehydroxylation of Glycerol and Polyols, *ChemSusChem* 4 (2011) 1017–1034, <https://doi.org/10.1002/cssc.201100162>.

[183] Y. Kon, M. Araque, T. Nakashima, S. Paul, F. Dumeignil, B. Katryniok, Direct Conversion of Glycerol to Allyl Alcohol Over Alumina-Supported Rhenium Oxide, *ChemistrySelect* 2 (2017) 9864–9868, <https://doi.org/10.1002/slct.201702070>.

[184] K. Chen, M. Tamura, Z. Yuan, Y. Nakagawa, K. Tomishige, One-Pot Conversion of Sugar and Sugar Polyols to n-Alkanes without C–C Dissociation over the Ir-ReO_x/SiO₂ Catalyst Combined with H-ZSM-5, *ChemSusChem* 6 (2013) 613–621, <https://doi.org/10.1002/cssc.201200940>.

[185] B. Op de Beeck, M. Duselier, J. Geboers, J. Holsbeek, E. Morré, S. Oswald, L. Giebel, B.F. Sels, Direct catalytic conversion of cellulose to liquid straight-chain alkanes, *Energy Environ. Sci.* 8 (2015) 230–240, <https://doi.org/10.1039/C4EE01523A>.

[186] Y. Liu, L. Chen, T. Wang, X. Zhang, J. Long, Q. Zhang, L. Ma, High yield of renewable hexanes by direct hydrolysis–hydrodeoxygenation of cellulose in an aqueous phase catalytic system, *RSC Adv.* 5 (2015) 11649–11657, <https://doi.org/10.1039/C4RA14304C>.

[187] Y. Liu, L. Chen, T. Wang, Q. Zhang, C. Wang, J. Yan, L. Ma, One-Pot Catalytic Conversion of Raw Lignocellulosic Biomass into Gasoline Alkanes and Chemicals over LiTaMoO₆ and Ru/C in Aqueous Phosphoric Acid, *ACS Sustain. Chem. Eng.* 3 (2015) 1745–1755, <https://doi.org/10.1021/acssuschemeng.5b00256>.

[188] Y. Guo, Y. Jing, Q. Xia, Y. Wang, NbO_x-Based Catalysts for the Activation of C–O and C–C Bonds in the Valorization of Waste Carbon Resources, *Acc. Chem. Res.* 55 (2022) 1301–1312, <https://doi.org/10.1021/acs.accounts.2c00097>.

[189] H. Shi, Valorization of Biomass-derived Small Oxygenates: Kinetics, Mechanisms and Site Requirements of H₂-involved Hydrogenation and Deoxygenation Pathways over Heterogeneous Catalysts, *ChemCatChem* 11 (2019) 1824–1877, <https://doi.org/10.1002/cctc.201801828>.

[190] W. Luo, W. Cao, P.C.A. Bruijninx, L. Lin, A. Wang, T. Zhang, Zeolite-supported metal catalysts for selective hydrodeoxygenation of biomass-derived platform molecules, *Green. Chem.* 21 (2019) 3744–3768, <https://doi.org/10.1039/C9GC01216H>.

[191] A.M. Robinson, J.E. Hensley, J.W. Medlin, Bifunctional Catalysts for Upgrading of Biomass-Derived Oxygenates: A Review, *ACS Catal.* 6 (2016) 5026–5043, <https://doi.org/10.1021/acscatal.6b00923>.

[192] S. De, B. Saha, R. Luque, Hydrodeoxygenation processes: Advances on catalytic transformations of biomass-derived platform chemicals into hydrocarbon fuels, *Bioresour. Technol.* 178 (2015) 108–118, <https://doi.org/10.1016/j.biortech.2014.09.065>.

[193] K. Tomishige, M. Yabushita, J. Cao, Y. Nakagawa, Hydrodeoxygenation of potential platform chemicals derived from biomass to fuels and chemicals, *Green. Chem.* 24 (2022) 5652–5690, <https://doi.org/10.1039/D2GC01289H>.

[194] L. Qu, X. Jiang, Z. Zhang, X.-g Zhang, G.-y Song, H.-i Wang, Y.-p Yuan, Y.-l Chang, A review of hydrodeoxygenation of bio-oil: model compounds, catalysts, and equipment, *Green. Chem.* 23 (2021) 9348–9376, <https://doi.org/10.1039/D1GC03183J>.

[195] S. Dutta, Hydro(deoxygenation) Reaction Network of Lignocellulosic Oxygenates, *ChemSusChem* 13 (2020) 2894–2915, <https://doi.org/10.1002/cssc.202000247>.

[196] S. Koso, I. Furukado, A. Shima, T. Miyazawa, K. Kunimori, K. Tomishige, Chemoselective hydrogenolysis of tetrahydrofurfuryl alcohol to 1,5-pentanediol, *Chem. Commun.* (2009) 2035–2037, <https://doi.org/10.1039/B822942B>.

[197] S. Koso, H. Watanabe, K. Okumura, Y. Nakagawa, K. Tomishige, Comparative study of Rh–MoO_x and Rh–ReO_x supported on SiO₂ for the hydrogenolysis of ethers and polyols, *Appl. Catal. B: Environ.* 111–112 (2012) 27–37, <https://doi.org/10.1016/j.apcatb.2011.09.015>.

[198] K. Chen, S. Koso, T. Kubota, Y. Nakagawa, K. Tomishige, Chemoselective Hydrogenolysis of Tetrahydropyran-2-methanol to 1,6-Hexanediol over Rhenium-Modified Carbon-Supported Rhodium Catalysts, *ChemCatChem* 2 (2010) 547–555, <https://doi.org/10.1002/cctc.201000018>.

[199] S. Koso, N. Ueda, Y. Shinmi, K. Okumura, T. Kizuka, K. Tomishige, Promoting effect of Mo on the hydrogenolysis of tetrahydrofurfuryl alcohol to 1,5-pentanediol over Rh/SiO₂, *J. Catal.* 267 (2009) 89–92, <https://doi.org/10.1016/j.jcat.2009.07.010>.

[200] K. Chen, K. Mori, H. Watanabe, Y. Nakagawa, K. Tomishige, C–O bond hydrogenolysis of cyclic ethers with OH groups over rhenium-modified supported iridium catalysts, *J. Catal.* 294 (2012) 171–183, <https://doi.org/10.1016/j.jcat.2012.07.015>.

[201] S. Koso, H. Watanabe, K. Okumura, Y. Nakagawa, K. Tomishige, Stable Low-Valence ReO_x Cluster Attached on Rh Metal Particles Formed by Hydrogen Reduction and Its Formation Mechanism, *J. Phys. Chem. C* 116 (2012) 3079–3090, <https://doi.org/10.1021/jp2114225>.

[202] S. Koso, Y. Nakagawa, K. Tomishige, Mechanism of the hydrogenolysis of ethers over silica-supported rhodium catalyst modified with rhenium oxide, *J. Catal.* 280 (2011) 221–229, <https://doi.org/10.1016/j.jcat.2011.03.018>.

[203] K. Tomishige, Y. Nakagawa, M. Tamura, Selective hydrogenolysis and hydrogenation using metal catalysts directly modified with metal oxide species, *Green. Chem.* 19 (2017) 2876–2924, <https://doi.org/10.1039/C7GC00620A>.

[204] Y.S. Yun, C.E. Berdugo-Díaz, D.W. Flaherty, Advances in Understanding the Selective Hydrogenolysis of Biomass Derivatives, *ACS Catal.* 11 (2021) 11193–11232, <https://doi.org/10.1021/acscatal.1c02866>.

[205] M. Chia, Y.J. Pagan-Torres, D. Hibbets, Q. Tan, H.N. Pham, A.K. Datye, M. Neurock, R.J. Davis, J.A. Dumesic, Selective Hydrogenolysis of Polyols and Cyclic Ethers over Bifunctional Surface Sites on Rhodium–Rhenium Catalysts, *J. Am. Chem. Soc.* 133 (2011) 12675–12689, <https://doi.org/10.1021/ja2038358>.

[206] T. Buntara, S. Noel, P.H. Phua, I. Melián-Cabrera, J.G. deVries, H.J. Heeres, Caprolactam from Renewable Resources: Catalytic Conversion of 5-Hydroxymethylfurfural into Caprolactone, *Angew. Chem., Int. Ed.* 50 (2011) 7083–7087, <https://doi.org/10.1002/anie.201102156>.

[207] T. Buntara, S. Noel, P.H. Phua, I. Melián-Cabrera, J.G. de Vries, H.J. Heeres, From 5-Hydroxymethylfurfural (HMF) to Polymer Precursors: Catalyst Screening Studies on the Conversion of 1,2,6-hexanetriol to 1,6-hexanediol, *Top. Catal.* 55 (2012) 612–619, <https://doi.org/10.1007/s11244-012-9839-6>.

[208] T. Buntara, I. Melián-Cabrera, Q. Tan, J.L.G. Fierro, M. Neurock, J.G. de Vries, H.J. Heeres, Catalyst studies on the ring opening of tetrahydrofuran–dimethanol to 1,2,6-hexanetriol, *Catal. Today* 210 (2013) 106–116, <https://doi.org/10.1016/j.cattod.2013.04.012>.

[209] J. He, S.P. Burt, M. Ball, D. Zhao, I. Hermans, J.A. Dumesic, G.W. Huber, Synthesis of 1,6-Hexanediol from Cellulose Derived Tetrahydrofuran–Dimethanol with Pt–WO_x/TiO₂ Catalysts, *ACS Catal.* 8 (2018) 1427–1439, <https://doi.org/10.1021/acscatal.7b03593>.

[210] B. Xiao, M. Zheng, X. Li, J. Pang, R. Sun, H. Wang, X. Pang, A. Wang, X. Wang, T. Zhang, Synthesis of 1,6-hexanediol from HMF over double-layered catalysts of Pd/SiO₂ + Ir–ReO_x/SiO₂ in a fixed-bed reactor, *Green. Chem.* 18 (2016) 2175–2184, <https://doi.org/10.1039/C5GC02228B>.

[211] S. Bhowmik, S. Darbha, Advances in solid catalysts for selective hydrogenolysis of glycerol to 1,3-propanediol, *Catal. Rev.* 63 (2021) 639–703, <https://doi.org/10.1080/01614940.2020.1794737>.

[212] Y. Amada, Y. Shinmi, S. Koso, T. Kubota, Y. Nakagawa, K. Tomishige, Reaction mechanism of the glycerol hydrogenolysis to 1,3-propanediol over Ir–ReO_x/SiO₂ catalyst, *Appl. Catal. B: Environ.* 105 (2011) 117–127, <https://doi.org/10.1016/j.apcatb.2011.04.001>.

[213] Y. Shinmi, S. Koso, T. Kubota, Y. Nakagawa, K. Tomishige, Modification of Rh/SiO₂ catalyst for the hydrogenolysis of glycerol in water, *Appl. Catal. B: Environ.* 94 (2010) 318–326, <https://doi.org/10.1016/j.apcatb.2009.11.021>.

[214] Y. Nakagawa, Y. Shinmi, S. Koso, K. Tomishige, Direct hydrogenolysis of glycerol into 1,3-propanediol over rhenium-modified iridium catalyst, *J. Catal.* 272 (2010) 191–194, <https://doi.org/10.1016/j.jcat.2010.04.009>.

[215] Y. Nakagawa, K. Tomishige, Heterogeneous catalysis of the glycerol hydrogenolysis, *Catal. Sci. Technol.* 1 (2011) 179–190, <https://doi.org/10.1039/C0CY00054J>.

[216] D.D. Falcone, J.H. Hack, A.Y. Klyushin, A. Knop-Gericke, R. Schlögl, R.J. Davis, Evidence for the Bifunctional Nature of Pt–Re Catalysts for Selective Glycerol Hydrogenolysis, *ACS Catal.* 5 (2015) 5679–5695, <https://doi.org/10.1021/acscatal.5b01371>.

[217] F. Wu, H. Jiang, X. Zhu, R. Lu, L. Shi, F. Lu, Effect of tungsten species on selective hydrogenolysis of glycerol to 1,3-propanediol, *ChemSusChem* 14 (2021) 569–581, <https://doi.org/10.1002/cssc.202002405>.

[218] R. Arundhathi, T. Mizugaki, T. Mitsudome, K. Jitsukawa, K. Kaneda, Highly Selective Hydrogenolysis of Glycerol to 1,3-Propanediol over a Boehmite-Supported Platinum/Tungsten Catalyst, *ChemSusChem* 6 (2013) 1345–1347, <https://doi.org/10.1002/cssc.201300196>.

[219] Y. Amada, H. Watanabe, M. Tamura, Y. Nakagawa, K. Okumura, K. Tomishige, Structure of ReO_x Clusters Attached on the Ir Metal Surface in Ir–ReO_x/SiO₂ for the Hydrogenolysis Reaction, *J. Phys. Chem. C* 116 (2012) 23503–23514, <https://doi.org/10.1021/jp308527F>.

[220] K. Tomishige, M. Tamura, Y. Nakagawa, Role of Re Species and Acid Cocatalyst on Ir–ReO_x/SiO₂ in the C–O Hydrogenolysis of Biomass-Derived Substrates, *Chem. Rec.* 14 (2014) 1041–1054, <https://doi.org/10.1002/tcr.201402026>.

[221] W. Zhou, J. Luo, Y. Wang, J. Liu, Y. Zhao, S. Wang, X. Ma, WOx domain size, acid properties and mechanistic aspects of glycerol hydrogenolysis over Pt/WOx/ZrO₂, *Appl. Catal. B: Environ.* 242 (2019) 410–421, <https://doi.org/10.1016/j.apcatb.2018.10.006>.

[222] S. García-Fernández, I. Gandarias, J. Requies, F. Soulimani, P.L. Arias, B. M. Weckhuysen, The role of tungsten oxide in the selective hydrogenolysis of glycerol to 1,3-propanediol over Pt/WOx/Al₂O₃, *Appl. Catal. B: Environ.* 204 (2017) 260–272, <https://doi.org/10.1016/j.apcatb.2016.11.016>.

[223] Y. Fan, S. Cheng, H. Wang, D. Ye, S. Xie, Y. Pei, H. Hu, W. Hua, Z.H. Li, M. Qiao, B. Zong, Nanoparticulate Pt on mesoporous SBA-15 doped with extremely low amount of W as a highly selective catalyst for glycerol hydrogenolysis to 1,3-propanediol, *Green. Chem.* 19 (2017) 2174–2183, <https://doi.org/10.1039/C7GC00317J>.

[224] Y. Amada, H. Watanabe, Y. Hirai, Y. Kajikawa, Y. Nakagawa, K. Tomishige, Production of Biobutanediols by the Hydrogenolysis of Erythritol, *ChemSusChem* 5 (2012) 1991–1999, <https://doi.org/10.1002/cssc.201200121>.

[225] S. Liu, Y. Okuyama, M. Tamura, Y. Nakagawa, A. Imai, K. Tomishige, Production of Renewable Hexanols from Mechanocatalytically Depolymerized Cellulose by Using Ir-ReO_x/SiO₂ catalyst, *ChemSusChem* 8 (2015) 628–635, <https://doi.org/10.1002/cssc.201403010>.

[226] L. Liu, J. Cao, Y. Nakagawa, M. Betchaku, M. Tamura, M. Yabushita, K. Tomishige, Hydrodeoxygenation of C4–C6 sugar alcohols to diols or mono-alcohols with the retention of the carbon chain over a silica-supported tungsten oxide-modified platinum catalyst, *Green. Chem.* 23 (2021) 5665–5679, <https://doi.org/10.1039/D1GC01486B>.

[227] H.W. Wijaya, T. Sato, H. Tange, T. Hara, N. Ichikuni, S. Shimazu, Hydrogenolysis of Furfural into 1,5-Pentanediol by Employing Ni-M (M = Y or La) Composite Catalysts, *Chem. Lett.* 46 (2017) 744–746, <https://doi.org/10.1246/cl.170129>.

[228] M. Al-Yusufi, N. Steinfeldt, R. Eckelt, H. Atia, H. Lund, S. Bartling, N. Rockstroh, A. Köckritz, Efficient base nickel-catalyzed hydrogenolysis of furfural-derived tetrahydrofurfuryl alcohol to 1,5-pentanediol, *ACS Sustain. Chem. Eng.* 10 (2022) 4954–4968, <https://doi.org/10.1021/acssuschemeng.1c08340>.

[229] Y. Nakagawa, K. Mori, K. Chen, Y. Amada, M. Tamura, K. Tomishige, Hydrogenolysis of CO bond over Re-modified Ir catalyst in alkane solvent, *Appl. Catal., A* 468 (2013) 418–425, <https://doi.org/10.1016/j.apcata.2013.09.021>.

[230] J. Tan, J. Cui, T. Deng, X. Cui, G. Ding, Y. Zhu, Y. Li, Water-Promoted Hydrogenation of Levulinic Acid to γ -Valerolactone on Supported Ruthenium Catalyst, *ChemCatChem* 7 (2015) 508–512, <https://doi.org/10.1002/cctc.201402834>.

[231] C. Michel, P. Gallezot, Why is ruthenium an efficient catalyst for the aqueous-phase hydrogenation of biosourced carbonyl compounds? *ACS Catal.* 5 (2015) 4130–4132, <https://doi.org/10.1021/acscatal.5b00707>.

[232] Y.M. Questell-Santiago, M.V. Galkin, K. Barta, J.S. Luterbacher, Stabilization strategies in biomass depolymerization using chemical functionalization, *Nat. Rev. Chem.* 4 (2020) 311–330, <https://doi.org/10.1038/s41570-020-0187-y>.

[233] X. Luo, Y. Li, N.K. Gupta, B. Sels, J. Ralph, L. Shuai, Protection strategies enable selective conversion of biomass, *Angew. Chem., Int. Ed.* 59 (2020) 11704–11716, <https://doi.org/10.1002/anie.201914703>.

[234] J.S. Luterbacher, J.M. Rand, D.M. Alonso, J. Han, J.T. Youngquist, C. T. Maravelias, B.F. Pfleger, J.A. Dumesic, Nonenzymatic sugar production from biomass using biomass-derived γ -valerolactone, *Science* 343 (2014) 277–280, <https://doi.org/10.1126/science.1246748>.

[235] K. Lee, Y. Jing, Y. Wang, N. Yan, A unified view on catalytic conversion of biomass and waste plastics, *Nat. Rev. Chem.* 6 (2022) 635–652, <https://doi.org/10.1038/s41570-022-00411-8>.

[236] M.W. Seo, S.H. Lee, H. Nam, D. Lee, D. Tokmurzin, S. Wang, Y.-K. Park, Recent advances of thermochemical conversion processes for biorefinery, *Bioresour. Technol.* 343 (2022), 126109, <https://doi.org/10.1016/j.biortech.2021.126109>.

[237] R. Vinu, L.J. Broadbelt, A mechanistic model of fast pyrolysis of glucose-based carbohydrates to predict bio-oil composition, *Energy Environ. Sci.* 5 (2012) 9808–9826, <https://doi.org/10.1039/C2EE22784C>.

[238] D. Lee, H. Nam, M. Won Seo, S. Hoon Lee, D. Tokmurzin, S. Wang, Y.-K. Park, Recent progress in the catalytic thermochemical conversion process of biomass for biofuels, *Chem. Eng. J.* 447 (2022), 137501, <https://doi.org/10.1016/j.cej.2022.137501>.

[239] H. Yue, Y. Zhao, X. Ma, J. Gong, Ethylene glycol: properties, synthesis, and applications, *Chem. Soc. Rev.* 41 (2012) 4218–4244, <https://doi.org/10.1039/C2CS15359A>.

[240] J. Pang, M. Zheng, R. Sun, A. Wang, X. Wang, T. Zhang, Synthesis of ethylene glycol and terephthalic acid from biomass for producing PET, *Green. Chem.* 18 (2016) 342–359, <https://doi.org/10.1039/C5GC01771H>.

[241] D.K. Sohounloue, C. Montassier, J. Barbier, Catalytic hydrogenolysis of sorbitol, *React. Kinet. Catal. Lett.* 22 (1983) 391–397, <https://doi.org/10.1007/BF02066210>.

[242] C. Montassier, J.C. Ménézo, L.C. Hoang, C. Renaud, J. Barbier, Aqueous polyol conversions on ruthenium and on sulfur-modified ruthenium, *J. Mol. Catal.* 70 (1991) 99–110, [https://doi.org/10.1016/0304-5102\(91\)85008-P](https://doi.org/10.1016/0304-5102(91)85008-P).

[243] I.T. Clark, Hydrogenolysis of sorbitol, *Ind. Eng. Chem.* 50 (1958) 1125–1126, <https://doi.org/10.1021/ie50584a026>.

[244] K. Wang, M.C. Hawley, T.D. Furney, Mechanism study of sugar and sugar alcohol hydrogenolysis using 1,3-diol model compounds, *Ind. Eng. Chem. Res.* 34 (1995) 3766–3770, <https://doi.org/10.1021/ie00038a012>.

[245] K.L. Deutsch, D.G. Lahr, B.H. Shanks, Probing the ruthenium-catalyzed higher polyol hydrogenolysis reaction through the use of stereoisomers, *Green. Chem.* 14 (2012) 1635–1642, <https://doi.org/10.1039/C2GC00026A>.

[246] M. Rivière, N. Perret, A. Cabiac, D. Delcroix, C. Pinel, M. Besson, Xylitol hydrogenolysis over ruthenium-based catalysts: effect of alkaline promoters and basic oxide-modified catalysts, *ChemCatChem* 9 (2017) 2145–2159, <https://doi.org/10.1002/cctc.201700034>.

[247] A.M. Ruppert, K. Weinberg, R. Palkovits, Hydrogenolysis goes bio: from carbohydrates and sugar alcohols to platform chemicals, *Angew. Chem., Int. Ed.* 51 (2012) 2564–2601, <https://doi.org/10.1002/anie.201105125>.

[248] P.J.C. Hausoul, L. Negahdar, K. Schute, R. Palkovits, Unravelling the Ru-catalyzed hydrogenolysis of biomass-based polyols under neutral and acidic conditions, *ChemSusChem* 8 (2015) 3323–3330, <https://doi.org/10.1002/cssc.201500493>.

[249] K. Tajvidi, P.J.C. Hausoul, R. Palkovits, Hydrogenolysis of cellulose over Cu-based catalysts – analysis of the reaction network, *ChemSusChem* 7 (2014) 1311–1317, <https://doi.org/10.1002/cssc.201300978>.

[250] J. Sun, H. Liu, Selective hydrogenolysis of biomass-derived xylitol to ethylene glycol and propylene glycol on supported Ru catalysts, *Green. Chem.* 13 (2011) 135–142, <https://doi.org/10.1039/C0GC00571A>.

[251] J. Zhou, G. Liu, Z. Sui, X. Zhou, W. Yuan, Hydrogenolysis of sorbitol to glycols over carbon nanofibers-supported ruthenium catalyst: The role of base promoter, *Chin. J. Cata.* 35 (2014) 692–702, [https://doi.org/10.1016/S1872-2067\(14\)60083-8](https://doi.org/10.1016/S1872-2067(14)60083-8).

[252] Y. Jia, H. Liu, Mechanistic insight into the selective hydrogenolysis of sorbitol to propylene glycol and ethylene glycol on supported Ru catalysts, *Catal. Sci. Technol.* 6 (2016) 7042–7052, <https://doi.org/10.1039/C6CY00928J>.

[253] X. Jin, J. Shen, W. Yan, P.S. Thapa, B. Subramaniam, R.V. Chaudhari, Sorbitol Hydrogenolysis over Hybrid Cu/Al₂O₃ catalysts: tunable activity and selectivity with solid base incorporation, *ACS Catal.* 5 (2015) 6545–6558, <https://doi.org/10.1021/acscatal.5b01324>.

[254] Z. Huang, J. Chen, Y. Jia, H. Liu, C. Xia, X. Liu, Selective hydrogenolysis of xylitol to ethylene glycol and propylene glycol over copper catalysts, *Appl. Catal. B: Environ.* 147 (2014) 377–386, <https://doi.org/10.1016/j.apcatb.2013.09.014>.

[255] B.M. Kabyemela, T. Adschiri, R.M. Malaluan, K. Arai, H. Ohzeki, Rapid and selective conversion of glucose to erythrose in supercritical water, *Ind. Eng. Chem. Res.* 36 (1997) 5063–5067, <https://doi.org/10.1021/ie9704354>.

[256] B.M. Kabyemela, T. Adschiri, R.M. Malaluan, K. Arai, Glucose and fructose decomposition in subcritical and supercritical water: detailed reaction pathway, mechanisms, and kinetics, *Ind. Eng. Chem. Res.* 38 (1999) 2888–2895, <https://doi.org/10.1021/ie9806390>.

[257] M. Sasaki, M. Furukawa, K. Minami, T. Adschiri, K. Arai, Kinetics and Mechanism of Cellobiose Hydrolysis and Retro-Aldol Condensation in Subcritical and Supercritical Water, *Ind. Eng. Chem. Res.* 41 (2002) 6642–6649, <https://doi.org/10.1021/ie020326b>.

[258] D.A. Cantero, A. Álvarez, M.D. Bermejo, M.J. Cocco, Transformation of glucose into added value compounds in a hydrothermal reaction media, *J. Supercrit. Fluids* 98 (2015) 204–210, <https://doi.org/10.1016/j.supflu.2014.12.015>.

[259] M. Sasaki, K. Goto, K. Tajima, T. Adschiri, K. Arai, Rapid and selective retro-aldol condensation of glucose to glycolaldehyde in supercritical water, *Green. Chem.* 4 (2002) 285–287, <https://doi.org/10.1039/B203968K>.

[260] S. Matsuoka, H. Kawamoto, S. Saka, Retro-aldol-type fragmentation of reducing sugars preferentially occurring in polyether at high temperature: Role of the ether oxygen as a base catalyst, *J. Anal. Appl. Pyrolysis* 93 (2012) 24–32, <https://doi.org/10.1016/j.jaap.2011.09.005>.

[261] Q. Jing, X. LÜ, Kinetics of Non-catalyzed Decomposition of D-xylose in High Temperature Liquid Water, *Chin. J. Chem. Eng.* 15 (2007) 666–669, [https://doi.org/10.1016/S1004-9541\(07\)60143-8](https://doi.org/10.1016/S1004-9541(07)60143-8).

[262] T.M. Aida, N. Shiraishi, M. Kubo, M. Watanabe, R.L. Smith, Reaction kinetics of d-xylose in sub- and supercritical water, *J. Supercrit. Fluids* 55 (2010) 208–216, <https://doi.org/10.1016/j.supflu.2010.08.013>.

[263] N. Pak Sung, Y. Matsumura, Decomposition of Xylose in Sub- and Supercritical Water, *Ind. Eng. Chem. Res.* 54 (2015) 7604–7613, <https://doi.org/10.1021/acs.iecr.5b01623>.

[264] M. Sasaki, T. Hayakawa, K. Arai, T. Adschiri, Measurement of the rate of retro-aldol condensation of d-xylose in subcritical and supercritical water, *Hydrothermal React. Tech.* (2003) 169–176.

[265] N. Pak Sung, R. Nagano, Y. Matsumura, Detailed mechanism of xylose decomposition in near-critical and supercritical water, *Energy Fuels* 30 (2016) 7930–7936, <https://doi.org/10.1021/acs.energyfuels.6b00918>.

[266] C.B. Schandl, M. Haj, C.M. Osmundsen, A.D. Jensen, E. Taarning, Thermal cracking of sugars for the production of glycolaldehyde and other small oxygenates, *ChemSusChem* 13 (2020) 688–692, <https://doi.org/10.1002/cssc.201902887>.

[267] G. Zhao, M. Zheng, R. Sun, Z. Tai, J. Pang, A. Wang, X. Wang, T. Zhang, Ethylene glycol production from glucose over W-Ru catalysts: Maximizing yield by kinetic modeling and simulation, *AIChE J.* 63 (2017) 2072–2080, <https://doi.org/10.1002/aiic.15589>.

[268] J. Zhang, B. Hou, A. Wang, Z. Li, H. Wang, T. Zhang, Kinetic study of the competitive hydrogenation of glycolaldehyde and glucose on Ru/C with or without AMT, *AIChE J.* 61 (2015) 224–238, <https://doi.org/10.1002/aiic.14639>.

[269] J. Zhang, B. Hou, A. Wang, Z. Li, H. Wang, T. Zhang, Kinetic study of retro-aldol condensation of glucose to glycolaldehyde with ammonium metatungstate as the catalyst, *AIChE J.* 60 (2014) 3804–3813, <https://doi.org/10.1002/aiic.14554>.

[270] Z. Xiao, S. Jin, G. Sha, C.T. Williams, C. Liang, Two-step conversion of biomass-derived glucose with high concentration over Cu–Cr catalysts, *Ind. Eng. Chem. Res.* 53 (2014) 8735–8743, <https://doi.org/10.1021/ie5012189>.

[271] A. Wang, T. Zhang, One-pot conversion of cellulose to ethylene glycol with multifunctional tungsten-based catalysts, *Acc. Chem. Res.* 46 (2013) 1377–1386, <https://doi.org/10.1021/ar3002156>.

[272] M. Zheng, J. Pang, R. Sun, A. Wang, T. Zhang, Selectivity control for cellulose to diols: dancing on eggs, *ACS Catal.* 7 (2017) 1939–1954, <https://doi.org/10.1021/acscatal.6b03469>.

[273] Y. Liu, C. Luo, H. Liu, Tungsten trioxide promoted selective conversion of cellulose into propylene glycol and ethylene glycol on a ruthenium catalyst, *Angew. Chem., Int. Ed.* 51 (2012) 3249–3253, <https://doi.org/10.1002/anie.201200351>.

[274] J.J. Wiesfeld, P. Persöhlja, F.A. Rollier, A.M. Elemans-Mehring, E.J.M. Hensen, Cellulose conversion to ethylene glycol by tungsten oxide-based catalysts, *Mol. Catal.* 473 (2019), 110400, <https://doi.org/10.1016/j.mcat.2019.110400>.

[275] N. Li, Y. Zheng, L. Wei, H. Teng, J. Zhou, Metal nanoparticles supported on WO₃ nanosheets for highly selective hydrogenolysis of cellulose to ethylene glycol, *Green. Chem.* 19 (2017) 682–691, <https://doi.org/10.1039/C6GC01327A>.

[276] N. Ji, M. Zheng, A. Wang, T. Zhang, J.G. Chen, Nickel-promoted tungsten carbide catalysts for cellulose conversion: effect of preparation methods, *ChemSusChem* 5 (2012) 939–944, <https://doi.org/10.1002/cssc.201100575>.

[277] R. Ooms, M. Dusselier, J.A. Geboers, B. Op de Beeck, R. Verhaeveren, E. Gobechiya, J.A. Martens, A. Redl, B.F. Sels, Conversion of sugars to ethylene glycol with nickel tungsten carbide in a fed-batch reactor: high productivity and reaction network elucidation, *Green. Chem.* 16 (2014) 695–707, <https://doi.org/10.1039/C3GC41431K>.

[278] G. Zhao, M. Zheng, A. Wang, T. Zhang, Catalytic conversion of cellulose to ethylene glycol over tungsten phosphide catalysts, *Chin. J. Cata.* 31 (2010) 928–932, [https://doi.org/10.1016/S1872-2067\(10\)60104-0](https://doi.org/10.1016/S1872-2067(10)60104-0).

[279] Y. Yang, W. Zhang, F. Yang, D.E. Brown, Y. Ren, S. Lee, D. Zeng, Q. Gao, X. Zhang, Versatile nickel–tungsten bimetallics/carbon nanofiber catalysts for direct conversion of cellulose to ethylene glycol, *Green. Chem.* 18 (2016) 3949–3955, <https://doi.org/10.1039/C6GC00703A>.

[280] G. Zhao, M. Zheng, J. Zhang, A. Wang, T. Zhang, Catalytic conversion of concentrated glucose to ethylene glycol with semicontinuous reaction system, *Ind. Eng. Chem. Res.* 52 (2013) 9566–9572, <https://doi.org/10.1021/ie400989a>.

[281] Z. Tai, J. Zhang, A. Wang, J. Pang, M. Zheng, T. Zhang, Catalytic conversion of cellulose to ethylene glycol over a low-cost binary catalyst of raney Ni and tungstic acid, *ChemSusChem* 6 (2013) 652–658, <https://doi.org/10.1002/cssc.201200842>.

[282] Z. Tai, J. Zhang, A. Wang, M. Zheng, T. Zhang, Temperature-controlled phase-transfer catalysis for ethylene glycol production from cellulose, *Chem. Commun.* 48 (2012) 7052–7054, <https://doi.org/10.1039/C2CC32305B>.

[283] J. Chai, S. Zhu, Y. Cen, J. Guo, J. Wang, W. Fan, Effect of tungsten surface density of WO₃–ZrO₂ on its catalytic performance in hydrogenolysis of cellulose to ethylene glycol, *RSC Adv.* 7 (2017) 8567–8574, <https://doi.org/10.1039/C6RA27524A>.

[284] Y. Cao, J. Wang, M. Kang, Y. Zhu, Efficient synthesis of ethylene glycol from cellulose over Ni–WO₃/SBA-15 catalysts, *J. Mol. Catal. A: Chem.* 381 (2014) 46–53, <https://doi.org/10.1016/j.molcata.2013.10.002>.

[285] Y. Liu, W. Zhang, C. Hao, S. Wang, H. Liu, Unveiling the mechanism for selective cleavage of C–C bonds in sugar reactions on tungsten trioxide-based catalysts, *Proc. Natl. Acad. Sci. U. S. A.* 119 (2022), e2206399119, <https://doi.org/10.1073/pnas.2206399119>.

[286] M.L. Hayes, N.J. Pennings, A.S. Serianni, R. Barker, Epimerization of aldoses by molybdate involving a novel rearrangement of the carbon skeleton, *J. Am. Chem. Soc.* 104 (1982) 6764–6769, <https://doi.org/10.1021/ja00388a047>.

[287] L. Petruš, M. Petrušová, Z. Hrincová, The Bilić Reaction, in: A.E. Stütz (Ed.), *Glycoscience: Epimerisation, Isomerisation and Rearrangements of Carbohydrates*, Springer Berlin Heidelberg, Berlin, Heidelberg, 2001, pp. 15–41.

[288] W.R. Gunther, Y. Wang, Y. Ji, V.K. Michaelis, S.T. Hunt, R.G. Griffin, Y. Román-Leshkov, Sn-Beta zeolites with borate salts catalyse the epimerization of carbohydrates via an intramolecular carbon shift, *Nat. Commun.* 3 (2012), 1109, <https://doi.org/10.1038/ncomms2122>.

[289] R. Bermejo-Deval, M. Orazov, R. Gounder, S.-J. Hwang, M.E. Davis, Active Sites in Sn-Beta for Glucose Isomerization to Fructose and Epimerization to Mannose, *ACS Catal.* 4 (2014) 2288–2297, <https://doi.org/10.1021/cs500466j>.

[290] H. Nguyen, V. Nikolakis, D.G. Vlachos, Mechanistic Insights into Lewis Acid Metal Salt-Catalyzed Glucose Chemistry in Aqueous Solution, *ACS Catal.* 6 (2016) 1497–1504, <https://doi.org/10.1021/acscatal.5b02698>.

[291] Y. Zhang, A. Wang, T. Zhang, A new 3D mesoporous carbon replicated from commercial silica as a catalyst support for direct conversion of cellulose into ethylene glycol, *Chem. Commun.* 46 (2010) 862–864, <https://doi.org/10.1039/B919182H>.

[292] N. Li, X. Liu, J. Zhou, Q. Ma, M. Liu, W. Chen, Enhanced Ni/W/Ti Catalyst Stability from Ti–O–W Linkage for Effective Conversion of Cellulose into Ethylene Glycol, *ACS Sustain. Chem. Eng.* 8 (2020) 9650–9659, <https://doi.org/10.1021/acssuschemeng.0c00836>.

[293] M.S. Hamdy, M.A. Eissa, S.M.A.S. Keshk, New catalyst with multiple active sites for selective hydrogenolysis of cellulose to ethylene glycol, *Green. Chem.* 19 (2017) 5144–5151, <https://doi.org/10.1039/C7GC02122D>.

[294] Q. Xin, L. Jiang, S. Yu, S. Liu, D. Yin, L. Li, C. Xie, Q. Wu, H. Yu, Y. Liu, Y. Liu, Bimetal oxide catalysts selectively catalyze cellulose to ethylene glycol, *J. Phys. Chem. C* 125 (2021) 18170–18179, <https://doi.org/10.1021/acs.jpcc.1c04446>.

[295] H. Xin, H. Wang, S. Li, X. Hu, C. Wang, L. Ma, Q. Liu, Efficient production of ethylene glycol from cellulose over Co@C catalysts combined with tungstic acid, *Sustain. Energy Fuels* 6 (2022) 2602–2612, <https://doi.org/10.1039/D2SE0038D>.

[296] I.G. Baek, S.J. You, E.D. Park, Direct conversion of cellulose into polyols over Ni/W/SiO₂–Al₂O₃, *Bioresour. Technol.* 114 (2012) 684–690, <https://doi.org/10.1016/j.biortech.2012.03.059>.

[297] S. Sreekanth, A. Arunima Kirali, B. Marimuthu, Enhanced one-pot selective conversion of cellulose to ethylene glycol over NaZSM-5 supported metal catalysts, *N. J. Chem.* 45 (2021) 19244–19254, <https://doi.org/10.1039/D1NJ03257G>.

[298] N. Enjamuri, S. Darbha, Advances in catalytic conversion of lignocellulosic biomass to ethylene glycol, *Catal. Rev.* (2022) 1–71, <https://doi.org/10.1080/01614940.2022.2111070>.

[299] R. Sun, M. Zheng, J. Pang, X. Liu, J. Wang, X. Pan, A. Wang, X. Wang, T. Zhang, Selectivity-Switchable Conversion of Cellulose to Glycols over Ni–Sn Catalysts, *ACS Catal.* 6 (2016) 191–201, <https://doi.org/10.1021/acscatal.5b01807>.

[300] J. Pang, M. Zheng, X. Li, Y. Jiang, Y. Zhao, A. Wang, J. Wang, X. Wang, T. Zhang, Selective conversion of concentrated glucose to 1,2-propylene glycol and ethylene glycol by using RuSn/AC catalysts, *Appl. Catal. B: Environ.* 239 (2018) 300–308, <https://doi.org/10.1016/j.apcatb.2018.08.022>.

[301] J. Xi, D. Ding, Y. Shao, X. Liu, G. Lu, Y. Wang, Production of Ethylene Glycol and Its Monoether Derivative from Cellulose, *ACS Sustain. Chem. Eng.* 2 (2014) 2355–2362, <https://doi.org/10.1021/sc500380c>.

[302] R. Sun, T. Wang, M. Zheng, W. Deng, J. Pang, A. Wang, X. Wang, T. Zhang, Versatile Nickel–Lanthanum(III) Catalyst for Direct Conversion of Cellulose to Glycols, *ACS Catal.* 5 (2015) 874–883, <https://doi.org/10.1021/cs501372m>.

[303] L. Zhou, A. Wang, C. Li, M. Zheng, T. Zhang, Selective Production of 1,2-Propylene Glycol from Jerusalem Artichoke Tuber using Ni–W2C/AC Catalysts, *ChemSusChem* 5 (2012) 932–938, <https://doi.org/10.1002/cssc.201100545>.

[304] R.D. Patria, M.K. Islam, L. Luo, S.-Y. Leu, S. Varjani, Y. Xu, J.W.-C. Wong, J. Zhao, Hydroxyapatite-based catalysts derived from food waste digestate for efficient glucose isomerization to fructose, *Green. Synth. Catal.* 2 (2021) 356–361, <https://doi.org/10.1016/j.gresc.2021.08.004>.

[305] Y. Román-Leshkov, M. Moliner, J.A. Labinger, M.E. Davis, Mechanism of glucose isomerization using a solid Lewis acid catalyst in water, *Angew. Chem., Int. Ed.* 49 (2010) 8954–8957, <https://doi.org/10.1002/anie.201004689>.

[306] I. Delidovich, Recent progress in base-catalyzed isomerization of D-glucose into D-fructose, *Curr. Opin. Green. Sustain. Chem.* 27 (2021), 100414, <https://doi.org/10.1016/j.cogsc.2020.100414>.

[307] C. Liu, C. Zhang, S. Sun, K. Liu, S. Hao, J. Xu, Y. Zhu, Y. Li, Effect of WO_x on Bifunctional Pd–WO_x/Al₂O₃ Catalysts for the Selective Hydrogenolysis of Glucose to 1,2-Propanediol, *ACS Catal.* 5 (2015) 4612–4623, <https://doi.org/10.1021/acscatal.5b00800>.

[308] X. Wang, L. Meng, F. Wu, Y. Jiang, L. Wang, X. Mu, Efficient conversion of microcrystalline cellulose to 1,2-alkanediols over supported Ni catalysts, *Green. Chem.* 14 (2012) 758–765, <https://doi.org/10.1039/C2GC15946E>.

[309] M. Gu, Z. Shen, L. Yang, W. Dong, L. Kong, W. Zhang, B.-Y. Peng, Y. Zhang, Reaction route selection for cellulose hydrogenolysis into C2/C3 glycols by ZnO-modified Ni–W/β-zeolite catalysts, *Sci. Rep.* 9 (2019), 11938, <https://doi.org/10.1038/s41598-019-48103-6>.

[310] A. Aho, S. Engblom, K. Eränen, V. Russo, P. Mäki-Arvela, N. Kumar, J. Wärnå, T. Salmi, D.Y. Murzin, Glucose transformations over a mechanical mixture of ZnO and Ru/C catalysts: Product distribution, thermodynamics and kinetics, *Chem. Eng. J.* 405 (2021), 126945, <https://doi.org/10.1016/j.cej.2020.126945>.

[311] Y. Hirano, K. Sagata, Y. Kita, Selective transformation of glucose into propylene glycol on Ru/C catalysts combined with ZnO under low hydrogen pressures, *Appl. Catal., A* 502 (2015) 1–7, <https://doi.org/10.1016/j.apcata.2015.05.008>.

[312] T.-t. Gao, Y.-g. Sun, Y.-b. Zhu, F. Lin, Y.-d. Zhong, Y.-y. Li, W.-x. Ji, Y.-l. Ma, Ni-Based multifunctional catalysts derived from layered double hydroxides for the catalytic conversion of cellulose to polyols, *N. J. Chem.* 46 (2022) 16058–16067, <https://doi.org/10.1039/D2NJ02104H>.

[313] M. Yang, H. Qi, F. Liu, Y. Ren, X. Pan, L. Zhang, X. Liu, H. Wang, J. Pang, M. Zheng, A. Wang, T. Zhang, One-Pot Production of Cellulosic Ethanol via Tandem Catalysis over a Multifunctional Mo/Pt/WO_x Catalyst, *Joule* 3 (2019) 1–12, <https://doi.org/10.1016/j.joule.2019.05.020>.

[314] C. Li, G. Xu, C. Wang, L. Ma, Y. Qiao, Y. Zhang, Y. Fu, One-pot chemocatalytic transformation of cellulose to ethanol over Ru–WO_x/HZSM-5, *Green. Chem.* 21 (2019) 2234–2239, <https://doi.org/10.1039/C9GC00719A>.

[315] H. Song, P. Wang, S. Li, W. Deng, Y. Li, Q. Zhang, Y. Wang, Direct conversion of cellulose into ethanol catalysed by a combination of tungstic acid and zirconia-supported Pt nanoparticles, *Chem. Commun.* 55 (2019) 4303–4306, <https://doi.org/10.1039/C9CC00619B>.

[316] D. Chu, Z. Luo, Y. Xin, C. Jiang, S. Gao, Z. Wang, C. Zhao, One-pot hydrogenolysis of cellulose to bioethanol over Pd–Cu–WO_x/SiO₂ catalysts, *Fuel* 292 (2021), 120311, <https://doi.org/10.1016/j.fuel.2021.120311>.

[317] J. Zhang, X. Liu, M. Sun, X. Ma, Y. Han, Direct Conversion of Cellulose to Glycolic Acid with a Phosphomolybdc Acid Catalyst in a Water Medium, *ACS Catal.* 2 (2012) 1698–1702, <https://doi.org/10.1021/cs300342k>.

[318] L. Yan, X. Qi, Degradation of Cellulose to Organic Acids in its Homogeneous Alkaline Aqueous Solution, *ACS Sustain. Chem. Eng.* 2 (2014) 897–901, <https://doi.org/10.1021/sc400507s>.

[319] A. Bayu, S. Karnjanakom, A. Yoshida, K. Kusakabe, A. Abudula, G. Guan, Polyoxomolybdates catalysed cascade conversions of cellulose to glycolic acid with molecular oxygen via selective aldohexoses pathways (an epimerization and a [2+4] Retro-aldol reaction), *Catal. Today* 332 (2019) 28–34, <https://doi.org/10.1016/j.cattod.2018.05.034>.

[320] Z. Jiang, Z. Zhang, J. Song, Q. Meng, H. Zhou, Z. He, B. Han, Metal-Oxide-Catalyzed Efficient Conversion of Cellulose to Oxalic Acid in Alkaline Solution under Low Oxygen Pressure, *ACS Sustain. Chem. Eng.* 4 (2016) 305–311, <https://doi.org/10.1021/acssuschemeng.5b01212>.

[321] G. Xu, A. Wang, J. Pang, X. Zhao, J. Xu, N. Lei, J. Wang, M. Zheng, J. Yin, T. Zhang, Chemocatalytic Conversion of Cellulosic Biomass to Methyl Glycolate,

Ethylene Glycol, and Ethanol, *ChemSusChem* 10 (2017) 1–6, <https://doi.org/10.1002/cssc.201601714>.

[322] J. He, L. Chen, S. Liu, K. Song, S. Yang, A. Riisager, Sustainable access to renewable N-containing chemicals from reductive amination of biomass-derived platform compounds, *Green. Chem.* 22 (2020) 6714–6747, <https://doi.org/10.1039/D0GC01869D>.

[323] N.K. Gupta, P. Reif, P. Palenicek, M. Rose, Toward Renewable Amines: Recent Advances in the Catalytic Amination of Biomass-Derived Oxygenates, *ACS Catal.* 12 (2022) 10400–10440, <https://doi.org/10.1021/acscatal.2c01717>.

[324] Y. Wang, S. Furukawa, X. Fu, N. Yan, Organonitrogen Chemicals from Oxygen-Containing Feedstock over Heterogeneous Catalysts, *ACS Catal.* 10 (2020) 311–335, <https://doi.org/10.1021/acscatal.9b03744>.

[325] G. Liang, A. Wang, L. Li, G. Xu, N. Yan, T. Zhang, Production of Primary Amines by Reductive Amination of Biomass-Derived Aldehydes/Ketones, *Angew. Chem., Int. Ed.* 56 (2017) 3050–3054, <https://doi.org/10.1002/anie.201610964>.

[326] M. Pelckmans, W. Vermandel, F. VanWaes, K. Moonen, B.F. Sels, Low-Temperature Reductive Aminolysis of Carbohydrates to Diamines and Aminoalcohols by Heterogeneous Catalysis, *Angew. Chem., Int. Ed.* 56 (2017) 14540–14544, <https://doi.org/10.1002/anie.201708216>.

[327] M. Pelckmans, T. Miayhavil, W. Faveere, J. Poissonnier, F. Van Waes, K. Moonen, G.B. Marin, J.W. Thibaut, K. Pierlot, B.F. Sels, Catalytic Reductive Aminolysis of Reducing Sugars: Elucidation of Reaction Mechanism, *ACS Catal.* 8 (2018) 4201–4212, <https://doi.org/10.1021/acscatal.8b00619>.

[328] L. Jia, M. Makha, C.-X. Du, Z.-J. Quan, X.-C. Wang, Y. Li, Direct hydroxyethylation of amines by carbohydrates via ruthenium catalysis, *Green. Chem.* 21 (2019) 3127–3132, <https://doi.org/10.1039/C9GC01195A>.

[329] C.B. Rasrendra, B.A. Fachri, I.G.B.N. Makertihartha, S. Adisasmitho, H.J. Heeres, Catalytic Conversion of Dihydroxyacetone to Lactic Acid Using Metal Salts in Water, *ChemSusChem* 4 (2011) 768–777, <https://doi.org/10.1002/cssc.201000457>.

[330] K.M.A. Santos, E.M. Albuquerque, G. Innocenti, L.E.P. Borges, C. Sievers, M. A. Fraga, The Role of Brønsted and Water-Tolerant Lewis Acid Sites in the Cascade Aqueous-Phase Reaction of Triose to Lactic Acid, *ChemCatChem* 11 (2019) 3054–3063, <https://doi.org/10.1002/cctc.201900519>.

[331] S. Lux, M. Siebenhofer, Synthesis of lactic acid from dihydroxyacetone: use of alkaline-earth metal hydroxides, *Catal. Sci. Technol.* 3 (2013) 1380–1385, <https://doi.org/10.1039/C3CY20859A>.

[332] R.M. West, M.S. Holm, S. Saravanamurugan, J. Xiong, Z. Beversdorf, E. Taarning, C.H. Christensen, Zeolite H-USY for the production of lactic acid and methyl lactate from C3-sugars, *J. Catal.* 269 (2010) 122–130, <https://doi.org/10.1016/j.jcat.2009.10.023>.

[333] P.Y. Dapsens, C. Mondelli, J. Pérez-Ramírez, Highly Selective Lewis Acid Sites in Desilicated MFI Zeolites for Dihydroxyacetone Isomerization to Lactic Acid, *ChemSusChem* 6 (2013) 831–839, <https://doi.org/10.1002/cssc.201200703>.

[334] P. Mäki-Arvela, I.L. Simakova, T. Salmi, D.Y. Murzin, Production of Lactic Acid/Lactates from Biomass and Their Catalytic Transformations to Commodities, *Chem. Rev.* 114 (2014) 1909–1971, <https://doi.org/10.1021/cr400203v>.

[335] F. de Clippel, M. Dusselier, R. Van Rompaey, P. Vanelderen, J. Dijkmans, E. Makshina, L. Giebel, S. Oswald, G.V. Baron, J.F.M. Denayer, P. Pescarmona, P.A. Jacobs, B.F. Sels, Fast and Selective Sugar Conversion to Alkyl Lactate and Lactic Acid with Bifunctional Carbon–Silica Catalysts, *J. Am. Chem. Soc.* 134 (2012) 10089–10101, <https://doi.org/10.1021/ja301678w>.

[336] W. Deng, P. Wang, B. Wang, Y. Wang, L. Yan, Y. Li, Q. Zhang, Z. Cao, Y. Wang, Transformation of cellulose and related carbohydrates into lactic acid with bifunctional Al(III)–Sn(II) catalysts, *Green. Chem.* 20 (2018) 735–744, <https://doi.org/10.1039/C7GC02975F>.

[337] J. Wang, G. Yao, F. Jin, One-pot catalytic conversion of carbohydrates into alkyl lactates with Lewis acids in alcohols, *Mol. Catal.* 435 (2017) 82–90, <https://doi.org/10.1016/j.mcat.2017.03.021>.

[338] M. Bicker, S. Endres, L. Ott, H. Vogel, Catalytical conversion of carbohydrates in subcritical water: A new chemical process for lactic acid production, *J. Mol. Catal. A: Chem.* 239 (2005) 151–157, <https://doi.org/10.1016/j.molcata.2005.06.017>.

[339] K. Nemoto, Y. Hirano, K.-i Hirata, T. Takahashi, H. Tsuneki, K.-i Tominaga, K. Sato, Cooperative In-Si catalyst system for efficient methyl lactate synthesis from biomass-derived sugars, *Appl. Catal. B: Environ.* 183 (2016) 8–17, <https://doi.org/10.1016/j.apcatb.2015.10.015>.

[340] S. Xu, Y. Wu, J. Li, T. He, Y. Xiao, C. Zhou, C. Hu, Directing the Simultaneous Conversion of Hemicellulose and Cellulose in Raw Biomass to Lactic Acid, *ACS Sustain. Chem. Eng.* 8 (2020) 4244–4255, <https://doi.org/10.1021/acscchemeng.9b07552>.

[341] X. Lei, F.-F. Wang, C.-L. Liu, R.-Z. Yang, W.-S. Dong, One-pot catalytic conversion of carbohydrate biomass to lactic acid using an ErCl₃ catalyst, *Appl. Catal. A* 482 (2014) 78–83, <https://doi.org/10.1016/j.apcata.2014.05.029>.

[342] F.-F. Wang, C.-L. Liu, W.-S. Dong, Highly efficient production of lactic acid from cellulose using lanthanum triflate catalysts, *Green. Chem.* 15 (2013) 2091–2095, <https://doi.org/10.1039/C3GC40836A>.

[343] F. Chambon, F. Rataboul, C. Pinel, A. Cabiac, E. Guillou, N. Essayem, Cellulose hydrothermal conversion promoted by heterogeneous Brønsted and Lewis acids: Remarkable efficiency of solid Lewis acids to produce lactic acid, *Appl. Catal. B: Environ.* 105 (2011) 171–181, <https://doi.org/10.1016/j.apcata.2011.04.009>.

[344] Y. Zhang, H. Luo, L. Kong, X. Zhao, G. Miao, L. Zhu, S. Li, Y. Sun, Highly efficient production of lactic acid from xylose using Sn-beta catalysts, *Green. Chem.* 22 (2020) 7333–7336, <https://doi.org/10.1039/D0GC02596H>.

[345] M.S. Holm, S. Saravanamurugan, E. Taarning, Conversion of Sugars to Lactic Acid Derivatives Using Heterogeneous Zeotype Catalysts, *Science* 328 (2010) 602–605, <https://doi.org/10.1126/science.1183990>.

[346] B. Tang, S. Li, W.-C. Song, E.-C. Yang, X.-J. Zhao, N. Guan, L. Li, Fabrication of Hierarchical Sn-Beta Zeolite as Efficient Catalyst for Conversion of Cellulosic Sugar to Methyl Lactate, *ACS Sustain. Chem. Eng.* 8 (2020) 3796–3808, <https://doi.org/10.1021/acscchemeng.9b07061>.

[347] Y. Sun, L. Shi, H. Wang, G. Miao, L. Kong, S. Li, Y. Sun, Efficient production of lactic acid from sugars over Sn-Beta zeolite in water: catalytic performance and mechanistic insights, *Sustain. Energy Fuels* 3 (2019) 1163–1171, <https://doi.org/10.1039/C9SE0020H>.

[348] L. Yang, J. Su, S. Carl, J.G. Lynam, X. Yang, H. Lin, Catalytic conversion of hemicellulosic biomass to lactic acid in pH neutral aqueous phase media, *Appl. Catal. B: Environ.* 162 (2015) 149–157, <https://doi.org/10.1016/j.apcata.2014.06.025>.

[349] D. Verma, R. Insany, Y.-W. Suh, S.M. Kim, S.K. Kim, J. Kim, Direct conversion of cellulose to high-yield methyl lactate over Ga-doped Zn/H-nanozeolite Y catalysts in supercritical methanol, *Green. Chem.* 19 (2017) 1969–1982, <https://doi.org/10.1039/C7GC00432J>.

[350] C. Kosri, S. Kiatphuengporn, T. Butburee, S. Youngjun, S. Thongratkaew, K. Faungnawakij, C. Yimsukanan, N. Chanlek, P. Kidkhunthod, J. Wittayakun, P. Khemthong, Selective conversion of xylose to lactic acid over metal-based Lewis acid supported on γ -Al2O3 catalysts, *Catal. Today* 367 (2021) 205–212, <https://doi.org/10.1016/j.cattod.2020.04.061>.

[351] S. Yamaguchi, M. Yabushita, M. Kim, J. Hirayama, K. Motokura, A. Fukuoka, K. Nakajima, Catalytic Conversion of Biomass-Derived Carbohydrates to Methyl Lactate by Acid–Base Bifunctional γ -Al2O3, *ACS Sustain. Chem. Eng.* 6 (2018) 8113–8117, <https://doi.org/10.1021/acscchemeng.8b00809>.

[352] S. Kiatphuengporn, A. Junkaew, C. Luadthong, S. Thongratkaew, C. Yimsukanan, S. Songtawee, T. Butburee, P. Khemthong, S. Namuangruk, M. Kunaseth, K. Faungnawakij, Roles of acidic sites in alumina catalysts for efficient d-xylose conversion to lactic acid, *Green. Chem.* 22 (2020) 8572–8583, <https://doi.org/10.1039/D0GC02573A>.

[353] J.W. Harris, M.J. Cordon, J.R. Di Iorio, J.C. Vega-Vila, F.H. Ribeiro, R. Gounder, Titration and quantification of open and closed Lewis acid sites in Sn-Beta zeolites that catalyze glucose isomerization, *J. Catal.* 335 (2016) 141–154, <https://doi.org/10.1016/j.jcat.2015.12.024>.

[354] M. Boronat, P. Concepción, A. Corma, M. Renz, S. Valencia, Determination of the catalytically active oxidation Lewis acid sites in Sn-beta zeolites, and their optimisation by the combination of theoretical and experimental studies, *J. Catal.* 234 (2005) 111–118, <https://doi.org/10.1016/j.jcat.2005.05.023>.

[355] W.N.P. van der Graaff, G. Li, B. Mezari, E.A. Pidko, E.J.M. Hensen, Synthesis of Sn-Beta with Exclusive and High Framework Sn Content, *ChemCatChem* 7 (2015) 1152–1160, <https://doi.org/10.1002/cctc.201403050>.

[356] R. Wischert, P. Florian, C. Copéret, D. Massiot, P. Sautet, Visibility of Al Surface Sites of γ -Alumina: A Combined Computational and Experimental Point of View, *J. Phys. Chem. C* 118 (2014) 15292–15299, <https://doi.org/10.1021/jp503277m>.

[357] S. Tølborg, S. Meier, S. Saravanamurugan, P. Fristrup, E. Taarning, I. Sádaba, Shape-selective Valorization of Biomass-derived Glycolaldehyde using Tin-containing Zeolites, *ChemSusChem* 9 (2016) 3054–3061, <https://doi.org/10.1002/cssc.201600757>.

[358] R. Zhang, A. Eronen, X. Du, E. Ma, M. Guo, K. Moslova, T. Repo, A catalytic approach via retro-aldol condensation of glucose to furanic compounds, *Green. Chem.* 23 (2021) 5481–5486, <https://doi.org/10.1039/D1GC01429C>.

[359] J.M. Bobbitt, Periodate Oxidation of Carbohydrates, in: M.L. Wolfrom, R. S. Tipson (Eds.), *Advances in Carbohydrate Chemistry*, Academic Press, 1956, pp. 1–41.

[360] R.D. Guthrie, The “Dialdehydes” from the Periodate Oxidation of Carbohydrates, in: M.L. Wolfrom (Ed.), *Advances in Carbohydrate Chemistry*, Academic Press, 1962, pp. 105–158.

[361] F. Jin, J. Yun, G. Li, A. Kishita, K. Tohji, H. Enomoto, Hydrothermal conversion of carbohydrate biomass into formic acid at mild temperatures, *Green. Chem.* 10 (2008) 612–615, <https://doi.org/10.1039/B802076K>.

[362] C. Wang, X. Chen, M. Qi, J. Wu, G. Gözaydin, N. Yan, H. Zhong, F. Jin, Room temperature, near-quantitative conversion of glucose into formic acid, *Green. Chem.* 21 (2019) 6089–6096, <https://doi.org/10.1039/C9GC02201E>.

[363] J. Yun, G. Yao, F. Jin, H. Zhong, A. Kishita, K. Tohji, H. Enomoto, L. Wang, Low-temperature and highly efficient conversion of saccharides into formic acid under hydrothermal conditions, *AIChE J.* 62 (2016) 3657–3663, <https://doi.org/10.1002/ai.15287>.

[364] H.S. Isbell, H.L. Frush, Mechanisms for hydroperoxide degradation of disaccharides and related compounds, *Carbohydr. Res.* 161 (1987) 181–193, [https://doi.org/10.1016/S0008-6215\(00\)90076-4](https://doi.org/10.1016/S0008-6215(00)90076-4).

[365] H.S. Isbell, R.G. Naves, Degradation of reducing disaccharides by alkaline hydrogen peroxide, *Carbohydr. Res.* 36 (1974) C1–C4, [https://doi.org/10.1016/S0008-6215\(00\)82019-4](https://doi.org/10.1016/S0008-6215(00)82019-4).

[366] Z. Tang, W. Deng, Y. Wang, E. Zhu, X. Wan, Q. Zhang, Y. Wang, Transformation of Cellulose and its Derived Carbohydrates into Formic and Lactic Acids Catalyzed by Vanadyl Cations, *ChemSusChem* 7 (2014) 1557–1567, <https://doi.org/10.1002/cssc.201400150>.

[367] E. Santillan-Jimenez, M. Crocker, Catalytic deoxygenation of fatty acids and their derivatives to hydrocarbon fuels via decarboxylation/decarbonylation, *J. Chem. Technol. Biotechnol.* 87 (2012) 1041–1050, <https://doi.org/10.1002/jctb.3775>.

[368] J. Fu, X. Lu, P.E. Savage, Hydrothermal Decarboxylation and Hydrogenation of Fatty Acids over Pt/C, *ChemSusChem* 4 (2011) 481–486, <https://doi.org/10.1002/cssc.201000370>.

[369] X. Yao, T.J. Strathmann, Y. Li, L.E. Cronmiller, H. Ma, J. Zhang, Catalytic hydrothermal deoxygenation of lipids and fatty acids to diesel-like hydrocarbons:

a review, *Green. Chem.* 23 (2021) 1114–1129, <https://doi.org/10.1039/D0GC03707A>.

[370] B.-S. Chen, Y.-Y. Zeng, L. Liu, L. Chen, P. Duan, R. Luque, R. Ge, W. Zhang, Advances in catalytic decarboxylation of bioderived fatty acids to diesel-range alkanes, *Renew. Sust. Energ. Rev.* 158 (2022), 112178, <https://doi.org/10.1016/j.rser.2022.112178>.

[371] Y. Chen, C. Wang, W. Lu, Z. Yang, Study of the co-deoxy-liquefaction of biomass and vegetable oil for hydrocarbon oil production, *Bioresour. Technol.* 101 (2010) 4600–4607, <https://doi.org/10.1016/j.biortech.2010.01.071>.

[372] Z. Liu, G. Han, Production of solid fuel biochar from waste biomass by low temperature pyrolysis, *Fuel* 158 (2015) 159–165, <https://doi.org/10.1016/j.fuel.2015.05.032>.

[373] G.J.S. Dawes, E.L. Scott, J. Le Nôtre, J.P.M. Sanders, J.H. Bitter, Deoxygenation of biobased molecules by decarboxylation and decarbonylation – a review on the role of heterogeneous, homogeneous and bio-catalysis, *Green. Chem.* 17 (2015) 3231–3250, <https://doi.org/10.1039/C5GC00023H>.

[374] F. Deng, J. Huang, E.E. Ember, K. Achterhold, M. Dierolf, A. Jentys, Y. Liu, F. Pfeiffer, J.A. Lercher, On the Mechanism of Catalytic Decarboxylation of Carboxylic Acids on Carbon-Supported Palladium Hydride, *ACS Catal.* 11 (2021) 14625–14634, <https://doi.org/10.1021/acscatal.1c03869>.

[375] Y. Gong, L. Lin, Oxidative Decarboxylation of Levulinic Acid by Silver(I)/Persulfate, *Molecules* 16 (2011) 2714–2725, <https://doi.org/10.3390/molecules16032714>.

[376] T. Mizugaki, K. Togo, Z. Maeno, T. Mitsudome, K. Jitsukawa, K. Kaneda, New Routes for Refinery of Biogenic Platform Chemicals Catalyzed by Cerium Oxide-supported Ruthenium Nanoparticles in Water, *Sci. Rep.* 7 (2017), 14007, <https://doi.org/10.1038/s41598-017-14373-1>.

[377] T. Mizugaki, K. Kaneda, Development of High Performance Heterogeneous Catalysts for Selective Cleavage of C–O and C–C Bonds of Biomass-Derived Oxygenates, *Chem. Rec.* 19 (2019) 1179–1198, <https://doi.org/10.1002/tcr.201800075>.

[378] J. Lv, Z. Rong, L. Sun, C. Liu, A.-H. Lu, Y. Wang, J. Qu, Catalytic conversion of biomass-derived levulinic acid into alcohols over nanoporous Ru catalyst, *Catal. Sci. Technol.* 8 (2018) 975–979, <https://doi.org/10.1039/C7CY01838J>.

[379] L. Chen, Y. Liu, C. Gu, G. Feng, X. Zhang, J. Liu, Q. Zhang, C. Wang, L. Ma, Selective Production of 2-Butanol from Hydrogenolysis of Levulinic Acid Catalyzed by the Non-precious NiMn Bimetallic Catalyst, *ACS Sustain. Chem. Eng.* 9 (2021) 15603–15611, <https://doi.org/10.1021/acssuschemeng.1c05771>.

[380] Y. Liu, C. Gu, L. Chen, W. Zhou, Y. Liao, C. Wang, L. Ma, Ru–MnO_x Interaction for Efficient Hydrodeoxygenation of Levulinic Acid and Its Derivatives, *ACS Appl. Mater. Interfaces* 15 (2023) 4184–4193, <https://doi.org/10.1021/acsami.2c22045>.

[381] J.Q. Bond, D.M. Alonso, D. Wang, R.M. West, J.A. Dumesic, Integrated Catalytic Conversion of γ -Valerolactone to Liquid Alkenes for Transportation Fuels, *Science* 327 (2010) 1110–1114, <https://doi.org/10.1126/science.1184362>.

[382] J. LeNôtre, S.C.M. Witte-vanDijk, J. vanHaveren, E.L. Scott, J.P.M. Sanders, Synthesis of Bio-Based Methacrylic Acid by Decarboxylation of Itaconic Acid and Citric Acid Catalyzed by Solid Transition-Metal Catalysts, *ChemSusChem* 7 (2014) 2712–2720, <https://doi.org/10.1002/cssc.201402117>.

[383] J. Li, T.B. Brill, Spectroscopy of Hydrothermal Solutions 18: pH-Dependent Kinetics of Itaconic Acid Reactions in Real Time, *J. Phys. Chem. A* 105 (2001) 10839–10845, <https://doi.org/10.1021/jp012501s>.

[384] A. Bohre, B. Hocevar, M. Grilc, B. Likozar, Selective catalytic decarboxylation of biomass-derived carboxylic acids to bio-based methacrylic acid over hexaaluminat catalysts, *Appl. Catal. B: Environ.* 256 (2019), 117889, <https://doi.org/10.1016/j.apcatb.2019.117889>.

[385] T. Li, G. Sun, L. Xiong, B. Zheng, Y. Duan, R. Yu, J. Jiang, Y. Wang, W. Yang, Transition-metal-free decarboxylation of D-glucaric acid to furan catalyzed by SnCl₄ in a biphasic system, *Mol. Catal.* 516 (2021), 111958, <https://doi.org/10.1016/j.mcat.2021.111958>.

[386] L. Claes, M. Janssen, D.E. DeVos, Organocatalytic Decarboxylation of Amino Acids as a Route to Bio-based Amines and Amides, *ChemCatChem* 11 (2019) 4297–4306, <https://doi.org/10.1002/cctc.201900800>.

[387] F. De Schouwer, L. Claes, N. Claes, S. Bals, J. Degrève, D.E. De Vos, Pd-catalyzed decarboxylation of glutamic acid and pyroglutamic acid to bio-based 2-pyrrolidone, *Green. Chem.* 17 (2015) 2263–2270, <https://doi.org/10.1039/C4GC02194K>.

[388] J. Verduyckt, M. Van Hoof, F. De Schouwer, M. Wolberg, M. Kurttepeli, P. Eloy, E. M. Gaigneaux, S. Bals, C.E.A. Kirschhock, D.E. De Vos, PdPb-Catalyzed Decarboxylation of Proline to Pyrrolidine: Highly Selective Formation of a Biobased Amine in Water, *ACS Catal.* 6 (2016) 7303–7310, <https://doi.org/10.1021/acscatal.6b02561>.

[389] S. Furukawa, A. Suga, T. Komatsu, Mechanistic Study on Aerobic Oxidation of Amine over Intermetallic Pd3Pb: Concerted Promotion Effects by Pb and Support Basicity, *ACS Catal.* 5 (2015) 1214–1222, <https://doi.org/10.1021/cs501695m>.

[390] J. Verduyckt, R. Coeck, D.E. De Vos, Ru-Catalyzed Hydrogenation–Decarbonylation of Amino Acids to Bio-based Primary Amines, *ACS Sustain. Chem. Eng.* 5 (2017) 3290–3295, <https://doi.org/10.1021/acssuschemeng.6b03140>.

[391] S. Xie, C. Jia, Z. Wang, S.S.G. Ong, M.-j Zhu, H. Lin, Mechanistic Insight into Selective Deoxygenation of L-Lysine to Produce Biobased Amines, *ACS Sustain. Chem. Eng.* 8 (2020) 11805–11817, <https://doi.org/10.1021/acssuschemeng.0c04052>.

[392] L. Claes, J. Verduyckt, I. Stassen, B. Lagrain, D.E. De Vos, Ruthenium-catalyzed aerobic oxidative decarboxylation of amino acids: a green, zero-waste route to biobased nitriles, *Chem. Commun.* 51 (2015) 6528–6531, <https://doi.org/10.1039/C5CC00181A>.

[393] L. Claes, R. Matthessen, I. Rombouts, I. Stassen, T. DeBaerdemaeker, D. Depla, J. A. Delcour, B. Lagrain, D.E. DeVos, Bio-Based Nitriles from the Heterogeneously Catalyzed Oxidative Decarboxylation of Amino Acids, *ChemSusChem* 8 (2015) 345–352, <https://doi.org/10.1002/cssc.201402801>.

[394] T. Thananathanachon, T.B. Rauchfuss, Efficient Production of the Liquid Fuel 2,5-Dimethylfuran from Fructose Using Formic Acid as a Reagent, *Angew. Chem., Int. Ed.* 49 (2010) 6616–6618, <https://doi.org/10.1002/anie.201002267>.

[395] S. Chen, R. Wojcieszak, F. Dumeignil, E. Marceau, S. Royer, How Catalysts and Experimental Conditions Determine the Selective Hydroconversion of Furfural and 5-Hydroxymethylfurfural, *Chem. Rev.* 118 (2018) 11023–11117, <https://doi.org/10.1021/acs.chemrev.8b00134>.

[396] J. Mitra, X. Zhou, T. Rauchfuss, Pd/C-catalyzed reactions of HMF: decarbonylation, hydrogenation, and hydrogenolysis, *Green. Chem.* 17 (2015) 307–313, <https://doi.org/10.1039/C4GC01520G>.

[397] Y.-B. Huang, Z. Yang, M.-Y. Chen, J.-J. Dai, Q.-X. Guo, Y. Fu, Heterogeneous Palladium Catalysts for Decarbonylation of Biomass-Derived Molecules under Mild Conditions, *ChemSusChem* 6 (2013) 1348–1351, <https://doi.org/10.1002/cssc.201300190>.

[398] Q. Meng, C. Qiu, G. Ding, J. Cui, Y. Zhu, Y. Li, Role of alkali earth metals over Pd/Al₂O₃ for decarbonylation of 5-hydroxymethylfurfural, *Catal. Sci. Technol.* 6 (2016) 4377–4388, <https://doi.org/10.1039/C5CY02248G>.

[399] D.P. Duarte, R. Martínez, L.J. Hoyos, Hydrodeoxygenation of 5-Hydroxymethylfurfural over Alumina-Supported Catalysts in Aqueous Medium, *Ind. Eng. Chem. Res.* 55 (2016) 54–63, <https://doi.org/10.1021/acs.iecr.5b02851>.

[400] Q. Meng, C. Qiu, H. Zheng, X. Li, Y. Zhu, Y. Li, Efficient decarbonylation of 5-hydroxymethylfurfural over an Pd/Al₂O₃ catalyst: Preparation via electrostatic attraction between Pd(II) complex and anionic Al₂O₃, *Mol. Catal.* 433 (2017) 111–121, <https://doi.org/10.1016/j.mcat.2017.02.035>.

[401] M. Chatterjee, T. Ishizaka, H. Kawanami, Accelerated decarbonylation of 5-hydroxymethylfurfural in compressed carbon dioxide: a facile approach, *Green. Chem.* 20 (2018) 2345–2355, <https://doi.org/10.1039/C8GC00174J>.

[402] F.M.A. Geilen, T. vomStein, B. Engendahl, S. Winterle, M.A. Liaw, J. Klankermayer, W. Leitner, Highly Selective Decarbonylation of 5-(Hydroxymethyl)furfural in the Presence of Compressed Carbon Dioxide, *Angew. Chem., Int. Ed.* 50 (2011) 6831–6834, <https://doi.org/10.1002/anie.201007582>.

[403] S. Sithisa, D.E. Resasco, Hydrodeoxygenation of Furfural Over Supported Metal Catalysts: A Comparative Study of Cu, Pd and Ni, *Catal. Lett.* 141 (2011) 784–791, <https://doi.org/10.1007/s10562-011-0581-7>.

[404] S. Bhogeswararao, D. Srinivas, Catalytic conversion of furfural to industrial chemicals over supported Pt and Pd catalysts, *J. Catal.* 327 (2015) 65–77, <https://doi.org/10.1016/j.jcat.2015.04.018>.

[405] R. Shekhar, M.A. Barreau, R.V. Plank, J.M. Vohs, Adsorption and Reaction of Aldehydes on Pd Surfaces, *J. Phys. Chem. B* 101 (1997) 7939–7951, <https://doi.org/10.1021/jp9710771>.

[406] V. Vorotnikov, G. Mpourmpakis, D.G. Vlachos, DFT Study of Furfural Conversion to Furan, Furfuryl Alcohol, and 2-Methylfuran on Pd(111), *ACS Catal.* 2 (2012) 2496–2504, <https://doi.org/10.1021/cs300395a>.

[407] S. Sithisa, W. An, D.E. Resasco, Selective conversion of furfural to methylfuran over silica-supported NiFe bimetallic catalysts, *J. Catal.* 284 (2011) 90–101, <https://doi.org/10.1016/j.jcat.2011.09.005>.

[408] C.P. Jiménez-Gómez, J.A. Cecilia, C. García-Sancho, R. Moreno-Tost, P. Maireles-Torres, Selective Production of Furan from Gas-Phase Furfural Decarbonylation on Ni-MgO Catalysts, *ACS Sustain. Chem. Eng.* 7 (2019) 7676–7685, <https://doi.org/10.1021/acssuschemeng.8b06155>.

[409] Y. Shi, Y. Zhu, Y. Yang, Y.-W. Li, H. Jiao, Exploring Furfural Catalytic Conversion on Cu(111) from Computation, *ACS Catal.* 5 (2015) 4020–4032, <https://doi.org/10.1021/acscatal.5b00303>.

[410] B. Liu, L. Cheng, L. Curtiss, J. Greeley, Effects of van der Waals density functional corrections on trends in furfural adsorption and hydrogenation on close-packed transition metal surfaces, *Surf. Sci.* 622 (2014) 51–59, <https://doi.org/10.1016/j.susc.2013.12.001>.

[411] S. Sithisa, T. Sooknoi, Y. Ma, P.B. Balbuena, D.E. Resasco, Kinetics and mechanism of hydrogenation of furfural on Cu/SiO₂ catalysts, *J. Catal.* 277 (2011) 1–13, <https://doi.org/10.1016/j.jcat.2010.10.005>.

[412] S. Wang, V. Vorotnikov, D.G. Vlachos, Coverage-induced conformational effects on activity and selectivity: hydrogenation and decarbonylation of furfural on Pd(111), *ACS Catal.* 5 (2015) 104–112, <https://doi.org/10.1021/cs5015145>.

[413] J. Luo, M. Monai, H. Yun, L. Arroyo-Ramírez, C. Wang, C.B. Murray, P. Fornasiero, R.J. Gorte, The H₂ Pressure Dependence of Hydrodeoxygenation Selectivities for Furfural Over Pt/C Catalysts, *Catal. Lett.* 146 (2016) 711–717, <https://doi.org/10.1007/s10562-016-1705-x>.

[414] S.H. Pang, J.W. Medlin, Adsorption and Reaction of Furfural and Furfuryl Alcohol on Pd(111): Unique Reaction Pathways for Multifunctional Reagents, *ACS Catal.* 1 (2011) 1272–1283, <https://doi.org/10.1021/cs200226h>.

[415] T. Ishida, K. Kume, K. Kinjo, T. Honma, K. Nakada, H. Ohashi, T. Yokoyama, A. Hamasaki, H. Murayama, Y. Izawa, M. Utsunomiya, M. Tokunaga, Efficient Decarbonylation of Furfural to Furan Catalyzed by Zirconia-Supported Palladium Clusters with Low Atomicity, *ChemSusChem* 9 (2016) 3441–3447, <https://doi.org/10.1002/cssc.201601232>.

[416] R.N. Monrad, R. Madsen, Rhodium-Catalyzed Decarbonylation of Aldoses, *J. Org. Chem.* 72 (2007) 9782–9785, <https://doi.org/10.1021/jo7017729>.

[417] F. van der Klis, L. Gootjes, J. van Haveren, D.S. van Es, J.H. Bitter, Selective terminal C–C scission of C5-carbohydrates, *Green. Chem.* 17 (2015) 3900–3909, <https://doi.org/10.1039/C5GC01012H>.

[418] P.J.C. Hausoul, A.K. Beine, L. Neghadar, R. Palkovits, Kinetics study of the Ru/C-catalysed hydrogenolysis of polyols – insight into the interactions with the metal surface, *Catal. Sci. Technol.* 7 (2017) 56–63, <https://doi.org/10.1039/C6CY02104B>.

[419] M. Rivière, N. Perret, D. Delcroix, A. Cabiac, C. Pinel, M. Besson, Solvent effect in hydrogenolysis of xylitol over bifunctional Ru/MnO/C catalysts under alkaline-free conditions, *ACS Sustain. Chem. Eng.* 6 (2018) 4076–4085, <https://doi.org/10.1021/acsuschemeng.7b04424>.

[420] M.O. Miranda, A. Pietrangle, M.A. Hillmyer, W.B. Tolman, Catalytic decarbonylation of biomass-derived carboxylic acids as efficient route to commodity monomers, *Green. Chem.* 14 (2012) 490–494, <https://doi.org/10.1039/C2GC16115J>.

[421] X. Zhang, F. Jordan, M. Szostak, Transition-metal-catalyzed decarbonylation of carboxylic acids to olefins: exploiting acyl C–O activation for the production of high value products, *Org. Chem. Front.* 5 (2018) 2515–2521, <https://doi.org/10.1039/C8QO00585K>.

[422] B. Katryniok, S. Paul, F. Dumeignil, Highly efficient catalyst for the decarbonylation of lactic acid to acetaldehyde, *Green. Chem.* 12 (2010) 1910–1913, <https://doi.org/10.1039/C0GC00203H>.

[423] M.D.R. Lutz, B. Morandi, Metal-catalyzed carbon–carbon bond cleavage of unstrained alcohols, *Chem. Rev.* 121 (2021) 300–326, <https://doi.org/10.1021/acs.chemrev.0c00154>.